



HAL
open science

Convergent assembly of natural benzophenanthridines and the chemistry of stable all-metal aromatic complexes

Pierre-Alexandre Deyris

► **To cite this version:**

Pierre-Alexandre Deyris. Convergent assembly of natural benzophenanthridines and the chemistry of stable all-metal aromatic complexes. Organic chemistry. Université Paris-Saclay, 2015. English. NNT : 2015SACLS109 . tel-01407351

HAL Id: tel-01407351

<https://theses.hal.science/tel-01407351>

Submitted on 2 Dec 2016

HAL is a multi-disciplinary open access archive for the deposit and dissemination of scientific research documents, whether they are published or not. The documents may come from teaching and research institutions in France or abroad, or from public or private research centers.

L'archive ouverte pluridisciplinaire **HAL**, est destinée au dépôt et à la diffusion de documents scientifiques de niveau recherche, publiés ou non, émanant des établissements d'enseignement et de recherche français ou étrangers, des laboratoires publics ou privés.

NNT : 2015SACLS109

THESE DE DOCTORAT
DE
L'UNIVERSITE PARIS-SACLAY
PREPAREE A
L'UNIVERSITE PARIS-SUD

INSTITUT DE CHIMIE DES SUBSTANCES NATURELLES

ECOLE DOCTORALE N°571 2MIB
Sciences chimiques : molécules, matériaux, instrumentation et biosystèmes

Spécialité : Chimie Organique

Par

Mr Pierre-Alexandre DEYRIS

Convergent assembly of natural benzophenanthridines
and the chemistry of stable all-metal aromatic complexes

Thèse présentée et soutenue à Gif-sur-Yvette, le 19 novembre 2015 :

Composition du Jury :

Mr GANDON, Vincent	Professeur – Université Paris-Sud	Président
Mr AMATORE, Christian	Directeur de Recherche – Ecole Normale Supérieure de Paris	Rapporteur
Mr PETIT, Marc	Chargé de Recherche – Université Pierre et Marie Curie	Rapporteur
Mr MALACRIA, Max	Professeur – Université Pierre et Marie Curie	Directeur de thèse
Mr MAESTRI, Giovanni	Assistant Professor – Università degli studi di Parma	Co-encadrant de thèse

A Papy,

*Personne n'aurait pu imaginer avoir
un meilleur grand-père que toi...*

“If you want to become a chemist, you will have to ruin your health. If you don't ruin your health studying, you won't accomplish anything these days in chemistry.”

Justus von Liebig — 19th century

REMERCIEMENTS

Je souhaiterais dans un premier temps remercier les Docteurs Christian Amatore et Marc Petit d'avoir accepté le rôle de rapporteur de mes travaux ainsi que le Professeur Vincent Gandon pour avoir présider ma soutenance. Je vous remercie tous les trois de vous être intéressé à mes travaux ainsi que d'avoir animé et participé à une riche discussion scientifique en cet après-midi du 19 novembre 2015.

Je tiens maintenant à remercier le Professeur Max Malacria pour m'avoir accueilli au sein de l'ICSN en tant qu'ancien directeur de l'Institut mais surtout en tant que directeur de thèse. Bien que tes fonctions de directeur ne nous ont pas permis de beaucoup nous voir durant la première année, tu as tout de même suivi nos projets respectifs, tu as toujours été à notre écoute quand quelque chose n'allait pas et ce jusqu'à notre soutenance. D'un point de vue plus personnel, les longues discussions sur la chimie, les années 70 (que tu affectionnes particulièrement), les femmes ou encore la politique ont été enrichissantes et m'ont aidé à prendre du recul et à voir le monde de manière différente. Je te remercie également pour les rencontres improvisées avec certain conférenciers (« Au fait, cet après-midi, il faut que tu parles avec le conférencier ! ») ou encore pour les referees à faire. Ça m'ennuyait sérieusement au début mais finalement l'expérience gagnée m'a fait relativiser les choses. Merci pour tout ! Mon seul regret, cependant, a été de ne pas t'avoir donné une formation accélérée sur Power Point !

Ensuite je souhaiterais remercier Giovanni Maestri. « Chef », tout d'abord merci de m'avoir recruté deux semaines avant le début du contrat ! Bien que le début de thèse fût difficile du point de vue chimie, tu as été là pour m'apprendre à passer du statut étudiant au statut de chercheur mais aussi à exploiter mes idées (quand j'en avais...). Merci de m'avoir confié le projet « triangle de palladium » avant ton départ pour l'Italie. Je ne connaissais pas du tout l'aromaticité métallique mais grâce à nos échanges de mails ainsi qu'aux rendez-vous Skype réguliers, j'ai pu totalement m'immerger dans ce grand projet qui j'espère continuera avec brio de l'autre côté des Alpes. A côté de ça, tu nous as laissé une grande liberté au laboratoire, c'était notre fief avec notre musique, nos photos, nos conneries et cela a beaucoup contribué à la bonne ambiance dans notre équipe. Je n'oublierai pas certaines soirées au cours desquelles tu nous disais « La sera leoni, la mattina coglioni », ce qui était un parfois vrai...! (Tout le temps en fait...) En tout cas, merci de la confiance que tu m'as accordé durant ces trois années.

Maintenant vient le moment de remercier Filipe « Filipé » Gomes. Je sais que tu n'aimes pas quand je dis ça mais merci beaucoup d'avoir pensé à moi pour la dernière bourse de thèse qui restait à

l'ICSN. Sans toi, je n'aurais pas été là et je n'aurais clairement pas pu vivre cette superbe aventure. Ensemble, on a réalisé un tas de conneries dont je citerai seulement quelques mots clés : Fléchettes, bombes, « dryce-ice », transpalette, fond d'écran, tortues ninja, septum... Cette liste est bien entendu non-exhaustive mais le point important est que cette complicité va grandement me manquer par la suite. Malgré une façade bourrue et un manque de tact certain (inhérent à ton côté portugais je pense :-P), tu es quelqu'un de droit, à qui on peut aisément faire confiance et je suis vraiment heureux de te compter parmi mes amis.

Vanessa « Franklin » Narbonne, ça a été un plaisir d'avoir été ton voisin de paillasse pendant cette thèse. Merci d'avoir supporté mes blagues pourries sans t'énerver (même si tu aurais parfois du...). J'espère que je t'ai donné l'envie de continuer à travailler ton second degré par la suite :-P Tu es enfin sortie de ta carapace, maintenant vis ta vie à fond et je te souhaite bon courage pour la suite !

Je tiens à remercier le reste de l'équipe 01 : Tatiana « abuelita », la gentillesse incarnée. Merci d'avoir travaillé avec moi sur le projet de m'avoir dépanné de temps en temps quand je n'avais plus de catalyseur ! Yanlan, je vais écrire en français alors j'espère que tu n'as pas oublié les bases de notre langue! Tu as abattu un boulot immense dont je présente une partie dans cette thèse. Merci beaucoup d'avoir travaillé à mes côtés ainsi que pour les discussions scientifiques poussées qui m'ont permis d'aller de l'avant. Je remercie aussi ma stagiaire Anne-Laure (Numéro 4) pour avoir contribué à l'avancement du projet des semi-réductions. Tu as toujours été volontaire, désireuse d'apprendre et également très méticuleuse. Ça a été un grand plaisir pour moi de t'encadrer et j'espère que tu te souviens du mécanisme de la Sonogashira :-P. Merci aussi aux autres stagiaires : Ghanio (Numéro 1), Emilie (Numéro 2) et Marion (Numéro 3) pour vous être si bien intégré dans l'équipe.

Un grand merci à deux amies au top du top : Laura et Corinne. Les souvenirs du séjour génialissime au Portugal avec vous ainsi que tout le reste resteront à jamais dans un coin de ma tête. Lolo, tes passages quotidiens au labo régulièrement accompagnés de petits post-it rigolo m'ont manqué depuis ton départ. Cocotte, il n'y a que toi qui adores le fromage autant que moi ! Bref, votre complicité à toute épreuve ainsi que votre gentillesse m'ont manqué depuis que vous êtes parties et même si je suis nul à chier pour garder contact et donner des news, sachez que je ne vous oublie pas et que je pense souvent à vous.

Cette thèse n'aurait pas été la même sans les membres du premier étage de l'aile est. Merci Manos, Trang, Angelica, Antje, Alexandra et Raphaël pour l'équipe Rodriguez. Entre autres, je retiendrai que la barrière « sale » de la langue a été outrepassée durant certains midis... Merci à vous ! Un grand merci à tous les membres de l'équipe Vauzeilles avec qui j'ai pu partager le petit déjeuner chaque vendredi matin. Tout d'abord merci Boris pour tes jeux de mots toujours excellents ainsi que pour nous avoir prêté la machine à café (élément indispensable dans la vie d'un thésard...). Aurélie, « Ainée », c'était un grand plaisir d'avoir une tête connue qui bossait dans le labo d'à côté. Merci pour

les pauses, pour tous les mails que tu as lu à ma place et pour ta gentillesse (bien cachée il faut se le dire :-P). Antoine et Jordi, merci de m'avoir fait autant rire lorsque vous chantiez *vivo per lei* dans le labo ainsi que pour les challenges de contrepèteries, les quelques verres en plastiques percés... Les « Salut Patrick » dans le couloir me manqueront ! Nathan, mon loulou, merci pour ta bonne humeur de tous les jours ainsi que de m'avoir suivi dans la plupart de mes délires parfois farfelus. Merci aussi d'avoir participé aux contrepèteries. T'es un mec au top! Roxane Ott « Hot », merci d'avoir participé à la bonne ambiance du groupe et souviens-toi, « Tout cul tendu, mérite son dû ! ». Merci également à Laura et Greg.

Merci au CEI 2013 pour toutes ces soirées et ces évènements à l'arrache. Bien que le mot « organisation » nous fût inconnu, tout le monde était au rendez-vous le jour-J et ceci a contribué à l'excellente ambiance de cette promo 2013. Je remercie notamment Amandine, et Matt le tout p'tit pour tous les bons moments partagés ensemble même si je n'ai pas fait l'ESOC à Marseille ! Lam, après 7 ans dans la même promo, nos chemins se séparent (enfin :-P) ! Bon vent pour la suite, nouille ;-). Aude, merci pour les moments où je pouvais me moquer de tes compétences en informatique ou quand je venais me plaindre en sortant du bureau de mon chef... Merci Tatiana pour ton mignon petit accent, ta maîtrise parfaite de la langue française et Val, mon coloc d'une semaine qui se faisait plaisir sous la douche, coquin va ! (:P). Avec une semaine complète en état d'ébriété, la SECO 52 à Morzine était une pure réussite et ça restera un des meilleurs souvenirs de la thèse. Je tiens aussi à te remercier, Camille, pour ta joie de vivre, ta pêche quasi constante, ta passion pour les petits plaisirs de la vie tels que le japonais, la petite, le fromage et la bonne bouffe de manière générale mais aussi pour ton rire tellement original qu'à l'autre bout de l'institut, je savais que tu étais là :-P

Je tiens également à remercier tous les membres de l'ICSN que j'ai pu côtoyer au cours de ces trois ans et notamment Odile, Franck et Nathalie pour m'avoir confié la précieuse GC-MS et m'avoir fait confiance pour son utilisation. Merci également au service informatique : Guillaume, David, Julien et Manu, je pensais que j'avais un humour assez « basique »... A la vue de votre excellent niveau, je me dis que j'ai encore du chemin à parcourir ;-) Merci à Lucie, Laurent, Margaux, Clément, Romain, Tiphaine, Coralie, Géraldine. Vous avez contribué, de différentes manières, à la bonne ambiance ainsi qu'au bon déroulement de cette thèse.

A défaut de savoir où l'on va, il ne faut certainement pas oublier d'où l'on vient. Je remercie mes loulous du M2R Chimie Organique d'Orsay 2011-2012 (et associées), nommément Filipe, Florian, Corentin & Eva, Bastien & Léa, Alexandre, Georges & Lilou, pour que cette promotion soit soudée autour de l'amitié, de l'entraide et de la bonne humeur. Par extension, je souhaite remercier certains membres de l'ICMMO, mon labo de substitution : Didier, Riccardo, Nicolas, Pierre, Rodolphe, Andrii, Morgan, Natacha, Terry, Pauline, Vincent, Florian, Claire, Valérie, Bastien, Olga, Jean-Pierre ainsi que La Marie. Vous m'avez toujours accueilli avec joie pour les nombreux apéros/pot de thèse/soirées et je me sentais comme chez moi dès que je mettais les pieds dans cette fameuse

bibliothèque du premier étage du bâtiment 410. Merci pour tout et « à ceux qui les montent !! ». Je remercie énormément mes amis du « 64 » (et associés) avec qui j'ai vécu des moments inoubliables : Ptit Gornyk & Eff, Puigstou et Luc & Clément. Même si j'étais beaucoup moins disponible qu'avant durant cette période de thèse, vous êtes restés les mêmes et avez su rester proche de moi ! Les habitudes telles que les soirées beaujolais annuelles ou les 7 Wonders ont la vie dure et cela compte vraiment beaucoup pour moi, merci les amis :-). Colinou, depuis ce retard mémorable en TP de chimie organique en L3, on s'est toujours suivi de près ou de loin. Même si tu as choisi le côté obscur de la chimie, tu as toujours été là pour me changer les idées autour d'un petit verre bien mérité ! Merci beaucoup ! Georges et Christophe, mes « shabs », même à distance la connerie reste un lien pour les gens et pour nous ça a toujours fonctionné ! Merci pour ces « gentils » week-ends strasbourgeois, les conversations délirantes sur hangout ou encore les vacances reposantes à la montagne. Cela m'a aidé à revenir en pleine forme pour continuer la chimie !

Je vais maintenant passer au plus important : la famille. Papa, Maman, malgré un début difficile dans les études supérieures, vous m'avez donné les moyens et vous m'avez supporté lorsque j'ai voulu me lancer dans la chimie. Grâce à vous, j'ai pu trouver ma voie et j'ai pu réaliser ce que je voulais faire depuis que je suis arrivé à l'IUT : Être docteur en chimie ! Vous avez cru en moi et je ne vous remercierai jamais assez pour tout ça. Je vous aime fort. Delphine, ma petite sœur préférée (en même temps je n'en ai qu'une :-P), merci également de ton soutien, des coups de téléphone quand ça n'allait pas à n'importe quelle heure ainsi que pour les petites soirées détente à regarder des films à la con. Toi aussi je t'aime fort ! Je tiens aussi à remercier mes grands-parents. Papy, Mamie, Daddy et Maddie, merci pour votre soutien moral et votre gentillesse même si je ne suis pas forcément doué pour vous donner des nouvelles. J'ai de la chance de vous avoir comme grands-parents.

ABBREVIATIONS

Ac :	acetyl
AO :	atomic orbital
Ar :	aryl
Bn:	benzyl
Bz:	benzoyl
CAAC :	cyclic (alkyl)(amino)carbene
cat. :	catalyst
cb	carbazole
Cp:	cyclopentadiene
Cp*:	cyclopentadienyl anion
DCE:	1,2-dichloroethane
DCM:	dichloromethane
DFT:	density functional theory
DMF :	dimethylformamide
dppf :	1,1'-Bis(diphenylphosphino)ferrocene
EDG :	electrodonating group
eq. :	equivalent
ESI-MS :	electrospray ionisation – mass spectrometry
Et :	ethyl
Et ₃ N :	triethylamine
EtOAc :	Ethyl acetate
EtOH :	ethanol
EWG :	electrowithdrawing group
FLP :	frustrated Lewis pair
GC-FID :	gas chromatography – flame ionisation detector
GC-MS :	gas chromatography – mass spectrometry
h :	hour
HOMO :	highest occupied molecular orbital
HRMS :	high resolution mass spectroscopy
ⁱ Pr :	isopropyl
LUMO :	lowest unoccupied molecular orbital

<i>m-</i> :	<i>meta-</i>
Me :	methyl
min. :	minutes
MO:	Molecular orbital
MTBE:	methyl <i>tert</i> -butyl ether
MW:	micro-wave
n.d.:	not determined
<i>n</i> -Bu:	normal butyl
NICS:	nucleus independent chemical shift
NMR :	nuclear magnetic resonance
<i>o-</i> :	<i>ortho-</i>
<i>p-</i> :	<i>para-</i>
ppm :	parts-per-million
PTSA :	<i>para</i> -toluenesulfonic acid
ref :	reflux
rt :	room temperature
SQUID :	superconducting quantum interference device
TBDPS:	<i>tert</i> -butyldiphenylsilyl
^t Bu :	<i>tert</i> -butyl
TEMPO :	2,2,6,6-Tetramethylpiperidin-1-yl)oxyl
Tf :	trifluoromethanesulfonyl
THF :	tetrahydrofuran
TS :	transition state
VB :	valence bond

REMERCIEMENTS	7
ABBREVIATIONS	13
GENERAL INTRODUCTION	21
PART 1: SYNTHESIS OF NATURAL BENZO[C]PHENANTHRIDINES BY PALLADIUM/NORBORNENE DUAL CATALYSIS	25
1.1. INTRODUCTION ON PALLADIUM/NORBORNENE CATALYSIS	25
1.2. STATE OF ART	35
1.2.1. BIOLOGICAL INTEREST OF BENZO[C]PHENANTHRIDINES	35
1.2.2. SYNTHESIS	36
1.2.2.1. Linear synthesis	36
1.2.2.1.1 Total synthesis of benzo[c]phenanthridines by Stermitz et al.	37
1.2.2.1.2. Total synthesis of benzo[c]phenanthridines by Ishihara et al.	38
1.2.2.2. Convergent synthesis	39
1.1.2.2.1. Synthesis of phenanthridines by Lautens <i>et al.</i>	39
1.2.2.2.2. Synthesis of phenanthridines by Catellani <i>et al.</i>	40
1.2.2.2.3. Synthesis of phenanthridines by Malacria <i>et al.</i>	41
1.3 RESULTS AND DISCUSSION	44
1.3.1. OBJECTIVES OF THE PROJECT	44
1.3.2. SYNTHESIS OF THE COUPLING PARTNERS	45
1.3.2.1. Synthesis of naphtyl triflates	45
1.3.2.2. Synthesis of o-bromobenzylamines	46
1.3.3 COUPLING STEP	47
1.4. CONCLUSION	51
1.5. SUPPORTING INFORMATION	55
1.5.1. GENERAL REMARKS	55
1.5.2. GENERAL PROCEDURES	55
1.5.3. COUPLING OF ORTHO-SUBSTITUTED ARYL IODIDES AND ORTHO-BROMOBENZYLAMINES	58
1.5.3.1. Preparation of the epoxynaphtalenes	58
1.5.3.2. Preparation of the naphtyl alcohols	59
1.5.3.3. Preparation of the naphtyl triflates	60
1.5.3.4. Preparation of the bromobenzylamines	61
1.5.3.5. Preparation of the bromobenzylamines	62
1.5.3.6. Benzo[c]phenanthridines compounds	63
PART 2 : ALL-METAL AROMATICITY	67
2.1. INTRODUCTION	67
2.1.1. CONCEPT OF AROMATICITY	67
2.1.1.1. Discovery of benzene	67
2.1.1.2. Electronic properties of aromatic compounds	72
2.1.2. ALL-METAL AROMATICITY	81

2.1.2.1. Nucleus Independent Chemical Shift (NICS)	83
2.1.2.2. δ -type aromaticity	84
2.1.2.3. Stable triangular all-metal aromatics	87
2.1.2.3.1. Robinson trigallium cluster	87
2.1.2.3.2. (tris)gold clusters	88
2.1.2.3.2.1. Sadighi's approach	88
2.1.2.3.2.2. Bertrand's approach	89
2.1.2.3.3. Fischer's trizinc clusters and zinc-copper heteroaromatics	90
2.1.2.3.4. Maestri's tripalladium cluster	91
2.1.2.3.4.1. First generation synthesis	91
2.1.2.3.4.2. Steric and electronic properties	93
2.2 RESULTS AND DISCUSSIONS	98
2.2.1. AIM OF THE PROJECT	98
2.2.2. SECOND GENERATION SYNTHESIS OF TRIPALLADIUM CLUSTERS	98
2.2.3. TOWARD THE SYNTHESIS OF ANALOGUES OF $[\text{Pd}_3]^+$	103
2.2.3.1. Analogues.	104
2.2.3.2. Mixed palladium and platinum heteroclusters	105
2.2.3. $[\text{Pd}_3]^+$ AS A LEWIS BASE, A NEW NUCLEOPHILIC LIGAND FOR LEWIS ACIDS	112
2.2.3.1. Non-covalent cation- π interactions	112
2.2.3.2. Tripalladium-based tetrahedral structures	113
2.4. CONCLUSIONS	120
2.5. SUPPORTING INFORMATION	123
2.5.1. GENERAL REMARKS	123
2.5.2. GENERAL PROCEDURES	123
2.5.3. SYNTHESIS OF TRIANGULAR HOMO- AND HETEROMETALLIC CLUSTERS	127
2.5.3.2. Preparation of tripalladium clusters	127
2.5.3.2. Preparation of triplatinum clusters	142
2.5.3.3. Preparation of heterobimetallic cluster 161	145
2.5.3.4. Preparation of heterobimetallic cluster 162	146
2.5.3.5. Preparation of silver-containing tetrahedral cluster	147
2.5.3.6. Preparation of gold-containing tetrahedral cluster 170	150
2.5.3.7. Preparation of copper-containing tetrahedral cluster 171	151
PART 3 : CATALYSIS WITH ALL-METAL AROMATICS	155

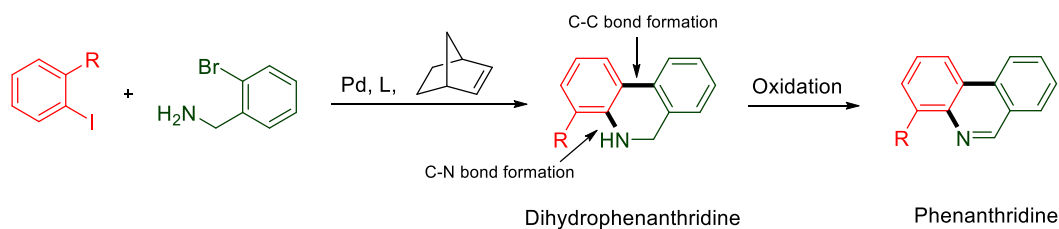
3.1. INTRODUCTION	155
3.2. STATE OF ART	156
3.2.1. SEMI-REDUCTION REACTIONS USING PALLADIUM CATALYSTS	157
3.2.2. METHOD USING FLP	161
3.2 RESULTS AND DISCUSSIONS	162
3.2.1. AIM OF THE PROJECT	162
3.2.2. OPTIMIZATION OF THE REACTION	163
3.2.3. ALKYNES SYNTHESSES	168
3.2.3.1. Synthesis of aromatic alkynes	168
3.2.3.2. Synthesis of aliphatic alkynes	169

3.2.4. EXTENSION OF THE SEMI-REDUCTION REACTION CATALYZED BY $[Pd_3]^+$ CATALYST	170
3.3. CYCLOISOMERIZATION OF ENYNES	177
3.4. CONCLUSIONS	179
3.5. SUPPORTING INFORMATION	183
3.5.1. GENERAL REMARKS	183
3.5.2. GENERAL PROCEDURES	184
3.5.3. SYNTHESIS OF AROMATIC ALKYNES	187
3.4.4. SYNTHESIS OF ALIPHATIC ALKYNES	190
3.4.5. CATALYTIC SEMI-REDUCTIONS OF ALKYNES	194
GENERAL CONCLUSION	221
<hr/>	
RESUME EN FRANCAIS	225

GENERAL INTRODUCTION

GENERAL INTRODUCTION

Since decades, transition-metal chemistry has made a remarkable headway, especially concerning palladium. Among the plethora of reactions catalyzed by palladium complexes, our group was interested by the dual palladium/norbornene catalysis in order to create polycyclic molecules. The use of norbornene in addition to palladium to achieve C-halide and C-H activations was first developed by the group of Catellani in the mid 1980's. Since then, numerous applications and extensions of this reaction have been realized around the world. Our group recently reported a new methodology to synthesize the phenanthridine framework starting from *ortho*-substituted aryl halides and bromobenzylamines. The catalytic cycle involves three palladium oxidation states (0, II and IV). We were interested to extend this methodology in order to achieve the synthesis of natural products (Scheme 1).



Scheme 1 : C-Amination coupling variant of the Catellani reaction.

The first part of my Ph D. took place into this perspective. Benzo[*c*]phenanthridines possess relevant biological activities that make them an interesting and challenging goal to extend this methodology.

The second part of this Ph D. work concerned a new family of metal-aromatic tripalladium complexes. Recently reported in our group, these complexes are the first noble metal stable analogues of the cyclopropenyl cation $[C_3H_3]^+$. These clusters possess a perfectly equilateral core as regular aromatics. Calculations interestingly predicted that in spite of the presence of a delocalized positive charge, they could have a Lewis basic character. The original route to these complexes was long and tedious. This synthesis was an impediment to study and exploit their special properties. Efforts were made to develop a concise and modular route to these platforms.

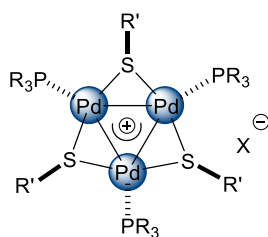


Figure 1 : Structure of tripalladium complexes family.

Taking advantage of the stability of these complexes, we wondered to know if their special properties could provide any catalytic activities. To answer this question, we chose to investigate a classical reaction in organic chemistry, namely the semi-reduction of alkynes.

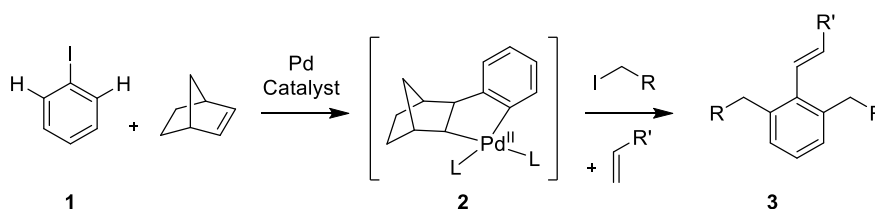
This manuscript will be divided in three chapters dealing respectively with benzophenanthridines synthesis, all-metal aromatic complexes and their applications in catalytic reactions. Each chapter will contain a bibliographical part in which the relevant literature background will be reviewed.

**PART 1: SYNTHESIS OF NATURAL
BENZO[C]PHENANTHRIDINES BY
PALLADIUM/NORBORNENE DUAL CATALYSIS**

PART 1: SYNTHESIS OF NATURAL BENZO[C]PHENANTHRIDINES BY PALLADIUM/NORBORNENE DUAL CATALYSIS

1.1. Introduction on palladium/norbornene catalysis

In the last three decades, recent advances in palladium chemistry allowed chemists to realize a wide panel of new reactions, such as selective C-C or C-Heteroatom bond formation under mild conditions. In the early 90's Catellani and coworkers¹ reported a palladium/norbornene reaction to create a trisubstituted aryl system **3** in a one-pot procedure, starting from phenyl iodide **1** (Scheme 2). The oxidative addition of Pd(0) into the C-I bond followed by the carbopalladation of norbornene give access to the palladacycle **2**. Indeed, norbornene is a strained olefin which cannot undergo a *syn*- β -hydride elimination and place the palladium well located to trigger aryl C-H activation.



Scheme 2 : Catellani's reaction.

Comforted by the work of Canty² and Echavarren,³ Catellani and coworkers⁴ postulated that palladacycle **2** could undergo another oxidative addition to form the Pd(IV) intermediate **4** (Scheme 3). Reductive elimination of **4** followed by a rotation of the norbornane-aryl bond and a new C-H activation provide **5**. Another C-C coupling between alkyl iodide and the aryl group could be realized. The norbornene extrusion step has been shown to occur only if the aromatic moiety is disubstituted.⁵ Catellani postulated that the C-C bond cleavage between aliphatic and aromatic carbon atoms appears to be driven by steric factors. After norbornene extrusion, a Pd(II) intermediate could be obtained, which is suitable to a classical Heck-type coupling reaction with a terminal olefin to form product **3**.

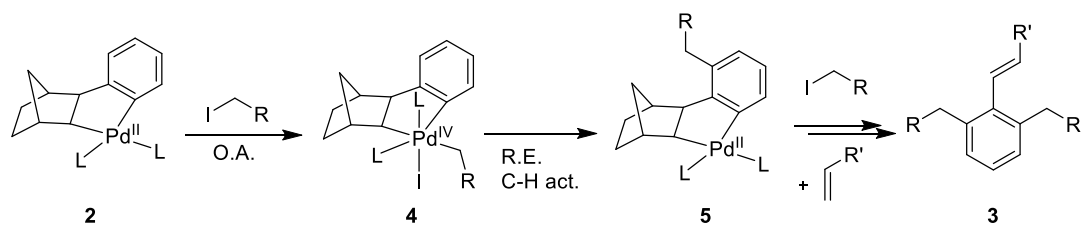
¹ M. Catellani, F. Frigiani, A. Rangoni, *Angew. Chem. Int. Ed. Engl.* **1997**, *36*, 119-122.

² a) A. J. Canty, *Acc. Chem. Res.*, **1992**, *25*, 83-90. b) D. Kruis, B. A. Markies, A. J. Canty, J. Boersma, G. van Koten, *J. Organomet. Chem.*, **1997**, *532*, 235-242.

³ a) D. J. Cardenas, C. Mateo, A. M. Echavarren, *Angew. Chem. Int. Ed. Engl.*, **1994**, *33*, 2445-2447. b) C. Mateo, D. J. Cardenas, C. Fernandez-Rivas, A. M. Echavarren, *Chem. Eur. J.*, **1996**, *2*, 1596-1606.

⁴ a) M. Catellani, G. P. Chiusoli, M. Costa, *J. Organomet. Chem.*, **1995**, *500*, 69-80.

⁵ M. Catellani, M. C. Fagnola, *Angew. Chem. Int. Ed. Engl.*, **1994**, *33*, 2421-2422.



Scheme 3 : Key intermediates in palladium/norbornene catalytic reactions.

In 2008, cyclovoltametric and kinetic studies by Amatore, Catellani and Jutand⁶ determined the presence of Pd(IV) intermediates in the mechanistic pathway showed above in scheme 3. However, authors expressed reservations concerning the application of their model to aromatic arylation.

In the case of sp^2 - sp^2 bond formation, the situation is different. It is commonly known that Ar-X can easily do oxidative addition on Pd(0) but the ability of the same species to realize oxidative addition on a Pd(II) complex was not experimentally proved at that time. Moreover, depending on the ligand used, the reductive elimination step can provide competitively sp^2 - sp^3 coupling between norbornene and the aryl moiety. This kind of coupling can lead to polycyclic molecules such as benzocyclobutene⁷ or benzocyclohexene⁸⁹ derivatives. Catellani and coworkers observed interesting activities with differently substituted aryl iodides.⁹ With *o*-substituted ones, they first observed the formation of the palladacycle **7** and then a total selectivity towards the sp^2 - sp^2 coupling, followed by extrusion of norbornene to give **8** (Scheme 4a). By contrast, the use of *m*- or *p*-substituted aryl iodides led to the formation of intermediate **10** which evolves through unselective sp^2 - sp^2 and sp^2 - sp^3 coupling eventually providing a mixture of complexes **11** and **12**, as reported for unsubstituted aryl iodides (Scheme 4b). They decided to screen several *ortho*-substituted aryl iodides to see the limits of the reaction.

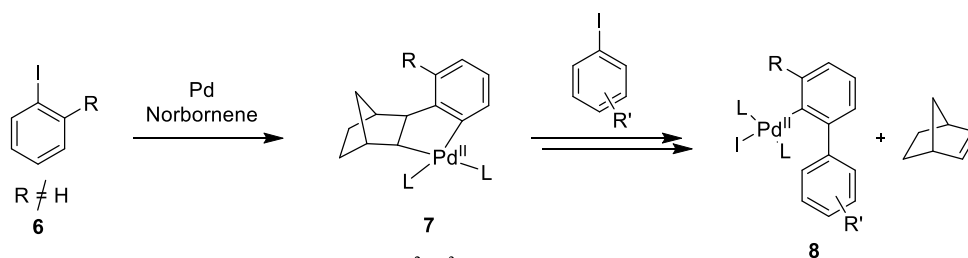
⁶ C. Amatore, M. Catellani, S. Deledda, A. Jutand, E. Motti, *Organometallics* **2008**, *27*, 4549-4554

⁷ M. Catellani, L. Ferioli, *Synthesis*, **1996**, 769-772.

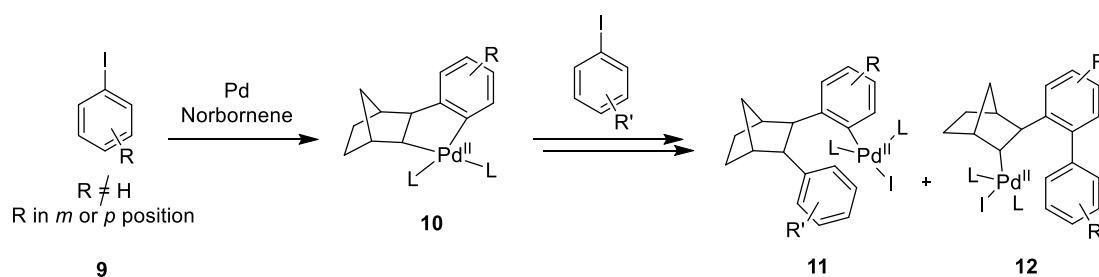
⁸ M. Catellani, G. P. Chiusoli, C. Castagnoli, *J. Organomet. Chem.*, **1991**, *407*, C30-C33.

⁹ M. Catellani, E. Motti, *New J. Chem.*, **1998**, *22*, 759-761.

a) Reaction with *o*-substituted aryl iodide leads to sp^2 - sp^2 coupling



b) Reaction with *m*- or *p*-substituted aryl iodide leads to sp^2 - sp^3 coupling



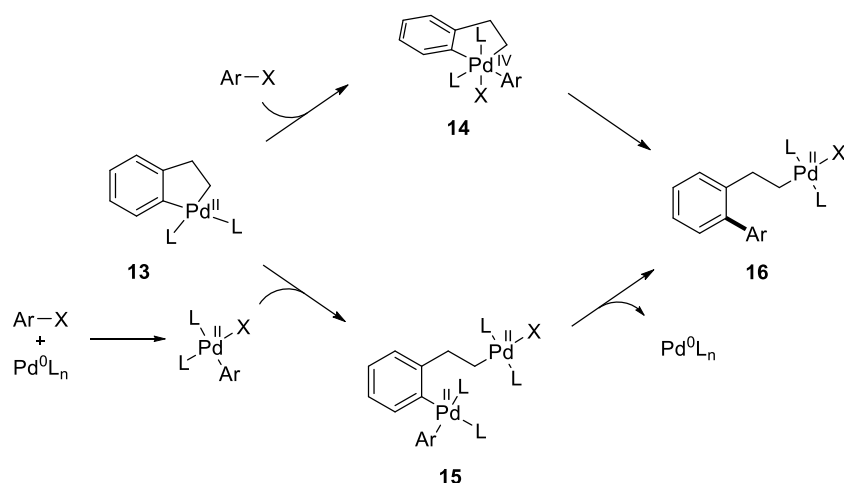
Scheme 4 : Results by employing differently substituted aryl iodides.

The direct arylation takes place in each case with good to excellent yields (61 to 99%) except for the bulky ^tBu- substituent, which leads to the benzocyclobutene⁸ compound resulting from reductive elimination of palladacycle **7**. Catellani supposed that the resulting coupling occurs thanks to a steric influence of R-substituent on the palladacycle. She called this observation the “*Ortho*-effect”.

If a substituent in *ortho*-position lead to selective aryl-aryl bond, the mechanism of this reaction was still unknown at that time. Catellani, Lautens and others¹⁰ invoked a Pd(IV) intermediate **14** to justify the C(sp^2)-C(sp^2) bond observed in final products but in 2006, Cardenas and Echavarren¹¹ postulated that the aryl-aryl bond could be engendered by a transmetalation pathway *via* intermediate **15** (Scheme 5).

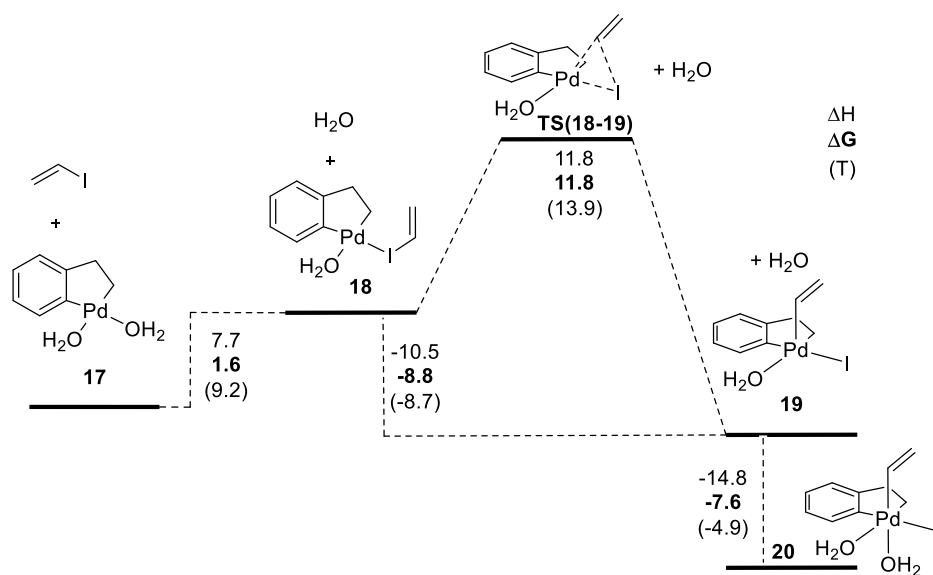
¹⁰ a) M. Catellani, *Top. Organomet. Chem.* **2005**, *14*, 21–53. b) M. Lautens, D. Alberico, C. Bressy, Y.-Q. Fang, B. Mariampillai, T. Wilhelm, *Pure Appl. Chem.* **2006**, *78*, 351–361. c) C. Bressy, D. Alberico, M. Lautens, *J. Am. Chem. Soc.* **2005**, *127*, 13148–13149. d) A. Rudolph, N. Rackelmann, M. Lautens, *Angew. Chem., Int. Ed.* **2007**, *46*, 1485–1488. e) K. M. Gericke, D. I. Chai, N. Bieler, M. Lautens, *Angew. Chem., Int. Ed.* **2009**, *48*, 1447–1451.

¹¹ D. J. Cárdenas, B. Martín-Matute, A. M. Echavarren, *J. Am. Chem. Soc.* **2006**, *128*, 5033–5040



Scheme 5 : Two possible routes to achieve aryl-aryl coupling.

They chose to study palladacycle **13** because of their *cis*-substitution with $\text{C}(\text{sp}^2)$ and $\text{C}(\text{sp}^3)$ and with PH_3 , water or formamide as ligand to simplify the calculations. They also chose to use vinyl iodide to model the $\text{C}(\text{sp}^2)\text{-X}$ bond of Ar-X . The results of calculations for Pd(IV) pathway is presented on figure 2.

Figure 2 : Palladium(IV) pathway calculations with H_2O as ancillary ligands. (B3LYP/LANL2AZ)

Palladacycle **17** proceeds to a ligand exchange between vinyl iodide and water to give intermediate **18**. Activation energy to reach transition state **TS(18-19)** is moderated ($11.8 \text{ kcal}\cdot\text{mol}^{-1}$) and afford pentacoordinated intermediate **19** after oxidative addition. Binding an additional ligand to complete the square-based bipyramide leads to intermediate **20** in an

energetically favored manner. The same calculations have been realized for the transmetalation pathway and are shown in figure 3.

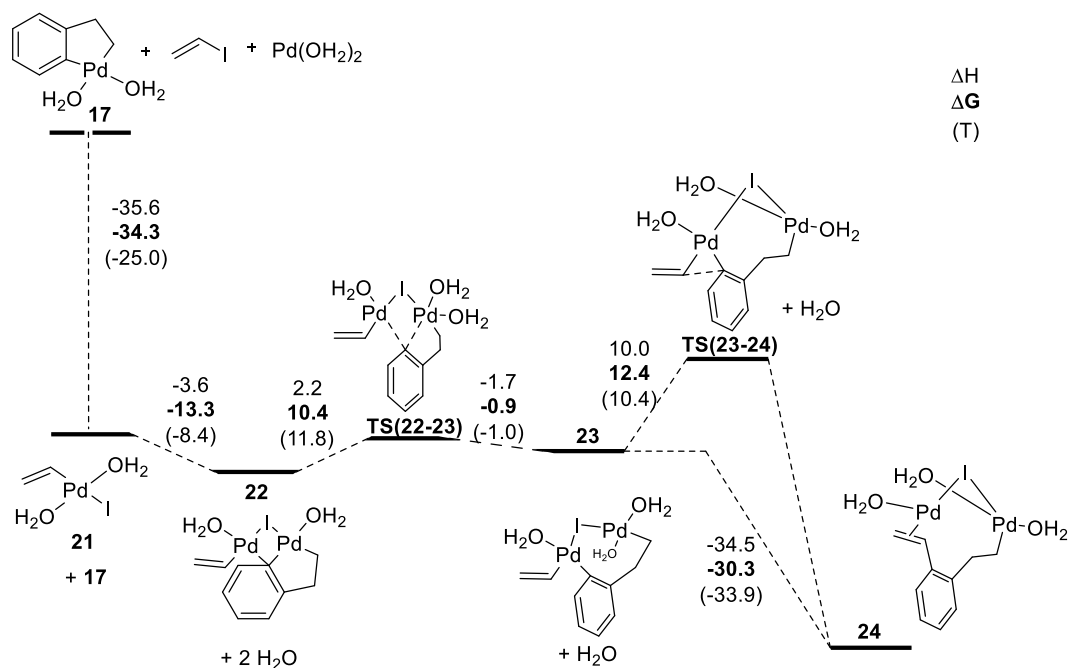


Figure 3 : Transmetalation pathway calculations with H₂O as ancillary ligands. (B3LYP/LANL2AZ)

The oxidative addition of vinyl iodide on Pd(0) provides intermediate **21** in a significantly exothermic way and the isomerization into the *trans* isomer proceeds easily. The coordination of **21** to **17** leads to the bimetallic species **22** in which an iodine atom bridges the two metal atoms and both palladium nuclei are coordinated to the *ipso* carbon of the aryl moiety. The transfer of aryl group leads endothermically to the formation of **23**. Transition state **TS(23-24)** requires roughly the same activation energy required to trigger Pd(IV) reductive elimination and affords intermediate **24**.

To summarize, the coordination previous to oxidative addition is exothermic for Pd(0) and endothermic for Pd(II). This greatly favors the transmetalation pathway in order to create new C-C bonds. By extension of these results, aryl halides could more easily react with unsaturated Pd(0) complexes than with Pd(II) metallacycles. Whereas formation of Pd(IV) intermediate was strongly supported by other experimental work²⁻⁴ in the Catellani reaction involving alkyl halides, their results showed that it should not be the case for aryl halides. However, the model utilized by Echavarren *et al.* greatly simplified the metalacycle, did not consider substituents on the alkyl chain and was unable to explain the so-called “*ortho*-rule” observed in Catellani reaction.

At that time, the real pathway of the aryl-aryl coupling was still a matter of debate because no significant proofs were reported in the literature to tip the balance towards one of the two proposed mechanisms.

In 2011, our group in collaboration with Catellani¹² reported computational analysis involving the real aryl-norbornyl metalacycle in order to get a better understanding the mechanism of aryl-aryl coupling step. They would like to understand the importance of a substituent on the *ortho*-position of the aryl moiety in the mechanistic pathway. They first started by the study of the mechanism using an unsubstituted metalacycle. Calculations have been realized for both of the pathways, in red, the Pd(IV) pathway and in blue the transmetalation one (Figure 4 and 5)

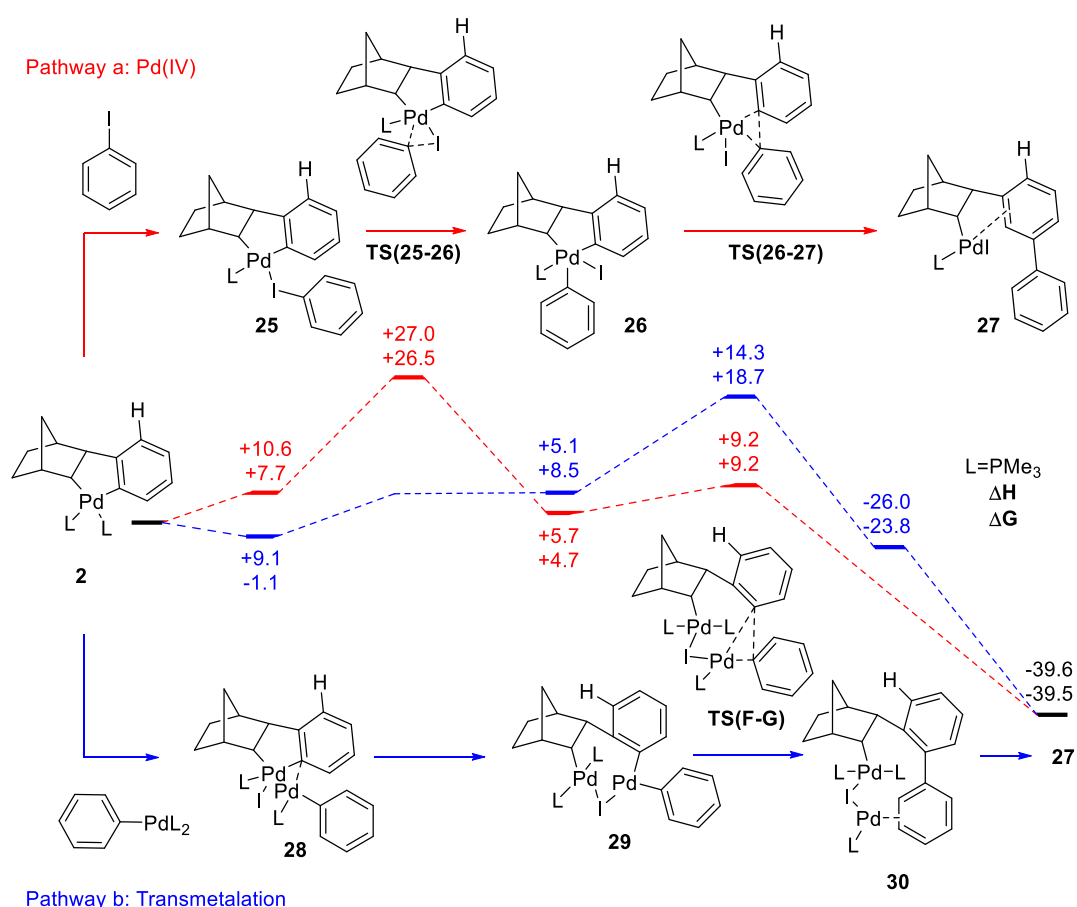


Figure 4 : Mechanistic studies of the reaction involving palladacycle with unsubstituted aryl.

For the Pd(IV) pathway, we can see that the transition state which leads to the crucial Pd(IV) intermediate, **TS(25-26)**, possesses the highest energy level ($\Delta G = +26.5$ kcal.mol⁻¹).

¹² G. Maestri, E. Motti, N. Della Ca', M. Malacria, E. Derat, M. Catellani, *J. Am. Chem. Soc.*, **2011**, *133*, 8574-8585.

For transmetalation pathway, it is the transition state of the reductive elimination **TS(29-30)** which possesses the higher level of energy. In comparison, the blue pathway needs less energy brought by the system than the red one to be achieved. They concluded that for an unsubstituted palladacycle the favored pathway would be that involving transmetalation between two Pd(II) species.

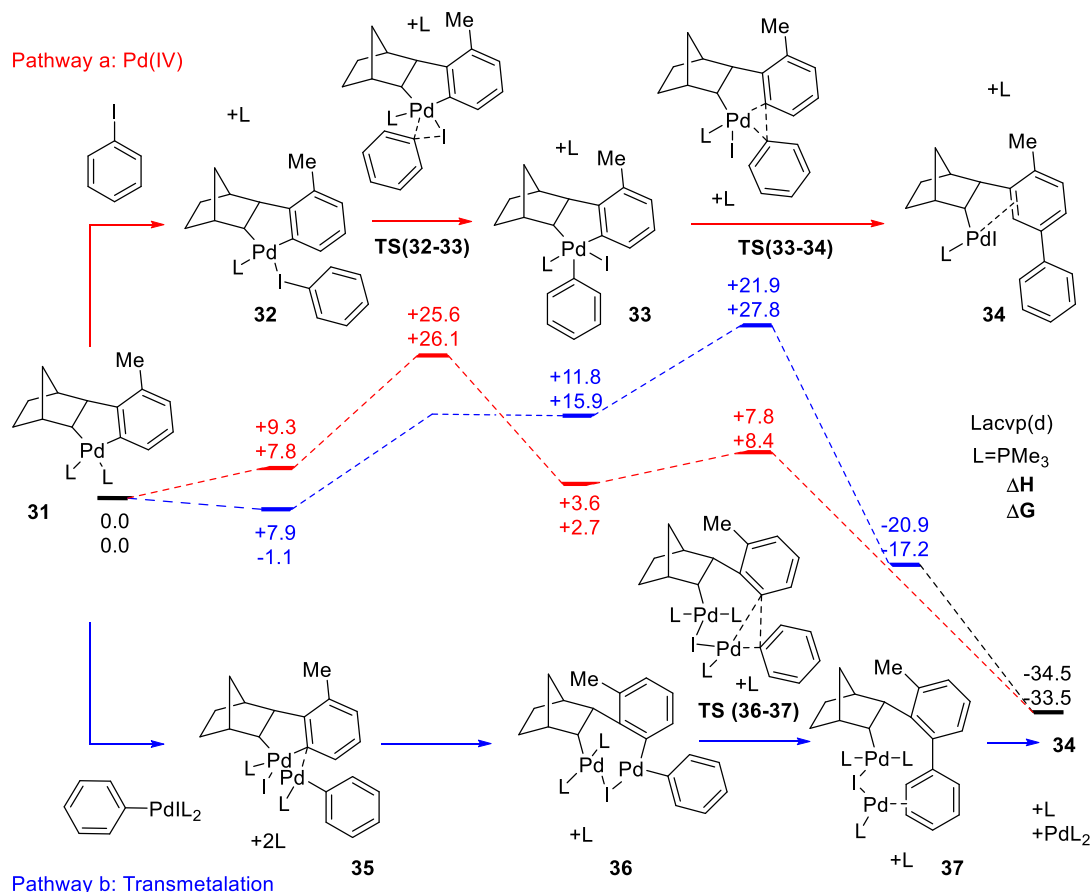


Figure 5 : Mechanistic studies of the reaction involving palladacycle with *ortho*-substituted phenyl iodide.

Now, let us consider a palladacycle which possess a methyl group as substituent on *ortho*-position. **TS(32-33)**, the transition state of the oxidative addition of phenyl iodide to the Pd(II) complex **32**, possesses the higher energy level ($\Delta G = +26.1$ kcal.mol⁻¹) of the red pathway. The energy of this transition state is very close to that has been calculated in the previous case for **TS(25-26)**. On the other side, the transition state **TS(36-37)** of the reductive elimination to form the aryl-aryl bond has a ΔG of +27.8 kcal.mol⁻¹ (more than 9 kcal.mol⁻¹ higher than previously) for transmetalation pathway. Then, in this case, the palladium(IV) pathway is favored.

These outcomes act complementary to those presented by Echavarren *et al.*¹¹ and go further. Now assuming that *ortho*-substituted metalacycles undergoes an oxidative addition to form a Pd(IV) cluster, the question of the total selectivity towards the sp^2 - sp^2 coupling still remains an outstanding issue. A possible rationalization of “*ortho*-effect” is explained in the same publication (Figure 6).

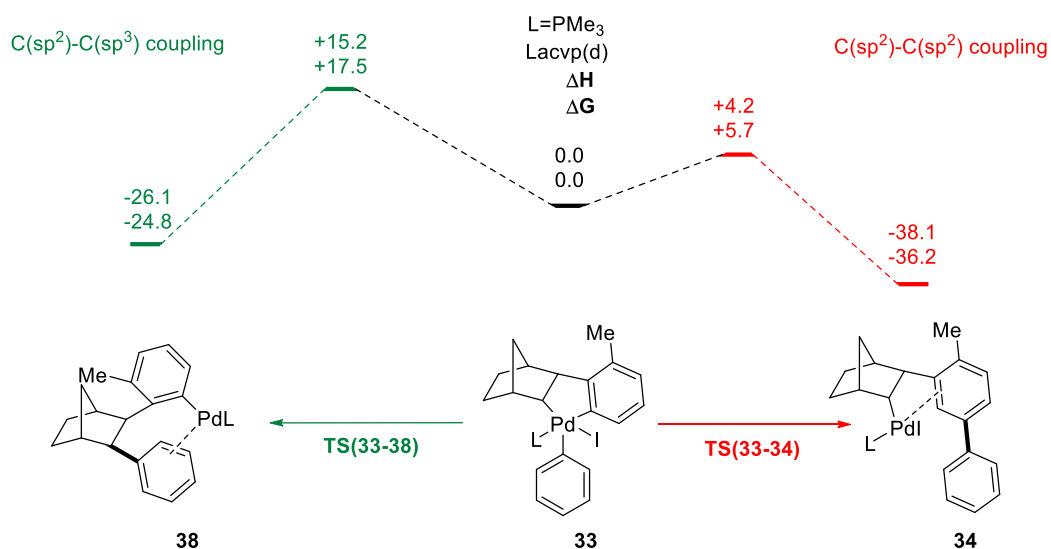


Figure 6 : Selectivity towards aryl-aryl coupling; explanation of the *ortho*-effect.

Calculations have been made for reductive elimination starting from palladium(IV) metalacycle **33**. Aryl-norbornyl coupling is represented in green, while aryl-aryl coupling is depicted in red. The transition state **TS(33-38)** has a higher energy level than **TS(33-34)** ($\Delta\Delta G = 11.8 \text{ kcal.mol}^{-1}$). This huge energetic difference shows why **38** has never been experimentally observed. For sake of comparison, several key intermediates are depicted in figure 7.

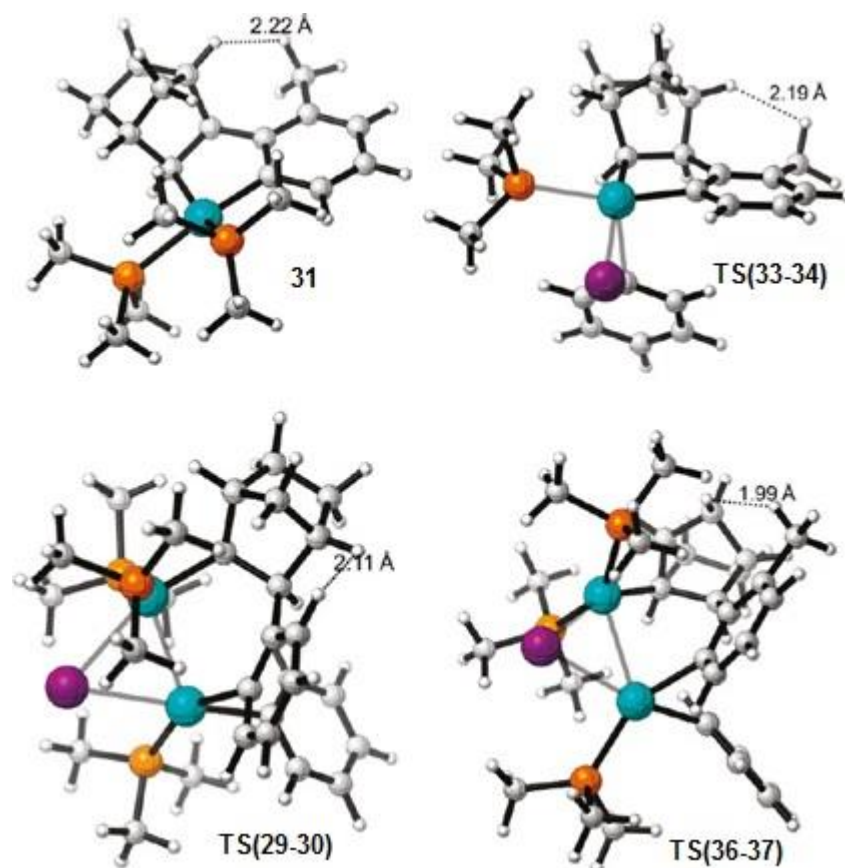
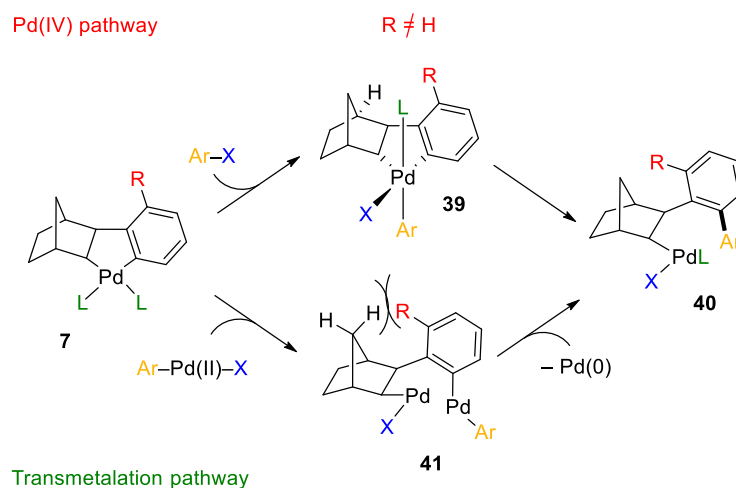


Figure 7 : Modeled structures of intermediates.

On the structure modeled for **31** metalacycle, we can see that all the atoms in the palladium-containing five-membered ring are on the same plane, including the aryl moiety and its methyl substituent. The distance between the hydrogen of the methyl group and the bridgehead hydrogen borne by the norbornyl moiety is 2.22 Å. For the representation of **TS(33-34)**, the planar conformation of the metalacycle remains nearly the same. The distance between the two hydrogens lowers only of 0.03 Å, which means that the steric effect does not have a big impact on the oxidative addition reaction. In the case of **TS(29-30)** and **TS(36-37)**, the insertion of a second palladium atom breaks the planar conformation of the system and induces a rotation of the aryl-norbornyl bond. For the transition state without *ortho*-substituent on aryl moiety **TS(29-30)**, the rotation of the C(sp²)-C(sp³) bond places the *ortho* hydrogen at 2.11 Å of distance from the bridgehead one of norbornene. For **TS(36-37)**, the rotation places the methyl group close to the norbornene upper face and the shortest hydrogen distance is about 1.99 Å. The steric effect is clearly more important in the latter situation and this is the reason why the transmetalation pathway is not favored compared to the Pd(IV) one.

This work is summarized in scheme 6. The presence of an R-substituent in *ortho*-position is very important for the selectivity of the reaction. If R=H, the reaction proceeds by a transmetalation pathway *via* intermediate **41**. However, if R≠H, the preferred pathway goes on through a Pd(IV) crucial intermediate **39** and its geometrical feature fully explain the selectivity in favor of sp^2 - sp^2 coupling (*ortho*-rule).



Scheme 6 : Conclusion of mechanistic studies.

With these results in hand, several chemists worldwide including our group were interested in changing the nature of aryl partners in order to synthesize nitrogen-containing heterocycles¹³ such as carbazoles **42**,¹⁴ phenanthridines **43**^{15,16,17} or dibenzoazepines **44**.¹⁸ (Figure 8)

¹³ a) A. Martins, B. Mariampillai, M. Lautens, *Top. Curr. Chem.* **2010**, 292, 1–33. b) M. Catellani, E. Motti, N. Della Ca', *Acc. Chem. Res.*, **2008**, 41, 1512-1522.

¹⁴ N. Della Ca', G. Sassi, M. Catellani, *Adv. Synth. Catal.*, **2008**, 350, 2179-2182.

¹⁵ a) D. A. Candito, M. Lautens, *Angew. Chem. Int. Ed.*, **2009**, 48, 6713-6716. b) M. Blanchot, D. A. Candito, F. Larnaud, M. Lautens, *Org. Lett.*, **2011**, 13, 1486-1489.

¹⁶ G. Maestri, M.-H. Larraufie, E. Derat, C. Ollivier, L. Fensterbank, E. Lacôte, M. Malacria, *Org. Lett.*, **2010**, 12, 5692-5695.

¹⁷ N. Della Ca', E. Motti, M. Catellani, *Adv. Synth. Catal.*, **2008**, 350, 2513-2516.

¹⁸ For dibenzo[*b,f*]azepine, see: N. Della Ca', G. Maestri, M. Malacria, E. Derat, M. Catellani, *Angew. Chem. Int. Ed.*, **2011**, 50, 12257-12261. For dibenzo[*c,e*]azepines, see: V. Narbonne, P. Retailleau, G. Maestri, M. Malacria, *Org. Lett.*, **2014**, 16, 628-631.

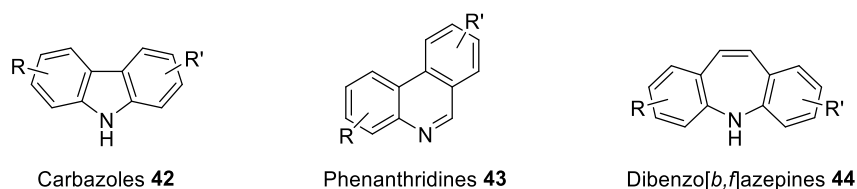


Figure 8 : Structures of nitrogen-containing heterocycles.

Our methodology, described in chapter 1.2.2.2.3, proved its robustness in term of yields and tolerates a lot of different functional groups. Several benzo[*c*]phenanthridines have been synthesized but none of them were reported to be found in natural products. According to the fact that the Institut de Chimie des Substances Naturelles is specialized on the synthesis of natural products, it was a great occasion to test our strategy in order to synthesize natural benzo[*c*]phenanthridines.

1.2. State of art

1.2.1. Biological interest of benzo[*c*]phenanthridines

Benzo[*c*]phenanthridines **46** (Figure 9b) are nitrogen-containing tetracyclic aromatic compounds, derived from the phenanthridine framework **45** (Figure 9a) and they bear a benzo- substituent on the *c*-bond position. These molecules are known since the middle of 19th century.¹⁹ These alkaloids have been isolated from *Papaveraceous* and *Rutaceous* plants during the 20th century. A lot of natural derivatives have been reported, adopting either neutral or iminium forms (Figure 9b and 9c).

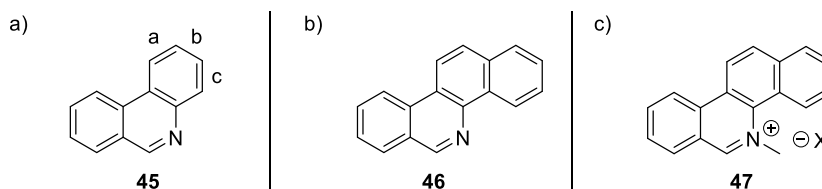


Figure 9: a) Phenanthridine b) Benzo[*c*]phenanthridine ; c) Benzo[*c*]phenanthridinium salt.

¹⁹ QM. Probst, *Ann*, **1839**, 29, 113-131

Some of them present relevant biological activities such as antifungal, antileukemic, antibacterial or antitumor properties.²⁰ For example, nitidine **50** and chelerythrine **51** (Figure 10) possess a good activity against *Mycobacterium tuberculosis* by inhibition of growth superior to 90% at 12.5 µg/mL.^{20a}

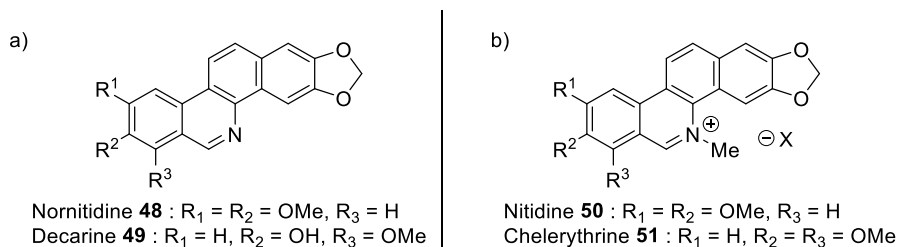


Figure 10 : Examples of bioactives benzo[*c*]phenanthridines.

The difference of biological activities lies in the molecular diversity on the substituents of benzo[*c*]phenanthridine core.

1.2.2. Synthesis

According to the relevant biological activities of benzo[*c*]phenanthridines, numerous syntheses have been reported since their discovery in the 20th century. These syntheses are categorized in two classes: linear and convergent syntheses.

1.2.2.1. Linear synthesis

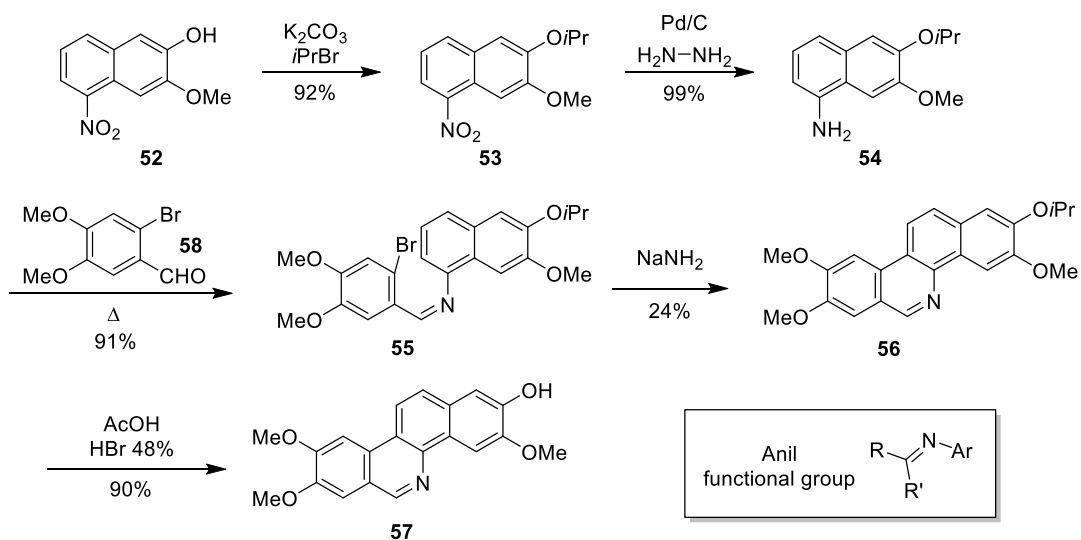
Many different linear syntheses have been employed to form benzo[*c*]phenanthridine derivatives. Nevertheless, these methodologies were tedious and provide the desired products with low overall yields or without diversity on the substituents.²¹ In reason of a very large library of reported synthesis, only two pertinent linear strategies will be showed below.

²⁰ a) T. Ishikawa, *Med. Res. Rev.*, **2001**, *21*, 61-71. b) W. A. Denny, *Curr. Med. Chem.*, **2002**, *9*, 1655-1665. c) P. H. Bernardo, K.-F. Wan, T. Sivaraman, J. Xu, F. K. Moore, A. W. Hung, H. Y. K. Mok, V. C. Yu, C. L. L. Chai, *J. Med. Chem.*, **2008**, *51*, 6699-6710. d) I. Kock, D. Heber, M. Weide, U. Wolschendorf, B. Clement, *J. Med. Chem.*, **2005**, *48*, 2772-2777.

²¹ a) Z. Dvorák, V. Kubán, B. Klejdus, J. Hlavác, J. Vicar, J. Ulrichová, V. Simánek, *Heterocycles*, **2006**, *68*, 2403-2422. b) H. Takashi, *Heterocycles*, **2005**, *65*, 697-713. c) I. Tsutomu, I. Hisashi, *Heterocycles*, **1999**, *50*, 627-639. d) L. Sripada, J. A. Teske, A. Deiters, *Org. Biomol. Chem.*, **2008**, *6*, 263-265.

1.2.2.1.1 Total synthesis of benzo[*c*]phenanthridines by Stermitz et al.

In 1974, Stermitz and coworkers published one of the first syntheses of norfagarone²² **57** in 6 steps with an overall yield of 18% starting from nitronaphtalene derivative **52**. (Scheme 7)

Scheme 7 : Stermitz *et al.* strategy.

²² a) F. R. Stermitz, J. P. Gillespie, L. G. Amoros, R. Romero, T. A. Stermitz, K. A. Larson, S. Earl, J. E. Ogg *J. Med. Chem.*, **1975**, 18, 708-713. b) J. P. Gillespie, L. G. Amoros, F. R. Stermitz, *J. Org. Chem.*, **1974**, 39, 3239-3241

The synthesis of **52** in a pure manner was delicate because of the non-selectivity of the nitration reaction with nitric acid. Furthermore, the key step of the reaction is the cyclisation of imine **55** using two equivalents of sodium amide. The first one attacks the imine group of to form an aminoamide. The negative charge of this intermediate is stabilized by the aryl substituent on the nitrogen. The second equivalent is used to form a benzyne intermediate. A rearrangement of the aminoamide leads to a nucleophilic carbon in the *ortho*-position of the naphthyl moiety, which can attack benzyne and creates a new C-C bond.²³ The protonation and rearomatization steps occur and a sodium amide molecule is released. Despite the beauty of this key-step, authors isolated the desired product with a poor 24% yield only. Later, this strategy has been extended to synthesize other benzo[c]phenanthridines.²⁴ Nevertheless, the starting material and protecting groups had to be modified depending on the nature of the desired product.

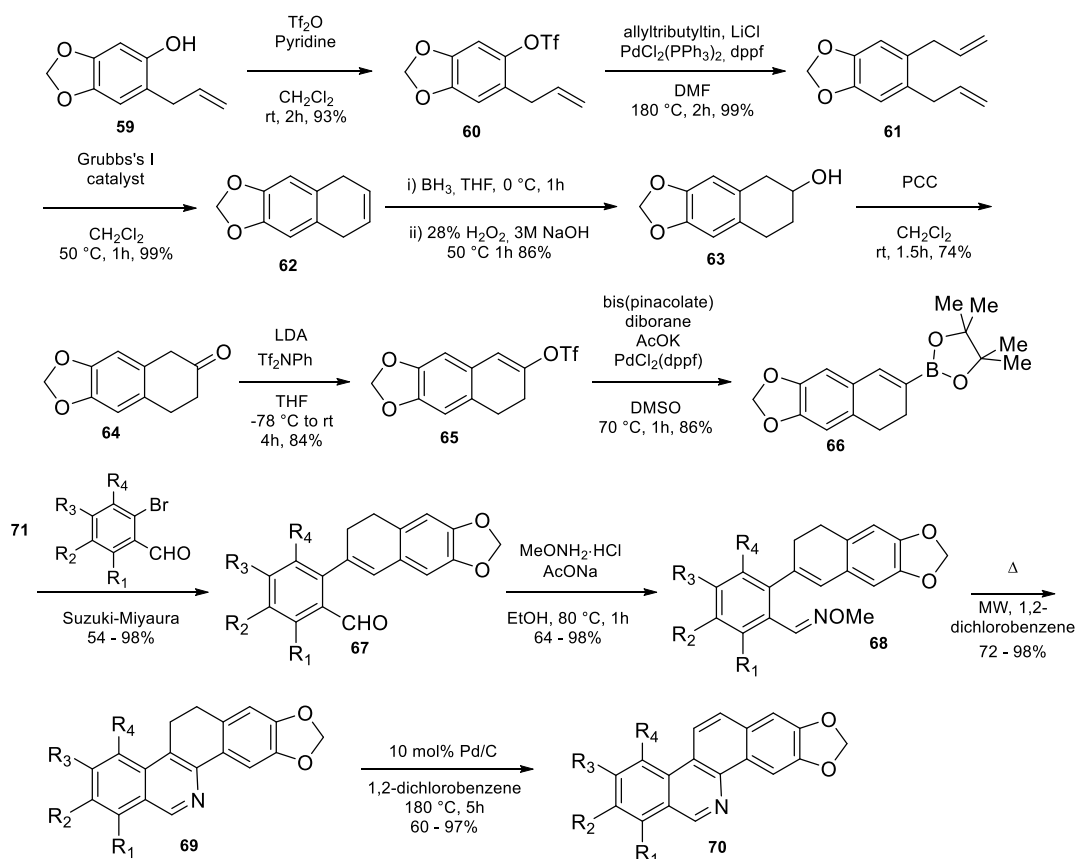
1.2.2.1.2. Total synthesis of benzo[c]phenanthridines by Ishihara et al.

In 2011, Ishihara and coworkers reported this linear total synthesis of benzo[c]phenanthridines in 11 steps.²⁵ The details of their strategy are described in scheme 8.

²³ S. V. Kessar, R. Gopal, M. Singh, *Tetrahedron*, **1973**, 29, 167-175. S. V. Kessar, D. Pal, M. Singh, *Tetrahedron*, **1973**, 29, 177-184.

²⁴ a) Nakanishi, T.; Suzuki, M. *Org. Lett.* **1999**, 1, 985-988. b) T. Harayama, H. Akamatsu, K. Okamura, T. Miyagoe, T. Akiyama, H. Abe, Y. Takeuchi, *Journal of the Chemical Society, Perkin Transactions* **2001**, 1, 523-528. c) H. Abe, N. Kobayashi, Y. Takeuchi, T. Harayama, *Heterocycles* **2010**, 80, 873-877. d) R. Beugelmans, J. Chastanet, H. Ginsburg, L. Quintero-Cortes, G. Roussi, *J. Org. Chem.* **1985**, 50, 4933-4938. e) S. V. Kessar, Y. P. Gupta, P. Balakrishnan, K. K. Sawal, T. Mohammad, M. Dutt, *J. Org. Chem.* **1988**, 53, 1708-1713. f) P. Ramani, G. Fontana, *Tetrahedron Letters* **2008**, 49, 5262-5264.

²⁵ Y. Ishihara, S. Azuma, T. Choshi, K. Kohno, K. Ono, H. Tsutsumi, T. Ishizu, S. Hibino, *Tetrahedron*, **2011**, 67, 1320-1333.

Scheme 8 : Synthesis of benzo[*c*]phenanthridines by Ishihara *et al.*.

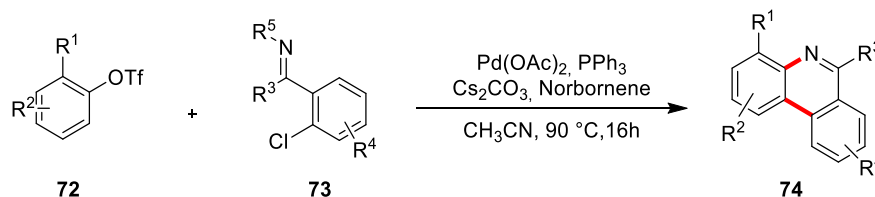
This strategy allowed to access eight natural and unnatural compounds with good overall yields between 18 and 39% depending of the different groups R^1 - R^4 . This functional-group tolerant synthesis uses two key-steps. The Suzuki-Miyaura couplings between boronate **66** and bromobenzaldehyde **71** were accomplished with moderate to excellent yields. The intramolecular, micro-wave assisted, aza-cyclisation affords dihydrophenanthridines **69** with comfortable yields. Pentacyclic molecule **69** undergoes oxidative dehydrogenation to get desired product **70** with good to excellent yields. However, the synthesis of the boronate **66** is rather long and limits the number of analogues which could be obtained.

1.2.2.2. Convergent synthesis

1.1.2.2.1. Synthesis of phenanthridines by Lautens *et al.*

A concise synthesis of phenanthridines from aryl triflates **72** and protected *o*-chlorobenzylimines **73** has been reported by Lautens and coworkers.¹⁵ The key step of this

strategy is the domino direct arylation followed by *N*-arylation in a one pot procedure (Scheme 9).

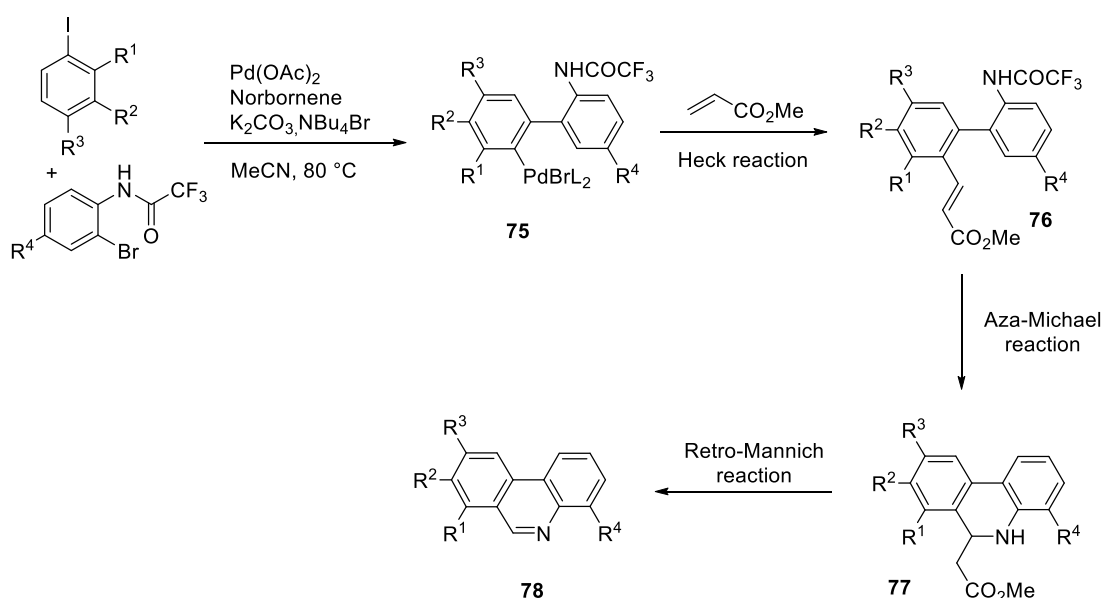


Scheme 9 : Lautens' approach.

This methodology gives phenanthridines¹⁵ **74** with yields between 38 and 85% and tolerates several functional groups such as halides, trifluoromethyl or morpholine moiety. However the protected imines are not very stable and uneasy to handle. The catalytic charge of palladium is up to 20 mol%.

1.2.2.2.2. Synthesis of phenanthridines by Catellani *et al.*

In 2010, Catellani reported a three-component reaction catalyzed by palladium/norbornene in order to synthesize phenanthridines in a one-pot procedure.²⁶ Her strategy is reported in scheme 10.



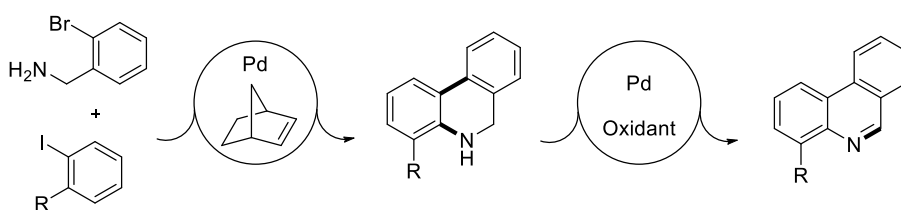
Scheme 10 : Catellani's methodology.

²⁶ N. Della Ca', E. Motti, A. Mega, M. Catellani, *Adv. Synth. Catal.*, **2012**, 352, 1451-1454.

The reaction starts with a classical Pd/Norbornene coupling to form the aryl-aryl bond and affords **75** after norbornene extrusion. This complex undergoes a Heck-type reaction with methyl acrylate to give **76**. The electron-poor olefin is attacked by the nitrogen to form the aza-Michael product **77**. This tricyclic compound easily realizes a retro-Mannich reaction and provides the desired phenanthridine **78**. This methodology affords differently substituted phenanthridines with good to excellent yields between 49 and 93%. However, this process is not very atom-economic. The use of methyl acrylate to insert only one carbon into the phenanthridine structure is not very elegant.

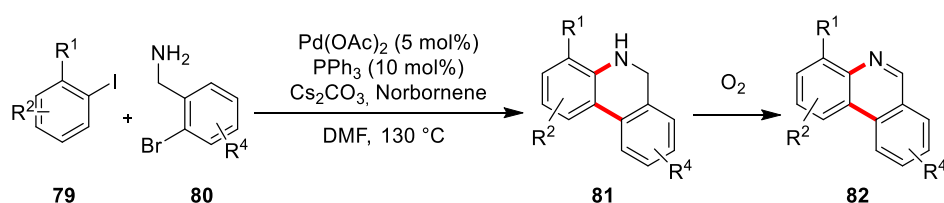
1.2.2.2.3. Synthesis of phenanthridines by Malacria *et al.*

Malacria's group reported a method for the synthesis of phenanthridines from aryl iodides **79** and *o*-bromobenzylamines **80** which uses palladium/norbornene dual catalysis.¹⁶ The general idea was to realize the synthesis of the phenanthridine core in a one-pot procedure without protecting groups. They reasoned that in presence of palladium, the creation of C-C and C-N bonds could be achieved in the first place and then the catalyst could realize an oxidative dehydrogenation in presence of an oxidant to afford the desired aromatic heterocycle (Scheme 11).



Scheme 11 : Envisaged strategy.

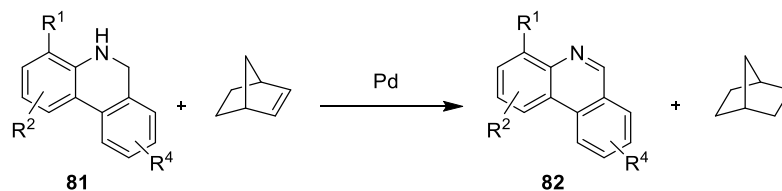
The proposed sequence uses the Catellani reaction to create C(sp²)-C(sp²) bond and ends via an intramolecular amination to obtain the dihydrophenanthridine **81**. The oxidative dehydrogenation of the C-N bond to form **82** is realized by adding a balloon of dioxygen after full conversion of the starting material (Scheme 12).



Scheme 12 : Malacria's approach.

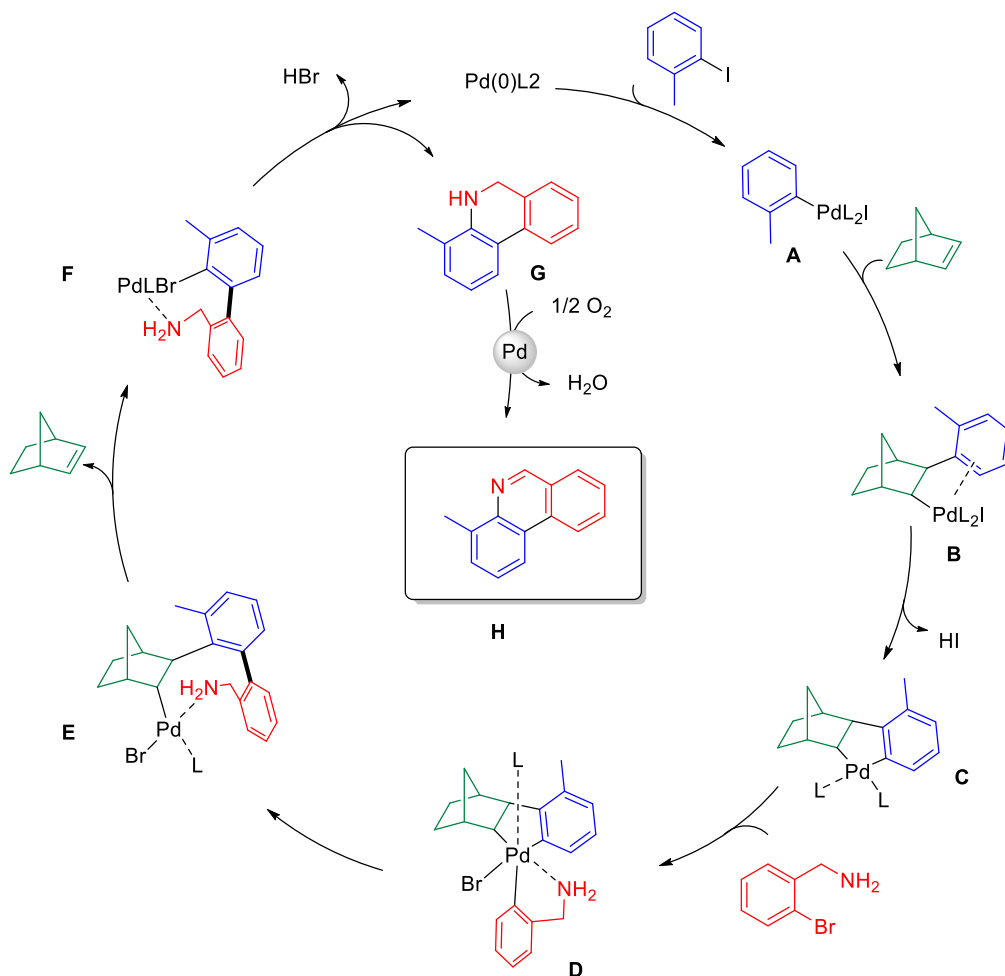
This protocol succeeded and provided differently substituted phenanthridines with yields between 22 and 97% and did not require a prefunctionalization of substrates or the presence of protecting groups.

During optimization of the oxidative dehydrogenation step, they found that when the palladium catalyst was missing, the transformation of **81** to **82** occurs but more slowly. This observation confirmed that palladium plays an essential role during this process. They also noticed that adding an excess of norbornene at 90% of conversion of starting material led to obtain the phenanthridine product (65% yield) without presence of dioxygen. This suggests that in presence of palladium catalyst, norbornene could act as sacrificial olefin and plays the role of formal “H₂” acceptor (Scheme 13).



Scheme 13 : Norbornene as sacrificial olefin.

The catalytic cycle is represented on scheme 14. It starts with the oxidative addition of palladium(0) formed *in situ* on the Ar-I bond to give intermediate **A** followed by the insertion of norbornene into the Ar-Pd bond to generate **B**. Arene C-H activation provides the palladacycle **C** which react with the bromobenzylamine to give Pd(IV) intermediate **D**. A reductive elimination step creates the aryl-aryl bond to form **E**.



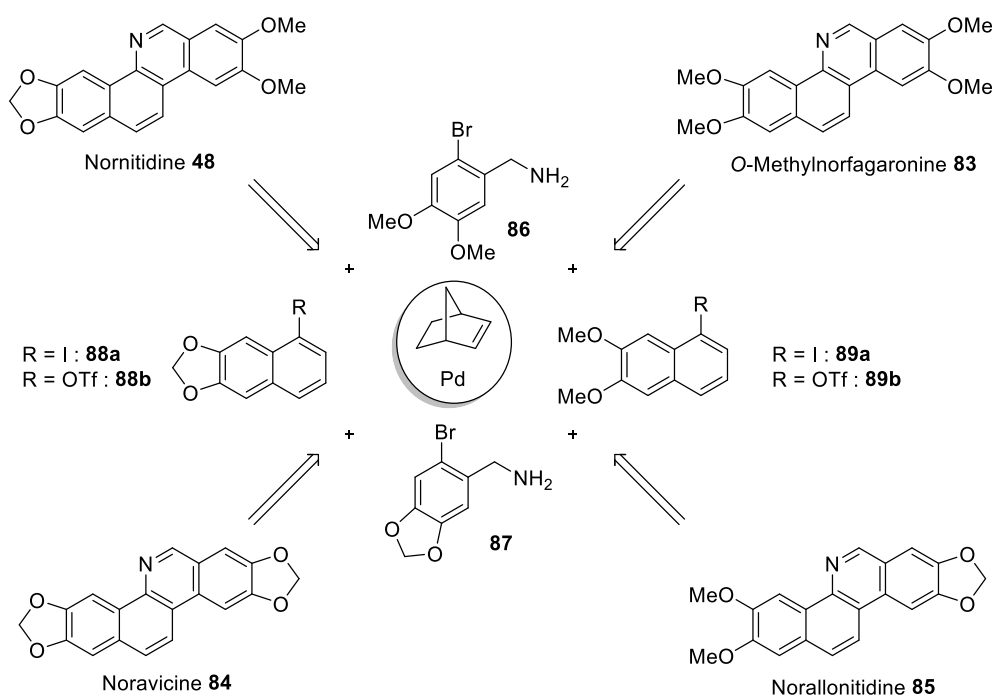
Scheme 14 : Catalytic cycle of formation of phenanthridines.

The steric hindrance of **E** forces norbornene to be eliminated. Complex **F** undergoes the intramolecular amination to afford dihydrophenanthridine **G**. Adding dioxygen after full conversion of aryl iodide in presence of $\text{Pd}(\text{II})$ leads to the catalytic dehydrogenation reaction and form the desired product **H** but also water as coproduct.

1.3 Results and discussion

1.3.1. Objectives of the project

The purpose of the present work,²⁷ realized in collaboration with Dr. Tatiana Cañeque-Cobo, Filipe Gomes and Vanessa Narbonne, is to synthesize four natural benzo[*c*]phenanthridines: Nornitidine **48**, *O*-Methylnorfagaronine **83**, Noravicine **84** and Norallonitidine **85** by the convergent strategy reported by our group in 2010. These natural alkaloids could be obtained by a palladium/norbornene coupling followed by a dehydrogenation step and starting from two *o*-bromobenzylamines **86** and **87** and two iodonaphthalene derivatives **88a** and **89a**. (Scheme 15) However, the limited stability of the two iodonaphthalene derivatives **88a** and **89a** prevents their uses as reagents in our cascade. Lautens and coworkers showed good results with triflates on this type of palladium catalyzed reactions, so we decided to choose to synthesize the **88b** and **89b** instead of the iodide derivatives ones.

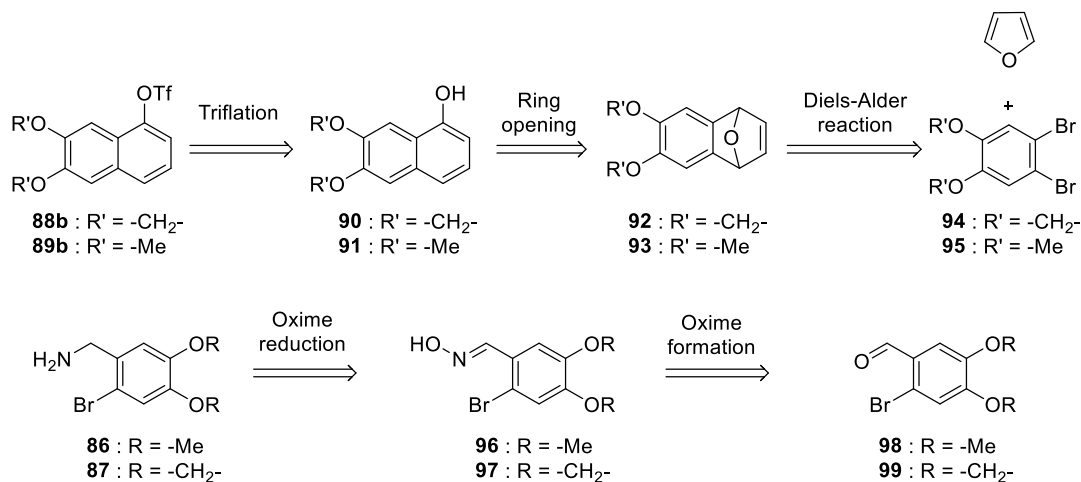


Scheme 15 : Retrosynthetic scheme.

The synthesis of triflates **88b** and **89b** could be realized in three steps by following Lautens method.^{15a} (Scheme 16) Triflates coupling partners **88b** and **89b** could be obtained by

²⁷ P.-A. Deyris, T. Cañeque-Cobo, F. Gomes, V. Narbonne, G. Maestri, M. Malacria, *Heterocycles*, **2014**, *88*, 807-815

the triflation of the corresponding alcohols **90** and **91**. Naphtol derivatives could be obtained by ring-opening of **92** and **93**. The oxygen-containing tricycle could be synthesized from dibromoaryl **94** and **95** by a Diels-Alder cycloaddition with furan.



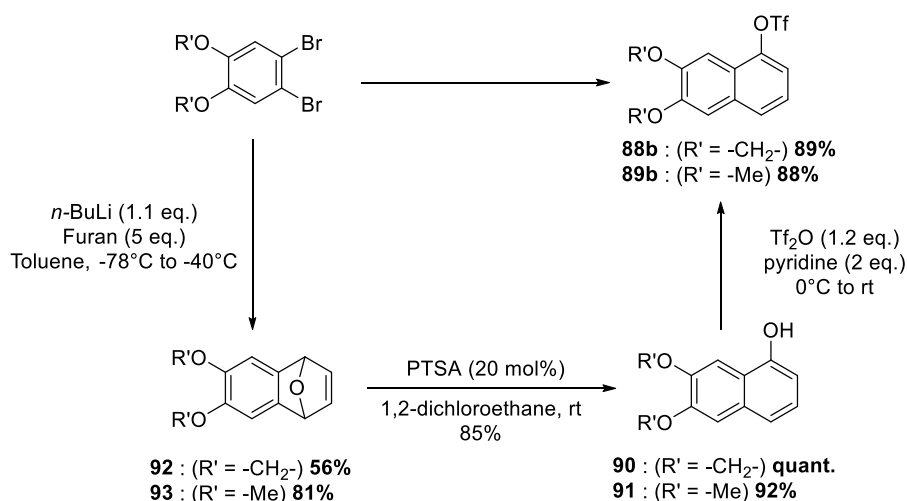
Scheme 16 : Retro-synthetic scheme for coupling partners.

In parallel, the *o*-bromobenzylamines **86** and **86** could be easily formed by the reduction of the corresponding oximes **96** and **97**. These oximes could be prepared from the condensation of hydroxylamine on commercially available *o*-bromobenzaldehydes **98** and **99**.

1.3.2. Synthesis of the coupling partners

1.3.2.1. Synthesis of naphthyl triflates

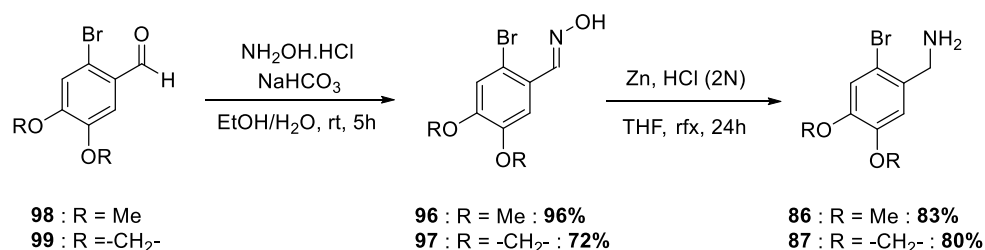
The synthesis starts with the Diels-Alder reaction involving dibromobenzenes **94** and **95** and furan (Scheme 17). The action of *n*-butyl lithium generates benzyne intermediate that can play the role of dienophile and form epoxynaphthalenes **92** and **93** with 56 and 81% yields respectively. Ring-opening step proceeds via the action of *p*-toluenesulfonic acid at 20 mol% in 1,2-dichloroethane to provide naphthalenols **90** and **91** with quantitative and 92% yield respectively. The triflation of alcohols using triflic anhydride in presence of pyridine delivers **88b** and **89b** with 89 and 88% yields.



Scheme 17 : Synthesis of naphtyltriflates.

1.3.2.2. Synthesis of *o*-bromobenzylamines

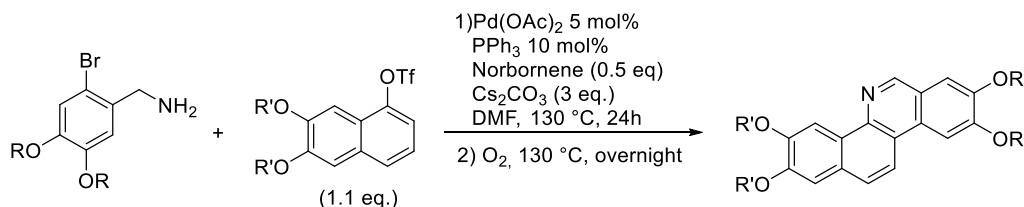
In parallel, we realized the synthesis of the second coupling partner (Scheme 18). The *o*-bromobenzaldehyde derivatives **98** and **99** react with hydroxylamine hydrochloride in presence of sodium bicarbonate in a mixture of water/ethanol to give the corresponding oximes **96** and **97** in 96 and 72% yield respectively.

Scheme 18 : Synthesis of *o*-bromobenzylamines.

These oximes were reduced by addition of solid zinc in a hydrochloric acid solution diluted in THF. After one day at reflux, *o*-bromobenzylamines **86** and **87** were obtained in 83 and 80% yield respectively after purification.

1.3.3 Coupling step

Having the two partners in hands, we were able to try the first attempt of the coupling reaction. We performed the reaction using conditions previously optimized in our group. (Scheme 19).



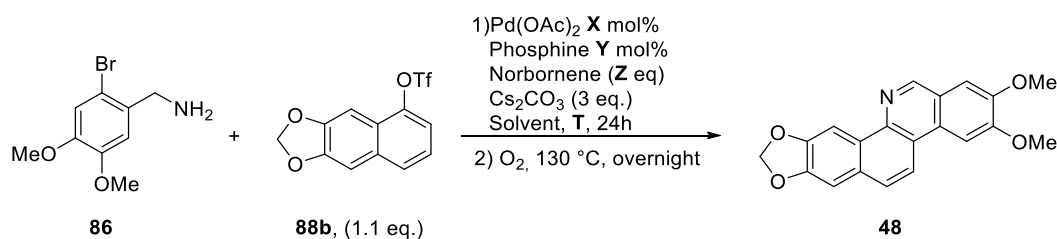
Scheme 19 : First attempt of coupling reaction.

The first trial was realized using 5 mol% of palladium catalyst, 10 mol% of triphenylphosphine and 50 mol% of norbornene in DMF. A balloon of dioxygen was added after 24h at reflux to operate the oxidative dehydrogenation and the solution was stirred overnight. The yields after purification are reported on table 1.

Compound	R	R'	Isolated Yield
Nornitidine 48	-Me	-CH ₂ -	18%
<i>O</i> -Methylnorfagaronine 83	-Me	-Me	63%
Noravicine 84	-CH ₂ -	-CH ₂ -	n.d.
Norallonitidine 85	-CH ₂ -	-Me	17%

Table 1 : First results on coupling reaction.

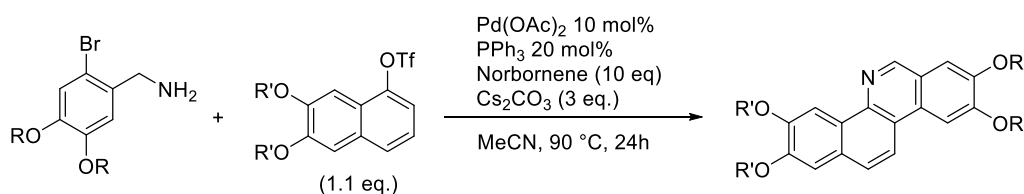
We were delighted to observe the formation of **83** in 63% yield considering that an electron-rich bromobenzylamine was not the best candidate to provide an oxidative addition on Pd(II) metallacycle. However **48** and **85** were isolated in poor 18 and 17% yields respectively while **84** was not even observed. A short optimization of conditions was performed on the synthesis of **48** varying reaction parameters (Table 2).



Entry	X (mol%)	Phosphine (Y mol%)	Z (eq.)	Solvent	T (°C)	Yield
1 ^a	5	PPh ₃ (10 mol%)	0.5	DMF	130	18%
2 ^a	5	PPh ₃ (10 mol%)	0.5	MeCN	90	22%
3 ^a	5	TFP (10 mol%)	0.5	MeCN	90	16%
4 ^a	10	PPh ₃ (20 mol%)	0.5	MeCN	90	29%
5 ^b	10	PPh ₃ (20 mol%)	10	MeCN	90	72%

Table 2 : Optimization of the reaction conditions for the synthesis of **48**. ^a: reaction has been performed with 3 eq. of Cs_2CO_3 during 24h before adding a balloon of dioxygen. ^b: Reaction performed with 3 eq. of Cs_2CO_3 during 24h.

Decreasing the temperature to 90 °C and changing the solvent to MeCN increased the yield by 4% (Table 2, Entries 1&2). Trifurylphosphine seems to be a less efficient ligand compared to triphenylphosphine (Table 2, Entry 3). When the catalyst charge is doubled, we obtain a yield of 29% (Table 2, Entry 4). We then thought that the reason of the poor yields observed for the last three products was due to the partial decomposition of their acetal groups. Oxidative dehydrogenation is a useful and atom-economic process to oxidize C-N bond into C=N bond but it forms water as coproduct. Water at 90 °C is able to transform acetals into the corresponding diols and thus decreases significantly the yields of the reaction. The presence of water is clearly a problem that we wanted to bypass. According to the observations presented in previous work by Malacria *et al.*,¹⁶ norbornene can play the role of an acceptor during oxidative dehydrogenation step. We showed that our hypothesis was true by performing the reaction with 10 eq. of norbornene (Table 2, Entry 5). The pentacyclic product **48** has been obtained with a comfortable 72% yield. Encouraged by these results, we applied these conditions (Scheme 20) to the synthesis of the other phenanthridines.



Scheme 20 : Optimized reaction conditions.

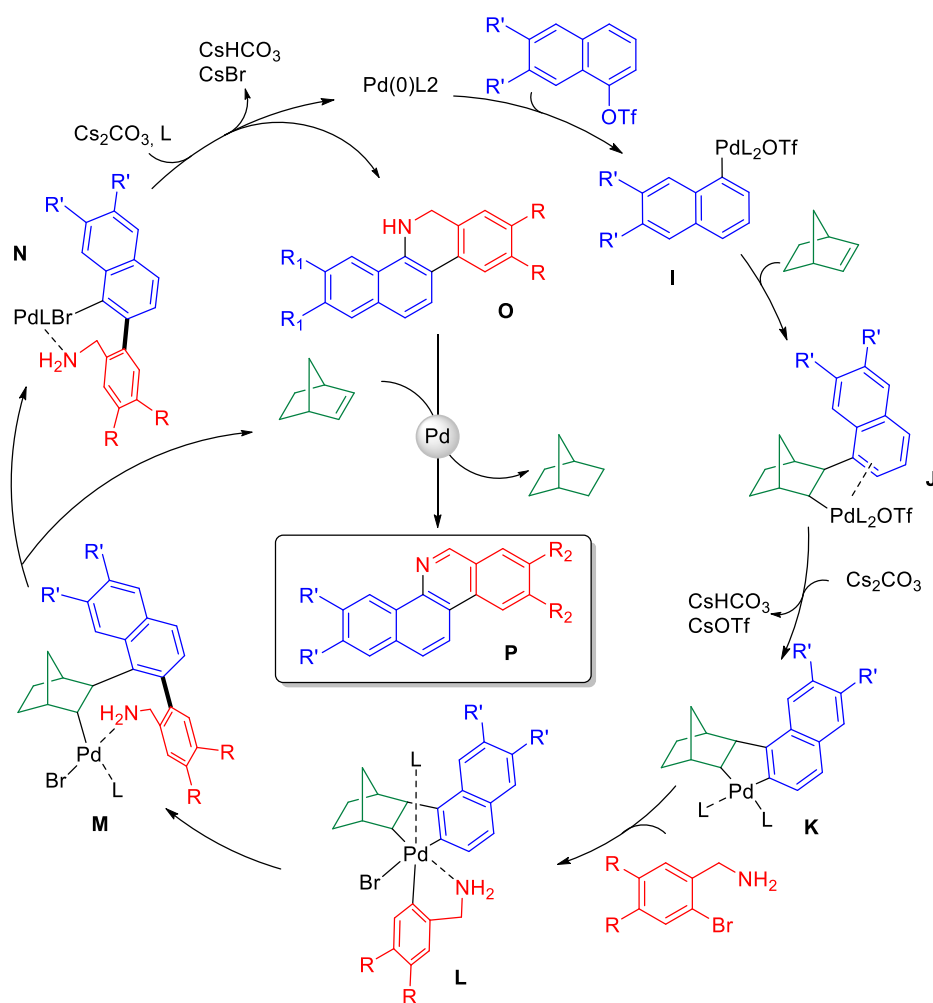
The results of the coupling step are reported on table 3. We were surprised to observe an increase of yields for **48** and **85** up to 72% and remarkable overall yields of 36 and 37% respectively. Regarding the first attempts with which we could not observe the presence of this alkaloid, we were excited for the yield of **84** (74%).

Compound	R	R'	Isolated Yield	Overall Yield
Nornitidine 48	-Me	-CH ₂ -	72%	36%
<i>O</i> -Methylnorfagaronine 83	-Me	-Me	64%	42%
Noravicine 84	-CH ₂ -	-CH ₂ -	74%	37%
Norallonitidine 85	-CH ₂ -	-Me	60%	35%

Table 3 : Coupling step with optimized conditions.

We completed the total synthesis of Noravicine **84** with 37% overall yield. Concerning *O*-Methylnorfagaronine **83**, the isolated yields of the coupling step are pretty the same and led to obtain the tetracyclic molecule with comfortable 42% overall yield. It seems like our hypothesis concerning the role of water in the deprotection of acetals was confirmed with these results.

Previous computational and experimental studies let us consider the mechanism depicted on scheme 21.



Scheme 21 : Proposed reaction mechanism.

The Pd(0) catalyst generated *in situ* undergoes oxidative addition by the naphthyl triflate and gives Pd(II) intermediate **I**. Insertion of norbornene into the Pd-C bond leads to intermediate **J** which is followed by the C-H activation on the *ortho* position of naphthyl moiety to give palladacycle **K**. This intermediate undergoes another oxidative addition of *o*-bromobenzylamine to provide the Pd(IV) intermediate **L**. The formation of the aryl-aryl bond is created by a reductive elimination step assisted by the primary amine (Intermediate **M**). Steric hinderance favors the extrusion of norbornene and form the complex **N** which is suitable to a Buchwald/Hartwig intramolecular amination. The creation of the C-N bond provides benzo[*c*]dihydrophenanthridine **O** and regenerates the Pd(0) catalyst. The corresponding phenanthridine **P** was obtained thanks to the excess of norbornene, which acts as sacrificial olefin. In presence of a palladium catalyst, the two hydrogen atoms on the HC-NH group can be formally transferred to an acceptor and form the desired product and norbornane as coproduct. The latter can be easily removed by vacuum.

1.4. Conclusion

By introducing an excess of norbornene and removing dioxygen, we have been able to exploit the dual nature of this olefin. In one side, it played the role of the co-catalyst of the coupling reaction. On the other hand, it acted as sacrificial olefin in a sequential palladium catalyzed dehydrogenation.

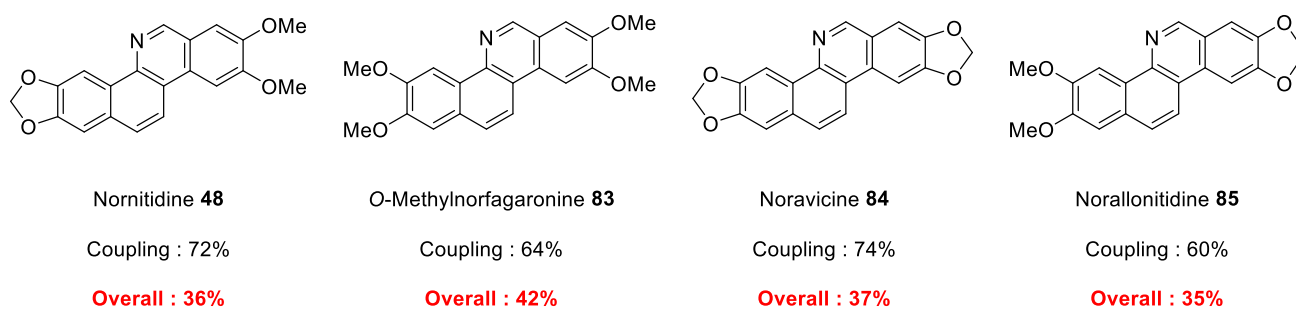


Figure 11 : Summary

Eventually, we achieved the total synthesis of four natural products in four steps only starting from four commercially available reagents. Overall yields ranged from 35 to 42% (Figure 11). In the same time we demonstrated the feasibility of our method towards the total synthesis of biologically relevant products.

SUPPORTING INFORMATION – PART 1

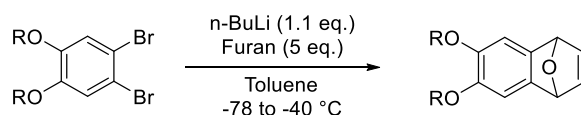
1.5. Supporting Information

1.5.1. General remarks

Reagents were obtained from commercial sources and used as received. **88b-89b**¹⁵ and **86-87**²⁸ were prepared according to reported procedures. Solvents were dried using microwave activated 3 Å molecular sieves, degassed by bubbling argon for 30 minutes and stored under an inert atmosphere. Reactions were carried out under argon using standard Schlenk technique. Flash column chromatography was performed on Merck Geduran SI 60 Å silica gel (40–63 μm) and thin-layer chromatography on Merck 60F254 plates. IR spectra were recorded with a PerkinElmer Spectrum 100 FT-IR Spectrometer. ¹H NMR and ¹³C NMR spectra were recorded in DMSO-*d*⁶ and chloroform-*d*³ on a Bruker 300 AVANCE spectrometer fitted with a QNP probehead at 300.1 and 75.4 MHz respectively, using the solvent as internal standard (7.26 ppm for ¹H NMR and 77.0 ppm for ¹³C NMR for chloroform and 2.50 ppm for ¹H NMR and 39.51 ppm for ¹³C NMR for DMSO). The reported assignments are based on decoupling, COSY, NOESY, HMBC, HSQC correlation experiments. Exact masses were recorded on a LCT Premier XE (Waters) equipped with an ESI ionization source and a TOF detector.

1.5.2. General procedures

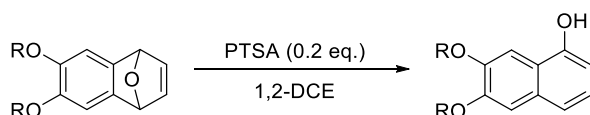
General procedure 1 (GP1): Synthesis of epoxynaphthalenes from corresponding dibromobenzenes.



A dried round-bottom flask was charged with the corresponding dibromoaryl (16.89 mmol, 1 eq) and furane (84.47 mmol, 5 eq.) in dry toluene (50 ml) under argon atmosphere. The solution was cooled at -78 °C and *n*-BuLi 1.6 M in THF (18.58 mmol, 1.1 eq.) was added dropwise to the solution. After complete addition, the solution was warmed up to -40°C and extracted with EtOAc (3x20 ml), dried over magnesium sulfate and concentrated under vacuum. The residue was purified by chromatography column (EtOAc/heptane).

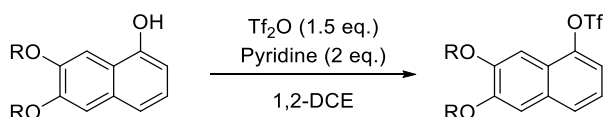
General procedure 2 (GP2): Synthesis of alcohols from corresponding epoxynaphthalenes.

²⁸ B. D. Chapsal, I. Ojima, *Organic. Lett.* 2006, **8**, 1395-1398.



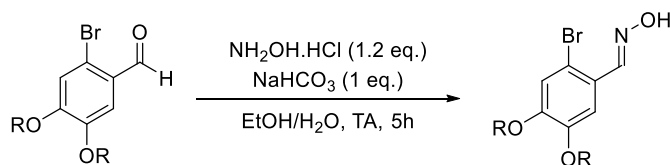
To a solution of the corresponding epoxy naphthalene (1.47 mmol) in DCE (10 ml) was added *p*-toluenesulfonic acid (0.29 mmol, 0.2 eq.) in DCE (2 ml). The reaction mixture was stirred at r.t overnight. The mixture was diluted with DCM, washed with water and brine, dried over magnesium sulfate and concentrated under vacuum. The products were used for the next step without further purification.

General procedure 3 (GP3): Synthesis of triflates from corresponding alcohols.



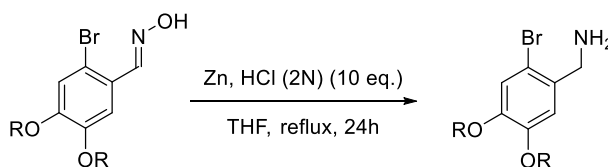
To a solution of the corresponding naphthol (6.86 mmol) and pyridine (13.72 mmol, 2 eq.) in DCM (40 ml) at 0 °C, was slowly added Tf₂O (10.29 mmol, 1.5 eq.). After complete addition the mixture was warmed to rt and stirred until completion (1h). The mixture then was diluted with Et₂O (20 ml), quenched with 10% aq HCl and washed with saturated NaHCO₃ solution and brine. After drying (Mg₂SO₄), the solvent was removed and the residue was purified by chromatography column (EtOAc/heptane) providing the desired product.

General procedure 4 (GP4): Synthesis of *ortho*-bromobenzoyloximes from corresponding aldehydes.



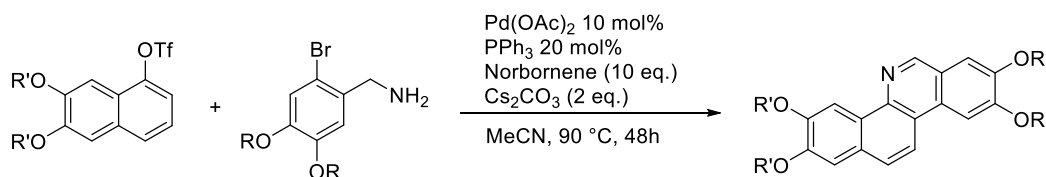
Hydroxylamine hydrochloride (0.775 g, 11.15 mmol, 1.2 eq.) was added to a solution of NaHCO₃ (0.915 g, 10.9 mmol, 1 eq.) in 25 mL of water. The solution was added to a vigorously stirred suspension of bromobenzaldehyde (10.9 mmol; 1 eq.) in EtOH (25 mL). The resulting mixture was stirred for 5h and then left at -20°C overnight. The suspension was filtered, washed with a few mL of cold ethanol and dried under vacuum to give the desired product.

General procedure 5 (GP5): Synthesis of *ortho*-bromobenzylamines from corresponding *ortho*-bromobenzoyloximes.



To a solution of the corresponding hydroxylamine (7 mmol; 1 eq.) in THF (80 mL) was added a 2N solution of HCl (35.3 mL; 70.7 mmol, 10 eq.), followed by zinc (4.62 g, 70.7 mmol, 10 eq.). The mixture was vigorously stirred under reflux for 2.5h until the reaction completed. The reaction mixture was cooled to room temperature, filtered through a celite pad to remove the excess of zinc and condensed under reduce pressure to remove THF. The aqueous layer was extracted with EtOAc (30 mL) and the pH of the aqueous layer was adjusted to >10 by addition of saturated ammonia solution then extracted with EtOAc (3x 30mL). The organic layers were combined and dried over anhydrous K_2CO_3 , filtered and evaporated to give the crude which was purified by flash column chromatography on silica gel (eluent: EtOAc/2% Et_3N).

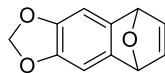
General procedure 6 (GP6): Coupling reactions between *ortho*-bromobenzylamines and naphthalene triflates.



To a Schlenk-type flask were added under argon Cs_2CO_3 (170 mg, 0.52 mmol, 2.0 eq.), triphenylphosphine (7 mg, 0.026 mmol, 0.10 eq.), a solution of MeCN (6 mL) containing the aryl triflate (0.29 mmol, 1.1 eq.), the 2-bromobenzylamine (0.26 mmol, 1 eq) and norbornene (245 mg, 2.6 mmol, 10 eq.) and $Pd(OAc)_2$ (6 mg, 0.026 mmol, 0.10 eq.). The same procedure could be adopted using 2-bromobenzylamines hydrochloric salts by adding 1 more equivalent of base in the reaction vessel. The resulting suspension was stirred with a magnetic bar at 130 °C until visible formation of palladium black (usually 48 h). Consumption of starting materials was assessed by 1H NMR. The mixture was then allowed to cool to room temperature, diluted with EtOAc (30 mL), washed with a saturated K_2CO_3 solution (3 × 30 mL) and dried over $MgSO_4$. The solvent was removed under reduced pressure and the products were isolated by flash column chromatography on silica gel.

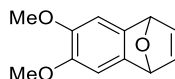
1.5.3. Coupling of ortho-substituted aryl iodides and ortho-bromobenzylamines

1.5.3.1. Preparation of the epoxynaphthalenes

5,8-dihydro-5,8-epoxynaphto[2,3-d][1,3]dioxo,¹⁵ **92**

Following **GP1**, from 5,6-dibromo-1,3-benzodioxole (4.73 g) were obtained 3.17 g of **92** (81% yield) as a white solid which was shown to be spectroscopically identical to the material described in the literature.

¹H-NMR (300 MHz, CDCl₃): δ (ppm) 7.07 (s, 2H), 6.86 (s, 2H), 5.96 (d, 1H, *J* = 1.4 Hz), 5.91 (d, 1H, *J* = 1.4 Hz), 5.66 (s, 2H).

1,4-dihydro-6,7-dimethoxy-1,4-epoxynaphthalene²⁹, **93**

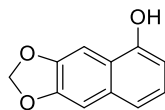
Following **GP1**, from 4,5-dibromoveratrol (5 g), 1.91 g of **93** (56% yield) were obtained as a white solid which was shown to be spectroscopically identical to the material described in the literature.

¹H-NMR (500 MHz, CDCl₃): δ (ppm) 7.01 (s, 1H), 6.94 (s, 1H), 5.65 (s, 1H), 3.82 (s, 6H).

²⁹ M. Lautens, K. Fagnou, D. Yang, *J. Am. Chem. Soc.* **2003**, *125*, 14884-14892

1.5.3.2. Preparation of the naphthyl alcohols

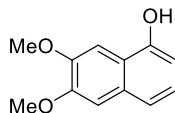
Benzo[*f*][1,3]benzodioxol-5-ol,¹⁵ **90**



Following **GP2**, from **92** (0.28 g), was obtained **90** as a white solid in quantitative yield. The product was shown to be spectroscopically identical to the material described in the literature.

¹H-NMR (300 MHz, CDCl₃) δ (ppm) 7.50 (s, 1H), 7.32-7.25 (m, 1H), 7.16 (t, 1H, *J* = 7.8 Hz), 7.11 (s, 1H), 6.70 (d, 1H, *J* = 7.4 Hz), 6.05 (s, 2H), 5.04 (s, 1H).

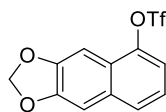
6,7-Dimethoxynaphthalen-1-ol,³⁰ **91**



Following **GP2**, from **93** (0.3 g), was obtained **91** as a white solid with 92% yield. The product was shown to be spectroscopically identical to the material described in the literature.

¹H-NMR (500 MHz, CDCl₃) δ (ppm) 7.44 (s, 1H), 7.28 (d, 1H, *J* = 8.0 Hz), 7.14 (apt, 1H, *J* = 7.4, 8.0 Hz), 7.08 (s, 1H), 6.68 (d, 1H, *J* = 7.4 Hz), 5.11 (s, 1H), 4.00 (s, 3H), 3.98 (s, 3H).

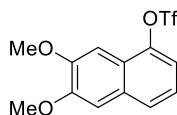
³⁰ M. Ballantine, M. L. Menard, Tam, W. *J. Org. Chem.* 2009, **74**, 7570-7573.

*1.5.3.3. Preparation of the naphthyl triflates***Naphtho[2,3-d][1,3]dioxol-5-yltrifluoromethanesulfonate,²⁸ 88b**

Following **GP3**, from **90** (1.29 g), were obtained 2.19 g (89% yield) of the product as a pale yellow solid which was shown to be spectroscopically identical to the material described.

¹H-NMR (500 MHz, CDCl₃) δ (ppm) 7.66 (dd, 1H, *J* = 3.6, 5.5 Hz), 7.33-7.31 (m, 3H), 7.16 (s, 1H), 6.11 (s, 2H).

¹³C-NMR (75 MHz, CDCl₃) δ (ppm) 149.4, 148.8, 145.3, 132.5, 127.3, 123.8, 123.5, 118.7 (c, *J* = 320.5 Hz), 116.4, 104.7, 101.7, 97.4.

6,7-Dimethoxynaphthalen-1-yltrifluoromethanesulfonate, 89b

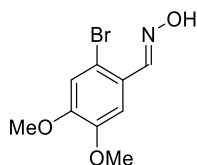
Following **GP3**, from **11** (1.40 g) were obtained 2.04 g (89% yield) of the product as a pale yellow solid.

¹H-NMR (500 MHz, CDCl₃) δ (ppm) 7.67 (dd, 1H, *J* = 1.6, 6.9 Hz), 7.32-7.28 (m, 3H), 7.14 (s, 1H), 4.00 (s, 3H), 3.99 (s, 3H).

¹³C-NMR (75 MHz, CDCl₃) δ (ppm) 151.1, 150.5, 144.7, 131.1, 126.6, 123.5, 122.0, 118.7 (c, *J* = 319.8 Hz), 116.4, 106.4, 99.3, 56.0, 55.9.

1.5.3.4. Preparation of the bromobenzyloximes

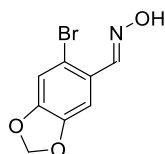
2-bromo-4,5-dimethoxy-benzaldehyde oxime, 28 96



Following **GP4**, from 2-bromo-4,5-dimethoxy-benzaldehyde (2.67 g), was obtained 2.72 g (96% yield) of the product as white crystals which was shown to be spectroscopically identical to the material described.

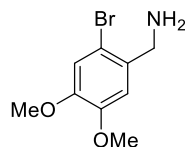
$^1\text{H NMR}$ (300 MHz, $\text{DMSO-}d_6$): δ (ppm) 11.41 (s, 1H), 8.19 (s, 1H), 7.27 (s, 1H), 7.16 (s, 1H), 3.79 (s, 3H), 3.76 (s, 3H).

6-bromo-1,3-benzodioxole-5-carbaldehyde oxime²⁸, 97



Following **GP4**, from 6-bromo-1,3-benzodioxole-5-carbaldehyde (2.50 g), was obtained 1.96 g (72% yield) of the product as white powder which was shown to be spectroscopically identical to the material described.

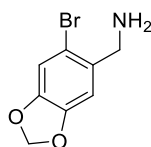
$^1\text{H NMR}$ (300 MHz, CDCl_3): δ (ppm) 8.44 (s, 1H), 7.29 (s, 1H), 7.00 (s, 1H), 6.01 (s, 2H).

*1.5.3.5. Preparation of the bromobenzylamines***2-Bromo-4,5-dimethoxybenzylamine,¹⁹ 86**

Following **GP5**, from **96** (1.82 g), was obtained 1.43 g (83% yield) of the product as white powder which was shown to be spectroscopically identical to the material described.

¹H NMR (300 MHz, CDCl₃): δ (ppm) 6.98 (s, 1H), 6.89 (s, 1H), 3.85-3.81 (m, 8H).

¹³C NMR (75 MHz, CDCl₃): δ (ppm) 148.5, 148.4, 134.2, 115.6, 113.2, 112.0, 56.2, 56.0, 46.6.

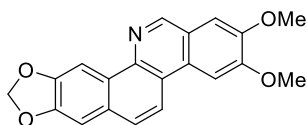
(6-Bromobenzo[d][1,3]dioxol-5-yl)methanamine,¹⁵ 87

Following **GP5**, from **97** (1.71 g) was obtained **87** (1.28 g, 80%) as light brownish soft solid.

¹H NMR (300 MHz, CDCl₃): δ (ppm) 6.99 (s, 1H), 6.88 (s, 1H), 5.96 (s, 2H), 3.80 (s, 2H), 1.56 (s, 2H).

¹³C NMR (75 MHz, CDCl₃): δ (ppm) 147.5, 147.2, 135.5, 113.6, 112.8, 109.1, 101.7, 46.8.

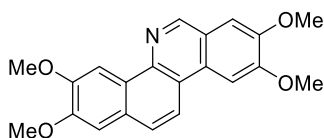
¹⁹ G. Satyanarayana, M. E. Maier, *Tetrahedron*, 2012, **68**, 1745-1749.

1.5.3.6. *Benzo[c]phenanthridines compounds***2,3-dimethoxy-[1,3]dioxolo[4',5':4,5]benzo[1,2-c]phenanthridine (Nornitidine), 48**

Following **GP6**, from the triflate **88b** (93 mg) and the bromobenzylamine **86** (64 mg), 62 mg were obtained as a white solid (72%).

¹H NMR (300 MHz, CDCl₃): δ (ppm) 9.33 (s, 1H), 8.65 (d, 1H, $J = 9.0$ Hz), 8.56 (s, 1H), 8.18 (s, 1H), 7.97 (d, 1H, $J = 9.0$ Hz), 7.73 (s, 1H), 7.53 (s, 1H), 6.22 (s, 2H), 4.10 (s, 3H), 3.99 (s, 3H).

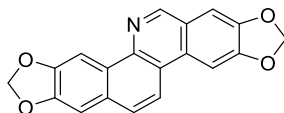
¹³C NMR (75.4 MHz, CDCl₃): δ 153.3, 149.7, 149.6, 148.0 (x2), 138.4, 129.3, 128.4, 127.9, 126.4, 121.8, 119.8, 119.2, 107.8, 104.5, 102.4, 101.4, 100.9, 56.2, 55.7.

2,3,8,9-Tetramethoxybenzo[c]phenanthridine (*O*-methylnorfagaronine), 83

Following **GP6**, from the triflate **89b** (97 mg) and the bromobenzylamine **86** (64 mg), 58 mg were obtained as a white solid (64%).

¹H NMR (300 MHz, CDCl₃): δ (ppm) 9.26 (s, 1H, H₆), 8.74 (s, 1H), 8.31 (d, 1H, $J = 8,9$ Hz), 7.91 (s, 1H), 7.87 (d, 1H, $J = 8,9$ Hz), 7.40 (s, 1H), 7.30 (s, 1H), 4.20 (s, 3H), 4.17 ppm (s, 3H), 4.10 (s, 3H), 4.08 (s, 3H).

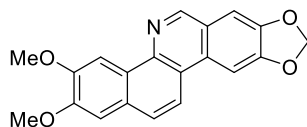
¹³C NMR (75.4 MHz, CDCl₃): δ 153.0, 150.0, 149.9, 149.7, 149.6 (C₆), 140.03, 128.9, 128.3, 127.5, 126.1, 122.1, 119.8, 118.0, 107.3, 107.0, 104.2, 101.6, 56.2, 56.1(x2), 56.0.

[1,3]dioxolo[4',5':4,5]benzo[1,2-c][1,3]dioxolo[4,5-j]phenanthridine (Noravicine), 84

Following the **GP6** from the triflate **88b** (93 mg) and the bromobenzylamine **87** (60 mg), 61 mg were obtained as a white solid (74%).

¹H NMR (500 MHz, CDCl₃): δ (ppm) 9.29 (s, 1H), 8.55 (s, 1H), 8.53 (d, 1H, $J = 9.2$ Hz), 8.34 (s, 1H), 7.95 (d, 1H, $J = 9.2$ Hz), 7.70 (s, 1H), 7.52 (s, 1H), 6.29 (s, 2H), 6.22 ppm (s, 2H).

¹³C NMR (75.4 MHz, CDCl₃): δ 151.8, 149.7, 148.1, 147.9, 141.9, 130.5, 129.6, 129.4, 126.7, 123.1, 122.4, 120.3, 119.2, 104.9, 104.6, 102.2, 101.5, 101.0, 100.1.

2,3-dimethoxybenzo[c][1,3]dioxolo[4,5-j]phenanthridine (Norallonitidine), 85

Following **GP6**, from the triflate **89b** (97 mg) and the bromobenzylamine **87** (60 mg), 52 mg were obtained as a white solid (60%)

¹H NMR (500 MHz, CDCl₃): δ (ppm) 9.29 (s, 1H), 8.63 (s, 1H), 8.51 (d, 1H, $J = 9.0$ Hz), 8.33 (s, 1H), 7.96 (d, 1H, $J = 9.0$ Hz), 7.69 (s, 1H), 7.54 (s, 1H), 6.29 (s, 2H), 4.02 (s, 3H) 3.96 (s, 3H).

¹³C NMR (75.4 MHz, CDCl₃): δ 151.5, 149.8, 149.5, 147.7, 139.6, 130.4, 128.0, 126.4, 126.1, 123.1, 119.9, 118.8, 107.5, 104.8, 103.7, 102.1, 100.0, 55.5 (x2).

PART 2: ALL-METAL AROMATICITY

PART 2 : ALL-METAL AROMATICITY

2.1. Introduction

2.1.1. Concept of aromaticity

2.1.1.1. Discovery of benzene

Benzene molecule was the first example of the aromatic compounds family that has been discovered. It was first isolated by Michael Faraday³¹ in 1825 when he was studying the fluid obtained during the compression of acetylene gas into the vessels used to illuminate the streets of London at the time. He just employed distillation method to isolate what he named “Bicarburet of hydrogen”. This compound was then synthesized in 1833 by Eilhard Mitscherlich³² *via* the degradation by distillation of benzoic acid, which was isolated from “benzoin resin”, in presence of Ca(OH)₂. Mitscherlich called this compound, “benzin” in reference to the corresponding aromatic resin. In 1836, the French scientist Auguste Laurent gave the name of “phène”³³ to the radical of the chlorophenesic acid, from the ancient Greek verb “φαινω” meaning bringing to light, because benzene was found in illuminating gas (acetylene). This word was the root of well-known words that chemists use nowadays, such as “phenyl” or “phenol”. At the time, all scientists worldwide pointed the differences between “benzin” and classical hydrocarbon chain but none of them had an idea about the chemical structure. The theory of carbon tetravalency³⁴ permitted scientists to assign structures to linear saturated molecules such as butane or hexane, but also to linear unsaturated products such as acetylene.³⁵ Nevertheless, no one could imagine a cyclic structure at that time. In 1865, August Kékule, a German chemist, was the first to postulate a cyclic structure in which “the carbon is more condensed than fatty substances”.³⁶ He described a sort of core composed by six carbon atoms common to all aromatic compounds. He followed the formulation reported by Hofmann in 1855 to classify a family of smelly acidic compounds he named ‘aromatics’.³⁷ In 1866, the French chemist Marcelin Berthelot was able to synthesize benzene from acetylene. The electric arc formed between carbon poles under hydrogen atmosphere in a

³¹ M. Faraday, *Philosophical Transactions of the Royal Society*, **1825** 115, 440–466.

³² E. Mitscherlich, *Annalen der Pharmacie*, **1834**, 9, 39–48 (German language).

³³ A. Laurent, *Annales de Chimie et de Physique*, **1836**, 63, 27–45.

³⁴ a) A. S. Couper *Annales de chimie et de physique*, **1858**, 53, 469–489. b) A. Kekulé, *Annalen der Chemie und Pharmacie*, **1858**, 106, 129–159 (German language).

³⁵ E. Davy, *The Transactions of the Royal Irish Academy*, **1839**, 18, 80–88

³⁶ A. Kekulé, *Bulletin de la Société Chimique de Paris*, **1865**, 3, 98–110.

³⁷ A. W. Hofmann, *Proceedings of the Royal Society*, **1856**, 8, 1–3. (abstract of lecture)

special glass that he called “œuf électrique” or also “calorimeter bomb” proved its usefulness in the synthesis of acetylene (Figure 12).³⁸

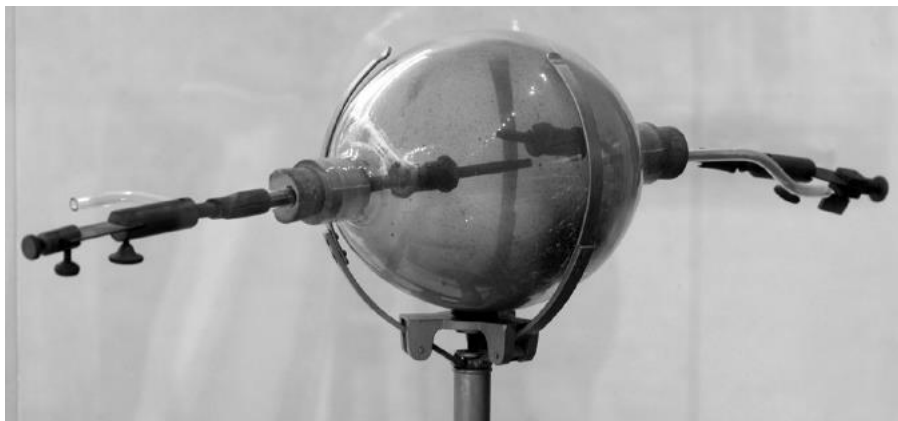


Figure 12 : Berthelot's "œuf électrique"

Berthelot used the same method to realize acetylene polymerization, forming mainly benzene but also toluene and styrene as byproducts. This was the first demonstration that it is possible to effect simple conversion of an aliphatic to an aromatic compound (and by the way, the first example of eco-compatible [2+2+2] cyclotrimerization).³⁹ Despite his success in acetylene and benzene synthesis, Berthelot remained outside the development of chemical structures pioneered by Butlerov and Kekulé. Instead of that, he distinguished chemical compounds according to their degrees of saturation, e.g. C_2H_6 was a “carbure complet”, C_2H_4 a “carbure incomplet” and C_2H_2 a second order “carbure incomplet”. According to this system, he considered benzene as an incomplete hydrocarbon of the fourth order.

It took until 1872 to see the first rational structure of benzene⁴⁰ represented on figure 13.

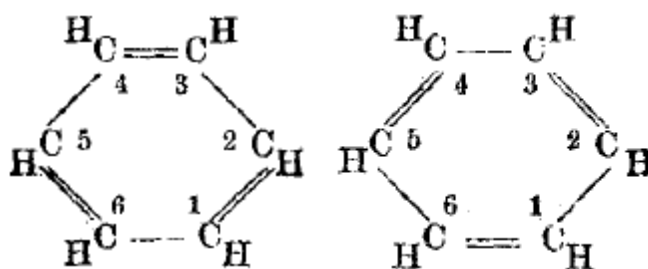


Figure 13 : First proposal for benzene structure.

³⁸ M. Berthelot, *J. Chem. Soc.*, **1864**, 17, 37-49.

³⁹ a) M. Berthelot, *Comptes rendus*, **1866**, 63, 479-484. b) M. Berthelot, *Comptes rendus*, **1866**, 63, 515-518. c) M. Berthelot, *Annales de Chimie et de Physique*, **1867**, 12, 52-63. d) M. Berthelot, *Annales de Chimie et de Physique*, **1867**, 12, 64-80.

⁴⁰ A. Kekulé, *Annalen der Chemie und Pharmacie*, **1872**, 162, 77-124 (German language).

Kekulé described two static structures containing three fixed double bonds in which each carbon atom is linked to one atom of hydrogen, one atom of carbon and twice to a second carbon nucleus. He reported two isomers of this triene (Figure 13), which will be proved later to be equivalent through the existence of the C_6 symmetry axis. At the end of 19th century, Kekulé's theory was not unanimous.⁴¹ Because of its three double bonds, benzene should react like ethylene but it does not. In occasion of the 25th anniversary of the German Chemical Society, Kekulé did have the opportunity to present his work during a prestigious congress in the Berlin City Hall in 1890.⁴² During this lecture, he spoke about the now famous dream that he had during a chilly night at Ghent University:

“During my stay in Ghent I resided in elegant bachelor quarters in the main thoroughfare. My study, however, faced a narrow side-alley and no daylight penetrated it. For the chemist who spends his day in the laboratory this mattered little. I was sitting writing at my textbook but the work did not progress; my thoughts were elsewhere. I turned my chair to the fire and dozed. Again the atoms were gamboling before my eyes. This time the smaller groups kept modestly in the background. My mental eye, rendered more acute by repeated visions of the kind, could now distinguish larger structures of manifold conformation: long rows, sometimes more closely fitted together all twining and twisting in snake-like motion. But look! What was that? One of the snakes had seized hold of its own tail, and the form whirled mockingly before my eyes. As if by a flash of lightning I awoke; and this time also I spent the rest of the night in working out the consequences of the hypothesis. Let us learn to dream, gentlemen, then perhaps we shall find the truth. But let us beware of publishing our dreams till they have been tested by the making understanding.”

Fredrich August Kekulé von Stradonitz
Translate to English by O. T. Benfey

⁴¹ a) A. K. L. Claus, *Theoretische Betrachtungen und deren Anwendungen zur Systematik der organischen Chemie*, **1867**. b) J. Dewar, *Proceedings of the Royal Society of Edinburgh*, **1867**, 6, 82–86. c) H. E. Armstrong, *Journal of the Chemical Society*, **1887**, 51, 258–268.

⁴² *Ber. D. Deutsch. Chem. Ges.*, **1890**, 23, 1302. (German language) Translation in English: O. T. Benfey, *J. Chem. Educ.*, **1958**, 35, 21–23.

The structure proposed by Kekulé was admitted by chemists but no significant proofs were added until the beginning of the 20th century. The discovery of the electron particle by Thomson⁴³ and the appearance of X-Ray analysis helped scientists to really move forward the understanding of carbon-carbon bonding. After the discovery of diamond structure in 1913 by the Bragg family (father and son rewarded by the Nobel Prize in 1915),⁴⁴ X-Ray was recognized as a very useful tool to analyze chemical compounds. Even if the complete elucidation of diamond has been given, the structure of graphite carbon, close to the benzene one, was not solved owing to the difficulty of obtaining good single crystals. At that time, results on graphite carbon powder led to two proposals (Figure 14).

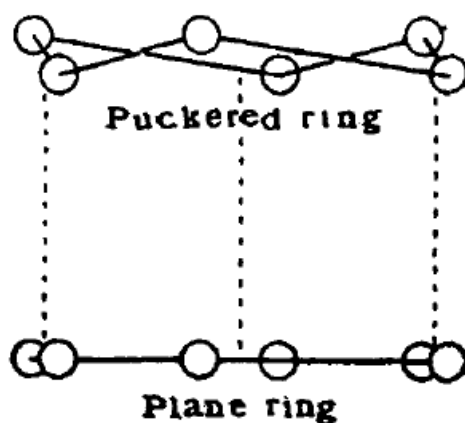


Figure 14 : Two proposed structures of benzene molecule

In one-side, the studies of Debye and Scherrer⁴⁵ stated that carbon atoms are arranged in a perfectly flat layer of linked hexagons and a carbon-carbon bond length of 1.45 Å (shorter than tetrahedral carbon of diamond possessing a C-C bond of 1.54 Å). This proposed bond length was special because it is an intermediate between classical σ bond (1.54 Å) and π double bond (1.33 Å). They also postulated that if graphite carbon occurred in a planar conformation, benzene should have the same arrangement. In the other side, Hull⁴⁶ proposed a hexagonal but puckered structure with carbon diameter of 1.54 Å. Each carbon of this structure possesses a tetrahedral arrangement and could be derived from diamond. But in fact,

⁴³ J. J. Thomson, *The Electrician*, **1897**, 39, 104

⁴⁴ W. H. Bragg, W. L. Bragg, *Proc. R. Soc. Lond. A*, **1913**, 89, 277-291.

⁴⁵ P. Debye, P. Scherrer, *Physik. Z.*, **1917**, 18, 291-301

⁴⁶ A. W. Hull, *Physical Rev.*, **1917**, 10, 661-697

the projection the puckered hexagon on the (0001) plane of graphite is perfectly identical to the planar structure described by Debye and Scherrer.

Because of the difficulty to obtain benzene crystals, investigations have been made on liquid benzene and powder. Many crystallographers studied the conformation of benzene units,⁴⁷ but so far the only facts established are the unit cell dimensions, the space group, the number and approximate positions of the molecules in the cell and the central but not planar symmetry of the molecule. In parallel, Bragg⁴⁸ and Plummer⁴⁹ exploited the more easily crystallizable naphthalene, anthracene and hexabromobenzene and showed that all the species were centro-symmetric and all their atoms are on the same plane embedded in a flat configuration. In the same time, Hassel and Mark⁵⁰ and, independently, Bernal⁵¹ solved the structure of carbon graphite. They found hexagonal units arranged in the form of superimposed sheets. The carbon-carbon bond lengths are all equally to 1.42 Å, very close to the value of 1.45 Å proposed by Scherrer and Debye eleven years ago. No critical proof was brought for several years and the problem remained at this stage.

Benzene nucleus structure was validated by the scientific community in 1929 after the report of hexamethylbenzene X-Ray analysis by Lonsdale.⁵² She found a C-C bond length of 1.42 ± 0.03 Å comparable to the value suggested by Hassel, Mark and Bernal for graphite. A few years later, in 1934, Pauling and Brockway⁵³ used the more precise new electron-diffraction method of gas molecules to reevaluate the bond length of benzene to 1.390 ± 0.005 Å. In 1939, Schomaker and Pauling⁵⁴ refined this value to 1.397 Å which is used as reference nowadays. However, if graphene's units are benzene molecules, one wonders why the C-C bond-lengths are that different. Pauling⁵⁵ described a relationship between the carbon-carbon bond length and the single-bond and double-bond character for molecules in resonance (Figure 15).

⁴⁷ a) P. Debye, P. Scherrer, *Gött. Nachr.*, **1916**, 16, 1-5. b) B. Broomé, *Physik. Z.*, **1923**, 24, 124-130. c) B. Broomé, *Z. Kristallogr.*, **1925**, 62, 325. d) E. D. Eastman, *J. Am. Chem. Soc.*, **1924**, 46, 917-923. e) J. R. Katz, *Physik Z.*, **1927**, 45, 97-113. f) E. G. Cox, *Nature*, **1928**, 122, 401.

⁴⁸ W. H. Bragg, *Z. Kristallogr.*, **1927**, 66, 22-32.

⁴⁹ W. G. Plummer, *Phil. Mag.*, **1925**, 50, 1214-1221.

⁵⁰ O. Hassel, H. Mark, *Physik Z.*, **1924**, 25, 317-337

⁵¹ J. D. Bernal, *Proc. R. Soc. Lond. A*, **1924**, 106, 749-773

⁵² K. Lonsdale, *Trans. Faraday Soc.*, **1929**, 25, 352-366.

⁵³ L. Pauling, L. O. Brockway, *J. Chem. Phys.*, **1934**, 2, 867-881.

⁵⁴ V. Schomaker, L. Pauling, *J. Am. Chem. Soc.*, **1939**, 61, 1769-1780.

⁵⁵ L. Pauling, *The nature of the chemical bond and the structure of molecules and crystals 3rd .ed.* (Cornell Univ. Press, N-Y, **1960**)

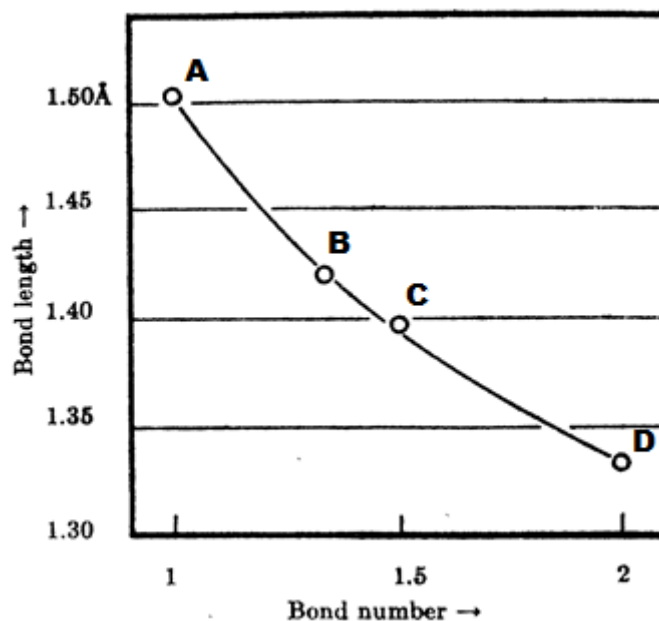


Figure 15 : Bond length in function of single- or double-bond character.

Point **A** describes a pure C-C single bond distance at 1.504 Å while point **D** shows a pure C=C double bond with no other conjugated double bonds aside at 1.334 Å. Point **B** represents graphite carbon at 1.420 Å and its bond character is evaluated at one third: one carbon atom realize one double bond and two single bonds. In the case of benzene (point **C**), each carbon atom does one single bond and one double bond which give a $\frac{1}{2}$ double bond character (C-H bond are omitted). The double bond character is stronger in benzene's case and thus leads to a smaller carbon-carbon bond length than graphite.

2.1.1.2. Electronic properties of aromatic compounds

The structure of benzene discovered by Kékule was admitted by the scientific community but experiments on benzene showed that this species is significantly more resistant to oxidizing and reducing agents than classical olefins. Thus, this structure was rapidly considered insufficient to describe the real chemical nature of this bonding mode. At that point, several scientists introduced different proposals concerning aromaticity. Bamberger⁵⁶ was the first to suggest an axiom in that six "potential valences" or "potential affinity" could cause an unsaturated ring to be aromatic and could justify the centric formula postulated by

⁵⁶ a) E. Bamberger, *Ber. Dtsch. Chem. Ges.*, **1891**, 24, 1758-1764. b) E. Bamberger, *Liebigs Ann. Chem.*, **1893**, 273, 373-379.

Armstrong⁵⁷ and von Baeyer⁵⁸ (Figure 16a). However, he did not gain recognition because of deficiencies in this axiom such as the case of nitrogen-containing compounds.

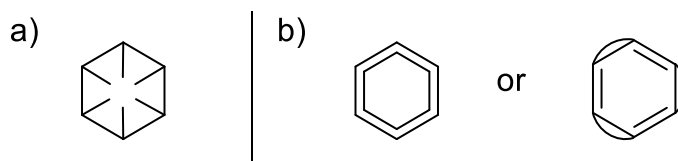


Figure 16 : Several proposition of the electronic structure of benzene.

Several years later, Thiele proposed a structure in which each bonds shares a partial valence with its neighbors in order to justify the weaker reactivity of benzene compared to olefins (Figure 16b). He also postulated that all cyclic compounds possessing a conjugated system of double bond are aromatic. Thiele's hypothesis was invalidated after the report of the synthesis of cyclooctatetraene by Willstätter⁵⁹ which proved to be an olefinic compound rather than an aromatic one.

The discovery of the electron and thus, of the electron theory of valence allowed chemists to think about benzene structure with a rather different approach. Much inspired by Lewis' octet-rule⁶⁰ and Crocker's work⁶¹, Armit and Robinson⁶² reported six-membered ring carbon cycle bearing a system of six electrons which resists disruption. They called this system the "aromatic sextet" and the representation is showed on figure 17.



Figure 17 : Armit and Robinson structure of benzene.

This delocalized system results from a combination of six π -electron in a stable association which is responsible for the aromatic character. This theory reminds what Armstrong proposed several years before if we replace the term "affinity" with the word "electron". Armit and Robinson pointed out that the sextet rule can be applied on

⁵⁷ H. E. Armstrong, *Phil. Mag.*, **1887**, 23, 73-109.

⁵⁸ A. v. Baeyer, *Liebigs Ann. Chem.*, **1888**, 245, 103-185.

⁵⁹ R. Willstätter, M. Heidelberger, *Ber. Dtsch. Chem. Ges.*, **1911**, 44, 3423-3445.

⁶⁰ G. N. Lewis, *J. Am. Chem. Soc.*, **1916**, 38, 762-785.

⁶¹ E. C. Crocker, *J. Am. Chem. Soc.*, **1921**, 44, 1618-1630.

⁶² J. M. Armit, R. Robinson, *J. Chem. Soc. Trans.*, **1925**, 127, 1604-1618.

heteroaromatics like pyridine for instance, but even to smaller molecules such as thiophene, pyrroles or furan. This implies the participation of one lone electron pair of the heteroatom to the delocalization of electrons. Thanks to this observation, they could reason, as others,⁶³ on the basicity or the acidity of several compounds (Figure 18).

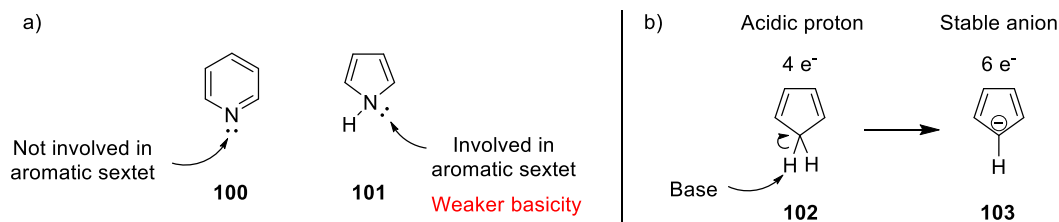


Figure 18 : Acidity and basicity

Pyridine **100** and pyrrole **101** are two nitrogen-containing aromatic heterocycles which respect the sextet rule but differences on their Brönsted basicity can be noted. In the case of pyridine (Figure 18a), the lone pair is not involved in aromaticity and thus remains available to play the role of a base. On the contrary, the lone pair on nitrogen in the pyrrole molecule is involved in the aromatic sextet and is not available anymore. This can justify why pyrrole is a weaker base. Another example is the Brönsted acidic character observed for the cyclopentadiene **102** (Figure 17b). The deprotonation of this compound leads to the stable anion **103** which possesses six π electrons. The aromatic sextet provides stability to this anion and explains its acidic character.

Several electronic benzene formulas have been reported but none of them were relevant and will not be discussed here.⁶⁴

After the birth of quantum mechanics, physical chemists attempt to solve the electronic benzene structure. The planar chemical structure was proven by Lonsdale⁵² but the question of the high stability of this ring still reminds unanswered. After seminal work by Biggs⁶⁵ and Slater⁶⁶ (first pictures of 2s and 2p orbitals), Erich Hückel reported its quantum theoretical contributions of what he called “the benzene problem” in 1931.⁶⁷ He was the first to

⁶³ a) F. R. Goss, C. K. Ingold, *J. Chem. Soc.*, **1928**, 127, 1268-1278. b) C. K. Ingold, H. A. Piggott, *J. Chem. Soc. Trans.*, **1923**, 123, 1469-1509.

⁶⁴ a) J. Beckenkamp, *Z. Anorg. Allg. Chem.*, **1924**, 137, 249-274. b) J. Beckenkamp, *Z. Anorg. Allg. Chem.*, **137**, 220-232. c) H. Burgarth, *Z. Elektrochem. Agew. Phys. Chem.*, **1926**, 32, 157-162. d) E. Schrörer, *Z. Elektrochem. Agew. Phys. Chem.*, **1925**, 31, 53-54. e) M. Ulmann, *Z. Elektrochem. Angew. Phys. Chem.*, **1928**, 41, 674-680. f) L. Pauling, *J. Am. Chem. Soc.*, **1926**, 48, 1132-1143. g) H. J. Lucas, *J. Am. Chem. Soc.*, **1926**, 46, 1827-1838.

⁶⁵ H. F. Biggs, *Philos. Mag.*, **1928**, 6, 659-664.

⁶⁶ J. C. Slater, *Phys. Rev.*, **1931**, 37, 481-489.

⁶⁷ E. Hückel, *Z. Physik*, **1931**, 70, 204-286.

dissociate π -electrons from the σ ones. According to the molecular orbital theory, it was stated that a double bond is composed by a σ -bond in which the recovery of the two atomic orbitals is linear and by a π -bond in which the recovery between two atomic orbitals is orthogonal (Figure 19).

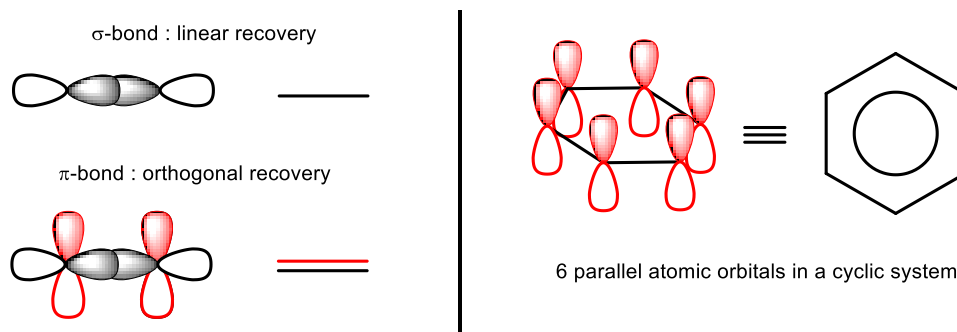


Figure 19 : Atomic orbitals.

Hückel examined the aromatic sextet with the two approximate methods of quantum chemistry available at that time, namely Valence Bond (VB) and Molecular Orbitals (MO). Without going into details, wave function for VB theory is a linear superposition of the wave functions that represent all the canonical structures. For the MO theory, the wave function is the linear combination of atomic orbitals of each atom contained in the molecule. Hückel concluded that because the MO method could explain the stability of aromatic sextet, it would be more suitable to treat π -electrons than the VB method. These results were contradicted by Pauling and Wheland in 1933, who found that benzene stability was due to the resonance of five canonical structures using VB method (Figure 20). However their results were considered uncertain because they indicate that cyclobutadiene should have been more stable than benzene.

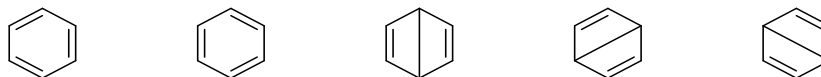
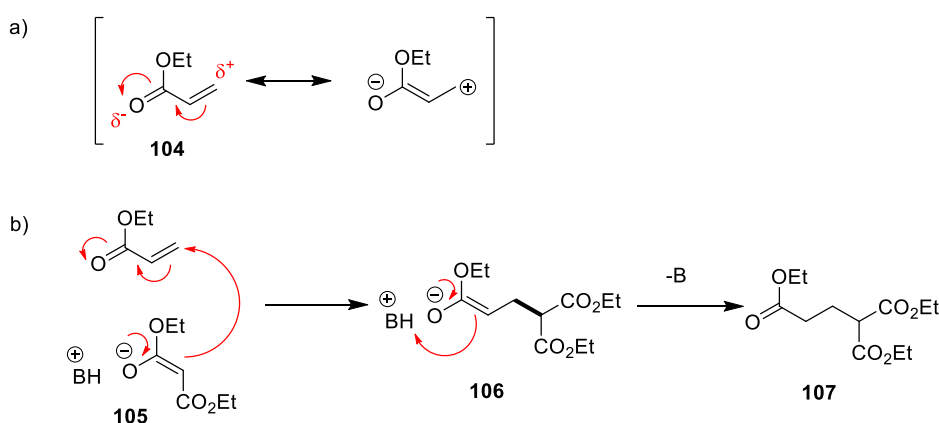


Figure 20 : Pauling's five canonical structures contributing to the normal state of the benzene molecule.

All these calculations were made taking into account only the six π -electrons but not the σ ones. This was the observation of Penney when he reported his results in 1934.⁶⁸ Using the VB method, he found that the stability of benzene mainly depended on the σ -bonds.

At that time, quantum mechanics did not provide clear results, perhaps because even if the methods of calculation were efficient, chemists' overview of the benzene problem was partially limited. Hückel and others were engaged in a global race for the discovery of what rules make aromatic compounds so stable. The answer of this question was very close and it was the introduction of the "mesomeric effect" theory which helped them to solve the problem.

In parallel to quantum mechanics studies, the discovery of the electron allowed organic chemistry to make a lot of progress, especially concerning the understanding of electronic effects on known chemical reactions, such as Michael addition or electrophilic aromatic substitutions. Ingold and coworkers⁶⁹ reported a theoretical analysis of the electrophilic partner in the Michael addition reaction. They postulated that ethyl acrylate **104** possesses a positive partial charge on the γ -carbon and a negative partial charge on the oxygen atom of the carbonyl group. With electron delocalization, a zwitterionic form could be written (Scheme 22a) and the system is stabilized in an intermediate state between these two forms. A mechanistic approach of the Michael addition resulting from this proposal is depicted on scheme 22b. The negative malonate ion **105**, stabilized by the two ester groups, can attack the electrophilic position of the acrylate moiety and create a C-C bond. The formed enolate **106** recovers a proton and regenerate the base to obtain the triester product **107**.



Scheme 22 : a) Mesomeric effect. b) Michael addition mechanism.

⁶⁸ W. G. Penney, *Proc. R. Soc. London A*, **1934**, 146, 223-238.

⁶⁹ K. E. Cooper, C. K. Ingold, E. H. Ingold, *J. Chem. Soc.*, **1926**, 129, 1868-1872.

This new vision of electronic effects was recognized to be possible by the scientific community and was applied to the case of aromatic electrophilic substitutions.⁷⁰ Experimentally, it is known that the selectivity of electrophilic substitutions on mono-substituted aryls depends on the type of the substituent (Figure 21a).

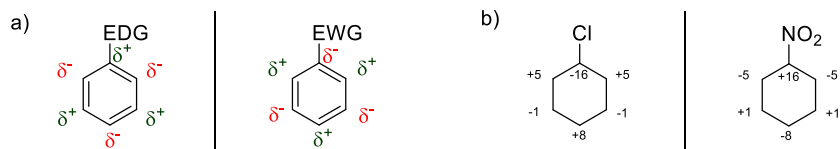
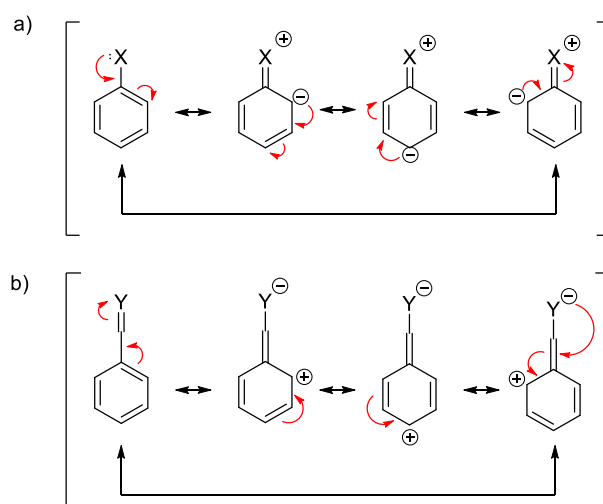


Figure 21 : a) Partial charges in function of the substituent. b) Hückel's calculated charge distribution (double bonds were omitted for clarity).

If the substituent is electronwithdrawing such as an ester or a nitro group, the orientation is in *meta*-position. On the contrary, if the substituent is an electrodonating group such as ethers or alkyl fragments, the orientation of the electrophilic substitution is in *ortho* and *para*-positions. After many argumentations between Hückel, Robinson and Ingold, calculations of aromatic sextet were made by Hückel⁷¹ to observe the charge distribution as a function of substituents in order to justify the selectivity experimentally observed (Figure 21b). The calculated charges were completely the opposite of what was observed at the bench. These results showed that the theory of the “aromatic sextet” was maybe not efficient enough to describe benzene bonding unlike that of mesomeric effects (Scheme 23).



Scheme 23 : Mesomeric effect depending of the substituents. a) Electron-donor group. b) Electron-withdrawing group.

⁷⁰ a) C. K. Ingold, E. H. Ingold, *J. Chem. Soc.*, **1926**, 129, 1310-1328. b) E. L. Leighton, C. K. Ingold, E. H. Ingold, *J. Chem. Soc.*, **1926**, 129, 1684-1690. c) A. Lapworth, R. Robinson, *Nature*, **1932**, 129, 278. d) A. Lapworth, R. Robinson, *Nature*, **1932**, 130, 273. e) E. Hückel, W. Hückel, *Nature*, **1932**, 129, 937-938.

⁷¹ E. Hückel, *Z. Physik*, **1931**, 72, 310-337.

The mesomeric effect of benzene bearing an electron-donating group leads to four canonic forms which can explain the selectivity of aromatic electrophilic substitution. The negative charge of the zwitterion created by the delocalization of electrons leads to three nucleophilic positions in *ortho* and *para* of mono-substituted rings. On the opposite, the presence of an electron-withdrawing group provides another delocalized system. The delocalization forms too a zwitterionic species but this time it is a positive charge that results stabilized on the aromatic ring. Electrophilic positions are found in *ortho* and *para* positions and so nucleophilic positions results in *meta*. This corresponds to the selectivity experimentally observed. Hückel accepted mesomerism principle and, through the aid of MO theory, he expressed what we call nowadays “Hückel’s rules” for aromaticity:

- A conjugated delocalized π -system, most of time, arranged in alternated single and double bond.
- All atoms of the molecule are on the same plane.
- Contributing atoms are arranged in one or several rings.
- $4n + 2$ delocalized π -electrons (n is a positive integer).

At that time these rules gained no credit however, because they were not applicable to the stable seven-membered ring tropolone’s family **108a-c** (Figure 22a) isolated in 1942. In 1945, Dewar attributed them a seven-membered ring structure and an aromatic character.⁷²

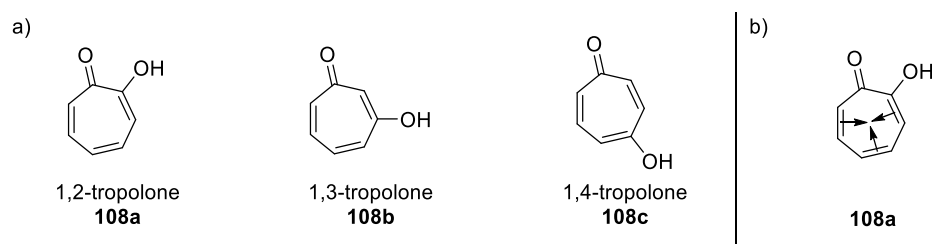


Figure 22 : a) Tropolone compounds family. b) Aromatic sextet rule justifying tropolone stability.

The tropone skeleton is composed of a conjugated triene part and a carbonyl group. At that time this structure was more easily explainable with the aromatic sextet rule than with Hückel’s rules (Figure 22b).⁷³ Other chemists such as Dauben Jr., thought that mesomerism

⁷² M. J. S. Dewar, *Nature*, **1945**, 155, 50-51.

⁷³ a) W. v. E. Doering, F. L. Detert, *J. Am. Chem. Soc.*, **1951**, 73, 876-877. b) W. v. E. Doering, L. H. Knox, *J. Am. Chem. Soc.*, **1952**, 74, 5683-5687.

theory could explain the stability of this ring by the delocalization of a positive charge (Figure 23).

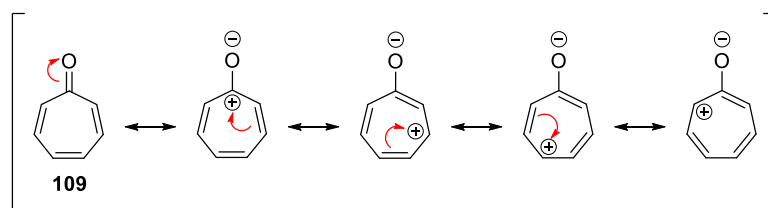
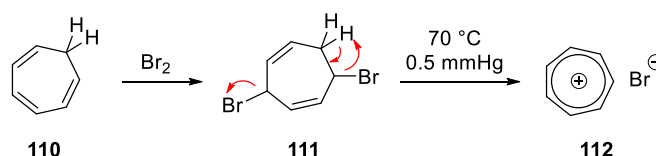


Figure 23 : Delocalization of the positive charge on tropone ring.

So far, experimental research on aromatic seven-membered rings was only at the initial stage, so it was impossible to determine which hypothesis was the most appropriate. This remained an open case until 1954 when Doering and coworkers reported the synthesis of the cycloheptatrienylium or tropylium cation **112** via 1,4-bromination and elimination of cyclohepta-1,3,5-triene **110** (Scheme 24).⁷⁴



Scheme 24 : Tropylium cation synthesis.

Doering stated that the degree of stabilization of the positive charge was very large and in accord with molecular orbital theory, therefore also with Hückel's rules. The cycloheptatrienylium cation appears as a new aromatic system in which very large resonance energy originates specifically from the cyclic nature of the system. At this point, the "aromatic sextet" rule was completely abandoned to describe aromatic systems in favor of Hückel's rules.

Hückel's rules have been accepted to describe monocyclic aromatic compounds however, as Roberts mentioned,⁷⁵ these rules cannot describe every polycyclic aromatic system, For example, pyrene **113** is a planar tetracycle which own a full delocalized double-bond system. It is yet considered as an aromatic compound while it possesses 16 delocalized π -electrons (Figure 24).

⁷⁴ W. v. E. Doering, L. H. Knox, *J. Am. Chem. Soc.*, **1954**, 76, 3203-3206.

⁷⁵ J. D. Roberts, A. Streitwieser Jr., C. M. Regan, *J. Am. Chem. Soc.*, **1952**, 74, 4579-4582.

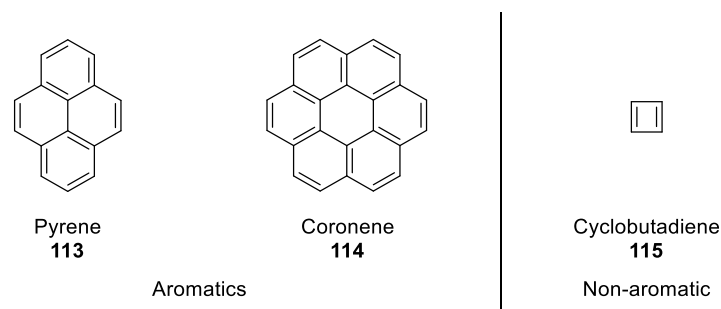
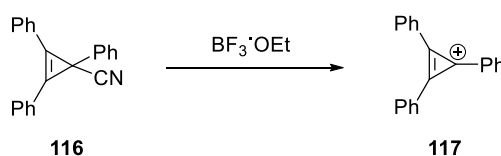


Figure 24 : Pyrene and coronene structures

The same observation has been made for coronene **114** which possesses 24 delocalized π -electrons and it is also planar. Since a long time, the case of cyclobutadiene **115** has been open to debate but it was classified as non-aromatic compound because of its only four delocalized π -electrons which did not respect Hückel's rules.^{68,71,76}

The smallest and simplest organic aromatic is the cyclopropenyl cation. Composed of two π -electron and a positive charge, the core of this species has been synthesized the first time in 1958 by Ronald Breslow.⁷⁷ This cation was obtained by removing a cyanide from **116** with boron trifluoride etherate (Scheme 25).



Scheme 25 : First synthesis of the cyclopropenyl cation by Breslow.

Breslow described the cationic compound **117** as a stable cycle in spite of its cycle strain. By NMR analysis, he only observed one phenyl signal compared to the two signals of the starting material **116**. Later, the synthesis has been improved⁷⁸ and the cyclopropenyl cation $[\text{C}_3\text{H}_3]^+$ has been isolated.

To summarize, aromaticity is a bonding mode that enables to minimize energetic levels of molecules. In most cases, it appears to be effective when these molecules, respect some

⁷⁶ a) G. W. Wheland, *J. Am. Chem. Soc.*, **1941**, 63, 2025-2027. b) C. A. Coulson, W. E. Moffitt, *Phil. Mag.*, **1949**, 40, 1-35. c) D. P. Craig, *Proc. Roy. Soc. Lond. A*, **1950**, 202, 498-506. d) D. P. Craig, *J. Chem. Soc.*, **1951**, 3175-3182.

⁷⁷ R. Breslow, C. Yuan, *J. Am. Chem. Soc.*, **1958**, 80, 5991-5994.

⁷⁸ a) R. Breslow, J. T. Groves, G. Ryan, *J. Am. Chem. Soc.*, **1967**, 89, 5048. b) D. G. Farnum, G. Mehta, G. Silberman, G. Robert, *J. Am. Chem. Soc.*, **1967**, 89, 5048-5049. c) R. Breslow, R. Haynie, J. Mirra, *J. Am. Chem. Soc.*, **1970**, 92, 984-987.

specific criteria, namely, Hückel's rules. Each aromatic molecule possesses resonance energies due to the delocalization of π -electrons in the orbitals that are orthogonal to the plane of the cyclic molecule. This system of parallel orbitals creates an electronic ring upon (and below) the cycle that stabilizes the whole structure. These observations are somehow straightforward nowadays for aromatic compounds containing main group elements because all of them have "s" and "p" electron shells. However, the concept of aromaticity can be also applied to molecules owing d-type electrons. They will be discussed in the following part.

2.1.2. All-Metal Aromaticity

All-metal aromaticity is a little bit different from classical aromaticity because it involves the participation of d- and sometimes f-atomic orbitals in the construction of delocalized molecular orbitals. The "d" electron shell is present in every atom from the fourth line of the periodic table to the end. In this group of atoms, transition metals are special because their "d" electronic shell is not completed and provides them remarkable and peculiar properties. Several years before the birth of all-metal aromatic compounds, Thorn and Hoffmann predicted that some hypothetical metallacycles **118** and **119** should exhibit delocalized bonding and some aromatic character (Figure 25).⁷⁹ They predicted that electrons in d_{xz} or d_{yz} atomic orbitals of metals could be involved in aromaticity. During the same year, Bursten and Fenske⁸⁰ introduced the term of "metalloaromaticity".

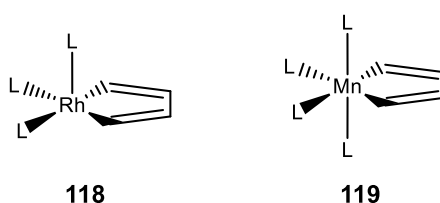


Figure 25 : Examples of predicted aromatic metallacycles.

Inspired by this work, several organometallic chemists isolated and characterized aromatic metallacycles (Figure 26).⁸¹ The first example of osmabenzene **120** was reported by

⁷⁹ D. L. Thorn, R. Hoffmann, *Nouv. J. Chim.*, **1979**, 3, 39-45.

⁸⁰ B. E. Bursten, R. F. Fenske, *Inorg. Chem.*, **1979**, 18, 1760-1765.

⁸¹ J. R. Bleeke, *Chem. Rev.*, **2001**, 101, 1205-1227.

Elliott in 1982.⁸² Iridabenzene derivatives **121** were synthesized by Bleeke and coworkers in the following years.⁸³ The first dimetallobenzene molecule **122** was reported by Rothwell *et al.*⁸⁴ Despite d- or f-orbitals from metal nuclei are involved in the electron delocalization of these clusters, the resulting aromaticity remains of π -like symmetry because of the pronounced contribution of p-orbitals from the organic fragments.

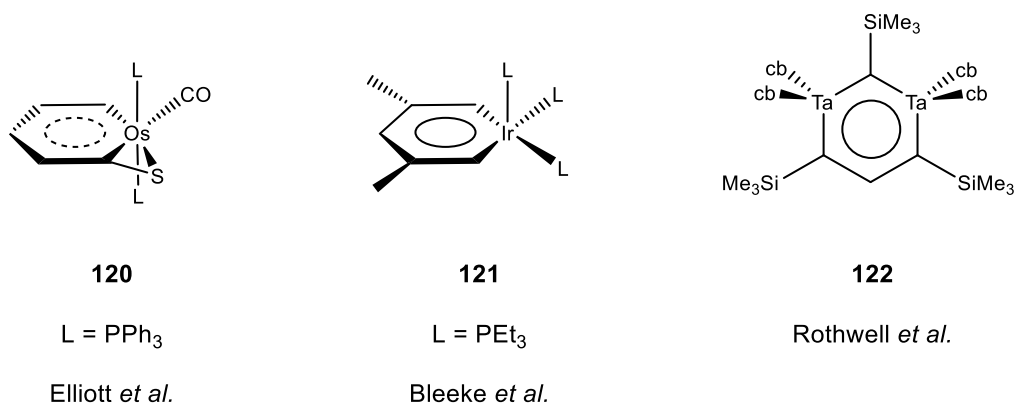


Figure 26 : Isolated mono- and bimetallo-cycles.

Though aromaticity in compound containing one or several transition-metal has already been shown for quite long time, aromaticity in all-metal systems was recognized only recently. The first all-metal aromatic compound, synthesized by Robinson in 1995,⁸⁵ presents a triangle of gallium Ga₃²⁻ **123** (Figure 27). Synthesis and properties of **123** will be discussed later but the aromaticity of this cyclogallene involving p-orbitals of gallium has been proven one year later by Robinson in collaboration with Schaefer.⁸⁶

⁸² G. P. Elliott, W. R. Roper, J. M. Waters, *J. Chem. Soc., Chem. Commun.*, **1982**, 811-813.

⁸³ a) J. R. Bleeke, Y.-F. Xie, W.-J. Peng, M. Chiang, *J. Am. Chem. Soc.*, **1989**, *111*, 4118-4120. b) J. R. Bleeke, R. Behm, Y.-F. Xie, T. W. Clayton Jr., K. D. Robinson, *J. Am. Chem. Soc.*, **1994**, *116*, 4093-4094.

⁸⁴ D. Robert, P. E. Fanwick, I. P. Rothwell, *Angew. Chem.* **1992**, *104*, 1277-1278. and *Angew. Chem. Int. Ed.*, **1992**, *31*, 1264-1263.

⁸⁵ X.-W. Li, W. T. Pennington, G. H. Robinson, *J. Am. Chem. Soc.*, **1995**, *117*, 7578-7579.

⁸⁶ a) X.-W. Li, Y. Xie, P. R. Schreiner, K. D. Gripper, R. C. Crittendon, C. F. Campana, H. F. Schaefer III, G. H. Robinson, *Organometallics*, **1996**, *15*, 3798-3803. b) Y. Xie, P. R. Schreiner, H. F. Schaefer III, X.-W. Li, G. H. Robinson, *J. Am. Chem. Soc.*, **1996**, *118*, 10635-10639.

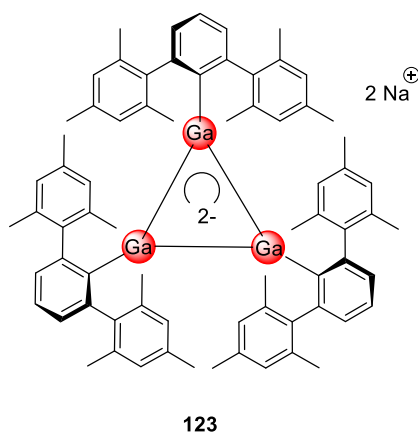


Figure 27 : Robinson's metal-aromatic cyclogallene.

The synthesis of this metalloaromatic complex paved the way to the discovery of plenty of metal and metalloid aromatic clusters.⁸⁷ Square planar metallic clusters such as Te_4^{2+} ,⁸⁸ Sb_4^{2-} and Bi_4^{2-} ⁸⁹ were reported to be valence isoelectronic to the prototypical aromatic $\text{C}_4\text{H}_4^{2-}$. Others pentagonal planar structures such as As_5^- , Sn_5^- and Pb_5^- are valence isoelectronic to cyclopentadienyl anion C_5H_5^- .⁹⁰ All previously cited clusters are composed by heavy atoms, which have a “d” electron shell, compared to classical aromatic compounds currently found in organic chemistry. Aromatic character is provided by the valence electron shell and in these cases the “ p_z ” ones, creating delocalized molecular orbitals of π symmetry, lead to π -aromaticity. It is reasonable to think that a possible new type of aromaticity involving d-type atomic orbitals exists.

2.1.2.1. Nucleus Independent Chemical Shift (NICS)

NICS was introduced by Schleyer in 1996⁹¹ and improved in the following years.⁹² NICS indices correspond to the negative of the magnetic shielding computed at chosen points in the vicinity of molecules. The negative values in interior positions of rings indicate the presence

⁸⁷ A. I. Boldyrev, L-S. Wang, *Chem. Rev.*, **2005**, *105* 3716-3757.

⁸⁸ a) R. J. Gillespie, J. Passmore, *Acc. Chem. Res.*, **1971**, *4*, 413-419. b) I. D. Brown, D. B. Crump, R. J. Gillespie, *Inorg. Chem.*, **1971**, *10*, 2319-2323.

⁸⁹ a) S. C. Critchlow, J. D. Corbett, *Inorg. Chem.*, **1984**, *23*, 770-774. b) A. Cisar, J. D. Corbett, *Inorg. Chem.*, **1977**, *16*, 2482-2487.

⁹⁰ a) O. J. Scherer, *Angew. Chem. Int. Ed.*, **1990**, *29*, 1104-1122. b) A. L. Rheingold, M. J. Foley, P. J. Sullivan, *J. Am. Chem. Soc.*, **1982**, *104*, 4727-4729. c) I. Todorov, S. C. Sevov, *Inorg. Chem.*, **2001**, *40*, 5042-5044.

⁹¹ P. v. R. Schleyer, C. Maerker, A. Dransfeld, H. Jiao, N. J. R. v. E. Hommes, *J. Am. Chem. Soc.*, **1996**, *118*, 6317-6318.

⁹² Z. Chen, C. S. Wannere, C. Corminboeuf, R. Puchta, P. v. R. Schleyer, *Chem. Rev.*, **2005**, *105*, 3842-3888.

of induced diatropic ring currents. This is a hallmark of aromaticity, whereas positive values denote paratropic ring current or anti-aromaticity. On the benzene example depicted on figure 28, all the values from 0 to 3 Å are negative as expected for an aromatic ring.

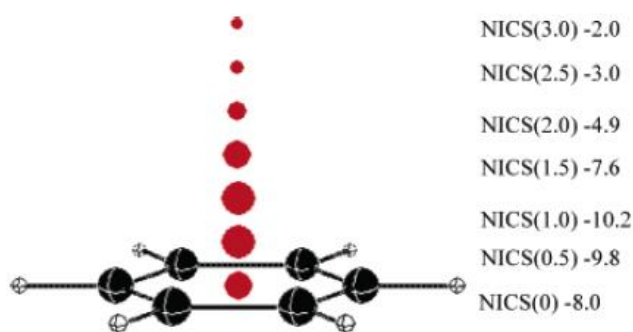


Figure 28 : NICS values for benzene molecule.

As Schleyer stated, NICS has several advantages compared to other aromaticity criteria. It does not require reference standards or increment schemes. It depends a little bit of the ring size but mostly of the number of delocalized π -electrons and it can be computed in an easy manner. All these advantages make NICS a method of choice to identify aromatic systems.

2.1.2.2. δ -type aromaticity

It would be improper to talk about δ -aromaticity without saying a few words about δ -bonding in metal-metal bonds. In 1964, Cotton and coworkers⁹³ reported the structure of $[\text{Re}_2\text{Cl}_8]^{2-}$ **124** in which the Re-Re bond is considered as very strong and unsupported by halide bridges (Figure 29). Quadruple Re-Re bond was measured 2.24 Å. This is lower than single Re-Re bond, 2.62 Å, but interestingly, higher than a triple Re-Re bond evaluated at 2.20 Å. The eclipsed conformation was justified by the overlapping between the two d_{xy} orbitals of each rhenium atoms which enabled a better stabilization despite the chlorine-chlorine interaction.

⁹³ F. A. Cotton, N. F. Curtis, C. B. Harris, B. F. G. Johnson, S. J. Lippard, J. T. Mague, W. R. Robinson, J. S. Wood, *Science*, **1964**, *145*, 1305-1307.

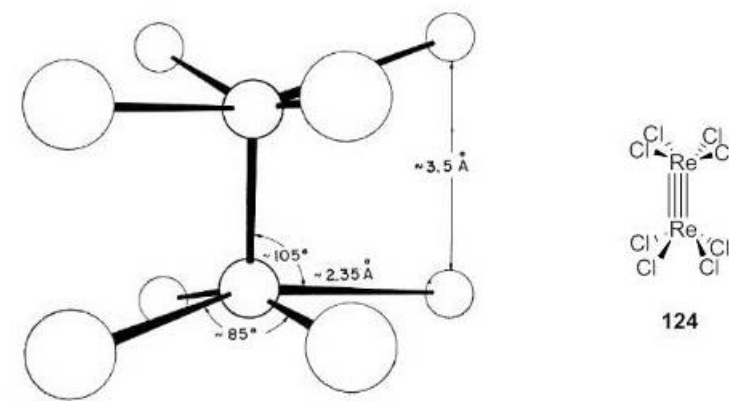


Figure 29 : X-Ray structure of $[\text{Re}_2\text{Cl}_8]^{2-}$.

More recently in 2005, Power *et al.*⁹⁴ reported a fivefold bonding ($\sigma^2\pi^4\delta^4$) between two chromium(I) atoms. Calculations of electron density (Figure 30 left) were realized for the bimetallic cluster **125** and are drawn on figure 30 right. The symmetries of the HOMO and the HOMO^{-1} come from the main contribution of d_{xy} and $d_{x^2-y^2}$ respectively and correspond to a δ -bond. HOMO^{-2} generated from d_{z^2} orbitals corresponds to a σ -bonding and HOMO^{-3} and HOMO^{-4} correspond to π -bonds by the main contribution of d_{yz} and d_{xz} atomic orbitals respectively.

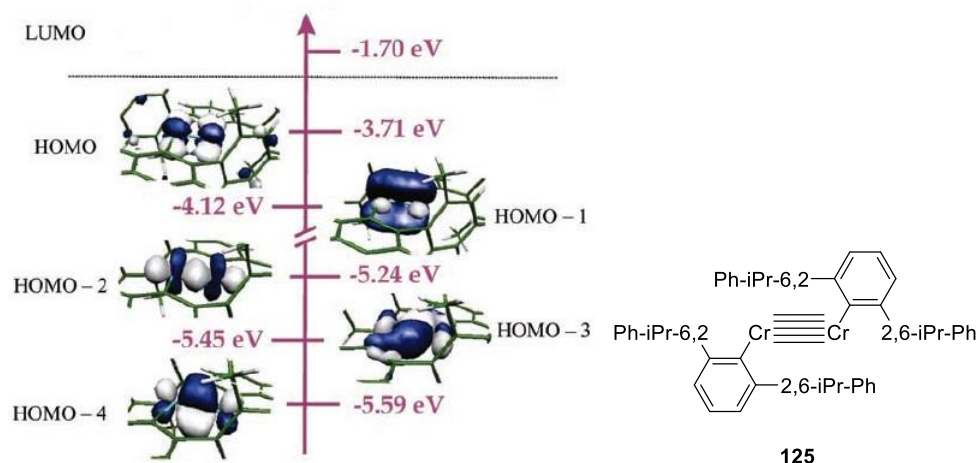


Figure 30 : (Left) Electron density surfaces and energies for the Cr-Cr bonding orbitals. (Right) Chemical structure of the fivefold Cr-Cr bond complex.

These studies showed that it was possible to observe and characterize δ -bonds in metal-metal bonding. The presence of this bonding mode suggests that cyclic multicenter species

⁹⁴ T. Nguyen, A. D. Sutton, M. Brynda, J. C. Fettinger, G. J. Long, P. P. Power, *Science*, **2005**, *310*, 844-847.

composed with transition metals and with completely delocalized δ -bond could exist and potentially provide δ -aromatic compounds as analogous of π -aromatic molecules made combining main group elements.

Indeed, the first δ -aromatic compound was identified by Boldyrev and Wang,⁹⁵ in the form of a tantalum triangular anion **126** in which each metal is bridged by an oxygen atom (Figure 31).

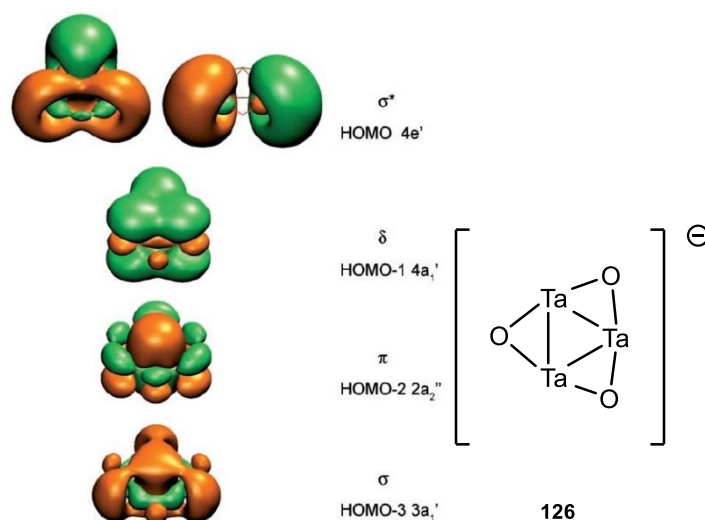


Figure 31 : (Left) Five valence molecular orbitals responsible for the Ta-Ta bonding. (Right) $[\text{Ta}_3\text{O}_3]^-$ complex.

According to the modeled molecular orbitals depicted on figure 31 left, the most interesting one is the HOMO^{-1} which possessed a δ -bonding nature. Boldyrev explained that this MO looked like a π -type MO because of its overlapping above and below the molecular plan but in fact it hold two nodal surfaces perpendicular to the C_{3v} axe. The observation of this δ -aromatic compound was a real progress in order to have a better understanding of δ -bonding mode, however, the weak point resided in the way to get it. Authors used a laser vaporization of solid tantalum under an oxygen atmosphere. The produced clusters were carried out by helium gas, separated by time of flight and analyzed by photoelectron spectroscopy. This method just afforded qualitative results and do not permit to isolate products.

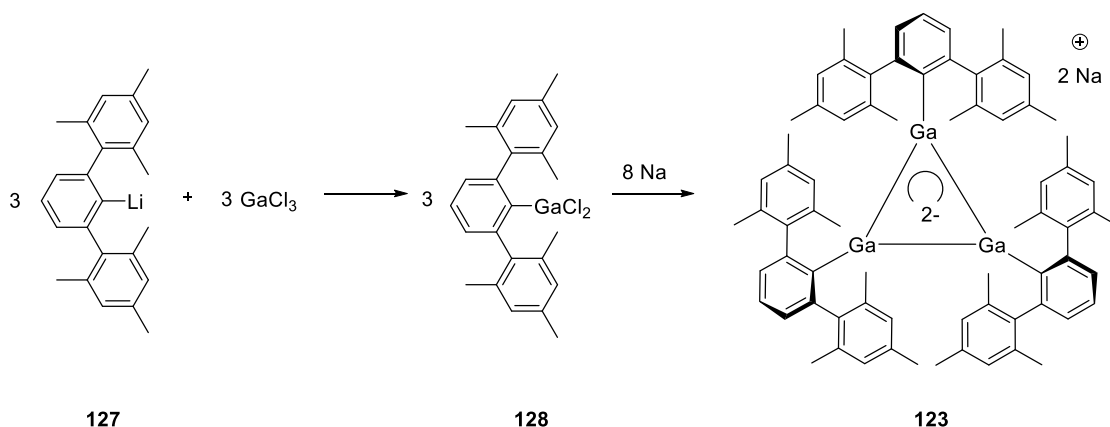
⁹⁵ H.-J. Zhai, B. B. Averkiev, D. Y. Zubarev, L.-S. Wang, A. I. Boldyrev, *Angew. Chem. Int. Ed.*, **2007**, *46*, 4277-4280.

2.1.2.3. Stable triangular all-metal aromatics

Since its opening 50 years ago, numerous triangular clusters have been deposited in the Cambridge Crystallographic Data Center. Though their numbers increased a lot these past years, only a few of them are metalloaromatics and will be shortly described in the following sessions.

2.1.2.3.1. Robinson trigallium cluster

In 1995, Robinson and coworkers⁸⁵ published the structure of a twice negative charged gallium triangle in which each gallium atom bears a bulky 2,6-mesitylphenyl ligand. The cluster was obtained from gallium trichloride and 2,6-mesitylphenyl lithium **127** and it was isolated in 50% yield after two steps (Scheme 26). This synthesis is however not easy to handle because it employs sensitive and harmful reagents. They required furthermore a glovebox to be safely manipulated.



Scheme 26 : Synthesis of Robinson's cyclogallene.

The trigallium core composes an equilateral triangle in which the three Ga-Ga-Ga angles are perfectly equal to 60°. All Ga-Ga bond lengths are equal to 2.441 Å. This is smaller than the Ga-Ga single bond of the dimer $[(\text{Me}_3\text{Si})_2\text{CH}]_2\text{Ga}]_2$ previously synthesized and than the diameter of gallium metal, 2.541 Å and 2.70 Å, respectively. Interestingly, the position of the two sodium atoms are above and below the triangular plane. They are arranged in a perfect trigonal pyramid in which the distance $[\text{Ga}_3]\text{-Na}$ is 3.220 Å. Concerning electronical properties, the gallium core can be considered as the association of two Gallium(0) with one Gallium(I). According to its π -aromatic character provided by 3p-orbitals of Gallium, it can

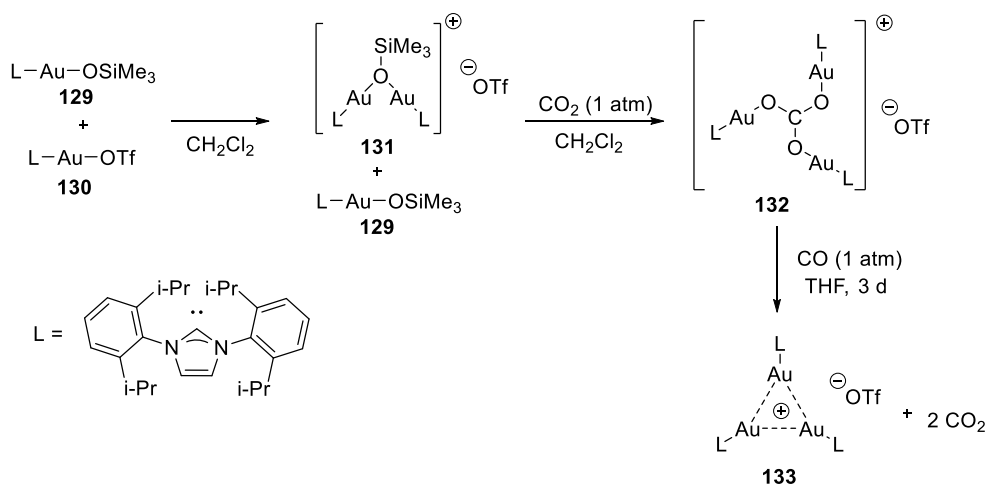
be also described as three Gallium(I) with two delocalized electrons. Anyway, the formal oxidation state of each gallium atom is not an integer but $1/3$ because there are two negative charges delocalized on three metallic centers. Compound **123** was the first π -aromatic all-metal analogue of the cyclopropenyl cation $[\text{C}_3\text{H}_3]^+$.

2.1.2.3.2. (tris)gold clusters

Very recently, Sadighi and Bertrand independently reported two different approaches towards aromatic (tris)gold complexes.

2.1.2.3.2.1. Sadighi's approach

In 2012, Sadighi and coworkers reported the synthesis of a (tris)gold monocation⁹⁶ which is an isolobal analogue of the $[\text{H}_3]^+$ cation. This cationic species bears a bulky NHC carbene ligand on each gold atom. The synthesis depicted on scheme 26 starts from two gold complexes **129** and **130** which forms the cationic siloxide-bridged digold cluster **131**. This intermediate reacts with another equivalent of **129** under a carbon dioxide atmosphere to give the cationic (tris)gold carbonate **132**. The slow reduction of **132** under a carbon monoxide atmosphere at room temperature provides the desired (tris)gold cluster **133** with 41% yield. However, a glovebox is also needed to prevent its decomposition by oxygen and moisture, as for Robinson's synthesis for $[\text{Ga}_3]^{2-}$.



Scheme 27 : Synthesis of Sadighi's (tris)gold cluster.

⁹⁶ T. J. Robilotto, J. Basca, T. G. Gray, J. P. Sadighi, *Angew. Chem. Int. Ed.*, **2012**, *51*, 12077-12080.

Contrary to what one might think, the (tris)gold core is not an equilateral triangle. Au-Au bonds are between 2.644 and 2.663 Å and the angles between 59.60° and 60.33°. Despite bond lengths are not equal, the σ -type highest occupied molecular orbital represented in figure 32, composed mainly from 5s orbitals of gold atoms, shows a completely delocalization of electron density on the three gold atoms. This is consistent with the presentation of this molecule as a σ -aromatic one.



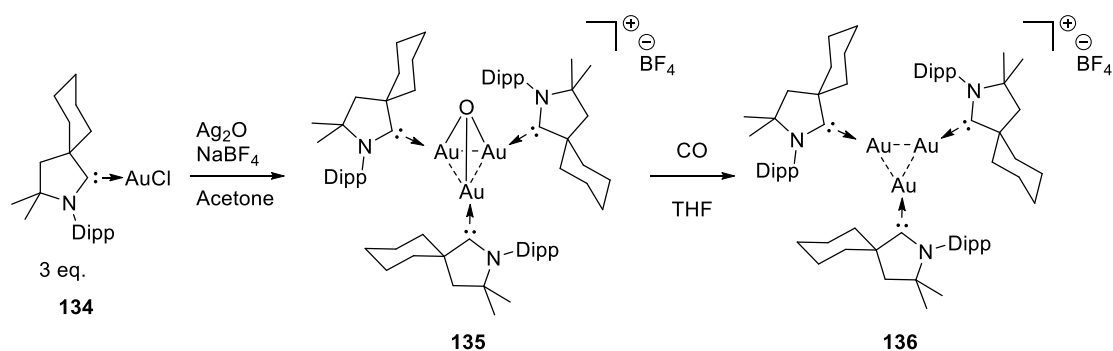
Figure 32 : Highest occupied molecular orbital of the simplified (tris)gold cation.

Furthermore, this cluster possesses a significant gap between its frontier orbitals of 5.42 eV, which is reminiscent of that found in $[\text{H}_3]^+$ and that makes this species relatively inert. Following the same principles of **123**, the formal oxidation state of each gold atom is +1/3.

2.1.2.3.2.2. Bertrand's approach

In 2014, Bertrand and coworkers proposed another method to synthesize a similar tris(gold) cluster (Scheme 28) by using cyclic (alkyl)(amino)carbenes (CAAC).⁹⁷ The reduction of **134** with Ag_2O in presence of NaBF_4 affords the (tris)gold based pyramid **135**. By putting **135** under a carbon monoxide atmosphere, a subsequent reduction step occurs to provide the desired product **136**.

⁹⁷ L. Jin, D. S. Weinberger, M. Melaimi, C. E. Moore, A. L. Rheingold, G. Bertrand, *Angew. Chem. Int. Ed.*, **2014**, *126*, 9205-9209.

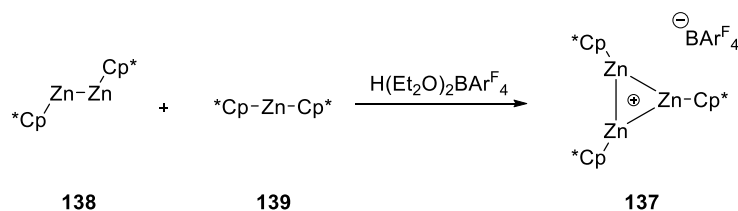


Scheme 28 : Bertrand's synthesis of (tris)gold clusters.

Bertrand stated that **136** is indefinitely air and moisture stable compared to **133**. This could be attributed to the chosen CAAC ligands⁹⁸ which are more electron donor than NHCs or phosphines and thus give a better stabilization to the cluster.

2.1.2.3.3. Fischer's trizinc clusters and zinc-copper heteroaromatics

Very recently, Fischer reported a (tris)zinc cluster⁹⁹ analogous of $[\text{H}_3]^+$ as Sadighi's and Bertrand's gold complex. Cluster **137** shown on figure 33, was synthesized by the condensation of Carmona's compound $[\text{Zn}_2\text{Cp}^*_2]$ **138** with $[\text{ZnCp}^*_2]$ **139** in presence of a stabilized boric acid derivative. In spite of a degradation of the starting material during the dissolution process, the desired cluster, when formed, has a rather slow decomposition rate and can be isolated.

Figure 33 : Fischer's (tris)zinc σ -aromatic cluster.

$[\text{Zn}_3]^+$ reveals almost perfect equilateral triangle with angles between 59.22° and 61.06° . The Zn-Zn bond lengths are almost identical with an average of $2.430(1) \text{ \AA}$ which is a little

⁹⁸ a) M. Melaimi, M. Soleilhavoup, G. Bertrand, *Angew. Chem. Int. Ed.*, **2010**, *49*, 8810-8849. b) D. Martin, M. Melaimi, M. Soleilhavoup, G. Bertrand, *Organometallics*, **2011**, *30*, 5304-5313.

⁹⁹ K. Freitag, C. Gemel, P. Jerabek, M. I. Oppel, R. W. Seidel, G. Frenking, H. Banh, K. Dilchert, R. A. Fischer, *Angew. Chem. Int. Ed.*, **2015**, *54*, 4370-4374.

bit longer than 2.305 Å in **138**. The σ -aromaticity of the triangle has been shown by NICS calculations which provided negatives values perpendicular to the plane of the ring.

Interestingly, by replacing ZnCp^*_2 **139** with $[\text{CuCp}^*]$ engendered *in situ* from the reaction between CuCl and LiCp^* , the formation of a new type of neutral heterocluster composed by two zinc and one copper atoms was observed.

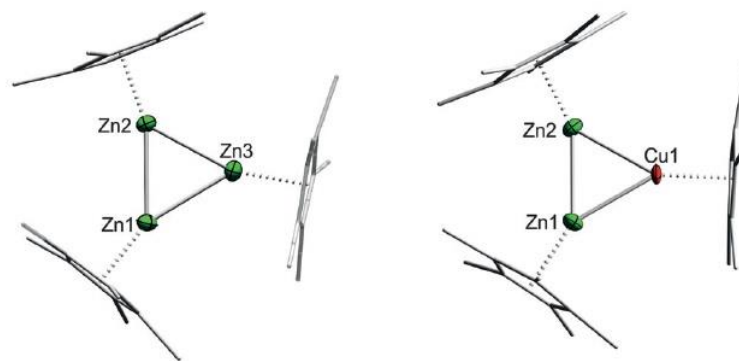


Figure 34 : Crystal structures of $[\text{Zn}_3]^+$ (left) and $[\text{Zn}_2\text{Cu}]$ (right).

This compound possesses similar properties to the tris(zinc) **137** even though its core is an isosceles triangle (Figure 34). Both Cu-Zn-Zn angles are of 60.34° whilst the Zn-Cu-Zn angle is of 59.33° . The two Cu-Zn bond distances (2.381 Å) are slightly shorter than in **137** and so as the Zn-Zn bond, which was 2.357 Å. The negative NICS values also confer an σ -aromatic character to this heterocluster. However these compounds are unfortunately not stable at room temperature and neither to air and moisture.

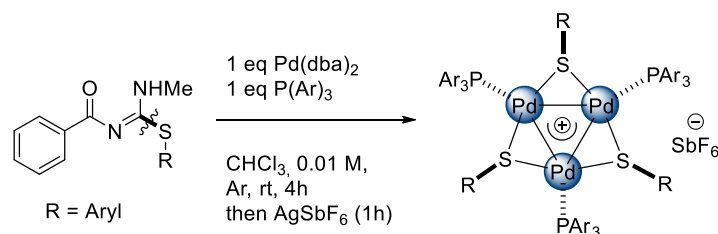
2.1.2.3.4. Maestri's tripalladium cluster

2.1.2.3.4.1. First generation synthesis

The structure of novel Pd_3^+ clusters was serendipitously found when our team was investigating the oxidative addition ability of the C-S bond of isothiourreas on low valent palladium complexes. The first generation synthesis of the Tripod cluster was realized with reaction conditions depicted in scheme 29.¹⁰⁰ The isothiourrea reacts with one equivalent of $\text{Pd}(\text{dba})_2$ and one equivalent of triarylphosphine in degassed dichloromethane under argon

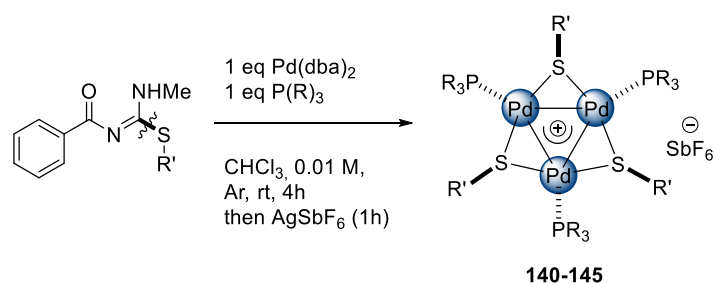
¹⁰⁰ S. Blanchard, L. Fensterbank, G. Gontard, E. Lacôte, G. Maestri, M. Malacria, *Angew. Chem. Int. Ed.* **2014**, 53, 1987-1991.

atmosphere. After adding silver hexafluoroantimonate at full conversion, the cluster can be isolated in the form of red powder after filtration and washings with cold diethylether. In contrast with previously reported all-metal aromatic clusters, these powders revealed to be very stable to air and moisture and can be stored without any drastic precautions. In comparison with Boldyrev's work,⁹⁵ this new family of tripalladium clusters is the first stable and isolable δ -aromatic species analogue of the cyclopropenyl cation.



Scheme 29 : Pd₃⁺ tripod first generation synthesis.

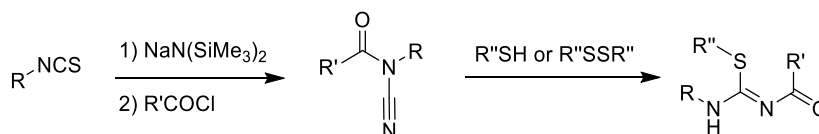
The formation of this triangular cluster seems to occur *via* oxidative addition of isothioureas's C-S bond on palladium(0) because only the presence of the thiolate moiety is observed in the final product. Whatever the nature of the aryl substituents R and R' (electron-donor or electron-withdrawing), this methodology provides Pd₃⁺ clusters **140-145** with good yields (Table 4).



Entry	R'	R	Product / isolated yield
1	4-Me-C ₆ H ₄ -	4-F-C ₆ H ₄ -	140 (93%)
2	4-Me-C ₆ H ₄ -	4-Me-C ₆ H ₄ -	141 (84%)
3	4-NH ₂ -C ₆ H ₄ -	4-F-C ₆ H ₄ -	142 (75%)
4	Ph	Ph	143 (88%)
5	4-MeO-C ₆ H ₄ -	Ph	144 (81%)
6	4-Cl-C ₆ H ₄ -	4-Me-C ₆ H ₄ -	145 (91%)

Table 4 : Synthesis of Tripod Pd₃⁺ clusters from isothioureas.

With this strategy, only clusters with aryl substituents could be obtained. If an alkyl phosphine or an alkyl isothiourea is used, intractable mixtures and very poor yield were observed. Despite the good selectivity towards the formation of the desired clusters, the synthesis of the isothioureas reveals to be much less convenient. According to the procedure reported by our group,¹⁰¹ isothioureas could be obtained in two steps from isothiocyanates derivatives (Scheme 30).



Scheme 30 : Synthesis of isothioureas in two steps from isothiocyanates.

This methodology provides differently substituted isothioureas with yields between 19 and 93% in a fast and convenient manner. For our cluster synthesis however, this procedure is not that effective because only the thiolate moiety of the starting material is kept in the palladium complex structure. This strategy is thus not atom-economic and need to be improved.

2.1.2.3.4.2. Steric and electronic properties

Our cluster of interest possesses a core of three palladium atoms perfectly arranged in an equilateral triangle. Each palladium atom bears a phosphine group and two palladium atoms are respectively bridged by a thiolate moiety (Figure 35 left).

¹⁰¹ a) G. Maestri, M.-H. Larraufie, C. Ollivier, M. Malacria, L. Fensterbank, E. Lacôte, *Org. Lett.*, **2012**, *14*, 5538-5541. b) M.-H. Larraufie, G. Maestri, M. Malacria, C. Ollivier, L. Fensterbank, E. Lacôte, *Synthesis*, **2012**, *44*, 1279-1292.

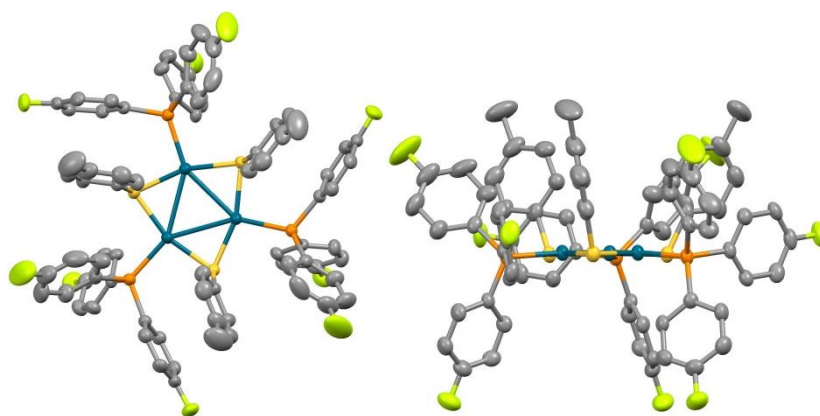


Figure 35 : X-Ray picture of Pd₃⁺ cluster 140.

Sulfur atoms are coplanar to the palladium core (Figure 34 right) and their substituents are nearly perpendicular to the plane (about 112.3°). For further understanding, it is important to point out that the distance between *ortho*-hydrogens on the tolyl group borne by the sulfur atom and the tripalladium plane is about 2.89 Å. About interatomic distances, all the Pd-Pd bonds have the same length at 2.8872 Å, which is clearly shorter than the sum of the Palladium van der Waals radii (3.26 Å). The angles of the palladium core have the same value of 60° and confer D_{3h} symmetry to the core of the cluster. The dihedral angle of 8.2° indicates that phosphorous atoms deviate slightly from the plane of the palladium core.

Concerning electronic properties, this cluster count 44 valence electrons that is quite rare among previously reported Pd₃ clusters. Only eight of them have the same electronic configuration and among them, our palladium tripod family is the only one which displays an equilateral kernel and overall C₃ symmetry. Formally, the triangular core is composed by two palladium(I) and one palladium(II) atoms, which carries a positive charge. Because of its high symmetry, it could be better regarded as a triangle that features metal in the +4/3 formal oxidation state. DFT calculations were achieved on **143** and relevant molecular orbitals are illustrated in figure 36. Energies are given relative to the HOMO and phenyl substituents are omitted for clarity.

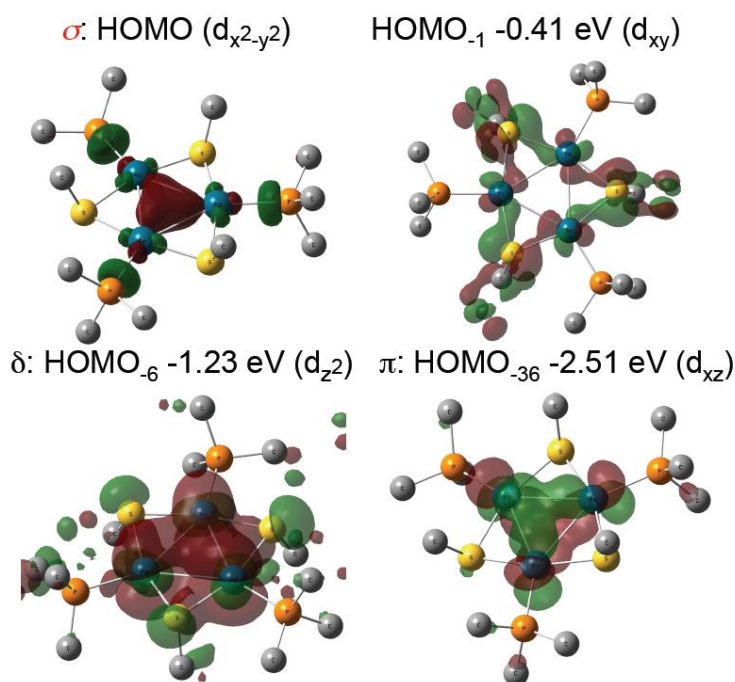


Figure 36 : Pictures of relevant molecular orbitals of 143.

According to its symmetry, the HOMO is a σ -type bonding orbital, clearly delocalized on the three palladium centers and results from the main contribution of the $d_{x^2-y^2}$ atomic orbitals of palladium atoms (Figure 36 top left). HOMO^{-1} at -0.41 eV represents a bonding MO in which the d_{xy} atomic orbitals are mainly involved in the back-donation from metals to the thiolate substituents (Figure 36 top right). Orthogonal to the core's plane, d_{z^2} orbitals provide HOMO^{-6} which lies at -1.23 eV below the HOMO (Figure 36 bottom left) and is a bonding δ -type molecular orbital. Indeed, it possesses two nodal surfaces perpendicular to the C_3 axis and a symmetry plane that contain the palladium core. It is commonly observed that in many Pd(II) dimers, their square planar configuration is not suitable to an adequate overlapping of d_{z^2} orbitals and this leads to increase the energy level of the corresponding molecular orbital, which is usually the HOMO instead.¹⁰² In the case of our cluster, the overlapping of these atomic orbitals is optimal and thus reduces the energy level of the corresponding MO. The last represented molecular orbital is the HOMO^{-36} which arises from the combination of d_{xz} AO and whose symmetry makes it a π -type bond (Figure 36 bottom right). This molecular orbital is also delocalized on the three palladium centers.

¹⁰² M. Weber, J. E. M. N. Klein, B. Miehlich, W. Frey, R. Peters, *Organometallics*, **2013**, 32, 5810-5817. b) T. Murahashi, H. Kurosawa, *Coord. Chem. Rev.*, **2002**, 231, 207-228, c) L. M. Mirica, J. R. Khusnutdinova, *Coord. Chem. Rev.*, **2013**, 257, 299-314. d) Y. Kajitani, K. Tsuge, Y. Sasaki, M. Kato, *Chem. Eur. J.*, **2012**, 18, 11196-11200. e) J. E. Bercaw, A. C. Durrell, H. B. Gray, J. C. Green, N. Hazari, J. A. Labinger, J. R. Winkler, *Inorg. Chem.*, **2010**, 49, 1801-1810. f) C. Eerdun, S. Hisanaga, J.-I. Setsune, *Angew. Chem. Int. Ed.*, **2013**, 52, 929-932. g) T. Murahashi, K. Takase, M.-A. Oka, S. Ogoshi, *J. Am. Chem. Soc.*, **2011**, 133, 14908-14911.

DFT calculations brought us another data which is interesting and strange at the same time. The measurement of the quadrupole moment, in fact the component towards z axis of the magnetic tensor, leads to a value of -52 Buckingham, which is largely negative. It is stated in the literature that molecules having a large negative quadrupolar moment possess a Lewis-basic character and thus should bind other cations. However, the palladium core also bears a delocalized positive charge which gives to it a Lewis-acidic character. These characteristics are reminiscent of Frustrated Lewis Pairs (FLP) which are pairs of molecules containing Lewis acid and Lewis base moieties. These observations will be discussed more thoroughly in the next part.

Nucleus independent chemical shifts (NICS) were calculated on **143** and also on its theoretical tricationic analogue in which the two electrons of the HOMO were voluntarily removed. The results are plotted in figure 37.

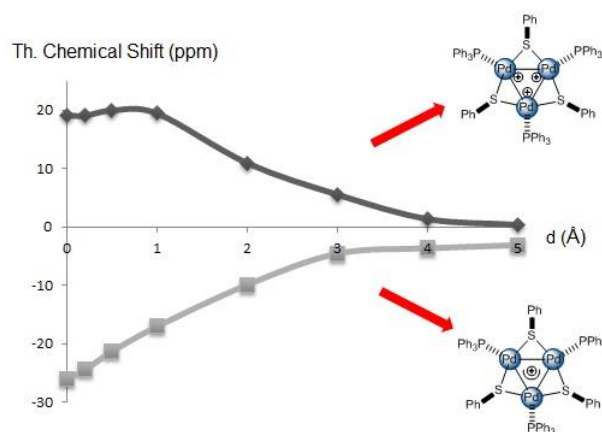


Figure 37 : NICS_{zz} calculations for complex **143** and its tricationic analogue.

Calculated chemical shifts for **143** showed to be negative from 0 to 5 Å above the palladium core plane. According to NICS theory, these results are in agreement with the presence of an aromatic ring current. Interestingly, the same calculations for the tricationic analogue of **143** showed positive theoretical chemical shifts at the same distances. As expected, the removal of two electrons of the HOMO resulted in the loss of the aromatic character of the cluster.

Concerning classical analysis, the tripalladium pattern coupled with its monocationic charge makes this cluster easily suitable for ESI-MS analysis (Figure 38).

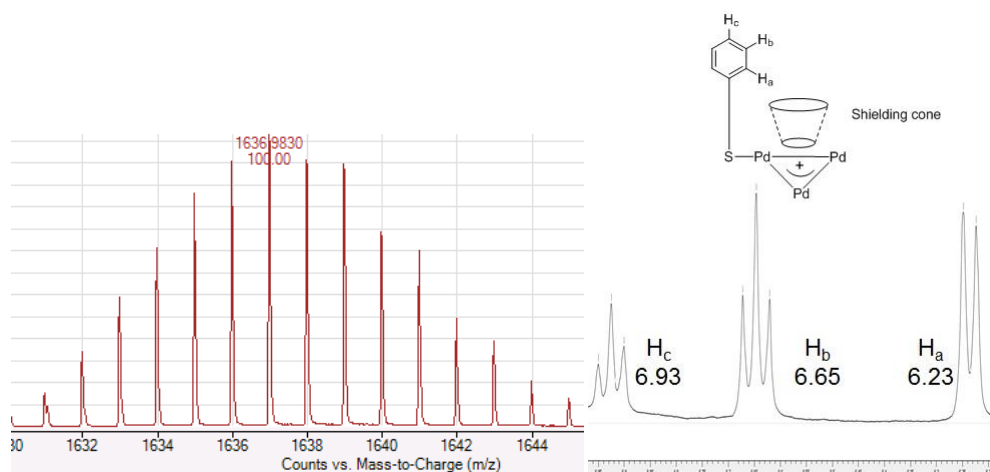


Figure 38 : Isotopic pattern of complex **140** in ESI-MS analysis (Left). NMR spectrum of phenylthiolate substituent in complex **143** (Right).

Besides its heavy molecular weight, the peculiar isotopic pattern of this cluster is very characteristic and renders it easy to identify (Figure 38 Left). Moreover, the NMR spectrum of thiolate substituents (Figure 38 Right) shows a particular chemical shift distribution. In most of palladium-thiolate clusters, chemical shifts lie in the area between 6.80 and 7.50 ppm and the distribution is usually in the *ortho/para/meta* order (from lower chemical shift to the higher) thanks to the inductive effect of the sulfur atom. In the case of our tripalladium cluster, the chemical shift is in *ortho/meta/para* order instead and this can be explained by the presence of a shielding cone perpendicular to the palladium-containing plane. Indeed, in every aromatic system, electron delocalization creates a magnetic field that can affect the electronic environment of each atom included in it even though its effect decreases with the distance.

To have more information on the electronic structure of this new family of clusters, measurements of magnetic susceptibility were realized by SQUID experiments on complex **143**. Usually, SQUID experiments are a tool to enhance the paramagnetic or the diamagnetic properties of chemical species.¹⁰³ For example, spin $\frac{1}{2}$ paramagnetic radical molecules such as 2,2,6,6-tetramethylpiperidin-1-oxyl (TEMPO) have a magnetic susceptibility value χT of 0.5 emu.K.mol⁻¹ at 300K. This value decreases proportionally with the temperature to zero value at 0 K. On the contrary, diamagnetic molecule does not exhibit magnetic susceptibility with a χT of 0 emu.K.mol⁻¹. Complex **143** showed an intermediate value of 0.41 emu.K.mol⁻¹ and also proved to be independent of the temperature between 300 and 20 K. The same

¹⁰³ a) J. Aihara, *J. Am. Chem. Soc.*, **2006**, *128*, 2873-2879. b) F. De Proft, P. v. R. Schleyer, J. H. van Lenthe, F. Stahl, P. Geerlings, *Chem. Eur. J.*, **2002**, *8*, 3402-3410. c) A. R. Katritzky, P. Barczynski, G. Musumarra, D. Pisano, M. Szafran, *J. Am. Chem. Soc.*, **1989**, *111*, 7-15.

peculiar observations were made for other species presenting π -electrons ring currents.¹⁰⁴ In agreement with these data, the presence of a ring current in diamagnetic complex **143** was justified.

2.2 Results and discussions

2.2.1. Aim of the project

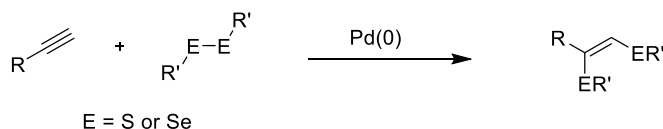
The previously described δ -aromatic tripalladium clusters were isolated in our team starting from isothioureas. However the way to get these compounds was not convenient and the first part of the project was to improve this synthesis. The second part concerned the extension of the synthesis towards analogues of the tripod cluster in order to verify if the principle of δ -aromaticity could be extend to heteroclusters, like Fischer proved for σ -aromaticity with $[\text{Zn}_3]^+$ and $[\text{Zn}_2\text{Cu}]$. The third part was to study the predicted Lewis-basic ability of the $[\text{Pd}_3]^+$ cluster to bind other cations in order to confirm or invalidate DFT results. The fourth part of the project was to exploit the stability of the cluster coupled with its potential Lewis dual-nature in order to realize the first catalytic application of an all-metal aromatic complex. This latest will be described in Part 3 of this manuscript.

2.2.2. Second generation synthesis of tripalladium clusters

The synthesis of palladium tripod from isothioureas was serendipitously found when our team was interested on the activation of carbon-sulfur bonds. However, the isolated product only bore the thiolate moiety. According to the fact that isothioureas are difficult to synthesize even with the methodology well developed in our group,¹⁰¹ we were concerned by the atom-economy of this synthesis. The loss of the aminoacetamide moiety during the process was a problem that we had to overcome. Moreover, the synthesis of tripalladium clusters using S-alkyl isothioureas led to intractable mixtures. It would be very appropriate to find a new way to synthesize our complex of interest by merging a more atom-economic process and a more substituent-tolerant synthesis.

¹⁰⁴ J. Jusélius, D. Sundholm, *Phys. Chem. Chem. Phys.*, **2000**, 2, 2145-2151.

To bypass these problems, we turned ourselves towards the activation of disulfides by transition metals. It is known since decades that palladium(0) can catalyze the addition of disulfides or diselenides on terminal alkynes (Scheme 31).¹⁰⁵



Scheme 31 : Disulfide or diselenide addition on terminal alkynes catalyzed by palladium(0).

Ananikov *et al.*¹⁰⁶ studied the mechanism and found that a palladium(II) dimeric species (Figure 39) was involved in the reaction as proposed by Graziani¹⁰⁷ several years ago.

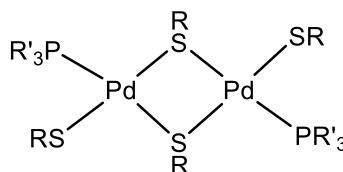
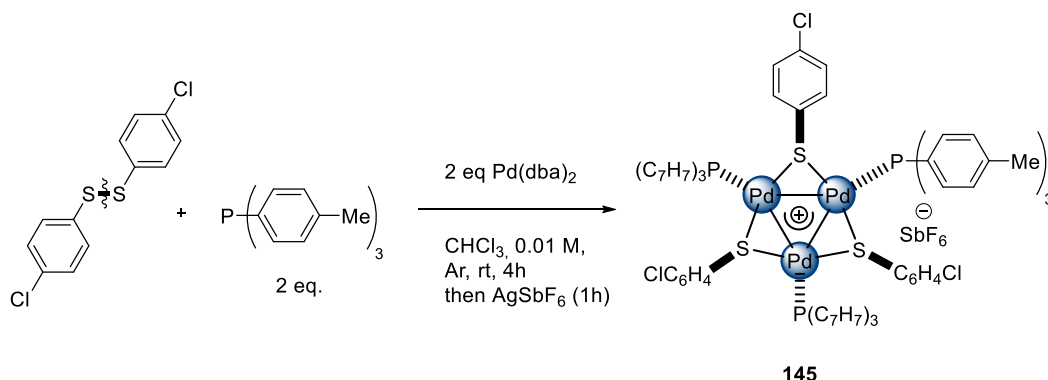


Figure 39 : Dimeric palladium(II) specie.

These works showed that palladium(0) is able to activate S-S bond and thus we decided to test this method in order to get the palladium tripod cluster. The first experiment that we tried was performed with one equivalent of 4-chlorophenyldisulfide, two equivalents of tri(*p*-tolyl)phosphine and two equivalents of Pd(dba)₂ in degassed chloroform (Scheme 32). In contrast with the first generation synthesis, reactions in dichloromethane did not work.



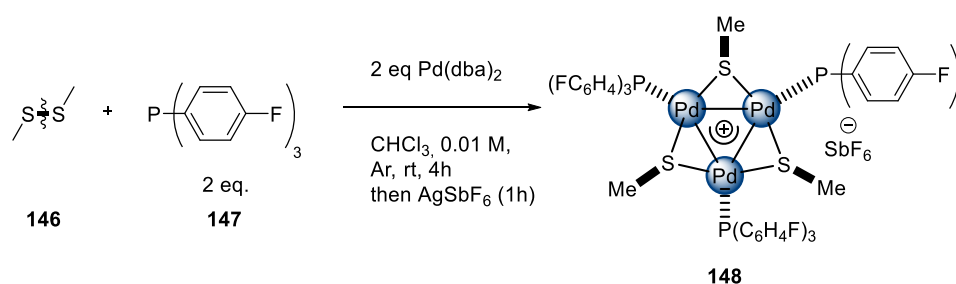
Scheme 32 : First trial involving disulfide as starting material.

¹⁰⁵ I. Beletskaya, C. Moberg, *Chem. Rev.*, **1999**, 99, 3435-3461.

¹⁰⁶ V. P. Ananikov, M. A. Kabeshov, I. P. Beletskaya, G. G. Aleksandro, I. L. Eremenko, *J. Organomet. Chem.*, **2003**, 687, 451-461

¹⁰⁷ R. Zanella, R. Ros, M. Graziani, *Inorg. Chem.*, **1973**, 12, 2736-2738.

After four hours stirring in chloroform at room temperature, the starting dark violet solution turned to dark orange and we were excited to observe the formation of the desired cluster almost without formation of any byproduct in crude ^1H NMR analysis. After addition of silver hexafluoroantimonate, we managed to purify the complex by the reported method. After evaporation of the solvent, the resulting dark brown solid was washed with cold diethyl ether *via* canula. The dark red solid obtained was solubilized in THF and filtered through a celite pad. THF was removed *in vacuo* and the desired cluster was isolated as red solid with 89% yield. We were particularly satisfied to observe that this method worked well with good selectivity starting from commercially available reagents in a one-pot procedure. Just by curiosity, we then wanted to go further and test other disulfides, especially alkyl ones, in order to synthesize other examples of $[\text{Pd}_3]^+$. We thus did the same reaction with dimethyl disulfide **146** and tri(4-Fluorophenyl)phosphine **147** (Scheme 33).



Scheme 33 : First experiment with dialkyl disulfide.

Crude ^1H NMR and ESI-MS analyzes of this sample were beyond our expectation. The starting material was totally consumed, the major product being tripalladium triangle **148** together with traces of phosphine oxide were observed. We managed to do the usual treatment to remove the excess of dibenzylideneacetone (dba) in order to purify the cluster but we observed that the cluster was partially soluble in cold diethyl ether (Table 5, Entry 1). According to this observation, another purification method needed to be found.

Entry	Solvent	Temperature (°C)	Observations
1	Et ₂ O	-78	148 partially soluble
2	MTBE	-78	Nothing soluble
3	MTBE	rt	148 partially soluble
4	<i>n</i> -hexane	-78	Nothing soluble
5	<i>n</i> -hexane	rt	dba soluble
6	<i>n</i> -pentane	-78	dba partially soluble
7	<i>n</i> -pentane	rt	dba soluble

Table 5 : Optimization of the purification step for complex 148.

We first thought that diethyl ether was a too polar solvent so we chose to try several less polar solvents, such as methyl *tert*-butyl ether (MTBE). MTBE at -78 °C did solubilize neither dba nor **148** while the same solvent at room temperature solubilized both. Indeed, ¹H NMR analysis of the fraction showed the presence of the cluster (Table 5, Entries 2 & 3). We then chose to use even less polar solvents. By using *n*-hexane at -78 °C, nothing was soluble. At room temperature, dba was slightly soluble but the cluster was not (Table 5, Entries 4 & 5). The use of several liters of *n*-hexane permitted us to isolate the desired complex with high yields, but through this method, the “green” side of our new synthesis would be badly affected. *n*-pentane solubilized dba at -78 °C and at room temperature (Table 5, Entries 6 & 7) but we could not use this solvent for the same reasons presented before for *n*-hexane.

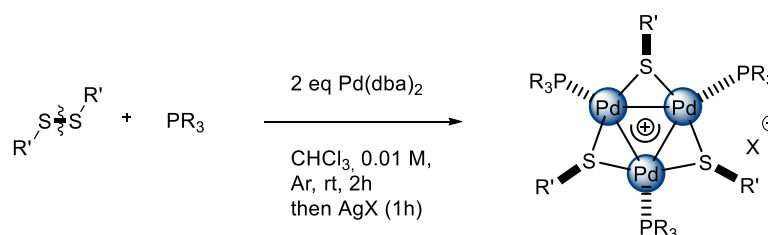
Not satisfied by these results, we then decided to search further. Instead of purifying the cluster by several washings, a precipitation method could be more appropriate. After evaporation of chloroform, the resulting solid is solubilized in the minimal quantity of polar solvent (Solvent A) and then an apolar solvent (Solvent B) is added under strong stirring. The results obtained with this method at room temperature are reported in table 6. The presented ratio of A/B volumes was evaluated after total precipitation; technically, if we stop stirring, big size orange-red particles should go down the Schlenk, releasing a limpid yellow solution.

Entry	Solvent A	Solvent B	Ratio A/B
1	Et ₂ O	<i>n</i> -hexane	1/42 ¹⁰⁸
2	MTBE	<i>n</i> -hexane	1/50
3	CHCl ₃	<i>n</i> -hexane	1/30
4	THF	<i>n</i> -hexane	1/46

Table 6 : Optimization of the precipitation method.

We tested four polar solvents coupled with *n*-hexane. According to the observed results, oxygen-containing solvents at room temperature were less efficient than chloroform to precipitate this cluster. Even if diethyl ether at 0 °C leads to the precipitation with a volume ratio of 1/30, we chose to keep the chloroform/*n*-hexane duet for the following of our studies.

Having this new method of purification in hands, we then applied it to the synthesis of other clusters (Table 7).



Entry	Complex	R'	R	X	Yield 1 st generation synthesis	Yield 2 nd generation synthesis
1	140	4-Me-C ₆ H ₄ -	4-F-C ₆ H ₄ -	SbF ₆ ⁻	93	89%
2	143	Ph-	Ph-	SbF ₆ ⁻	88	99%
3	145	4-Cl-C ₆ H ₄ -	4-Me-C ₆ H ₄ -	SbF ₆ ⁻	91	97%
4	149	4-Cl-C ₆ H ₄ -	4-F-C ₆ H ₄ -	SbF ₆ ⁻	-	90%
5	150	4-Cl-C ₆ H ₄ -	4-Me-C ₆ H ₄ -	F ₃ CCO ₂ ⁻	-	89%
6	151	4-Cl-C ₆ H ₄ -	4-MeO-C ₆ H ₄ -	SbF ₆ ⁻	-	80%
7	148	Me-	4-F-C ₆ H ₄ -	SbF ₆ ⁻	-	85%
8	152	Me-	4-Me-C ₆ H ₄ -	SbF ₆ ⁻	-	94%
9	153	4-Me-C ₆ H ₄ -	Et-	SbF ₆ ⁻	-	98%
10	154	4-Cl-C ₆ H ₄ -	Et-	SbF ₆ ⁻	-	97%

Table 7 : Straightforward synthesis of tripod clusters.

¹⁰⁸ The precipitation at 0 °C with Et₂O/*n*-hexane worked at a ratio 1/30 (v/v).

We first wanted to obtain clusters which were synthesized with the first generation method in order to compare the efficiency of the synthesis (Table 7, Entries 1 to 3). Despite cluster **140** get a 4% lower yield than the first generation synthesis, **143** and **145** were isolated instead with almost quantitative yields. Classical NMR and mass analyses revealed to be the same and this proved that the second generation is at least as efficient as the first one. The synthesis tolerates others silver salts (Table 7, Entry 5) and other donating groups on phosphines (Table 7, Entry 6). The use of alkyl disulfides such as the dimethyl one worked well and complexes **148** and **152** were isolated in 85 and 94% yields respectively (Table 7, Entries 7 & 8). Full of joy at the belief of seeing results with alkyl disulfides, we decided to test the reaction with an alkyl phosphine (Table 7, Entries 9 & 10). Even though clusters **153** and **154** are a little less stable to air and moisture, excellent isolated yields of 98 and 97% respectively were achieved.

Regarding X-ray analyses, all clusters possess a C_3 symmetry and a nearly D_{3h} symmetric core. Pd_3 is arranged in a perfect equilateral triangle with Pd-Pd-Pd angles of 60° and a single Pd-Pd distance. The latter is always below the sum of their Van der Waals radii. **152** presents Pd-Pd distances at 2.8419(6) Å, which are smaller than that of S-aryl cluster **145** at 2.8731(8) Å (Table 7, Entries 3 & 7). This difference could be explained by the steric hindrance that is more important in the case of S-aryl clusters than in S-methyl ones.

Good to excellent yields were observed for the synthesis of tripalladium aromatic clusters in a one pot procedure and starting from commercially available reagents. The robustness and the flexibility of this synthesis have been tested and it tolerates alkyl and aryl substituents that the first generation synthesis could not support. To go further, we proposed to extend this outstanding methodology to the creation of analogues of $[Pd_3]^+$ clusters.

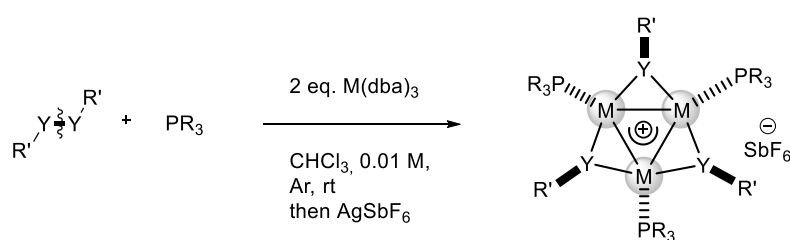
2.2.3. Toward the synthesis of analogues of $[Pd_3]^+$

At this point, we hoped that our methodology could be extended to other clusters. According to Beletskaya *et al.*,¹⁰⁶ palladium(0) easily undergoes oxidative addition on disulfides but also on diselenide which can be a good starting point to our trials. In another

side nickel and platinum are valence isoelectronic to palladium and could provide the same reactivity. This work was realized in collaboration with Dr. Yanlan Wang.¹⁰⁹

2.2.3.1. Analogues.

To extend our methodology to platinum analogues, we first had to synthesize $\text{Pt}(\text{dba})_3$ by using standard procedure reported in the literature.¹¹⁰ This compound in hands, we put it in reaction in order to get $[\text{Pt}_3]^+$ (Table 8).



Entry	Complex	R'	R	M	Y	Yield
1	155	4-Cl-C ₆ H ₄ -	4-F-C ₆ H ₄ -	Pt	S	60%
2	156	Me-	4-Me-C ₆ H ₄ -	Pt	S	40%
3	157	Ph-	4-F-C ₆ H ₄ -	Pd	Se	50%
4	158	Ph-	4-F-C ₆ H ₄ -	Pt	Se	41%

Table 8 : Synthesis of analogue clusters of $[\text{Pd}_3]^+$.

Our methodology permitted us to obtain two examples of triplatinum clusters. **155** and **156** (Table 8, Entry 1 & 2) were isolated in 60 and 40% yields respectively. We also tried reactions with diphenyl diselenide in order to insert another bridging atom in the complex structure. Syntheses of selenide-bridged tripalladium **157** and triplatinum **158** were achieved in moderate 50 and 41% yields. All these clusters possessed a perfectly triangular core with a unique M-M bond length and angles of 60° as the original Pd_3 complex. They also expressed an overall C_3 symmetry and a nearly D_{3h} -symmetric core. Metals and heteroatoms were nearly coplanar, with a largest dihedral angle below 5°. By comparison to its palladium analogue **152** ($\text{Pd-Pd} = 2.8419(6) \text{ \AA}$), metal-metal bond lengths were just slightly longer in **156**, with Pt-Pt distances equal to $2.8672(7) \text{ \AA}$ (Table 7, Entry 8 and Table 8, Entry 2). This curious

¹⁰⁹ Y. Wang, P.-A. Deyris, T. Caneque, F. Blanchard, Y. Li, F. Bigi, R. Maggi, S. Blanchard, G. Maestri, M. Malacria, *Chem. Eur. J.*, **2015**, *31*, 12271-12274.

¹¹⁰ L. T. Kliman, S. N. Mlynarski, J. P. Morken, *J. Am. Chem. Soc.*, **2010**, *132*, 13949-13949. H. E. Burks, L. T. Kliman, J. P. Morken, *J. Am. Chem. Soc.*, **2009**, *131*, 9134-9135.

observation could be attributed to the lanthanide contraction effect.¹¹¹ Replacing the thiolate-bridge by a selenide-bridge increased the size of triangular core. The Pd-Pd distance is 2.9302(8) Å in **157** instead of 2.8731(8) Å found for **149** (Table 7, Entry 4 and Table 8, Entry 3).

Technically speaking, triplatinum clusters are less easy to obtain. Indeed, purification by precipitation removed efficiently the dibenzylideneacetone but the reaction provides platinum containing byproducts which can only be removed by flash chromatography. Unfortunately, several species including our cluster of interest have almost the same polarity on silica. This meant that at least four chromatography columns are required to isolate the pure product.

Measurements of magnetic susceptibility by SQUID for $[\text{Pt}_3]^+$ **155** were comparable to those observed for $[\text{Pd}_3]^+$ **149** (0.44. emu.K.mol⁻¹ at 300K).¹⁰⁰ **155** had χT of 0.48 emu.K.mol⁻¹ at 300K and thus confirmed the presence of cyclic electron delocalization.

Even if analogues of $[\text{Pd}_3]^+$ were isolated with modest yields, the methodology proved its feasibility in term of tolerance of functional groups. According to the fact that platinum has isoelectronic properties of palladium, we wondered that if we could be able to synthesize mixed bimetallic Pd/Pt clusters in order to study their metal-metal bonding.

2.2.3.2. Mixed palladium and platinum heteroclusters

In the large library of trimetallic-core complexes, almost 300 X-ray structures contains Pd₃ or Pt₃ triangle pattern. However, no PdPt₂ cluster has been reported yet and only two clusters containing the Pd₂Pt core were described (Figure 40).

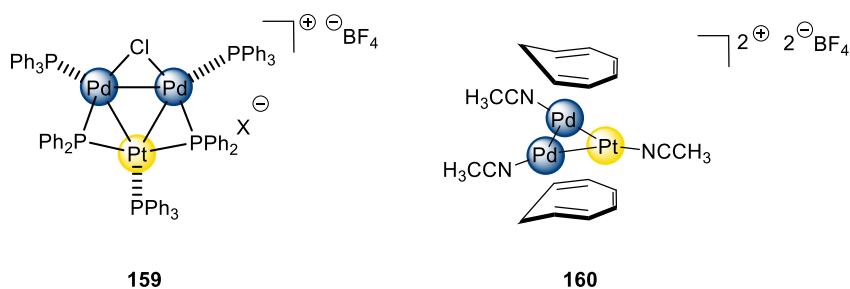
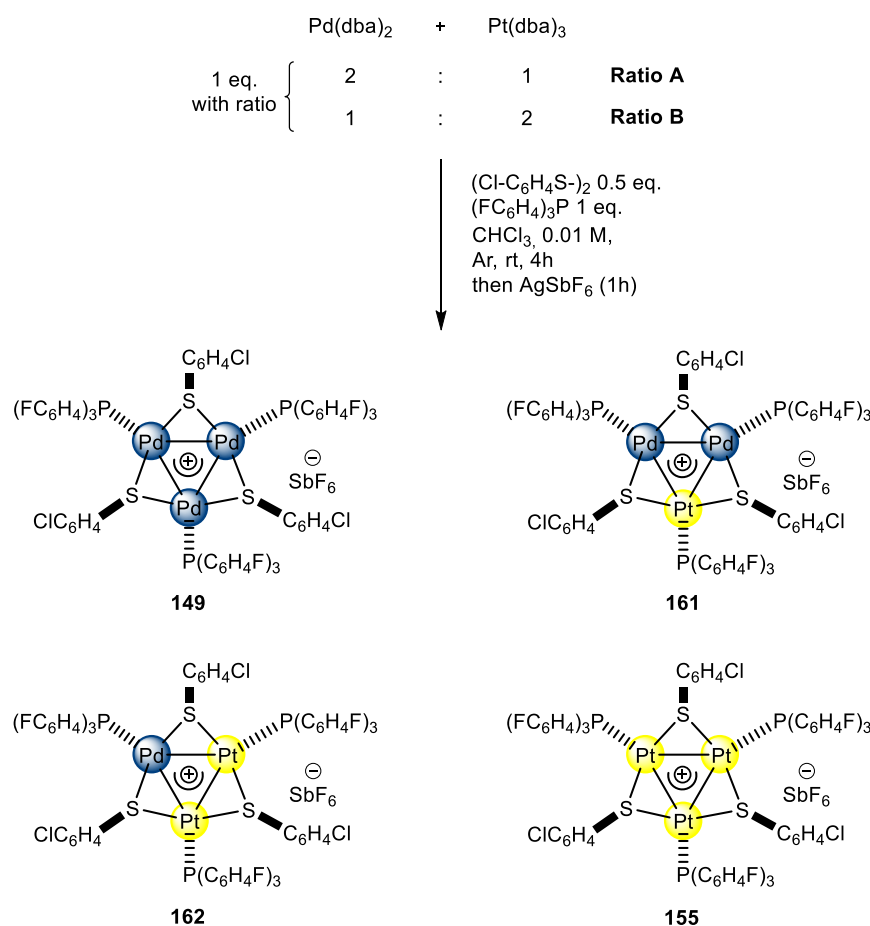


Figure 40 : Two Pd₂Pt metallic core clusters.

¹¹¹ a) D. J. Gorin, D. Toste, *Nature*, **2007**, *446*, 395-403. b) A. Fürstner, P. W. Davies, *Angew. Chem. Int. Ed.*, **2007**, *46*, 3410-3449. c) A. S. K. Hashmi, *Chem. Rev.*, **2007**, *107*, 3180-3211.

In 1985, Berry and coworkers reported the X-ray diffraction picture of **159** (Figure 40 left).¹¹² This heterometallic cluster presents 44 valence electrons and each metal bears a triphenylphosphine ligand. The two palladium atoms are bridged by a chlorine atom while platinum and palladium are bridged by phosphanide moiety. This cluster possesses an averaged metal-metal bond of 2.89 Å but it is not symmetric. More recently, Murahashi *et al.* published the structure of a sandwich complex including the Pd₂Pt kernel **160** (Figure 40 right).¹¹³ Each metal bears an acetonitrile ligand and two molecules of cycloheptatriene close the sandwich above and below the trimetallic plan. This unsymmetrical cluster possesses an isosceles triangular Pd₂Pt core with two equally Pd-Pt bonds (2.7161(7) Å) while the Pd-Pd distance is much longer (2.8974(9) Å). Concerning heteronuclear triangular structure, Suzuki *et al.* reported examples of nearly equilateral pattern composed of ruthenium and osmium.¹¹⁴

Applying our already established reaction, we mixed Pd(dba)₂ and Pt(dba)₃ in 2:1 and 1:2 ratios with bis(4-chlorophenyl)disulfide and tri(4-fluorophenyl)phosphine (Scheme 34).



Scheme 34 : Synthesis of trimetallic heteroclusters.

¹¹² D. E. Berry, G. W. Bushnell, K. R. Dixon, P. M. Moroney, C. Wan, *Inorg. Chem.*, **1985**, *24*, 2625-2634.

¹¹³ T. Murahashi, K. Usui, Y. Tachibana, S. Kimura, S. Ogoshi, *Chem. Eur. J.*, **2012**, *18*, 8886-8890.

¹¹⁴ H. Kameo, T. Shima, Y. Nakajima, H. Suzuki, *Organometallics*, **2009**, *28*, 2535-2545.

groups borne by the phosphine and those from the thiolate. Regarding crystal structures, both **161** and **162** presented an asymmetric unit identical to **149** and **155** (Figure 42). Beside the non-coordinating counter-anion, each unit was composed of only one metal atom, a thiolate fragment and a phosphine moiety. They presented a statistical disorder on the nature of the metal ion. The refinement procedure has been realized to obtain the best model of the site occupation factor of the metallic position.

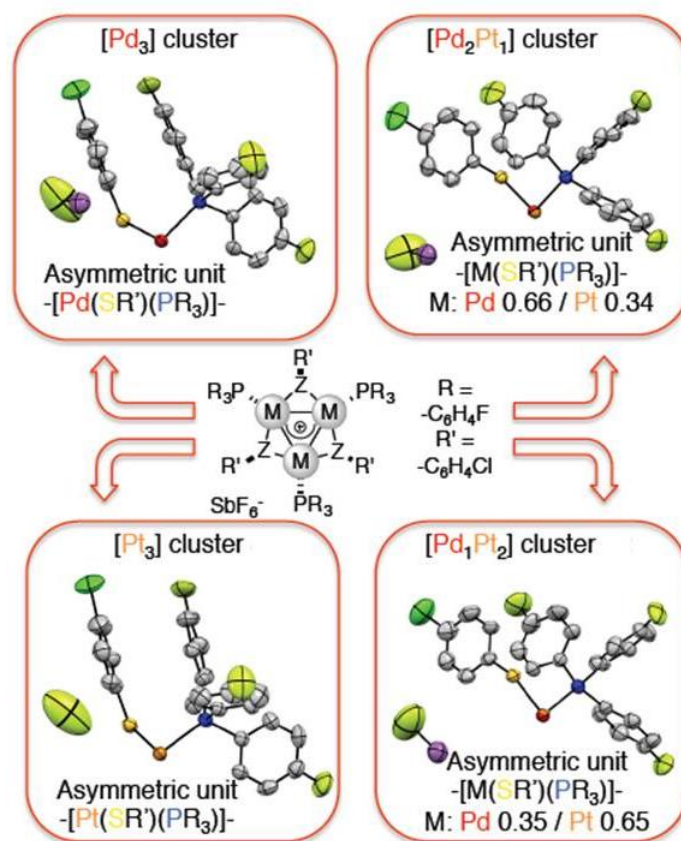


Figure 42 : X-ray asymmetric units.

The results showed occupancy of 66% palladium and 34% platinum for **161** while **162** presented occupancy of 35% for palladium and 65% for platinum. Considering the experimental error, these data were in agreement with the respective stoichiometry previously observed in HRMS analysis and confirmed the $[Pd_2Pt]$ pattern for **161** and the $[PdPt_2]$ one for **162**. The two heteronuclear metallic triangles are equilateral with angles of 60° and an averaged metal-metal bond length of $2.87(4)$ Å for **161** and $2.86(3)$ Å for **162**. These distances are nearly identical to their respective homonuclear peers **149** and **155** and also very close to the average metal-metal distance of 2.89 Å described by Berry and coworkers for **159**.

Magnetic susceptibilities were measured by SQUID experiments and gave the values of 0.22 and 0.26 emu.K.mol⁻¹ respectively for complexes **161** and **162**. These values were much lower compared to those observed for their homonuclear analogues but significantly higher than the quasi-symmetric but non-aromatic triangular cluster [Pd(CO)PPh₃]₃ which had a value of 0.04 emu.K.mol⁻¹.¹¹⁵ The decreases of these values are not very surprising according to the fact that heteroarenes usually presents lower diamagnetic susceptibility than the corresponding arenes.¹⁰³ The measured susceptibilities reminded almost independent from temperature above 20 K, in agreement with the presence of a ring current in these diamagnetic clusters.

Molecular modeling based on the crystalline structures of **149**, **161**, **162** and **155** was realized. After optimization of the structures without any symmetry constraint, we were surprised to observe that these four complexes had the same bonding HOMOs (Figure 43). The major part of the electron density of each of these MO is composed by combination of d_{x²-y²} orbitals of metals and is delocalized on the trimetallic core. These bonding molecular orbitals have a sigmoidal symmetry and thus provide a σ-aromatic character to these clusters. HOMOs -36 of these clusters are depicted in Figure 44. As for HOMOs, HOMOs -36 were identical among these four clusters and were formed by combining d_{xz} atomic orbitals of each metal. The symmetry of these MO revealed to be π-like. A δ-type molecular orbitals has been found in **155** (HOMO -12) which was totally delocalized on the trimetallic core, as previously observed in the case of [Pd₃]⁺ clusters.¹⁰⁰ These observations conferred to **155** triple aromaticity (σ, π and δ).

¹¹⁵ V. Bonuccelli, T. Funaioli, P. Leoni, F. Marchetti, L. Marchetti, *Inorg. Chem.*, **2013**, 52, 8759-8769.

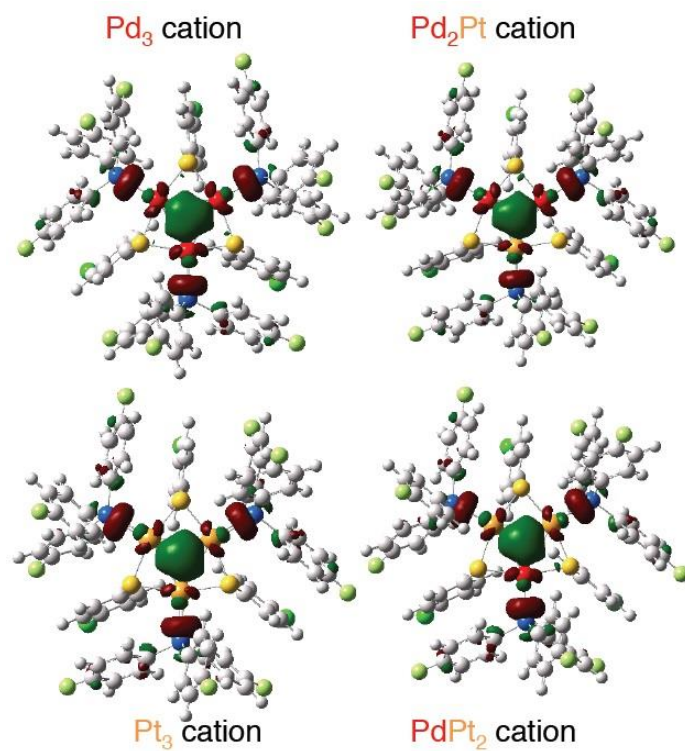


Figure 43 : Representations of HOMOs for cationic clusters 149, 161, 162 and 155.

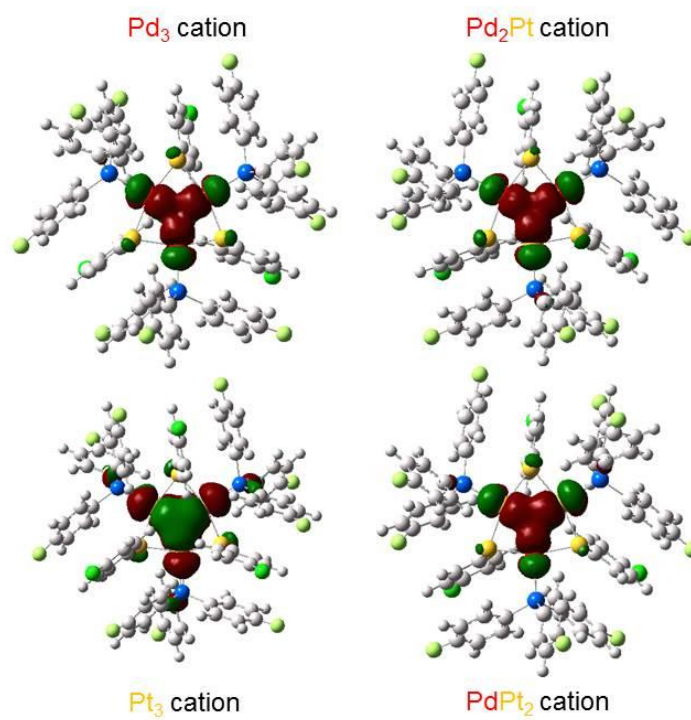


Figure 44 : Representations of HOMOs -36 for cationic clusters 149, 161, 162 and 155.

NICS have been also realized on these four clusters and the results are plotted on Figure 45.

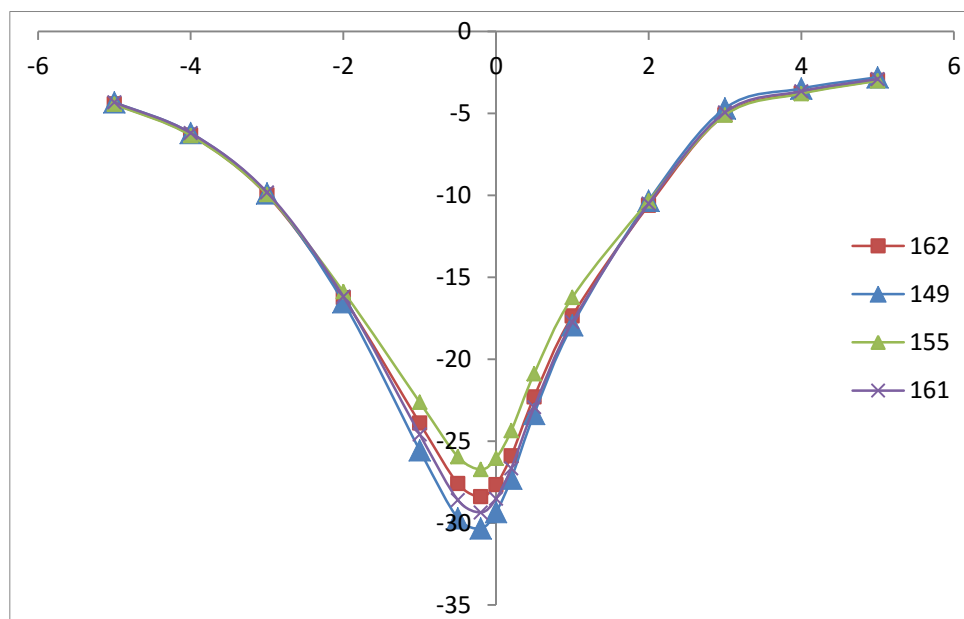


Figure 45 : NICS values.

Theoretical chemical shifts have been calculated from a distance of 0, 0.2, 0.5, 1, 2, 3, 4 and 5 Å respectively above and below the metallic plane. The chart showed that they display negative values for all calculated points and thus confirmed the presence of cyclic delocalization of electrons. The trend of the curves parallel that described for Pd₃ triangles obtained from S-aryl isothiureas.

In conclusion, the second generation synthesis of all-metal aromatic [Pd₃]⁺ clusters was optimized in our group, especially the purification method. This method showed good to excellent yields from commercially available reagents compared to the first generation one. Most of all, it proved its robustness and its feasibility enabling an extension to analogue clusters. Platinum triangles [Pt₃]⁺ could be isolated and showed a triple aromaticity (σ, π and δ) as their palladium homonuclear palladium peers. Doubly (σ and π) aromatic heteronuclear clusters [Pd₂Pt]⁺ and [PdPt₂]⁺ owned the same electronic and structural properties as homonuclear ones. On this pattern, palladium and platinum were equivalent and shared the formal +4/3 oxidation state.

2.2.3. $[\text{Pd}_3]^+$ as a Lewis base, a new nucleophilic ligand for Lewis acids2.2.3.1. Non-covalent cation- π interactions

Non-covalent π -interactions are weak interaction compared to covalent bonding but they help to stabilize the relevant structures. Carbon graphite described above is a key example. With its superimposed planar sheets in which π -electrons are fully delocalized, the total structure is stabilized by π - π -interactions between these sheets.^{50,51} Among these weak interactions, cation- π interactions are usually observed in biology and chemistry. This non-covalent interaction between a cationic species and delocalized electrons on an aromatic ring are theoretically well-documented for main group aromatics.¹¹⁶ A correlation between the quadrupolar moment of aromatic compounds and their ability to bind ions has been established. According to that, differently substituted arenes could be predicted to bind cations or anions (Figure 46)

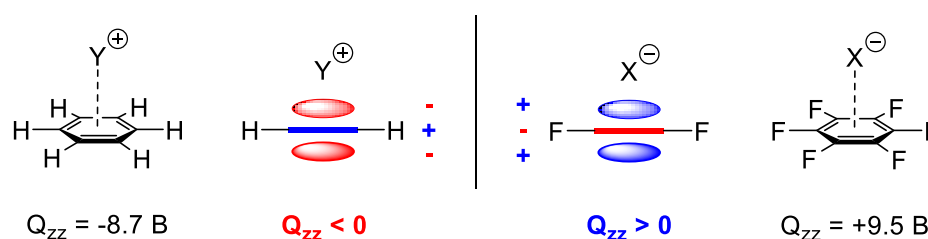


Figure 46 : Quadrupole moment and anion/cation affinities.

For the case of benzene (Figure 46 left), hydrogen substituents are electron-donor that make the ring electron-rich. The quadrupole moment is -8.7 B and the electron density is thus polarized to bind cationic species. On the contrary, with electron-withdrawing substituent such as fluorine in the case of hexafluorobenzene (Figure 46 right), its quadrupole moment is +9.5 B and the electron density is polarized to bind anions. The energy of ion- π interactions with aromatics such as benzene or hexafluorobenzene is of course too weak to afford complexes that could be isolated. However, Matile and coworkers¹¹⁷ synthesized a very electron-deficient naphthalenediimide derivative which possessed a quadrupole moment value of +39 B. This large negative value indicated that the π -electron density was very polarized

¹¹⁶ a) J. C. Ma, D. A. Dougherty, *Chem. Rev.*, **1997**, 97, 103-1324. b) E. A. Meyer, R. K. Castellano, F. Diederich, *Angew. Chem. Int. Ed.*, **2003**, 42, 1210-1250. c) B. L. Schottel, H. T. Chifotides, K. R. Dunbar, *Chem. Soc. Rev.*, **2008**, 37, 68-83. d) A. Clements, M. Lewis, *J. Phys. Chem. A*, **2006**, 110, 12705-12710. e) S. Kolakkandy, S. Pratihari, A. J. A. Aquino, H. Wang, W. L. Hase, *J. Phys. Chem. A*, **2014**, 118, 9500-9511.

¹¹⁷ R. E. Dawson, A. Hennig, D. P. Weimann, D. Emery, V. Ravikumar, J. Montenegro, T. Takeuchi, S. Gabutti, M. Mayor, J. Marenda, C. A. Schalley, S. Matile, *Nat. Chem.*, **2010**, 2, 533-538.

and suitable for binding anions. Matile proved the existence of the chlorine-bound species depicted in figure 47 by using several specific analyses. However, no X-ray data were available.

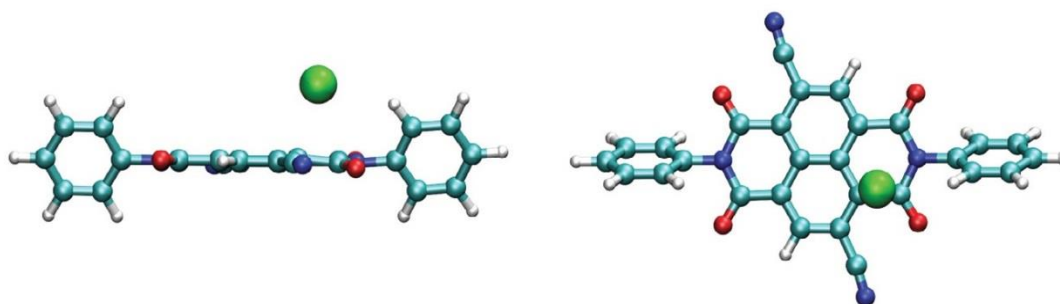


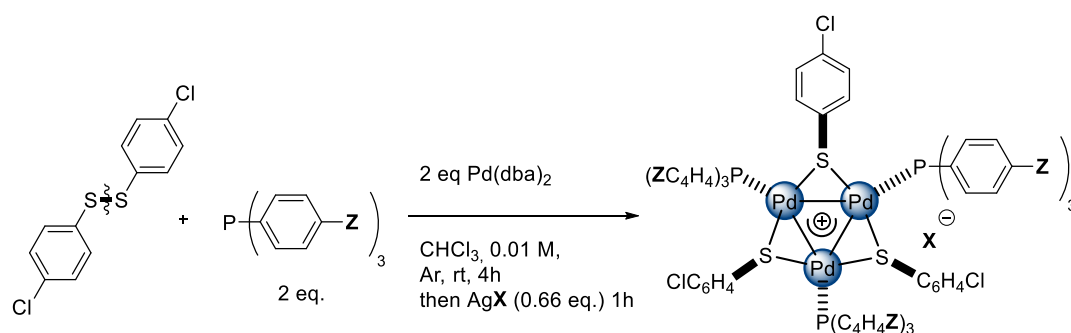
Figure 47 : Molecular modeling of Matile's naphthalenediimide binding a chlorine atom.

In the previous part of this manuscript, the large negative quadrupole moment of $[\text{Pd}_3]^+$ clusters (-52 B) was evoked. According to this data, $[\text{Pd}_3]^+$ should be able to bind cationic species. In addition to this observation, Tsipis and Tsipis predicted by calculations the tendency of ligand-stabilized aromatic trigold clusters to interact with Lewis acids.¹¹⁸ To the best of our knowledge, no stable all-metal aromatic compound possessing a large negative quadrupole moment has been isolated yet. In spite of the possibility that the charge repulsion between two positively charged moieties could be a too severe cliff for our experiments, we were interested in studying the potential of $[\text{Pd}_3]^+$ to bind other cationic species such as Li^+ , Cu^+ or Ag^+ .

2.2.3.2. Tripalladium-based tetrahedral structures

To prevent a potential anion metathesis between $[\text{Pd}_3]^+\text{X}^-$ clusters and general salts $\text{Y}^+\text{X}'^-$, a library of $[\text{Pd}_3]^+\text{X}^-$ was previously synthesized varying their counter-anion (Table 9).

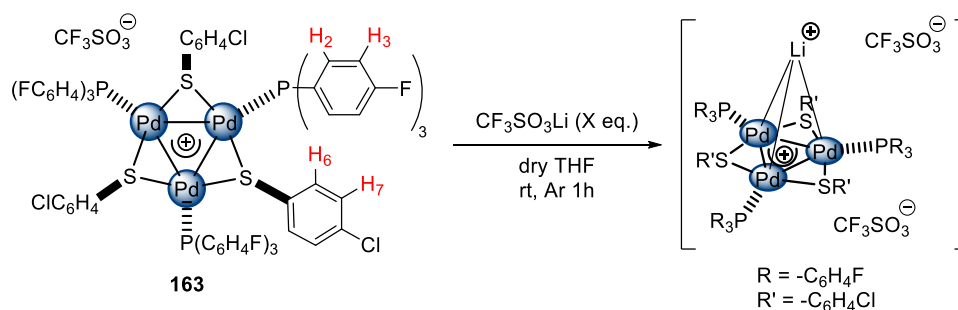
¹¹⁸ A. C. Tsipis, C. A. Tsipis, *J. Am. Chem. Soc.*, **2005**, *127*, 10623-10638.



Cluster	Z	X ⁻	Yield
163	F-	F ₃ CSO ₃ ⁻	91%
149	F-	SbF ₆ ⁻	90%
164	F-	BF ₄ ⁻	85%
165	F-	F ₃ CCO ₂ ⁻	86%
166	H-	SbF ₆ ⁻	92%

Table 9 : Synthesis tripalladium clusters by changing the silver salt.

We first started by performing reactions in dry THF at room temperature involving **163** and lithium triflate. Several experiments were realized by varying the molar ratio of the lithium salt (Scheme 35).

Scheme 35 : Synthesis of pyramidal [Pd₃Li]²⁺.

After one hour of reaction and filtration through a celite pad to remove unsolubilized salts, we examined the products by ¹H NMR analyses (Figure 48)

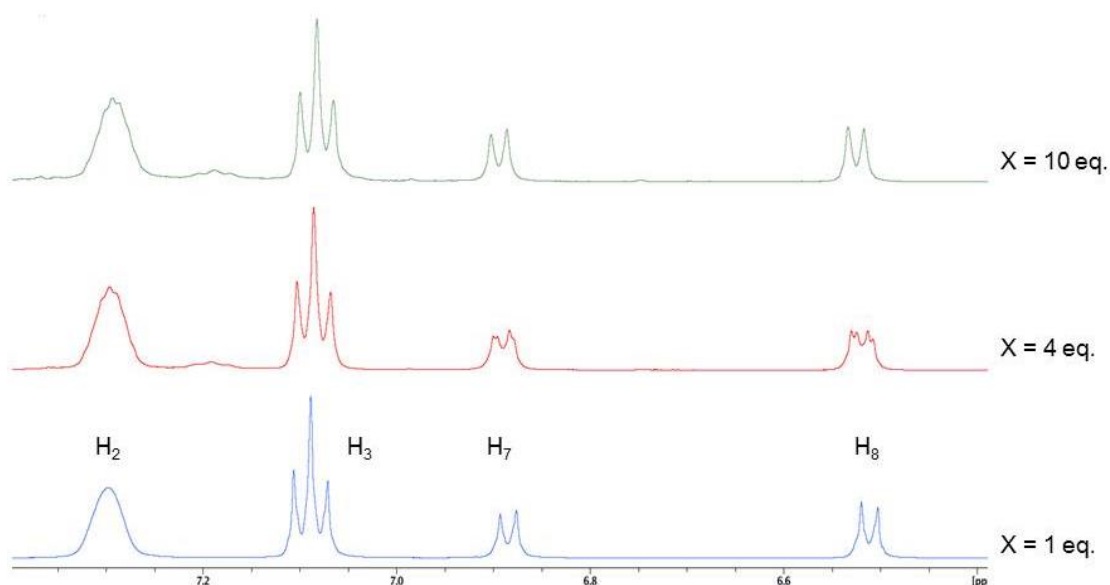
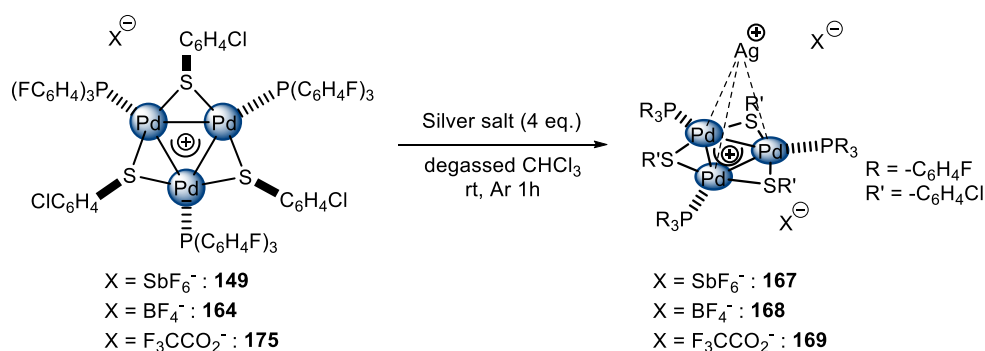


Figure 48 : ^1H NMR of reactions with X eq. of lithium triflate.

^1H NMR showed that with one equivalent of lithium salt, the spectrum did not change compared to the naked $[\text{Pd}_3]^+$ **163** (Figure 48 blue spectrum). When 10 equivalents were added, the chemical shifts of H_2 and H_3 stayed unchanged but we observed a slightly shift of 0.01-0.02 ppm to the left of the spectrum for protons on the thiolate H_7 and H_8 (Figure 48 green spectrum). Surprisingly, with only four equivalents of lithium, we distinguished a double signal around thiolate chemical shifts that implies the presence of two species. One was the naked triangle and the other could have a new molecule, maybe the pyramidal cluster we were looking for. The same observation was made by treating compound **164** with an excess of LiBF_4 and a shift of 0.02-0.04 ppm of the thiolate signals was identified while phosphine ones remain unchanged. We then turned to HRMS and X-ray analyses to get more information of this new compound. Unfortunately, HRMS analysis gave only the m/z isotopic pattern of the “naked” triangle **163**. We thought that the ionization potential used in electrospray apparatus was strong enough to break the weak interaction between lithium ion and $[\text{Pd}_3]^+$ cluster. Sadly, X-ray analyses were as lackluster as HRMS. After many attempts, crystals revealed to be also the classical naked triangle and ^1H NMR of the crystals confirmed it did not show anymore shifts presented in figure 48. As HRMS, the potential lithium-containing compound possibly degraded during the crystallization process.

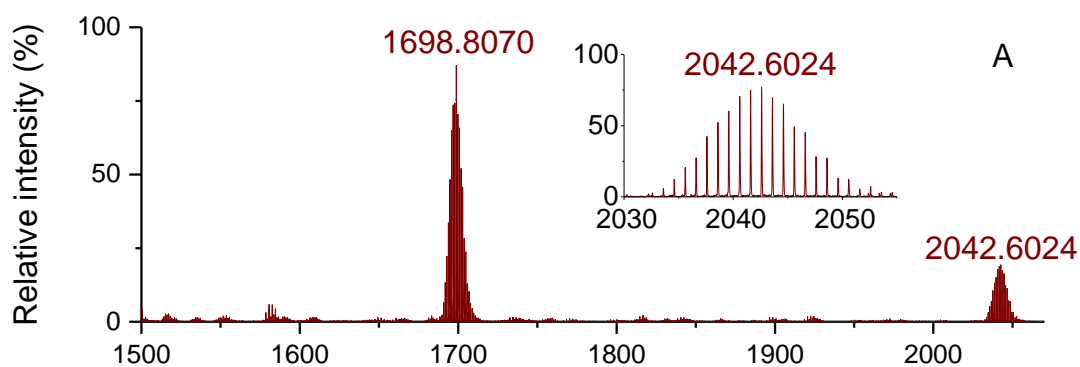
Disappointed by the results with lithium, we kept the faith and we turned ourselves to more Lewis acidic compounds such as silver salts. We realized several reactions which turned out to be more fruitful than the previous ones (Table 10).



Entry	Cluster	Silver salt	Isolated yield
1	149	AgSbF_6	76%
2	164	AgBF_4	78%
3	165	AgO_2CCF_3	72%

Table 10 : Synthesis of pyramidal $[\text{Pd}_3\text{Ag}]\text{X}_2$ clusters.

We were glad to observe the typical slight shifts of thiolate protons in ^1H NMR for the three presented attempts (0.01-0.11 ppm). ^{31}P NMR presented shifts of 0.35 to 2.55 ppm to the lower field. The presence of a cationic atom perpendicularly to the trimetallic plan should disturb the electron density of the aromatic system. In addition to NMR analyses, HRMS measurements gave us a supplementary clue to confirm the presence of the pyramidal clusters (Figure 49).

Figure 49 : HRMS analysis of **167**.

HRMS analysis of **167** showed two isotopic patterns which fit to tripalladium compounds. The one at $m/z = 2042.6024$ fitted with the calculated mass of **167**. The other at $m/z = 1698.8070$ corresponded to the original triangle **149** that was probably afforded by the decomposition of the pyramid in the ionization source as we supposed for lithium

experiments. Mass analysis for compounds **168** and **169** also matched the calculated mass with $m/z = 1892.7208$ and 1918.7033 respectively, despite the presence of the naked $[\text{Pd}_3]^+$ cluster. With great luck, we were able to crystallize compounds **167** and **168** (Figure 50).

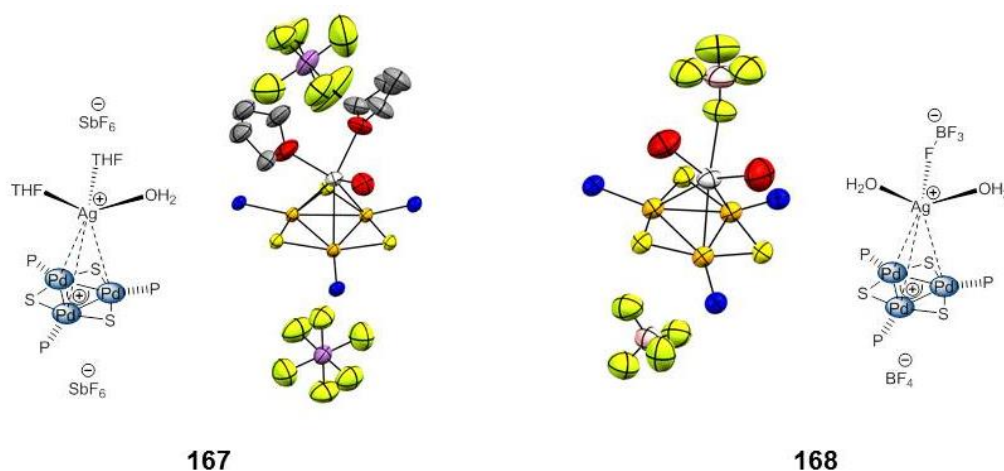


Figure 50 : X-ray pictures of pyramidal clusters **167** and **168**. Hydrogens and substituent on sulfur and phosphorous atoms were omitted for clarity.

X-ray picture of **167** (Figure 50 left) showed that the silver atom is tetracoordinated. It has a $[\text{Pd}_3]^+$ that acts an ancillary ligand, two molecules of THF (crystallization solvent) and one molecule of water. The two non-coordinating anions lied far from the tetranuclear core. Ag-Pd distances were between 2.824 and 2.853 Å. A slight distortion that breaks the perfect symmetry of the palladium triangle occurred. Two Pd-Pd distances are 2.899 Å and the third one is 2.917 Å, rendering it isosceles. The case of **168** (Figure 50 right) was a little bit different. The silver atom is also tetracoordinated but there was a participation of the counter-anion BF_4^- into the coordination. The palladium triangle is closer to the silver atom with Ag-Pd distances between 2.793 and 2.819 Å that formed a slightly distorted pyramid. Interestingly in both of the cases, the silver atom adopts a tetrahedral conformation. Both complexes can be regarded as typical 18 electrons Ag(I) complexes with four ancillary ligands. Therefore, this observation suggests that the tripalladium complex plays the role of L-type ligand and give two electrons to the silver atom as drawn on figure 51. So far this new type of bonding mode has never been described. Several metallic tetrahedral structures have already been published, mostly using neutral partners. We did not find any analogies of present results in the literature. However, we found a single precedent that we associate to this bonding mode. By adding a cation on a 44 cve triplatinum monocationic triangle, Braunstein *et al.* concluded that their $[\text{Pt}_3]^+$ cluster is electron-rich enough to bind cationic metallic

species without further explanation of this phenomenon.¹¹⁹ Even if their triplatinum cluster was not perfectly symmetrical, they probably missed the metal-aromatic character which could adequately justify the cation-cation bonding.

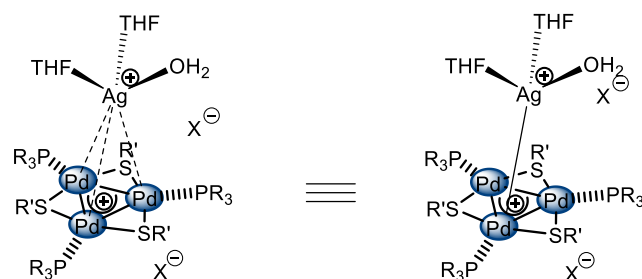
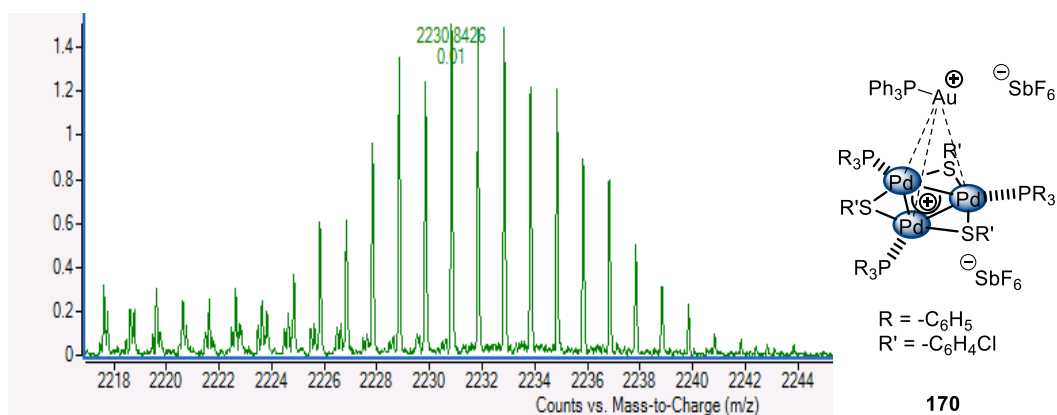


Figure 51 : Two different representations of complex 167.

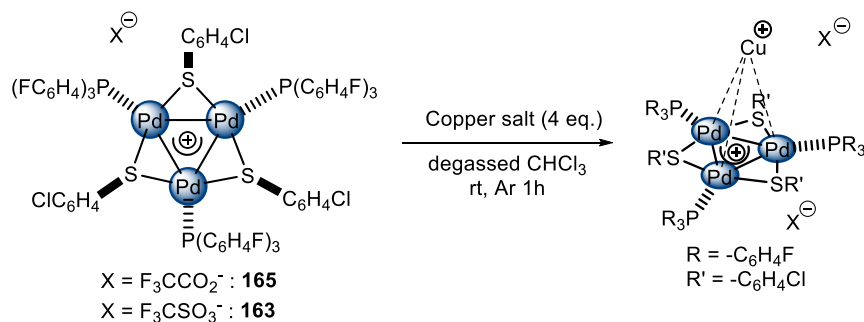
Encouraged by these probative results, we managed to test several other Lewis acids, such as FeCl_3 , $\text{Fe}(\text{OTf})_2$, $\text{Fe}(\text{OTf})_3$, $\text{Sc}(\text{OTf})_3$, $\text{Yb}(\text{OTf})_3$, $\text{Bu}_2\text{Sn}(\text{OTf})_2$, $\text{Hg}(\text{OTf})_2$, $\text{Bi}(\text{OTf})_3$, $\text{Dy}(\text{OTf})_3$. In all cases reactions were tested with 4 and 8 equivalents. Unfortunately, none of these triflates worked and the starting material was recovered.

We also tried the gold complex $\text{AuPPh}_3\text{SbF}_6$ with triangular $[\text{Pd}_3]^+$ **149**. This reaction led to a mixture of complexes in which the triphenylphosphine ligand of the gold complex was exchanged with the tri(4-fluorophenyl)phosphine of the tripalladium cluster. To overcome this problem, we tried complex **166** that possessed triphenylphosphine as ligand. Hopefully, the gold atom was coordinated by the triangle of palladium. No small shifts were detected by ^1H NMR however, but HRMS proved the formation the desired pyramid **170** with $m/z = 2230.8426$ as expected for a Pd_3Au core (Figure 52).

¹¹⁹ C. Archambault, R. Bender, P. Braunstein, Y. Dusausoy, R. Welter, *Dalton Trans.*, **2014**, 43, 8609-8619.



Compared to the Lewis acidic silver(I) and gold(I) salts, the introduction of less Lewis acidic copper was more difficult (Table 11).



Entry	Cluster	Copper salt	Isolated yield
1	165	$\text{Cu}(\text{MeCN})_4\text{PF}_6$	-
2	165	$\text{CF}_3\text{CO}_2\text{Cu}$	-
3	165	$(\text{CF}_3\text{CO}_2)_2\text{Cu}$	-
4	165	$\text{CH}_3\text{CO}_2\text{Cu}$	-
5	163	$(\text{CF}_3\text{SO}_3\text{Cu})_2 \cdot \text{PhMe}$	75%

Table 11 : Attempts to synthesize pyramidal cluster incorporating copper.

We were a little bit frustrated when we saw that the palladium triangle did not coordinate any classical copper salt. The Lewis acidic character of these salt was not strong enough to be bound by $[\text{Pd}_3]^+$ **165**. After some struggles, we found that commercially available $(\text{CF}_3\text{SO}_3\text{Cu})_2 \cdot \text{PhMe}$ should have been a better Lewis acid compound. Fortunately, through the use of the reagent, the $\text{CF}_3\text{SO}_3\text{Cu}$ fragment stacked $[\text{Pd}_3]^+$ cluster **163** affording pyramidal compound **171** in 72% yield.

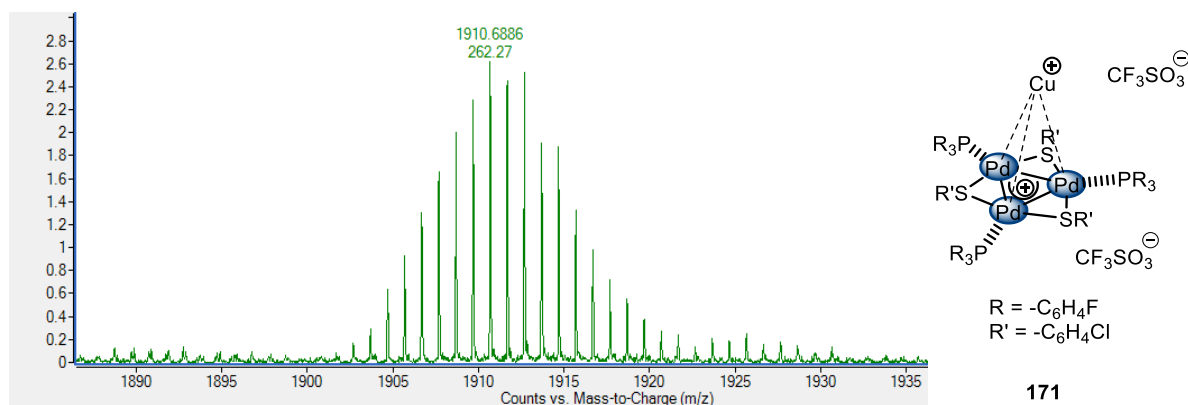


Figure 53 : HRMS analysis of compound 171.

As for pyramidal gold-containing cluster **170**, no shifts of thiolate signals were observed in ^1H NMR but HRMS analysis provides us the correct mass of the desired tetrahedral compound (Figure 53).

2.4. Conclusions

During this work, we developed and optimized a new methodology in order to synthesize previously reported all-metal δ -aromatic $[\text{Pd}_3]^+$ clusters. This very convenient synthetic way uses commercially available reagents and affords desired clusters in good to excellent yields in one-pot, without chromatography columns. Moreover, it tolerated several other types of ligands (trialkylphosphine or alkyl disulfide) that the first method did not allow to use. This robust method could be extended to the synthesis of homo- and heteronuclear analogues which revealed to have a metal-aromatic character too. One of the most promising properties of all-metal aromaticity was the theoretical and peculiar property of tripalladium clusters to realize sort of cation π -interactions mimicking regular donor ligand formed assembling main group elements. In this case, cation d-orbital-interaction seems a more appropriate definition of this bonding mode. Despite the unavoidable charge repulsion, we were able to prove this ability by the identification of several metallic tetrahedral complexes $[\text{M}_3\text{M}']^{2+}$.

SUPPORTING INFORMATION – PART 2

2.5. Supporting Information

2.5.1. General remarks

Disulfides, diselenides, phosphines and Pd(dba)₂ were purchased from commercial sources and used as received. Pt(dba)₃ was synthesized according to the procedure described in the literature.¹ Solvents were degassed by bubbling argon for at least 30 minutes prior to use. Reactions and filtrations were carried out under argon using standard Schlenk technique. ¹H NMR, ¹³C NMR, ³¹P NMR and ¹⁹⁵Pt NMR spectra were recorded in CDCl₃ or acetone-*d*₆ at 300 K on a Bruker 500 AVANCE spectrometer fitted with a BBFO probe head at 500, 125, 202 and 107 MHz respectively, using the solvent as internal standard (7.26 and 2.05 ppm for ¹H NMR and 77.16 and 29.84 ppm for ¹³C NMR respectively). For ³¹P and ¹⁹⁵Pt NMR, H₃PO₄ and K₂PtCl₄ were respectively used as external standards. ¹⁹F NMR spectra were recorded in CDCl₃ or acetone-*d*₆ at 300 K on a Bruker 300 AVANCE spectrometer fitted with a BBFO probe head at 282 MHz. Reported assignments are based on COSY, decoupling, HMBC, HSQC, NOESY and ROESY correlation experiments. The terms m, s, d, t, and q represent multiplet, singlet, doublet, triplet and quadruplet respectively, and the term br means a broad signal. Exact masses were recorded on a Agilent Q-TOF 6540 spectrometer (electrospray source). IR spectra were recorded with a Bruker Tensor 27 ATR diamant PIKE spectrometer and UV-visible spectra were recorded on a Shimadzu UV-2101 spectrophotometer. Magnetic measures were made on a MPMS-5S SQUID apparatus setting the applied field and collecting data while cooling from 300 to 2 K.

2.5.2. General procedures

General procedure 1 (GP1): Synthesis of triangular tripalladium clusters.

Pd(dba)₂ (0.2 mmol, 115 mg, 1 eq.) was added to a 50 mL Schlenk-type flask. The vessel underwent at least three vacuum/Ar cycles. 20 mL of freshly degassed CHCl₃ were then syringed under Ar. The desired phosphine (0.2 mmol, 1 eq.) and the disulfide or diselenide (0.1 mmol, 0.5 eq.) were immediately added to the mixture under Ar. The resulting solution was kept under stirring at r.t. for 2 hours, the desired silver salt (0.067 mmol, 0.33 eq.) was then added under Ar and the solution was put in the dark. Stirring was maintained for 1 hour and the mixture was then filtered through a short pad of celite under Ar to remove traces of black metals. The solvent was removed under vacuum to leave a deep red solid that was purified by CHCl₃/hexane washings (1/30 v/v, 3 x 30 mL). Evaporation of solvents under

vacuum afforded pure clusters as orange/red solids. Crystals suitable for X-Ray diffractions were obtained by vapor diffusion using THF/hexane or CHCl₃/hexane.

General procedure 2 (GP2): Synthesis of triangular triplatinum clusters.

Pt(dba)₃ (0.1 mmol, 89.7 mg, 1 eq.) was added to a 50 mL Schlenk-type flask. The vessel underwent at least three vacuum/Ar cycles. 10 mL freshly degassed CHCl₃ were then syringed under Ar. The desired phosphine (0.1 mmol, 1 eq.) and the disulfide or diselenide (0.05 mmol, 0.5 eq.) were immediately added to the mixture under Ar. The resulting solution was kept under stirring at r.t. for 2 hours, AgSbF₆ (0.033 mmol, 11.4 mg, 0.33 eq.) was then added under Ar and the solution was put in the dark. Stirring was maintained for 1 hour and the mixture was then filtered under Ar through a short pad of celite to remove traces of black metals. The solvent was removed under vacuum to leave a deep yellow-brown solid that was washed with a CHCl₃/hexane solution (1/30 v/v, 3 x 30 mL). Desired clusters were purified by chromatography using acetone/hexane (1/2 v/v) as eluent. Evaporation of solvents under vacuum provided pure complexes as yellow solids. Crystals suitable for X-Ray diffraction were obtained by vapor diffusion using THF/hexane.

General procedure 3 (GP3): Synthesis of triangular heterobimetallic cluster **161**.

Pt(dba)₃ (89.7 mg, 0.1 mmol, 0.33 eq.) and Pd(dba)₂ (115 mg, 0.2 mmol, 0.66 eq.) were added to a 100 mL Schlenk-type flask. The vessel underwent at least three vacuum/Ar cycles. 50 mL of freshly degassed CHCl₃ were then syringed under Ar and the solution became deeply violet. Tri(4-fluorophenyl)phosphine (94.9 mg, 0.3 mmol, 1 eq.) and bis(4-chlorophenyl)disulfide (43.1 mg, 0.15 mmol, 0.5 eq.) were immediately added to the mixture under Ar and the resulting solution was kept under stirring at r.t. for 2 hours. AgSbF₆ (34.2 mg, 0.1 mmol, 0.33 eq.) was eventually added and the solution was put in the dark. Stirring is maintained for 1 hour and the mixture was filtered through a short pad of celite under Ar. Solvent was removed under vacuum to leave an orange-red solid. The latter was washed with a CHCl₃/hexane solution (1/30 v/v, 5 x 50 mL). The crude orange-red solid was dried under vacuum providing 178.2 mg of a mixture of triangular complexes **149**, **155**, **161** and **162**. Their relative ratio (Pd₃:Pd₂Pt:PtPt₂:Pt₃ = 66:21:7:2) was estimated comparing the total ion current of each trimetallic cation *via* HRMS. Comparable results were obtained comparing ¹H and ³¹P NMR signals. The mixture of complexes was purified by chromatography using acetone/hexane (1/2 v/v) as eluent. Complexes were collected in twelve fractions that were separately analyzed by NMR revealing that the polarity follows the order **149** < **161** < **162** <

155 ($\text{Pd}_3\text{Pd}_2\text{Pt}<\text{PdPt}_2<\text{Pt}_3$). Desired Pd_2Pt cluster **161** was more abundant in fractions 7-9, which were then separately dried in vacuum. Crystals of **161** suitable for X-Ray diffraction were obtained by recrystallization of the content of fraction 8 (vapor diffusion using THF/hexane).

General procedure 4 (GP4): Synthesis of triangular heterobimetallic cluster **162**.

$\text{Pt}(\text{dba})_3$ (179.4 mg, 0.2 mmol, 0.67 eq.) and $\text{Pd}(\text{dba})_2$ (57.5 mg, 0.1 mmol, 0.33 eq.) were added to a 100 mL Schlenk-type flask. The vessel underwent at least three vacuum/Ar cycles. 50 mL of freshly degassed CHCl_3 were then syringed under Ar and the solution became deeply violet. Tri(4-fluorophenyl)phosphine (94.8 mg, 0.3 mmol, 1 eq.) and bis(4-chlorophenyl)disulfide (43.2 mg, 0.15 mmol, 0.5 eq.) were immediately added to the mixture under Ar and the resulting solution was kept under stirring at r.t. for 2 hours. AgSbF_6 (34.2 mg, 0.1 mmol, 0.33 eq.) was eventually added and the solution was put in the dark. Stirring is maintained for 1 hour and the mixture was filtered through a short pad of celite under Ar. Solvent was removed under vacuum to leave an orange solid. The latter was washed with a CHCl_3 /hexane solution (1/30 v/v, 5 x 50 mL). The crude orange solid was dried under vacuum providing 134.2 mg of a mixture of triangular complexes **149**, **155**, **161** and **162**. Their relative ratio ($\text{Pd}_3\text{Pd}_2\text{Pt}:\text{PdPt}_2:\text{Pt}_3 = 15:11:51:21$) was estimated comparing the total ion current of each trimetallic cation *via* HRMS. Comparable results were obtained comparing ^1H and ^{31}P NMR signals. The mixture of complexes was purified by chromatography using acetone/hexane (1/2 v/v) as eluent. Complexes were collected in twelve fractions that were separately analyzed by NMR. Desired PdPt_2 cluster **161** was more abundant in fractions 6-9, which were then separately dried in vacuum. Crystals of **161** suitable for X-Ray diffraction were obtained by recrystallization of the content of fraction 7 (vapor diffusion using THF/hexane).

General procedure 5 (GP5): Synthesis of silver-containing tetrahedral clusters **167**, **168** and **169**.

AgX (0.0444 mmol, 4 eq.) was added to a solution of $[\text{Pd}_3]\text{X}$ (0.0111 mmol, 1 eq.) in 5 mL of CHCl_3 in a Schlenk-type flask under Ar. The deep red solution was put in the dark. Stirring was maintained for 1 hour and the mixture was then filtered through a short celite pad under Ar. The solvent was removed under vacuum to afford a deep red solid. Then the compound was further purified by recrystallization. Crystals of **6** suitable for X-Ray diffractions were obtained by vapor diffusion using THF/hexane.

General procedure 6 (GP6): Synthesis of gold-containing tetrahedral cluster **170**.

AuPPh₃Cl (0.0667 mmol, 1 eq.) and AgSbF₆ (0.0667 mmol, 1 eq.) were added to freshly degassed CHCl₃ 10 mL in a Schlenk-type flask under argon and the mixture stirred for 1h in the dark. After filtration through a celite pad to remove the formed AgCl, the solvent was evaporated to dryness under vacuum, the residue was dissolved in THF 10 mL and the resulting solution was added to a solution of **5** (0.0667 mmol, 1 eq.) in THF 10 mL under Ar. The mixed solution was put in the dark. Stirring was maintained for 1 hour and the mixture was then filtered through a short celite pad under Ar. Evaporation of solvents under vacuum afforded orange/red solids. Then the compound was further purified by recrystallization by vapor diffusion using THF/hexane.

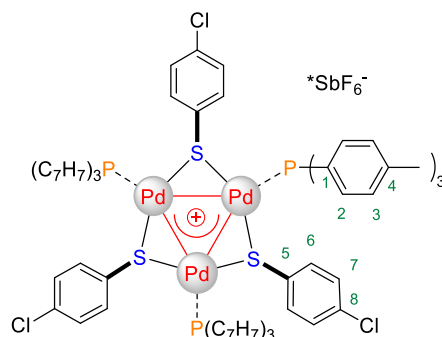
General procedure 7 (GP7): Synthesis of gold-containing tetrahedral cluster **171**.

(CF₃SO₃Cu)₂•PhCH₃ (0.0222 mmol, 4 eq.) was added to a solution of compound **1** (0.0111 mmol, 1 eq.) in CHCl₃ 5 mL in a Schlenk-type flask under Ar. The deep red solution was put in the dark. Stirring was maintained for 1 hour and the mixture was then filtered through a short pad of Celite under Ar. The solvent was removed under vacuum to afford a deep red solid. Then the compound was further purified by recrystallization by vapor diffusion using THF/hexane.

2.5.3. Synthesis of triangular homo- and heterometallic clusters

2.5.3.2. Preparation of tripalladium clusters

Complex 145



Following **GP1**, from tri(*p*-tolyl)phosphine and di(4-chlorophenyl)disulfide, was obtained 123 mg (97% yield) of **145** as an deep-red powder which was shown to be spectroscopically identical to the material described.¹⁰⁰

¹H NMR (300 MHz, CDCl₃): δ (ppm): 7.02 – 6.92 (m, 36H, **H2**, **H3**), 6.58 (d, 6H, *J* = 8.4 Hz, **H7**), 6.16 (d, 6H, *J* = 8.4 Hz, **H6**), 2.32 (s, 27H, **CH₃**).

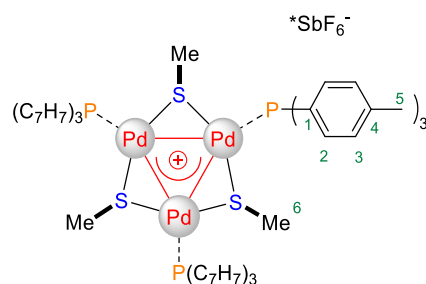
¹³C NMR (75 MHz, CDCl₃): δ (ppm) 140.9 (**C4**), 135.7 (**C6**), 134.7 (**C8**), 133.4 (**C2**), 133.3 (**C5**), 129.0 (**C3**), 128.8-128.0 (m, **C1**), 127.9 (**C7**), 21.3 (**CH₃**)

³¹P NMR (CDCl₃): δ (ppm) 15.72

HRMS calcd. for C₈₁H₇₅P₃Pd₃S₃⁺ 1663.0437, found 1663.0424.

IR (cm⁻¹): 3019, 2920, 2864, 1597, 1496, 1469, 1189, 1092, 802, 654.

Complex 152



Following **GP1**, from tri(*p*-tolyl)phosphine and dimethyldisulfide, was obtained 104 mg (97% yield) of **152** as an deep-red powder.

$^1\text{H NMR}$ (300 MHz, CDCl_3): δ (ppm): 7.35 (dd, 18H, $J = 7.5$ Hz, 10.8 Hz, **H2**), 7.20 (d, 18H, $J = 7.8$ Hz, **H3**), 2.38 (s, 27H, **H5**), 1.04 (s, 9H, **H6**).

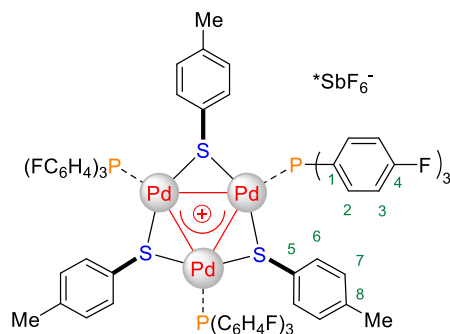
$^{13}\text{C NMR}$ (75 MHz, CDCl_3): δ (ppm) 141.2 (**C4**), 133.9 (**C2**), 129.4 (**C1**, **C3**), 21.4 (**C5**), 17.8 (**C6**).

$^{31}\text{P NMR}$ (CDCl_3): δ (ppm) 16.06.

HRMS calcd. for $\text{C}_{66}\text{H}_{72}\text{P}_3\text{Pd}_3\text{S}_3^+$ 1373.1151, found 1373.1147.

IR (cm^{-1}): 2919, 1597, 1496, 1445, 1396, 1303, 1189, 1094, 1017, 946, 803, 708, 653.

Complex 140



Following **GP1**, from tri(4-Fluorophenyl)phosphine and di(*p*-tolyl)disulfide and on 0.4 mmol scale of Pd(dba)₂, was obtained 216 mg (87% yield) of **140** as an orange-red powder. Spectroscopic data correspond to the literature.¹⁰⁰

¹H NMR (300 MHz, CDCl₃) δ (ppm): 7.12 – 7.06 (m, 18H, **H2**), 6.83 (d, 18H, *J* = 8.0 Hz, **H3**), 6.61 (d, 6H, *J* = 7.5 Hz, **H7**), 6.21 (d, 6H, *J* = 7.5 Hz, **H6**), 2.17 (s, 9H, **CH₃**).

¹³C NMR (75 MHz, acetone-*d*₆): δ (ppm) 165.1 (d, *J* = 251.2 Hz, **C4**), 139.1 (**C8**), 136.7 (ddd, *J* = 13.9, 7.3, 4.7 Hz, **C2**), 135.6 (**C6**), 133.6 (**C5**), 130.1 (**C7**), 128.5-127.9 (m, **C1**), 116.6 (ddd, *J* = 21.8, 7.9, 4.0 Hz, **C3**), 21.0 (**CH₃**).

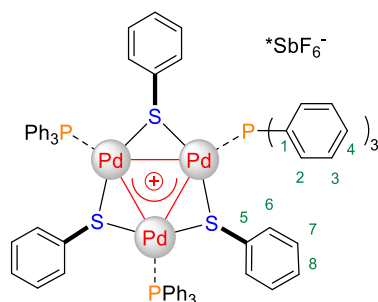
³¹P NMR (CDCl₃): δ (ppm) 14.93.

¹⁹F NMR (CDCl₃): δ (ppm) -109.99.

HRMS calcd. for C₇₅H₅₇F₉P₃Pd₃S₃⁺ 1636.9836, found 1636.9830.

IR (cm⁻¹): 3069, 2923, 1588, 1494, 1394, 1232, 1159, 1092, 825, 806, 655.

Complex 143



Following **GP1**, from triphenylphosphine and diphenyldisulfide, was obtained 108 mg (97% yield) of **143** as a deep red powder. Spectroscopic data correspond to the literature.¹⁰⁰

¹H NMR (300 MHz, CDCl₃): δ (ppm): 7.31 (t, 9H, *J* = 6.9 Hz, **H4**), 7.16 – 7.07 (m, 36H, **H2**, **H3**), 6.93 (t, 3H, *J* = 7.5 Hz, **H8**), 6.65 (t, 6H, *J* = 7.8 Hz, **H7**), 6.23 (d, 6H, **H6**).

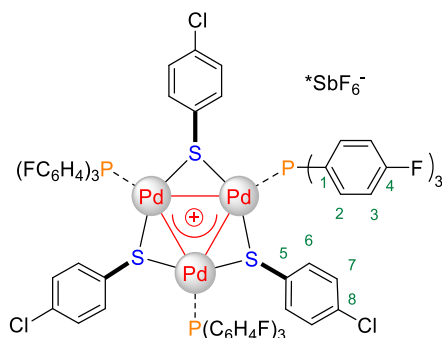
¹³C NMR (75 MHz, CDCl₃): δ (ppm) 136.2 (**C5**), 134.5 (**C6**), 133.5 (**C3**), 131.6 – 131.1 (m, **C1**), 130.6 (**C4**), 128.3 (**C2**, **C7**), 127.3 (**C8**).

³¹P NMR (CDCl₃): δ (ppm) 14.93.

HRMS calcd. for C₇₂H₆₀P₃Pd₃S₃⁺ 1433.0214, found 1433.0201.

IR (cm⁻¹): 3053, 2926, 1585, 1573, 1479, 1434, 1094, 998, 738, 688, 654.

Complex 149



Following **GP1**, from tri(4-Fluorophenyl)phosphine and di(4-Chlorophenyl)disulfide, was obtained 116 mg (90% yield) of **149** as a deep red powder. Spectroscopic data correspond to the literature.¹⁰⁰

¹H NMR (300 MHz, acetone-*d*₆): δ (ppm) 7.30 (br s, 18H, **H2**), 7.09 (t, *J* = 8.6 Hz, 18H, **H3**), 6.87 (d, *J* = 8.4 Hz, 6H, **H7**), 6.48 (d, *J* = 8.1 Hz, 6H, **H6**).

¹³C NMR (125 MHz, acetone-*d*₆): δ (ppm) 165.2 (d, *J* = 251.9 Hz, **C4**), 137.0 (br s, **C2**), 136.9 (s, **C6**), 135.7 (**C8**), 134.8 (**C5**), 129.5 (**C7**), 128.0 (br s, **C1**), 116.9 (d, *J* = 21.9 Hz, **C3**).

³¹P NMR (acetone-*d*₆): δ (ppm) 12.66.

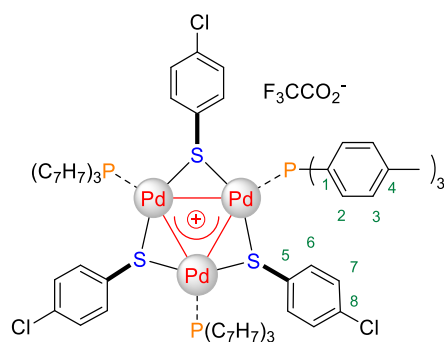
¹⁹F NMR (acetone-*d*₆): δ (ppm) -109.38.

HRMS calcd. for C₇₂H₄₈P₃Pd₃S₃Cl₃F₉⁺ 1698.8170, found 1698.8122.

IR (cm⁻¹): ν 3069, 2955, 2924, 2855, 1587, 1493, 1470, 1392, 1236, 1158, 1092, 1011, 940, 824, 814, 744.

UV-vis: *c* = 1.59 × 10⁻⁵ mol/L in CHCl₃, λ_{max} = 244 nm, ε_{max} = 0.44 × 10⁵ M⁻¹ cm⁻¹.

Complex 150



Following **GP1**, from tri(*p*-tolyl)phosphine and di(4-Chlorophenyl)disulfide, was obtained 105 mg (89% yield) of **150** as a deep red powder.

¹H NMR (300 MHz, CDCl₃): δ (ppm) 7.01-6.91 (m, 36H, **H2**, **H3**), 6.58 (d, *J* = 8.4 Hz, 6H, **H7**), 6.16 (d, *J* = 8.4 Hz, 6H, **H6**), 2.32 (s, 27H, **CH₃**).

¹³C NMR (75 MHz, CDCl₃): δ (ppm) 141.1 (**C4**), 135.9 (**C6**), 134.9 (**C8**), 133.8-133.2 (m, **C2**), 130.1-128.8 (m, **C3**, **C1**), 128.5 (**C5**), 128.0 (**C7**), 21.5 (**CH₃**).

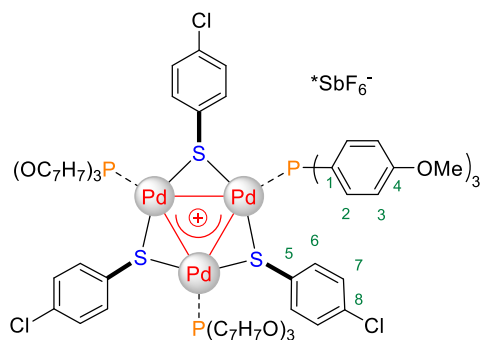
³¹P NMR (CDCl₃): δ (ppm) 15.49.

HRMS calcd. for C₈₁H₇₅Cl₃P₃Pd₃S₃⁺ 1663.0437, found 1663.0424.

IR (cm⁻¹): ν 3019, 2920, 2864, 1597, 1496, 1469, 1189, 1092, 802, 654.

UV-vis: *c* = 1.18 × 10⁻⁵ mol/L in CHCl₃, λ_{max} = 246 nm, ε_{max} = 4.9 × 10⁴ M⁻¹cm⁻¹.

Complex 151



Following **GP1**, from tri(4-Methoxyphenyl)phosphine and di(4-Chlorophenyl)disulfide and on 0.4 mmol scale of Pd(dba)₂, was obtained 218 mg (80% yield) of **151** as a deep red powder.

¹H NMR (300 MHz, CDCl₃): δ (ppm): 7.09 – 7.00 (m, 18H, **H2**), 6.65 (d, 24H, *J* = 8.1 Hz, **H7**, **H3**), 6.30 (d, 6H, *J* = 7.8 Hz, **H6**), 3.79 (s, 27H, -OCH₃).

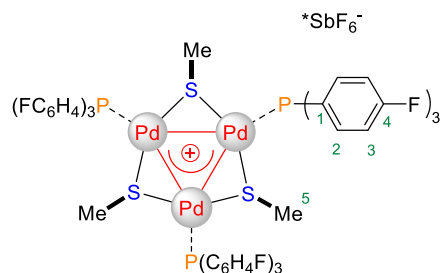
¹³C NMR (75 MHz, CDCl₃): δ (ppm) 161.2 (**C4**), 136.0 (**C6**), 135.0 (**C2**), 133.1 (**C8**), 128.1 (**C7**), 123.6-122.7 (m, **C1**), 113.7 (**C3**), 55.3 (-OCH₃).

³¹P NMR (CDCl₃): δ (ppm) 13.60.

HRMS calcd. for C₈₁H₇₅Cl₃O₉P₃Pd₃S₃⁺ 1806.9979, found 1806.9972.

IR (cm⁻¹): ν 2958, 2923, 2853, 1590, 1497, 1467, 1253, 1176, 1094, 1021, 1011, 795, 655.

Complex 148



Following **GP1**, from tri(4-Fluorophenyl)phosphine and dimethyldisulfide, was obtained 93 mg (85% yield) of **148** as an deep-red powder.

¹H NMR (300 MHz, CDCl₃): δ (ppm): 7.47 (ddd, 18H, *J* = 11.1, 8.4, 5.4 Hz, **H2**), 7.20 (dd, 18H, *J* = 8.4, 8.4 Hz, **H3**), 1.14 (s, 9H, **H5**).

¹³C NMR (75 MHz, CDCl₃): δ (ppm) 164.4 (d, *J* = 253.1 Hz (**C4**), 136.1 (dd, *J* = 8.7, 13.0 Hz, **C2**), 127.4 (dd, *J* = 31.6, 13.0 Hz, **C1**), 116.4 (ddd, *J* = 20.0, 6.6, 3.4 Hz, **C3**), 17.6 (**C5**).

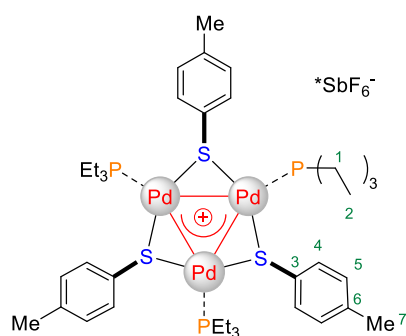
³¹P NMR (CDCl₃): δ (ppm) 14.63

HRMS calcd. for C₅₇H₄₅P₃Pd₃S₃⁺ 1408.8890, found 1408.8894.

IR (cm⁻¹): 3070, 2920, 1586, 1493, 1393, 1230, 1160, 1091, 1012, 945, 824, 812, 653.

UV-vis: *c* = 1.12 × 10⁻⁵ mol/L in CHCl₃, λ_{max} = 241 nm, ε_{max} = 4.8 × 10⁴ M⁻¹ cm⁻¹.

Complex 153



Following **GP1**, from triethylphosphine and di(*p*-tolyl)disulfide, was obtained 80 mg (98% yield) of **153** as an deep-red powder.

¹H NMR (300 MHz, CDCl₃): δ (ppm): 7.12 (d, *J* = 4.5 Hz, 6H, **H5**), 6.98 (d, *J* = 4.8 Hz, 6H, **H4**), 2.27 (br s, 9H, **H7**), 1.69 (br s, 18H, **H1**), 0.81 (m, 27H, **H2**).

¹³C NMR (75 MHz, CDCl₃): δ (ppm) 138.4 (C6), 134.6 (C4), 134.2 (C3), 129.6 (C5), 21.2 (C7), 19.3 (dd, *J* = 15.7, 8.7 Hz, C1), 8.1 (C2).

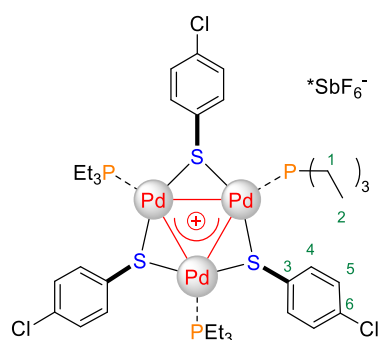
³¹P NMR (CDCl₃): δ (ppm) 13.61.

HRMS calcd. for C₃₉H₆₆P₃Pd₃S₃⁺ 1043.0666, found 1043.0618.

IR (cm⁻¹): 2968, 2934, 2878, 1485, 1452, 1414, 1253, 1032, 1015, 811, 770, 751.

UV-vis: *c* = 1.67 × 10⁻⁵ mol/L in CHCl₃, λ_{max} = 244 nm, ε_{max} = 1.2 × 10⁴ M⁻¹ cm⁻¹.

Complex 154



Following **GP1**, from triethylphosphine and di(4-Chlorophenyl)disulfide, was obtained 71 mg (97% yield) of **154** as an deep-red powder.

¹H NMR (500 MHz, CDCl₃): δ (ppm): 7.21 (d, *J* = 9.0 Hz, 6H, **H5**), 7.18 (d, *J* = 9.0 Hz, 6H, **H4**), 1.79-1.67 (br s, 18H, **H1**), 0.92-0.85 (m, 27H, **H2**).

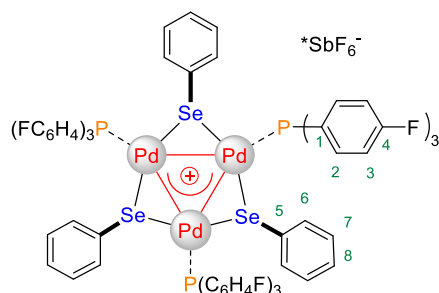
¹³C NMR (125 MHz, CDCl₃): δ (ppm) 136.1 (**C6**), 135.9 (**C4**) 134.6 (**C3**), 129.1 (**C5**), 19.6-19.4 (m, **C1**), 8.2 (**C2**).

³¹P NMR (CDCl₃): δ (ppm) 14.39.

HRMS calcd. for C₃₆H₅₇Cl₃P₃Pd₃S₃⁺ 1100.9005, found 1100.9004.

IR (cm⁻¹): 2973, 2940, 2902, 1470, 1450, 1385, 1237, 1086, 1031, 1009, 831, 766, 737, 649, 624.

Complex 157



Following **GP1** and purification by flash chromatography (acetone/hexane = 1:2, $R_f = 0.30$), from tri(4-Fluorophenyl)phosphine and diphenyldiselenide, was obtained 52.6 mg (50% yield) of **157** as an deep-red powder.

$^1\text{H NMR}$ (500 MHz, acetone- d_6): δ (ppm) 7.39-7.25 (m, 15H, **P-Ar**), 7.17 (t, $J = 7.2$ Hz, 3H, **H8**), 7.14-7.08 (m, 3H, **P-Ar**), 7.02 (t, $J = 8.4$ Hz, further split, 18H, **H2**), 6.93 (t, $J = 7.5$ Hz, 6H, **H7**), 6.62, 6.56, 6.52 (three d, $J = 7.6$ Hz, 6H, **H6**).

$^{13}\text{C NMR}$ (125 MHz, acetone- d_6): δ (ppm) 165.0 (d, $J = 251.5$ Hz, **C4**), 137.3 (m, **C5**), 137.1 (**C6**), 136.6 (**C2**), 130.1 (**C1**), 129.8 (**C7**), 128.6 (**C8**), 116.6 (d, $J = 21.7$ Hz, **C3**).

$^{31}\text{P NMR}$ (acetone- d_6): δ (ppm) 11.95.

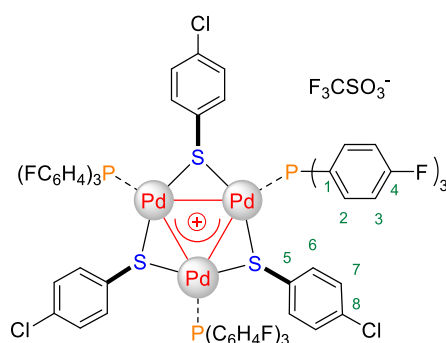
$^{19}\text{F NMR}$ (acetone- d_6): δ (ppm) -109.83.

HRMS calcd. for $\text{C}_{72}\text{H}_{51}\text{F}_9\text{P}_3\text{Pd}_3\text{Se}_3^+$ 1736.7720, found 1736.7649.

IR (cm^{-1}): 3360, 2956, 2925, 2852, 1736, 1589, 1495, 1470, 1234, 1161, 1093, 1013, 827, 772, 938, 658.

UV-vis: $c = 1.56 \times 10^{-5}$ mol/L in CHCl_3 , $\lambda_{\text{max}} = 254$ nm, $\epsilon_{\text{max}} = 0.37 \times 10^5 \text{ M}^{-1} \text{ cm}^{-1}$.

Complex 163



Following **GP1**, from tri(4-Fluorophenyl)phosphine, di(4-Chlorophenyl)disulfide and silver triflate, was obtained 99 mg (90% yield) of **163** as a deep red powder.

$^1\text{H NMR}$ (500 MHz, acetone- d_6): δ (ppm) 7.29 (br s, 18H, **H2**), 7.09 (t, $J = 8.8$ Hz, 18H, **H3**), 6.88 (d, $J = 8.5$ Hz, 6H, **H7**), 6.51 (d, $J = 8.5$ Hz, 6H, **H6**).

$^{13}\text{C NMR}$ (125 MHz, acetone- d_6): δ (ppm) 165.2 (d, $J = 252.0$ Hz, **C4**), 137.1 (s, **C2**), 136.9 (br s, **C6**), 135.7 (**C8**), 134.8 (**C5**), 129.6 (**C7**), 128.0 (br s, **C1**), 116.8 (d, $J = 22.0$ Hz, **C3**).

$^{31}\text{P NMR}$ (acetone- d_6): δ (ppm) 13.64.

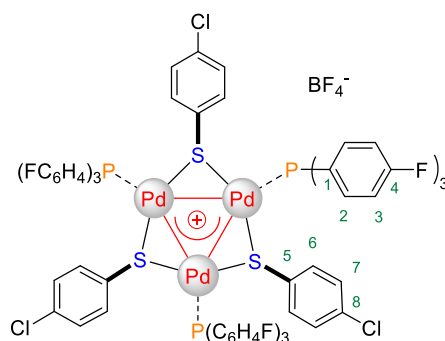
$^{19}\text{F NMR}$ (acetone- d_6): δ (ppm) -109.45 (s, $\text{P}(\text{C}_6\text{H}_4\text{F})_3$), -78.78 (s, CF_3SO_3^-).

HRMS calcd. for $\text{C}_{72}\text{H}_{48}\text{Cl}_3\text{F}_9\text{P}_3\text{Pd}_3\text{S}_3^+$ 1698.8170, found 1698.8167.

IR (cm^{-1}): ν 3071, 2926, 2853, 1589, 1497, 1470, 1394, 1271, 1238, 1162, 1093, 1030, 1011, 827.

UV-vis.: $c = 8.5 \times 10^{-6}$ mol/L in CHCl_3 , $\lambda_{\text{max}} = 243$ nm, $\epsilon_{\text{max}} = 9.5 \times 10^4$ $\text{M}^{-1} \text{cm}^{-1}$.

Complex 164



Following **GP1**, from tri(4-Fluorophenyl)phosphine, di(4-Chlorophenyl)disulfide and silver trifluoroborate, was obtained 101 mg (85% yield) of **164** as a deep red powder.

$^1\text{H NMR}$ (300 MHz, acetone- d_6): δ (ppm) 7.29 (br s, 18H, **H2**), 7.09 (t, $J = 8.7$ Hz, 18H, **H3**), 6.88 (d, $J = 8.5$ Hz, 6H, **H7**), 6.50 (d, $J = 8.5$ Hz, 6H, **H6**).

$^{13}\text{C NMR}$ (125 MHz, acetone- d_6): δ (ppm) 165.2 (d, $J = 251.9$ Hz, **C4**), 137.1 (br s, **C2**), 136.9 (s, **C6**), 135.6 (**C8**), 134.8 (**C5**), 129.6 (**C7**), 128.0 (br s, **C1**), 116.9 (d, $J = 22.2$ Hz, **C3**).

$^{31}\text{P NMR}$ (acetone- d_6): δ (ppm) 13.60.

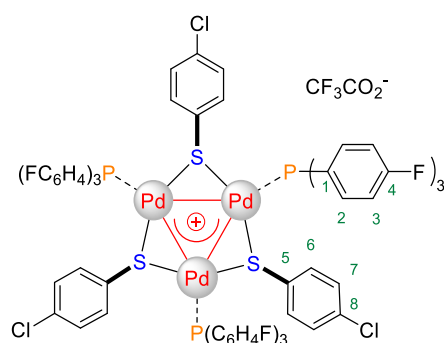
$^{19}\text{F NMR}$ (acetone- d_6): δ (ppm) -109.39 (s, $\text{P}(\text{C}_6\text{H}_4\text{F})_3$), -151.66 (s, BF_4^-).

HRMS calcd. for $\text{C}_{72}\text{H}_{48}\text{Cl}_3\text{F}_9\text{P}_3\text{Pd}_3\text{S}_3^+$ 1698.8170, found 1698.8167.

IR (cm^{-1}): ν 3068, 2925, 2853, 1711, 1588, 1494, 1472, 1394, 1234, 1161, 1089, 1050, 1010, 825.

UV-vis.: $c = 1 \times 10^{-5}$ mol/L in CHCl_3 , $\lambda_{\text{max}} = 244$ nm, $\epsilon_{\text{max}} = 9.3 \times 10^4$ $\text{M}^{-1} \text{cm}^{-1}$.

Complex 165



Following **GP1**, from tri(4-Fluorophenyl)phosphine, di(4-Chlorophenyl)disulfide and silver trifluoroborate, was obtained 116 mg (89% yield) of **165** as a deep red powder.

$^1\text{H NMR}$ (500 MHz, acetone- d_6): δ (ppm) 7.32 (br s, 18H, **H2**), 7.07 (br s, 18H, **H3**), 6.88 (d, $J = 7.1$ Hz, 6H, **H7**), 6.49 (br s, 6H, **H6**).

$^{13}\text{C NMR}$ (125 MHz, acetone- d_6): δ (ppm) 165.2 (d, $J = 251.9$ Hz, **C4**), 137.0 (br s, **C2**), 136.9 (s, **C6**), 135.7 (**C8**), 134.8 (**C5**), 129.5 (**C7**), 128.2 (br s, **C1**), 116.8 (d, $J = 22.1$ Hz, **C3**).

$^{31}\text{P NMR}$ (acetone- d_6): δ (ppm) 13.97.

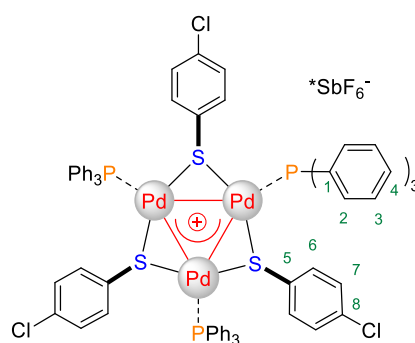
$^{19}\text{F NMR}$ (acetone- d_6): δ (ppm) -109.50 (s, $\text{P}(\text{C}_6\text{H}_4\text{F})_3$), -73.91 (s, CF_3CO_2^-)

HRMS calcd. for $\text{C}_{72}\text{H}_{48}\text{Cl}_3\text{F}_9\text{P}_3\text{Pd}_3\text{S}_3^+$ 1698.8170, found 1698.8132.

IR (cm^{-1}): ν 3067, 2954, 2922, 2853, 1686, 1667, 1586, 1495, 1470, 1394, 1232, 1154, 1088, 1010, 811, 751, 705.

UV-vis.: 5×10^{-6} mol/L in CHCl_3 , $\lambda_{\text{max}} = 242$ nm, $\epsilon_{\text{max}} = 7.2 \times 10^4$ $\text{M}^{-1} \text{cm}^{-1}$.

Complex 166



Following **GP1**, from triphenylphosphine and di(4-Chlorophenyl)disulfide, was obtained 108 mg (92% yield) of **166** as a deep-red powder.

$^1\text{H NMR}$ (500 MHz, acetone- d_6): δ (ppm) 7.43 (br s, 9H, **H4**), 7.29 (br s, 18H, **H3**), 7.24 (br s, 18H, **H2**), 6.76 (d, $J = 7.1$ Hz, 6H, **H7**), 6.35 (d, $J = 7.1$ Hz, 6H, **H6**).

$^{13}\text{C NMR}$ (125 MHz, acetone- d_6): δ (ppm) 136.9 (**C6**), 136.0 (**C8**), 134.5 (br s, **C3**), 134.2 (**C5**), 131.8 (br s, **C4**), 129.5 (br s, **C1**, **C2**), 129.2 (**C7**).

$^{31}\text{P NMR}$ (acetone- d_6): δ (ppm) 16.15.

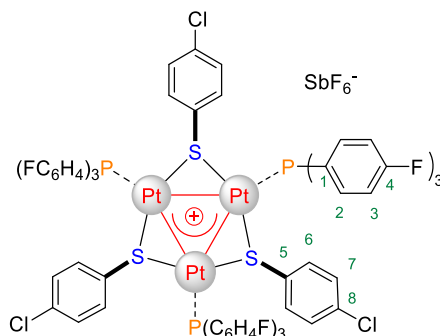
HRMS calcd. for $\text{C}_{72}\text{H}_{57}\text{Cl}_3\text{P}_3\text{Pd}_3\text{S}_3^+$ 1536.8901, found 1536.8946.

IR (cm^{-1}): ν 3056, 2922, 2857, 1700, 1588, 1572, 1479, 1470, 1435, 1388, 1216, 1185, 1094, 1010, 823, 743, 691.

UV-vis.: $c = 1 \times 10^{-5}$ mol/L in CHCl_3 , $\lambda_{\text{max}} = 246$ nm, $\epsilon_{\text{max}} = 6.2 \times 10^4$ $\text{M}^{-1} \text{cm}^{-1}$.

2.5.3.2. Preparation of triplatinum clusters

Complex 155



Following **GP2**, from tri(4-Fluorophenyl)phosphine and di(4-Chlorophenyl)disulfide, was obtained 88 mg (60% yield) of **155** as a yellow powder.

$^1\text{H NMR}$ (500 MHz, acetone- d_6): δ (ppm) 7.42-7.18 (m, 18H, **H3**), 7.11 (br s, 18H, **H2**), 6.92 (d, $J = 8.0$ Hz, 6H, **H7**), 6.64 (d, $J = 8.0$ Hz, 6H, **H6**).

$^{13}\text{C NMR}$ (125 MHz, acetone- d_6): δ (ppm) 165.4 (d, $J = 252.1$ Hz, **C4**), 136.9 (br s, **C2**), 136.6 (**C5**), 136.5 (**C6**), 135.3 (**C8**), 129.3 (**C7**), 127.5 (br s, **C1**), 116.7 (dt, $J = 20.9$ Hz, 5.6 Hz, **C3**).

$^{31}\text{P NMR}$ (acetone- d_6): δ (ppm) -1.58 (apparent tt, $^1J_{\text{P-Pt}} = 4223$ Hz, $^2J_{\text{P-Pt}} = 93$ Hz).

$^{19}\text{F NMR}$ (acetone- d_6): δ (ppm) -109.03.

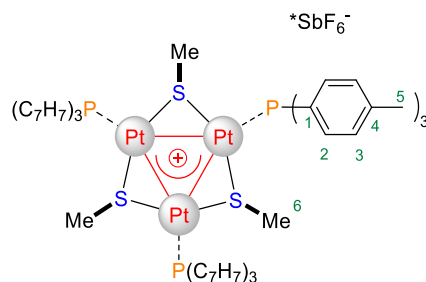
$^{195}\text{Pt NMR}$ (107 MHz, acetone- d_6): δ (ppm) -5680 (apparent dt, $^1J_{\text{Pt-P}} = 4271$ Hz, $^2J_{\text{Pt-P}} = 96$ Hz).

HRMS calcd. for $\text{C}_{72}\text{H}_{48}\text{Cl}_3\text{F}_9\text{P}_3\text{Pt}_3\text{S}_3^+$ 1963.9975, found: 1963.9880.

IR (cm^{-1}): ν 2958, 2919, 2851, 1587, 1494, 1470, 1393, 1260, 1233, 1160, 1093, 1010, 817, 742, 709, 655.

UV-vis.: $c = 1.40 \times 10^{-5}$ mol/L in CHCl_3 , $\lambda_{\text{max}} = 241$ nm, $\epsilon_{\text{max}} = 0.50 \times 10^5 \text{ M}^{-1} \text{ cm}^{-1}$.

Complex 156



Following **GP2**, from tri(*p*-tolyl)phosphine and dimethyldisulfide, was obtained 50 mg (40% yield) of **156** as a yellow powder.

$^1\text{H NMR}$ (500 MHz, acetone- d_6): δ (ppm) 7.43 (br s, 18H, **H3**), 7.35 (d, $J = 7.6$ Hz, 18H, **H2**), 2.41 (s, 27H, **H5**), 0.97 (t, $J = 19.2$ Hz, 9H, **H6**).

$^{13}\text{C NMR}$ (125 MHz, acetone- d_6): δ (ppm) 142.7 (s, **C4**), 134.7 (t, $J = 6.0$ Hz, **C2**), 130.2-130.1 (m, **C3**), 129.9-129.3 (**C1**), 21.3 (s, **C5**), 18.2 (br s, **C6**).

$^{31}\text{P NMR}$ (acetone- d_6): δ (ppm) -0.76 (apparent tt, $^1J_{\text{P-Pt}} = 4285$ Hz, $^2J_{\text{P-Pt}} = 85$ Hz).

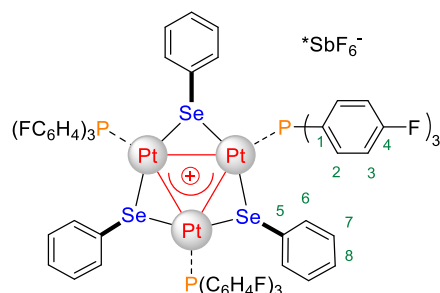
$^{195}\text{Pt NMR}$ (107 MHz, acetone- d_6): δ (ppm) -5724 (apparent dt, $^1J_{\text{Pt-P}} = 4228$ Hz, $^2J_{\text{Pt-P}} = 96$ Hz).

HRMS calcd. for $\text{C}_{66}\text{H}_{72}\text{P}_3\text{Pt}_3\text{S}_3^+$ 1639.2925, found 1639.2920.

IR (cm^{-1}): ν 2959, 2923, 2853, 1598, 1497, 1456, 1189, 1098, 806, 711, 658.

UV-vis.: 1.64×10^{-5} mol/L in CHCl_3 , $\lambda_{\text{max}} = 243$ nm, $\epsilon_{\text{max}} = 0.40 \times 10^5 \text{ M}^{-1} \text{ cm}^{-1}$.

Complex 158



Following **GP2**, from tri(4-Fluorophenyl)phosphine and diphenyldiselenide, was obtained 61 mg (41% yield) of **158** as a yellow powder.

$^1\text{H NMR}$ (300 MHz, acetone- d_6): δ (ppm) 7.57-7.31 (m, 18H, **H3**), 7.23 (t, $J = 7.6$ Hz, 3H, **H8**), 6.98 (t, $J = 8.5$ Hz, 18H, **H2**), 6.91 (t, $J = 7.6$ Hz, 6H, **H7**), 6.28 (d, $J = 7.6$ Hz, 6H, **H6**).

$^{13}\text{C NMR}$ (75 MHz, acetone- d_6): δ (ppm) 165.0 (d, $J = 251.9$ Hz, **C4**), 137.8 (**C7**), 137.3 (**C2**), 135.8 (**C8**), 129.4 (**C5**), 129.0 (**C6**), 128.4 (br s, **C1**), 116.4 (**C3**).

$^{31}\text{P NMR}$ (acetone- d_6): δ (ppm) 0.65 (apparent tt, $^1J_{\text{P-Pt}} = 4301$ Hz, $^2J_{\text{P-Pt}} = 74$ Hz).

$^{19}\text{F NMR}$ (acetone- d_6): δ (ppm) -109.57.

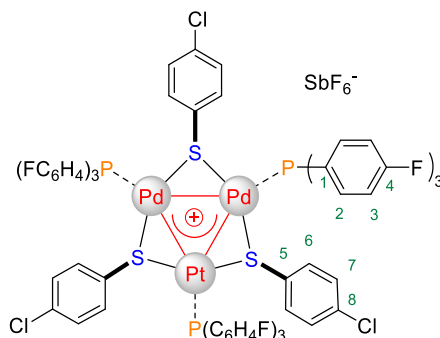
$^{195}\text{Pt NMR}$ (107 MHz, acetone- d_6): δ (ppm) -5474 (d, $^1J_{\text{Pt-P}} = 4400$ Hz).

HRMS calcd. for $\text{C}_{72}\text{H}_{51}\text{F}_9\text{P}_3\text{Pt}_3\text{Se}_3^+$ 2001.9528, found: 2001.9459.

IR (cm^{-1}): ν 3064, 2328, 1590, 1496, 1394, 1238, 1162, 1095, 1013, 828, 737, 659.

UV-vis.: $c = 2.10 \times 10^{-5}$ mol/L in CHCl_3 , $\lambda_{\text{max}} = 246$ nm, $\epsilon_{\text{max}} = 0.43 \times 10^5 \text{ M}^{-1} \text{ cm}^{-1}$.

2.5.3.3. Preparation of heterobimetallic cluster 161



Following **GP3**, **161** could be isolated as orange crystals.

¹H NMR (500 MHz, acetone-*d*₆): δ (ppm) 7.40-7.24 (m, 18H, **H3**), 7.15-7.08 (m, 18H, **H2**), 6.90-6.82 (m, 6H, **H7**), 6.56-6.47 (m, 6H, **H6**).

¹³C NMR (125 MHz, acetone-*d*₆): δ (ppm) 165.4 (d, *J* = 252.1 Hz, **C4**), 137.0 (**C6**), 136.9 (br s, **C2**), 136.8 (**C7**), 136.7 (**C8**), 129.4 (**C5**), 127.9 (br s, **C1**), 116.8 (m, **C3**).

³¹P NMR (acetone-*d*₆): δ (ppm) 12.57 (br, 2P, **Pd-P**), 6.53 (apparent t, 1P, ¹*J*_{P-Pt} = 4132 Hz, **Pt-P**).

¹⁹F NMR (acetone-*d*₆): δ (ppm) -109.36 (s, 1F, **Pt-P**), -109.01 (s, 2F, **Pd-P**).

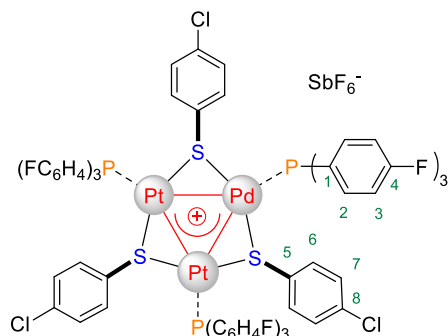
¹⁹⁵Pt NMR (107 MHz, acetone-*d*₆): δ (ppm) -5713 (d, ¹*J*_{Pt-P} = 4224 Hz).

HRMS calcd. for C₇₂H₄₈Cl₃F₉P₃Pd₂PtS₃⁺ 1786.8772, found 1786.8723.

IR (cm⁻¹): ν 2959, 2928, 2853, 1657, 1630, 1586, 1494, 1470, 1392, 1235, 1160, 1096, 1010, 942, 820, 747, 709, 656.

UV-vis.: *c* = 1.00 × 10⁻⁵ mol/L in CHCl₃, λ_{max} = 241 nm, ε_{max} = 0.90 × 10⁵ M⁻¹ cm⁻¹.

2.5.3.4. Preparation of heterobimetallic cluster 162



Following **GP4**, **162** could be isolated as orange crystals.

^1H NMR (500 MHz, acetone- d_6): δ (ppm) 7.46-7.22 (m, 18H, **H3**), 7.17-7.09 (m, 18H, **H2**), 6.87 (d, $J = 8.6$ Hz, 6H, **H7**), 6.55 (d, $J = 8.3$ Hz, 6H, **H6**).

^{13}C NMR (125 MHz, acetone- d_6): δ (ppm) 165.4 (d, $J = 252.1$ Hz, **C4**), 137.5-136.4 (m, **C2**, **C6**, **C7**, **C8**), 129.4 (**C5**), 127.9 (br s, **C1**), 117.1-116.4 (m, **C3**).

^{31}P NMR (acetone- d_6): δ (ppm) 6.10 (apparent t, $^1J_{\text{Pt-P}} = 4159$ Hz, 2P, **Pt-P**), 3.60 (br s, 1P, **Pd-P**).

^{19}F NMR (acetone- d_6): δ (ppm) -109.44 (s, 2F, **Pt-P**), -109.03 (s, 1F, **Pd-P**).

^{195}Pt NMR (107 MHz, acetone- d_6): δ (ppm) -5713 (d, $^1J_{\text{Pt-P}} = 4274$ Hz).

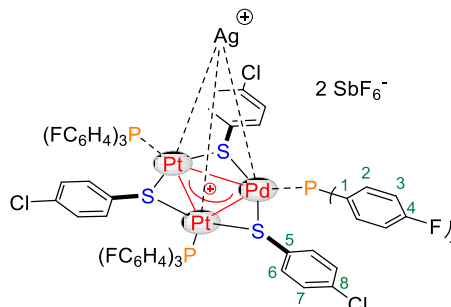
HRMS calcd. for $\text{C}_{72}\text{H}_{48}\text{Cl}_3\text{F}_9\text{P}_3\text{PdPt}_2\text{S}_3^+$ 1875.9376, found 1875.9320.

IR (cm^{-1}): ν 2959, 2928, 2856, 1737, 1657, 1632, 1589, 1494, 1465, 1366, 1230, 1215, 1204, 1162, 1092, 1012, 890, 827, 770, 707, 658.

UV-vis.: $c = 0.90 \times 10^{-5}$ mol/L in CHCl_3 , $\lambda_{\text{max}} = 240$ nm, $\epsilon_{\text{max}} = 0.87 \times 10^5 \text{ M}^{-1} \text{ cm}^{-1}$.

2.5.3.5. Preparation of silver-containing tetrahedral cluster

Complex 167



Following **GP5** and using AgSbF_6 , was obtained 19 mg (76% yield) of **167** as a red crystals.

$^1\text{H NMR}$ (500 MHz, acetone- d_6): δ (ppm) 7.30 (br s, 18H, **H2**), 7.09 (t, $J = 8.7$ Hz, 18H, **H3**), 6.88 (d, $J = 8.4$ Hz, 6H, **H7**), 6.50 (d, $J = 8.4$ Hz, 6H, **H6**).

$^{13}\text{C NMR}$ (125 MHz, acetone- d_6): δ (ppm) 165.3 (d, $J = 252.3$ Hz, **C4**), 137.0 (br s, **C2**), 136.8 (s, **C6**), 135.2 (**C8**), 134.7 (**C5**), 129.8 (**C7**), 127.2-127.8 (br, **C1**), 116.9 (d, $J = 21.4$ Hz, **C3**).

$^{31}\text{P NMR}$ (acetone- d_6): δ (ppm) 13.92.

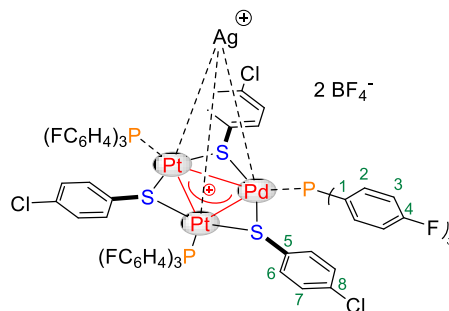
$^{19}\text{F NMR}$ (acetone- d_6): δ (ppm) -108.47 (s, $\text{P}(\text{C}_6\text{H}_4\text{F})_3$), -109.65 (s, SbF_6^-).

HRMS calcd. for $\text{C}_{72}\text{H}_{48}\text{Cl}_3\text{F}_9\text{P}_3\text{Pd}_3\text{S}_3\text{AgSbF}_6^+$ 2042.6163, found 2042.6026.

IR (cm^{-1}): ν 2959, 2928, 2856, 1737, 1657, 1632, 1589, 1494, 1465, 1366, 1230, 1215, 1204, 1162, 1092, 1012, 890, 827, 770, 707, 658.

UV-vis.: $c = 5 \times 10^{-6}$ mol/L in CHCl_3 , $\lambda_{\text{max}} = 242$ nm, $\epsilon_{\text{max}} = 7.8 \times 10^4$ $\text{M}^{-1} \text{cm}^{-1}$.

Complex 168



Following **GP5** and using AgBF_4 , was obtained 17 mg (78% yield) of **168** as a red crystals.

$^1\text{H NMR}$ (500 MHz, acetone- d_6): δ (ppm) 7.28 (br s, 18H, **H2**), 7.10 (t, $J = 8.0$ Hz, 18H, **H3**), 6.94 (d, $J = 7.4$ Hz, 6H, **H7**), 6.61 (d, $J = 7.3$ Hz, 6H, **H6**).

$^{13}\text{C NMR}$ (125 MHz, acetone- d_6): δ (ppm) 165.3 (d, $J = 252.1$ Hz, **C4**), 137.2 (br s, **C2**), 137.0 (s, **C6**), 135.2 (**C8**), 134.4 (**C5**), 129.9 (**C7**), 127.5 (br s, **C1**), 116.9 (d, $J = 20.7$ Hz, **C3**).

$^{31}\text{P NMR}$ (acetone- d_6): δ (ppm) 15.35.

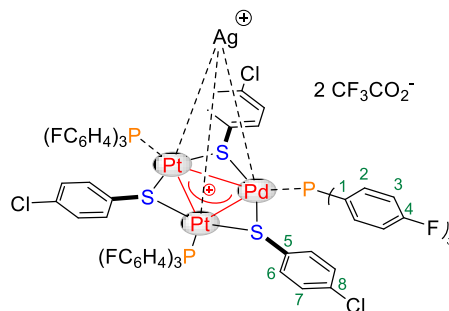
$^{19}\text{F NMR}$ (acetone- d_6): δ (ppm) -109.15 (s, $\text{P}(\text{C}_6\text{H}_4\text{F})_3$), -151.93 (s, BF_4^-).

HRMS calcd. for $\text{C}_{72}\text{H}_{48}\text{Cl}_3\text{F}_9\text{P}_3\text{Pd}_3\text{S}_3\text{AgBF}_4^+$ 1891.7261, found 1891.7207.

IR (cm^{-1}): ν 2955, 2926, 2857, 1657, 1587, 1498, 1468, 1392, 1232, 1160, 1092, 1011, 826.

UV-vis.: $c = 5 \times 10^{-6}$ mol/L in CHCl_3 , $\lambda_{\text{max}} = 245$ nm, $\epsilon_{\text{max}} = 9.4 \times 10^4 \text{ M}^{-1} \text{ cm}^{-1}$.

Complex 169



Following **GP5** and using AgO_2CCF_3 , was obtained 16 mg (72% yield) of **169** as a red crystals.

$^1\text{H NMR}$ (500 MHz, acetone- d_6): δ (ppm) 7.37 (br s, 18H, **H2**), 6.99 (br, 18H, **H3**), 6.87 (d, $J = 7.4$ Hz, 6H, **H7**), 6.35 (br, 6H, **H6**).

$^{13}\text{C NMR}$ (125 MHz, acetone- d_6): δ (ppm) 165.2 (d, $J = 252.0$ Hz, **C4**), 136.9-137.2 (br, **C2**), 137.0 (**C6**), 135.6 (**C8**), 134.9 (**C5**), 129.7 (**C7**), 127.8-128.5 (br, **C1**), 116.8 (ddd, $J = 22.8, 7.2, 4.0$ Hz, **C3**).

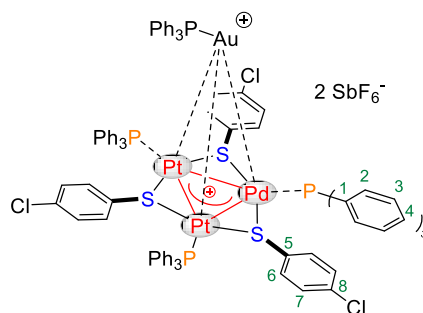
$^{31}\text{P NMR}$ (acetone- d_6): δ (ppm) 14.32.

$^{19}\text{F NMR}$ (acetone- d_6): δ (ppm) -109.50 (s, $\text{P}(\text{C}_6\text{H}_4\text{F})_3$), -73.69 (s, CF_3CO_2^-).

HRMS calcd. for $\text{C}_{72}\text{H}_{48}\text{Cl}_3\text{F}_9\text{P}_3\text{Pd}_3\text{S}_3\text{CF}_3\text{CO}_2\text{Ag}^+$ 1918.7072, found 1918.7033.

IR (cm^{-1}): ν 3069, 2926, 2854, 1899, 1664, 1586, 1495, 1470, 1394, 1237, 1195, 1160, 1089, 1010, 814, 798, 721.

UV-vis.: $c = 5 \times 10^{-6}$ mol/L in CHCl_3 , $\lambda_{\text{max}} = 242$ nm, $\epsilon_{\text{max}} = 6.2 \times 10^4$ $\text{M}^{-1} \text{cm}^{-1}$.

2.5.3.6. Preparation of gold-containing tetrahedral cluster **170**

Following **GP6**, was obtained 18 mg (72% yield) of **170** as a red crystals.

^1H NMR (500 MHz, acetone- d_6): δ (ppm) 7.66-7.73 (br, 15H, Ph/AuPPh $_3^+$), 7.43 (br s, 9H, **H4**), 7.29 (br s, 18H, **H3**), 7.22 (br s, 18H, **H2**), 6.76 (d, $J = 8.4$ Hz, 6H, **H7**), 6.36 (d, $J = 8.4$ Hz, 6H, **H6**).

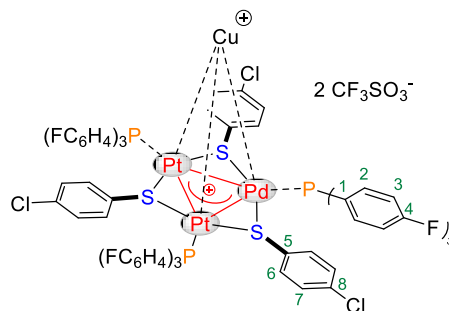
^{13}C NMR (125 MHz, acetone- d_6): δ (ppm) 136.9 (s, **C6**), 136.0 (**C8**), 135.2 (Ph/AuPPh $_3^+$), 134.4 (br s, **C3**), 134.2 (**C5**), 133.4 (br s, Ph/AuPPh $_3^+$), 131.8 (br s, **C4**), 130.7 (Ph/AuPPh $_3^+$), 129.4 (br s, **C1**, **C2**), 129.2 (**C7**).

^{31}P NMR (acetone- d_6): δ (ppm) 15.81 (s, PPh $_3$), 44.33 (s, AuPPh $_3^+$).

HRMS calcd. for $\text{C}_{90}\text{H}_{72}\text{Cl}_3\text{F}_6\text{P}_4\text{Pd}_3\text{S}_3\text{SbAu}^+$ 2230.8547, found 2230.8426.

IR (cm^{-1}): ν 3058, 2923, 2853, 1572, 1479, 1470, 1435, 1388, 1308, 1216, 1185, 1095, 1070, 1010, 820, 744, 691.

UV-vis.: $c = 1 \times 10^{-5}$ mol/L in CHCl_3 , $\lambda_{\text{max}} = 244$ nm, $\varepsilon_{\text{max}} = 5.2 \times 10^4$ $\text{M}^{-1} \text{cm}^{-1}$.

2.5.3.7. Preparation of copper-containing tetrahedral cluster **171**

Following **GP7**, was obtained 17 mg (75% yield) of **171** as a red crystals.

$^1\text{H NMR}$ (500 MHz, acetone- d_6): δ (ppm) 7.30 (br s, 18H, **H2**), 7.09 (t, $J = 8.7$ Hz, 18H, **H3**), 6.89 (d, $J = 8.4$ Hz, 6H, **H7**), 6.51 (d, $J = 8.4$ Hz, 6H, **H6**).

$^{13}\text{C NMR}$ (125 MHz, acetone- d_6): δ (ppm) 165.2 (d, $J = 251.9$ Hz, **C4**), 137.1 (br s, **C2**), 137.0 (dq, $J = 9.3, 5.2$ Hz, **C6**), 135.6 (**C8**), 134.7 (**C5**), 129.6 (**C7**), 128.1 (br s, **C1**), 116.8 (dq, $J = 22.8, 4.0$ Hz, **C3**).

$^{31}\text{P NMR}$ (acetone- d_6): δ (ppm) 13.67.

$^{19}\text{F NMR}$ (acetone- d_6): δ (ppm) -109.47 (s, $\text{P}(\text{C}_6\text{H}_4\text{F}_3)_3$), -78.38 (s, CF_3SO_3^-).

HRMS calcd. for $\text{C}_{72}\text{H}_{48}\text{Cl}_3\text{F}_9\text{P}_3\text{Pd}_3\text{S}_3\text{CF}_3\text{SO}_3\text{Cu}^+$ 1910.6981, found 1910.6886.

IR (cm^{-1}): ν 3100, 3070, 2925, 2845, 1699, 1589, 1497, 1470, 1395, 1265, 1237, 1161, 1093, 1030, 1011, 827.

UV-vis.: $c = 7.5 \times 10^{-6}$ mol/L in CHCl_3 , $\lambda_{\text{max}} = 244$ nm, $\epsilon_{\text{max}} = 8.7 \times 10^4$ $\text{M}^{-1} \text{cm}^{-1}$.

**PART 3: CATALYSIS WITH ALL-METAL
AROMATICS**

PART 3 : CATALYSIS WITH ALL-METAL AROMATICS

3.1. Introduction

In Part 2 of this manuscript, we demonstrated the predicted Lewis base properties of $[\text{Pd}_3]^+$ complexes and their ability to bind cations in spite of charge repulsion. However we did not insist on the delocalized positive charge borne by the palladium core. This positive charge lowered the LUMO and provided a Lewis acidic character to the cluster. Dual Lewis nature on the same molecule obviously reminded the principle of Frustrated Lewis Pairs (Figure 54)

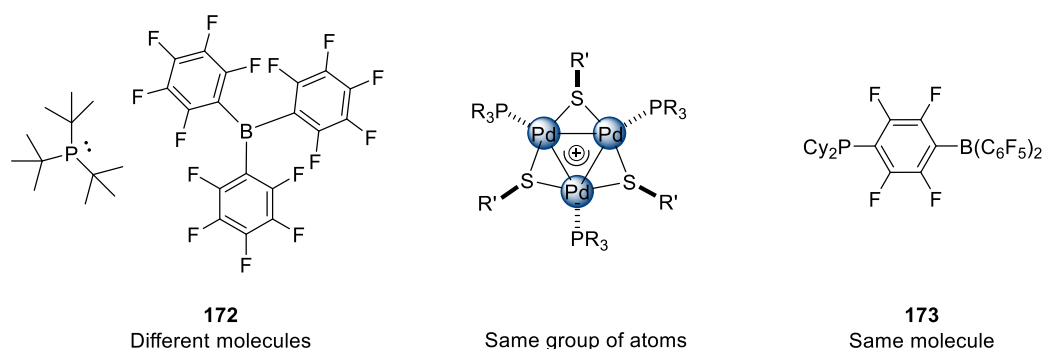
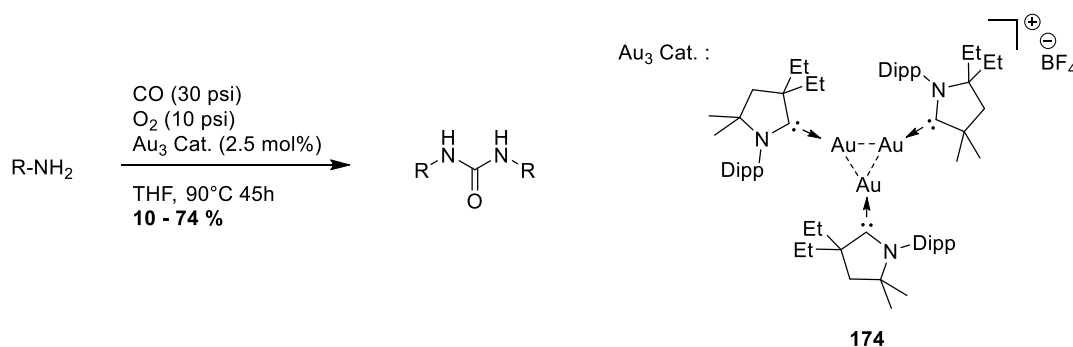


Figure 54 : Different types of Frustrated Lewis Pairs.

A Frustrated Lewis Pair (FLP) is by definition, a compound containing both Lewis acidic and Lewis basic moieties, where the formation of a Lewis adduct is prevented by steric hindrance. Seminal work on FLP has been realized by the group of Stephan. He reported at least two types of FLP. The first example (Figure 54, left) showed Lewis basic and Lewis acidic character on two distinguished molecules. **172** was composed by one tri(*t*-butyl)phosphine molecule which acts as Lewis base and by tri(pentafluorophenyl)borane that brings the Lewis acidic character. The second example **173** (Figure 54, right) presented a Lewis basic phosphorous moiety separated from the Lewis acidic boron moiety by a tetrafluorophenyl ether. The two Lewis species were on the same molecule. Concerning the tripalladium complex, both Lewis characters were located on the same group of atoms. To the best of our knowledge, these special properties of $[\text{Pd}_3]^+$ cluster were not referenced yet.

In parallel, we reported a new synthesis to easily access to $[\text{Pd}_3]^+$ clusters with diversity on its substituents. This method could be greatly valued if the clusters could provide any catalytic reactions. So far, only one example involving all-metal aromatics in catalytic reactions was reported by Bertrand and coworkers (Scheme 36).⁹⁷ With 2.5 mol% of trigold cluster **174** they realized catalytic carbonylation of amines in presence of 30 psi of carbon monoxide and 10 psi of dioxygen to form the corresponding urea.



Scheme 36 : Catalytic amine carbonylation by using aromatic trigold catalyst.

This reaction provided very modest to good yields and also other transition metal catalysts were efficient to do this transformation such as palladium, ruthenium or nickel¹²⁰. However it was the first application of all-metal aromatics in catalysis.

We thought semi-reduction of alkynes appropriate in order to exploit the high stability of $[\text{Pd}_3]^+$ cluster and its peculiar dual Lewis nature.

3.2. State of art

Since several decades, alkynes semi-reduction reactions have been well-studied and many methods to realize this transformation have been reported.¹²¹ According to that, only a non-exhaustive list of the most recent and relevant homogeneous methods will be described in this manuscript.

¹²⁰ D. J. Diaz, A. K. Darko, L. McElwee-White, *Eur. J. Org. Chem.*, **2007**, 27, 4453-4465. b) F. Ragaini, *Dalton Trans.*, **2009**, 32, 6251-6266. c) X.-F. Wu, H. Neumann, M. Beller, *ChemSusChem*, **2013**, 6, 229-241.

¹²¹ a) C. Oger, L. Balas, T. Durand, J. M. Galano, *Chem. Rev.*, **2013**, 113, 1313-1350. b) R. Chinchilla, C. Najera, *Chem. Rev.*, **2014**, 114, 1783-1826. c) I. N. Michaelides, D. J. Dixon, *Angew. Chem. Int. Ed.*, **2013**, 52, 806-808. d) J. G. de Vries, C. J. Elsevier, *Handbook of Homogeneous Hydrogenation*, Wiley- VCH, Weinheim, **2007**. e) S. Gladiali, E. Alberico, *Chem. Soc. Rev.*, **2006**, 35, 226-236. f) J. S. M. Samec, J.-E. Bäckvall, P. G. Anderson, P. Brandt, *Chem. Soc. Rev.*, **2006**, 35, 237-248. g) D. Wang, D. Astruc, *Chem. Rev.*, **2015**, 115, 661-6686.

3.2.1. Semi-reduction reactions using palladium catalysts

Among reported alkyne semi-reduction methods, the majority were realized *via* palladium catalysis. Lindlar reported the first poisoned palladium catalyst in 1952.¹²² However this method using gaseous dihydrogen was not convenient because it presented some reproducibility issues and if the reaction was not stopped immediately after full conversion of alkyne, the formed alkene could react with excess of hydrogen and afford over-reduction products. Since then, a lot of progress has been made in heterogeneous and homogenous catalysis.

Elsevier and coworkers developed a new type of palladium(0) catalyst (Figure 55).

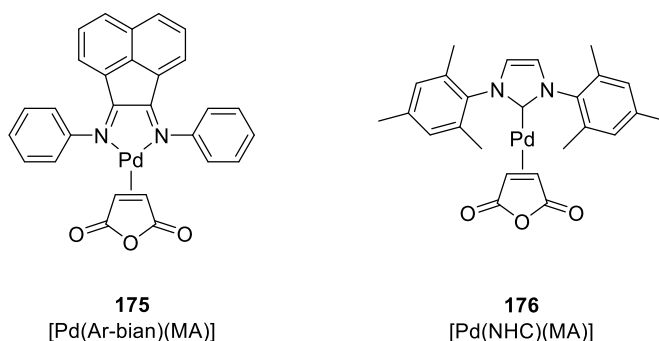
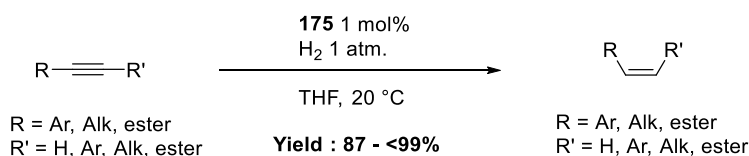


Figure 55 : Palladium(0) catalysts

First generation complex **175** is composed by a bidentate bis(arylimino)acenaphthalene ligand and a molecule of maleic anhydride as ancillary ligands (Figure 55, left).¹²³ By activation of dihydrogen and ligand exchange between maleic anhydride and alkyne, they could be able to selectively reduce alkyne to alkene under mild conditions (Scheme 37).



Scheme 37 : Semi-reduction of alkynes by using Elsevier's first generation catalyst.

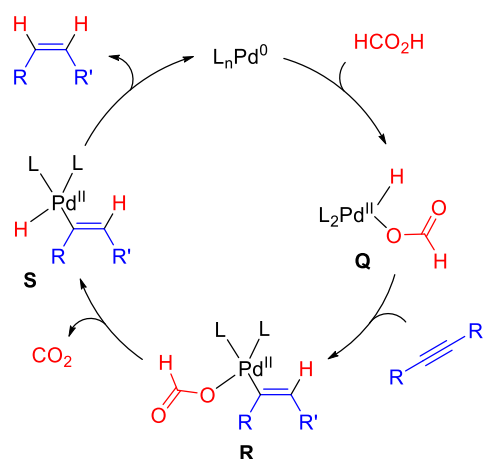
¹²² a) H. Lindlar, *Helv. Chim. Act.*, **1952**, 57, 446-450. b) H. Lindlar, R. Dubuis, *Org. Synth.*, **1966**, 46, 89-91.

¹²³ a) M. W. van Laren, C. J. Elsevier, *Angew. Chem. Int. Ed.*, **1999**, 38, 3715-3717. b) A. M. Kluwer, T. S. Koblenz, T. Jonischkeit, K. Woelk, C. J. Elsevier, *J. Am. Chem. Soc.*, **2005**, 127, 15470-15480.

They obtained good to excellent selectivities with terminal and internal alkynes either electron-rich or electron-poor. However, this method provided over-reduction products for some examples (between 3 and 13% yields). The hydrogenation method using gaseous dihydrogen was not really controllable even if the catalyst was rendered less active by adding excess ligands or other metallic salts.

In parallel, studies have been realized on transfer hydrogenation by using hydrogen donor instead of hazardous gaseous dihydrogen.¹²⁴ So far, many hydrogen donors have been listed such as ammonium formiates, 1,4-cyclohexadiene¹²⁵ or Hantzsch esters¹²⁶ to cite the most famous ones.

Reactions of alkynes with formic acid/triethylamine in presence of palladium(0) catalyst gave preferentially *Z*-alkene.¹²⁷ In 1993, Sato proposed a mechanism of the transfer hydrogenation (Scheme 38).¹²⁸



Scheme 38 : Sato's proposed mechanism of transfer hydrogenation by $\text{HCO}_2\text{H}/\text{Et}_3\text{N}$.

This mechanism used two oxidation states of palladium (0 and +II). The first step was the oxidative addition of the O-H bond of formic acid on palladium(0) to give intermediate **Q**. Alkyne moiety was inserted into the Pd-H bond in a *cis* configuration to afford intermediate **R**. The latter underwent decarboxylation to provide Palladium (II) intermediate **S**. Classical

¹²⁴ a) G. Brieger, T. J. Nestruck, *Chem. Rev.*, **1974**, 74, 567-580. b) R. A. W. Johnstone, A. H. Wilby, *Chem. Rev.*, **1985**, 85, 129-170.

¹²⁵ B. Michelet, C. Bour, V. Gandon, *Chem. Eur. J.*, **2014**, 20, 14488-14492.

¹²⁶ C. Zheng, S.-L. You, *Chem. Rev.*, **2012**, 41, 2498-2518.

¹²⁷ R. A. W. Johnstone, A. h. Wilby, I. D. Entwistle, *Chem. Rev.*, **1985**, 85, 129-170.

¹²⁸ K. Tani, N. Ono, S. Okamoto, F. Sato, *J. Chem. Soc., Chem. Commun.*, **1993**, 386-387.

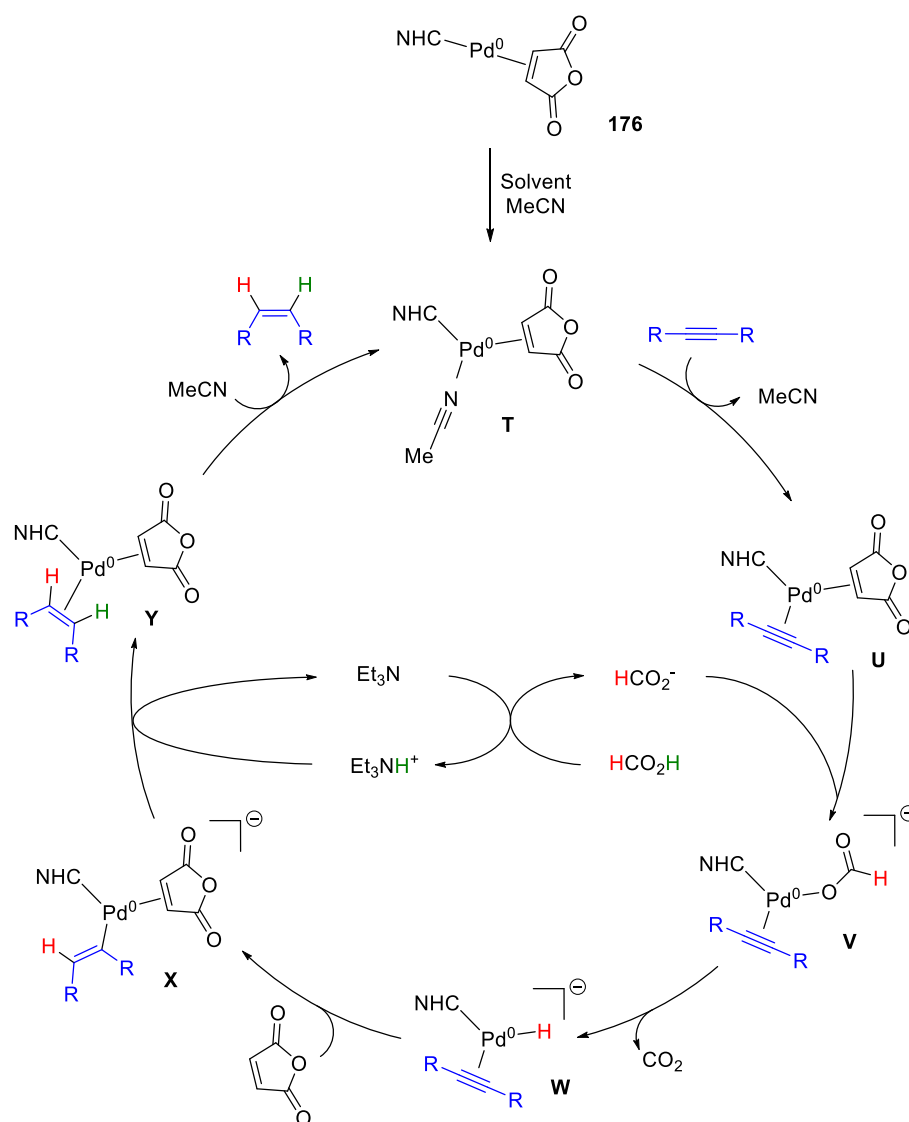
reductive elimination step released the desired Z-alkene and regenerated the catalyst. Even if this mechanism could be acceptable, it did not take into account the role of trimethylamine. Nevertheless, this method afforded alkanes if the electron density of the alkyne was affected by the presence of strongly electron-withdrawing or electron-donor groups.

The second generation catalyst of Elsevier *et al.* **176** possessed a hindered monodentate symmetrical NHC carbene as ligand (Figure 55 right).¹²⁹ By using this palladium(0) catalyst coupled with triethylammonium formate as hydrogen source, they could be able to realize Z-selective semi-reduction of alkyne.¹³⁰ They also investigated the mechanism¹³¹ that is depicted on scheme 39.

¹²⁹ a) J. W. Sprengers, J. Wassenaar, N. D. Clement, K. J. Cavell, C. J. Elsevier, *Angew. Chem. Int Ed.*, **2005**, *44*, 2026-2029.

¹³⁰ a) P. Hauwert, G. Maestri, J. W. Sprengers, M. Catellani, C. J. Elsevier, *Angew. Chem. Int. Ed.* **2008**, *47*, 3223-3226. b) P. Hauwert, J. J. Dunsford, D. S. Tromp, J. J. Weigand, M. Lutz, K. J. Cavell, C. J. Elsevier, *Organometallics*, **2012**, *32*, 131-140.

¹³¹ P. Hauwert, R. Boerleider, S. Warsink, J. J. Weigand, C. J. Elsevier, *J. Am Chem. Soc.*, **2010**, *132*, 16900-16910.



Scheme 39 : Proposed mechanism for alkyne semi-reduction.

In an acetonitrile solution, the precatalyst **176** was complexed by a MeCN molecule to give the active species **T**. By ligand exchange, MeCN was replaced by an alkyne molecule to form intermediate **U**. In parallel, formic acid was deprotonated by triethylamine to afford the corresponding formiate which could coordinate the palladium complex to give anionic intermediate **V**. After decarboxylation, **V** was transformed in palladium-hydride complex **W**. Hydrogen transfer into alkyne followed by insertion of maleic anhydride provided intermediate **X**. Protonolysis of **X** by triethylammonium cation afforded tricoordinated palladium(0) intermediate **Y**. A ligand exchange step released the desired Z-alkene and regenerated the active specie **T**. Deuterium labelling experiments showed that hydrogens kept their identity during the reaction. The selectivity towards alkene was justified by the life-time

of intermediate **Y** but also by the coordinative properties of the solvent. Acetonitrile possess a good coordination property which helps to operate a ligand exchange with the alkene ligand. However, if alkene has good π -accepting properties (electron-withdrawing substituents), the strength of Pd-alkene bond will increase and so does intermediate **Y** lifetime. The competition between the two ligands is no longer in favor of acetonitrile, thus **Y** is more suitable to undergo another catalytic cycle and provide the corresponding over-reduced product.

Up to now, all reported palladium-catalyzed methods for semi-reduction of alkyne used palladium(0) catalyst.

3.2.2. Method using FLP

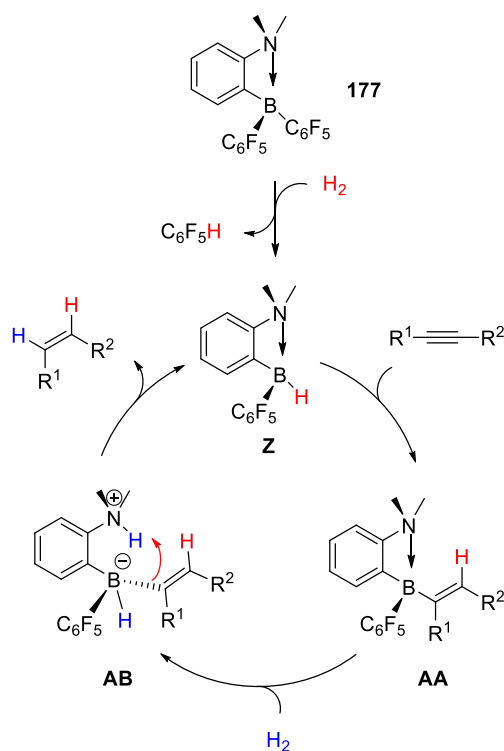
Since last decade, the utilization of Frustrating Lewis Pairs to realize metal-free reactions has been stated.¹³² These species are known to activate dihydrogen in order to reduce polarized multiple bond such as imines, enamides, silyl ether,¹³³ α,β -enones¹³⁴ or ynones¹³⁵ with very mild conditions. Very recently, Papai and Repo reported a method to semi-hydrogenate alkyne to *Z*-alkene by using aminoborane FLP **177** (Scheme 40)

¹³² a) D. W. Stephan, *Acc. Chem. Res.*, **2015**, *48*, 306-316. b) D. W. Stephan, G. Erker, *Angew. Chem. Int. Ed.*, **2015**, *54*, 2-44.

¹³³ D. W. Stephan, *Org. Biomol.*, **2012**, *10*, 5740-5746.

¹³⁴ G. Eros, H. Mehdi, I. Papai, T. A. Rokob, P. Kiraly, G. Tarkanyi, T. Soos, *Angew. Chem. Int. Ed.*, **2010**, *49*, 6559-6563.

¹³⁵ B-H. Xu, G. Kehr, R. Frölich, B. Wibbeling, B. Schirmer, S. Grimme, G. Erker, *Angew. Chem. Int. Ed.*, **2011**, *50*, 7183-7186.



Scheme 40 : Semi-reduction of alkyne by using FLP

The precatalyst **177** was activated by a first molecule of dihydrogen to give the reactive specie **Z**, releasing in the same time a molecule of pentafluorobenzene. Alkyne moiety inserted into the boron-hydrogen bond to afford **AA** and then the system activates a second molecule of H_2 to provide intermediate **AB**. The carbon-boron bond attacked the hydrogen atom borne by the ammonium ion and the desired alkene was released regenerating the active catalyst. This method proved to be efficient at 2.2 bar of H_2 and 5 mol% of organocatalyst. Several alkynes were synthesized with excellent selectivities except for electron rich or bulky alkynes for which the conversion was low and the selectivity modest. However, with this metal-free method no alkanes were detected.

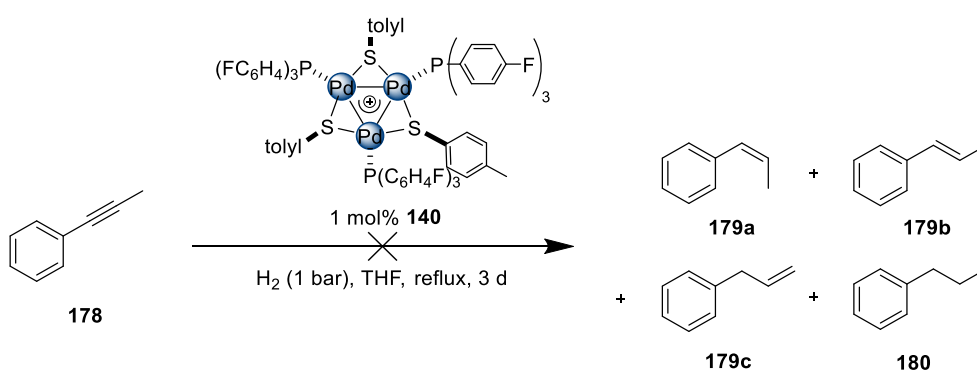
3.2 Results and discussions

3.2.1. Aim of the project

The purpose of the project was not to just add a new method to the plethora already listed. The real aim was to observe the potential catalytic activity of our stable $[\text{Pd}_3]^+$ species on a simple and already well-investigated reaction in order to gain insights on their behavior pivoting on existing literature to understand analogies and differences.

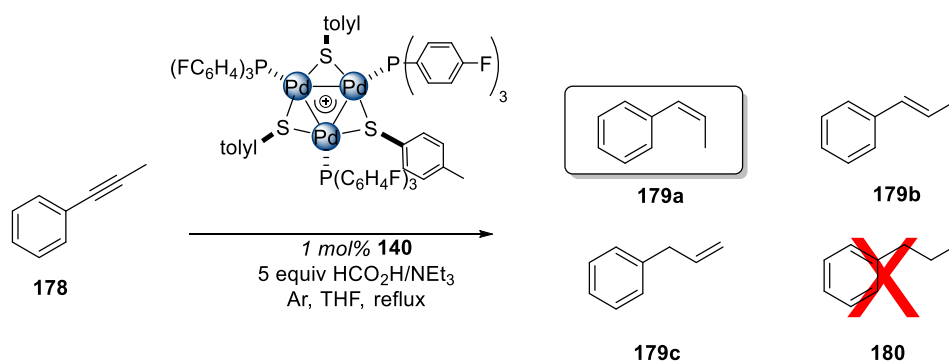
3.2.2. Optimization of the reaction

Inspired by the work of Elsevier¹²⁹ with its first generation catalyst, we started our investigation by the reaction depicted on scheme 41.



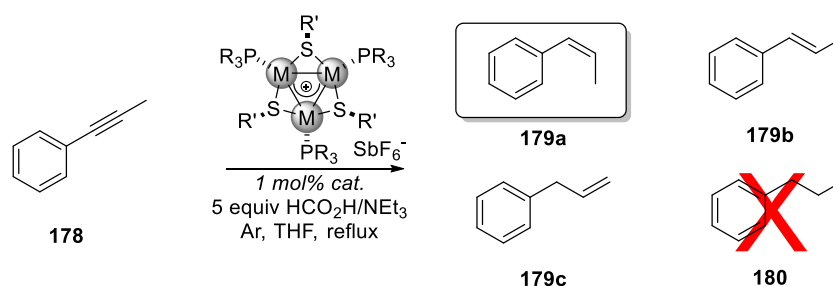
Scheme 41 : First catalytic reaction with dihydrogen.

We performed the first reaction by using phenylprop-1-yne **178** as model substrate with 1 mol% of catalyst **140** in THF under dihydrogen atmosphere. The reaction was then stirred during one day at room temperature (25 °C). GC-MS analysis of the crude reaction showed no conversion of the starting material so we decided to warm the solution to reflux in THF. Sadly, after three days stirring at reflux, no conversion was observed. We thought that 1 bar of dihydrogen pressure was not enough. Unfortunately, Institut de Chimie des Substances Naturelles was not equipped to realize high pressure hydrogenation. We thus decided to replace hazardous gaseous dihydrogen by a safer hydrogen source, namely the couple formic acid/triethylamine (Scheme 42).



Scheme 42 : Reaction with formic acid/triethylamine as hydrogen donor.

The reaction was conducted with the same conditions presented above but with five equivalents of formic acid and triethylamine under argon (Table 12, Entry 1). After 24h, we were excited to see a conversion of 20% of the starting material by GC-MS. The reaction was stirred for three additional days until the observation of black particles stuck on the sides of the Schlenk. Conversion stopped at 86% a surprising selectivity of 92% towards the Z-alkene **179a** was observed. Small quantities of E-alkene **179b** (3%) and double-bond isomerization product allylbenzene **179c** (5%) were identified. Moreover, no presence of the over-reduced product **180** was detected. It seems that the current method worked pretty well, however incomplete conversion upon four days meant that parameters needed to be improved. We thus decided to screen several [Pd₃]⁺ complexes previously synthesized in Part 2 of this manuscript (Table 12).



Entry	Complex	M	R	R'	T (h)	Conv. (%)	Selectivity
							179a/179b/ 179c/180 (%)
1	140	Pd	4-FC ₆ H ₄ -	4-MeC ₆ H ₄ -	96	86%	92/3/5/0
2	145	Pd	4-MeC ₆ H ₄ -	4-ClC ₆ H ₄ -	64	quant.	82/15/3/0
3	143	Pd	Ph-	Ph-	48	54	83/8/9/0
4	154	Pd	Et-	4-ClC ₆ H ₄ -	96	-	-
5	153	Pd	Et-	4-MeC ₆ H ₄ -	96	-	-
6	148	Pd	4-FC ₆ H ₄ -	Me-	64	34	82/12/6/0
7	152	Pd	4-MeC ₆ H ₄ -	Me-	10	quant.	93/3/4/0
8	156	Pt	4-MeC ₆ H ₄ -	Me-	96	-	-

Table 12 : Screening of [Pd₃]⁺ catalysts.

Inversion of electron-withdrawing and electron-donating groups on fragments increased the activity of the catalyst to the detriment of the selectivity of the reaction (Table 12, Entries 1 & 2). All-phenyl substituted cluster provided a selectivity of 83% toward Z-alkene **179a** but revealed to be inactive after 48h (Table 12, Entry 3). Modification of the electronic structure seemed to have no beneficial effects on the reaction. We thus turned to modify the steric arrangement of the catalyst. Complexes bearing alkyl phosphine substituents remained completely inactive (Table 12, Entries 4 & 5). Nevertheless, small alkyl groups on thiolate substituents afforded more attractive results. Despite the bad conversion with an electron-withdrawing phosphine, the cluster **152** composed with tri(*p*-tolyl)phosphine and methylthiolate groups, provided total conversion in only 10h and a selectivity of 93% towards Z-alkene **179a** (Table 12, Entries 6 & 7) As observed for the other tested complexes, no over-

reduction was observed during the process even if heating was prolonged for additional 24 hours. The platinum analogue **156** was also tested but interestingly stayed inactive even after four days (Table 12, Entry 8). To get a better understanding of this phenomenon, we analyzed the frontier orbitals of $[\text{Pd}_3]^+$ **152** and $[\text{Pt}_3]^+$ **156** (Figure 56).

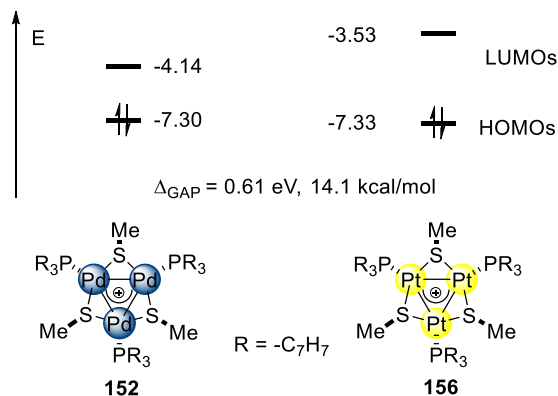
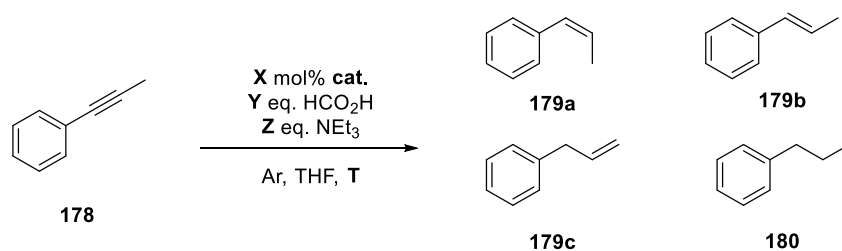


Figure 56 : Frontier orbitals of complexes **152** (left) and **156** (right).

This chart showed a significant difference of 0.61 eV between the LUMO of **152** and that of **156**. Whereas the HOMOs possessed nearly the same energy level, the difference of the LUMOs made $[\text{Pd}_3]^+$ **152** a better Lewis acid than $[\text{Pt}_3]^+$ **156** and could explain why the reaction did not work with triplatinum catalyst (vide infra). These results were counterintuitive considering the mono-platinum clusters are more electrophilic than their palladium peers.¹³⁶ Having the best catalyst in hands, further optimization and comparison tests were realized, varying several parameters (Table 13).

¹³⁶ a) T. Caneque, F. M. Truscott, R. Rodriguez, G. Maestri, M. Malacria, *Chem. Soc. Rev.*, **2014**, *43*, 2916-2926. b) L. Fensterbank, M. Malacria, *Acc. Chem. Res.*, **2014**, *47*, 953-965. c) C. Obradors, A. M. Echavarren, *Acc. Chem. Res.*, **2014**, *47*, 902-912.



Entry	Catalyst	X (mol %)	Y (eq.)	Z (eq.)	T (°C)	Reaction time (h)	Conv. (%)	Selectivity
								179a/179b/ 179c/180 (%)
1	152	0.1	5	5	Rfx	120	9	84/6/10/0
2	152	1	5	5	80 (μW)	0.5	< 1	-
3	152	1	5	0	Rfx	24	-	-
4	152	1	5	0.1	Rfx	7	18%	78/14/8/0
5	-	-	5	5	Rfx	24	-	-
6	Pd(dba) ₂	1	5	5	Rfx	24	Quant.	81/11/0/8
7	Pd(dba) ₂	3	5	5	Rfx	24	Quant.	25/15/0/60

Table 13 : Optimization and comparison tests

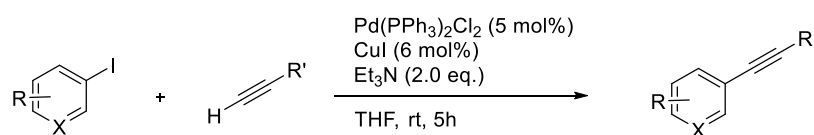
Reaction with 0.1 mol% of **152** provided a correct selectivity however, after 120 hours of stirring, the conversion stopped at only 9% (Table 13, Entry 1). We were also interested to investigate micro-wave heating which should warm the solution more homogeneously but unfortunately after 30 minutes at 80 °C, the conversion was less than 1% (Table 13, Entry 2). According to the proposed mechanism by Elsevier¹³¹ (Scheme 39), triethylamine should be catalytic. Reaction without triethylamine showed no conversion, which indicated that the catalyst is not able to activate the O-H bond of formic acid (Table 13, Entry 3). Adding only 0.1 eq of triethylamine afforded 18% of conversion and a correct selectivity of 78% towards Z-alkene without over-reduced product (Table 13, Entry 4). As expected, no conversion was observed for the reaction without catalyst (Table 13, Entry 5). As **152** was composed of three palladium atoms, we were curious to see the comparison of results with 1 and 3% of palladium(0) catalyst (Table 13, Entries 6 & 7). Reaction using 1 mol% of Pd(dba)₂ gave a

good selectivity 81% towards Z-alkene, but 8% of over-reduced product was detected. Increasing the catalytic amount to 3 mol% of palladium(0) provided 60% of the corresponding alkane **180**. The two latter experiments showed the efficiency and the chemoselectivity of $[\text{Pd}_3]^+$ catalyst. In agreement with the good results obtained with the model substrate phenylprop-1-yne **178**, we wanted to extend the reaction to differently substituted alkynes.

3.2.3. Alkynes syntheses

3.2.3.1. Synthesis of aromatic alkynes

The synthesis of aromatic alkynes was realized by a classical Sonogashira-type coupling using palladium(II) reduced *in situ* and copper iodide (Table 14).



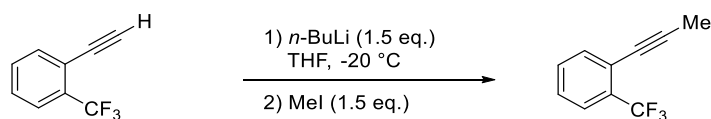
Entry	R	R'	X	Product	Yield (%)
1	4-MeO	(CH ₂) ₃ CN	C	183	80
2	4-CO ₂ Me	4-MeO-C ₆ H ₄	C	188	82
3	4-CO ₂ Me	4-Cl-C ₆ H ₄	C	189	94
4	4-CO ₂ Me	4-MeO ₂ C-C ₆ H ₄	C	190	60
5	H	4-Me-C ₆ H ₄	N	191	92

Table 14 :Synthesis of aromatic alkynes

With this method, aromatic alkynes were obtained in moderate to excellent yields and were purified in order to be engaged in semi-reduction reactions. We tuned the electronic environment of alkynes with electron-withdrawing and electron-donating groups such as methyl ester or methoxy group.

Aromatic alkyne **184** was obtained by a different method. Starting from the corresponding terminal alkyne, deprotonated by *n*-butyllithium and then sequential

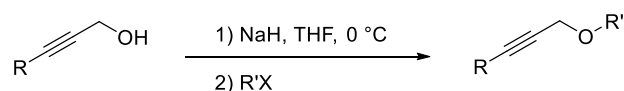
methylation with methyl iodide by a S_N2 type reaction delivered **184** in 63% yield (Scheme 43).



Scheme 43 : Synthesis of alkyne 184.

3.2.3.2. Synthesis of aliphatic alkynes

To be very rigorous concerning the nature of our scope, we performed the syntheses of other aliphatic alkynes bearing different type of functional groups starting from propargylic alcohol derivatives (Table 15).



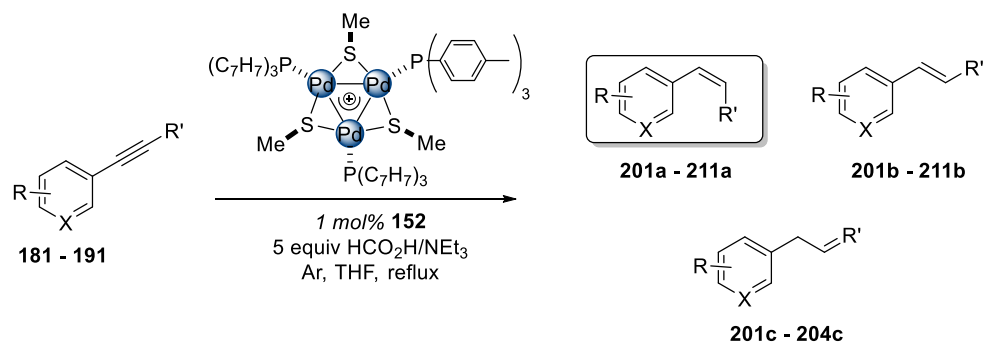
Entry	R	R'	X	Yield (%)
1	Me	TBDPS	Cl	193 82%
2	Me	Ph-CH ₂	Br	194 52%
3	Me	4-CF ₃ -C ₆ H ₄ -CH ₂	Br	195 90%
4	Me	2-F-C ₆ H ₄ -CH ₂	Br	196 40%
5	Me	3-Br-C ₆ H ₄ -CH ₂	Br	197 41%
6	Me	Ph(C=O)	Cl	198 86%
7	Ph	4-CN-C ₆ H ₄ (C=O)	Cl	199 45%

Table 15 : Synthesis of aliphatic alkynes.

No optimization was realized for these synthesis but seven aliphatic alkynes **193** – **199** were isolated with moderate to good yields and were suitable for semi-hydrogenation reactions.

3.2.4. Extension of the semi-reduction reaction catalyzed by $[\text{Pd}_3]^+$ catalyst

We first tested the semi-reduction reaction on previously synthesized and commercial aromatic alkynes. These species are known to be more difficult to reduce than aliphatic ones because of their stabilization by π -electrons delocalization with the conjugated aromatic ring. The results were presented on table 16.



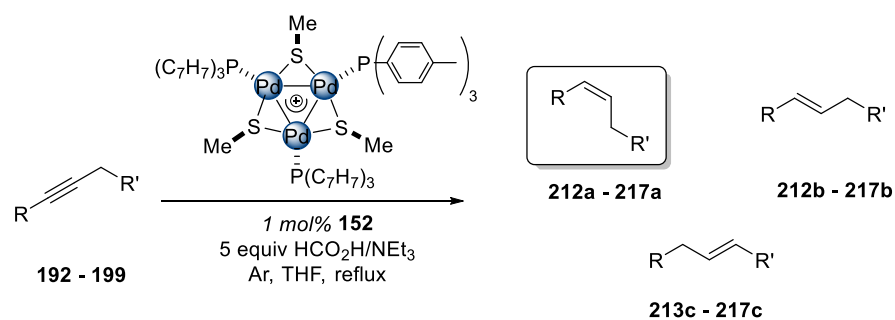
Entry	Alkyne	R	R'	X	t	Selectivity Z/E/Isom
1	181	Ph	C ₂ H ₅	C	22	78/21/1
2	182	Ph	C ₃ H ₇	C	67	70/29/1
3	183	4-MeO-C ₆ H ₄	(CH ₂) ₃ CN	C	88	83/13/4
4	184	2-CF ₃ -C ₆ H ₄	Me	C	96	92/4/4
5	185	Ph	(CO)CH ₃	C	4	0/100/0
6	186	Ph	CO ₂ H	C	4	93/7/0
7	187	Ph	Ph	C	7	98/2/0
8	188	4-MeO-C ₆ H ₄	4-MeO ₂ C-C ₆ H ₄	C	9	99/1/0
9	189	4-Cl-C ₆ H ₄	4-MeO ₂ C-C ₆ H ₄	C	9	99/1/0
10	190	4-MeO ₂ C-C ₆ H ₄	4-MeO ₂ C-C ₆ H ₄	C	10	100/0/0
11	191	Ph	4-Me-C ₆ H ₄	N	18	100/0/0

Table 16 : Semi-reduction of aromatic alkynes.

Compared to the results obtained with phenylprop-1-yne **178**, increasing the length of the aliphatic side chain demanded a longer reaction time to achieve full conversion and implied a fall of selectivity to 78 and 70% in favor of alkenes **201a** and **202a** respectively (Table 16,

Entries 1 & 2). The tripalladium catalyst **152** kept cyano and trifluoromethyl groups untouched (Table 16, Entries 3 & 4). Alkyne **185** bearing a conjugated ketone was semi-reduced into *Z*-alkene **205a**, which isomerized *in situ* to give 100% of the *E*-product **205b** upon full conversion (Table 16, Entry 5). Electron-poor olefins are very sensitive to hydrogenation condition but no traces of corresponding alkane was detected (Table 16, Entries 5 & 6). Alkynes substituted by two aryl groups were semi-reduced with excellent selectivities between 98 and 100% towards *Z*-alkene **207a–211a** whatever the electron-withdrawing or electron-donating characters of the substituents (Table 16, Entries 7-11). It seemed that the catalyst also tolerated chlorine atoms, which was interesting and not common for a palladium complex (Table 16, Entry 9). A tolerance for heterocyclic molecules was shown with total selectivity obtained for pyridine containing alkyne **191** (Table 16, Entry 11). According to these results, we interestingly noticed that the $[\text{Pd}_3]^+$ catalyst was more effective with biaryl substituted alkynes. This observation could be due to potential π -stacking interactions between aryl group on the phosphine and those borne by the alkyne which favored the coordination of the alkyne to the palladium cluster.

Satisfied by the good results obtained with aromatic alkynes, we thus turned ourselves to aliphatic alkynes (Table 17).



Entry	Alkyne	R	R'	t (h)	Selectivity
					Z/E/Isom
1	192	C(CH ₃) ₂ OH	NMe ₂	4	100/0/0
2	193	Me	TBDPSO	22	90/6/4
3	194	Me	BnO	18	83/14/3
4	195	Me	4-CF ₃ -BnO	15	76/19/5
5	196	Me	2-F-BnO	16	74/21/5
6	197	Me	3-Br-BnO	17	87/11/2
7	198	Me	BzO	18	-
8	199	Ph	4-CN- BzO	20	29/27/44

Table 17 : Semi-reductions of aliphatic alkynes.

Compound **192** was semi-reduced in 4 hours affording **212a** in quantitative yield (Table 17, Entry 1). Silyl ethers-containing alkyne **193** was also tolerated by the catalyst and produced Z-alkene **213a** with a selectivity of 90% (Table 17, Entry 2). Benzyl protecting groups on alcohol were known to be reduced by hydrogenation conditions but in our case, they were not affected (Table 17, Entries 3-6). Despite the presence of a bromide on compound **197**, the catalyst remained selective for towards carbon-carbon triple bonds and provided **217a** in 87% yield (Table 17, Entry 6). These two positions were suitable for isomerization but experimentally we only observed the thermodynamically less stable terminal alkene, likely for steric reasons (Figure 57).

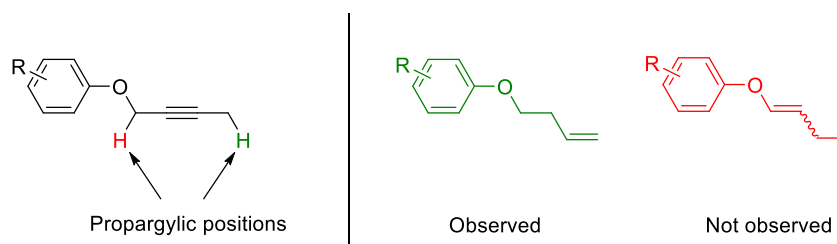
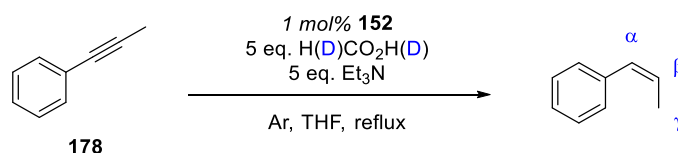


Figure 57 : Possible double-bond isomerization products.

Reaction with propargylic ester **198** gave an unexpected outcome (Table 17, Entry 7). After 18 hours, full conversion was achieved but no reduction product or polymers were obtained. To understand what happened, we realized the reaction with a heavier alkyne **199** (Table 17, Entry 8). After 20 hours, we isolated a mixture of three isomers of phenylpropene **179a**, **179b** and **179c** in a 29/27/44 respective ratio. The cleavage of propargylic esters under hydrogenation conditions¹³⁷ has been already described for monometallic complexes¹³⁸ in order to synthesize allenes.¹³⁹ These observation led us to think that $[Pd_3]^+$ cluster could act as its mono-nuclear electrophilic peers.

We also realized reactions on the model substrate phenylprop-1-yne **178** with deuterium-labeled formic acids in order to get a better understanding of the mechanism (Scheme 44).



Scheme 44 : Semi-reduction reactions using deuterated formic acids.

Three different deuterated formic acids were used for this study: HCO_2D , DCO_2H and DCO_2D . We first observed that with HCO_2D , the reaction required ten hours to achieve full conversion as observed with regular formic acid. However, with deuterium on the formiate position, the reaction time to reach full conversion increased to 24 hours. This data suggested that hydride transfer had an impact on the catalytic cycle and might be the rate-determining

¹³⁷ R. Shen, T. Chen, Y. Zhao, R. Qui, Y. Zhou, S. Yin, X. Wang, M. Goto, L.-B. Han, *J. Am. Chem. Soc.*, **2011**, *133*, 17037-17044.

¹³⁸ A. Correa, N. Marion, L. Fensterbank, M. Malacria, S. P. Nolan, L. Cavallo, *Angew. Chem. Int. Ed.*, **2008**, *47*, 718-721. J. Marco-Contelles, E. Soriano, *Chem. Eur. J.*, **2007**, *13*, 1350-1357.

¹³⁹ N. Krause, A. Hoffmann-Roder, *Tetrahedron*, **2004**, *60*, 11671-11694. C. Deutsch, B. H. Lipshutz, N. Krause, *Org. Lett.*, **2009**, *11*, 5010-5012.

step of the reaction. Moreover, we observed a non-selective distribution of the deuterium atom in ^2D NMR (Figure 58).

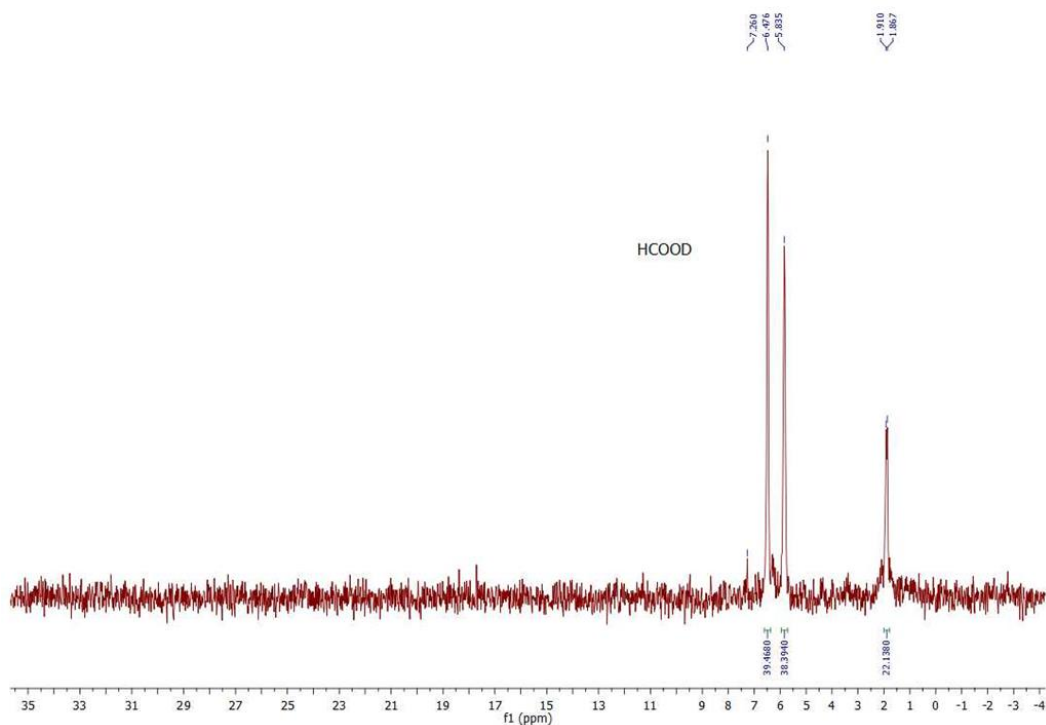
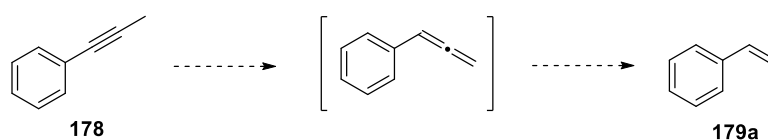


Figure 58 : Deuterium NMR of deuterated phenylpropene.

A $\alpha/\beta/\gamma$ ratio of 39/39/22 was determined for reaction with HCO_2D . Deuterium was incorporated on the two non-aromatic sp^2 carbon atoms but also on the terminal carbon. Similar ratios were observed for reactions with DCO_2H and DCO_2D . These unprecedented observations,¹³¹ suggested that the reaction could proceed via an allene intermediate (Scheme 45), possibly due to electrophilic activation of the alkyne by the $[\text{Pd}_3]^+$ complex.

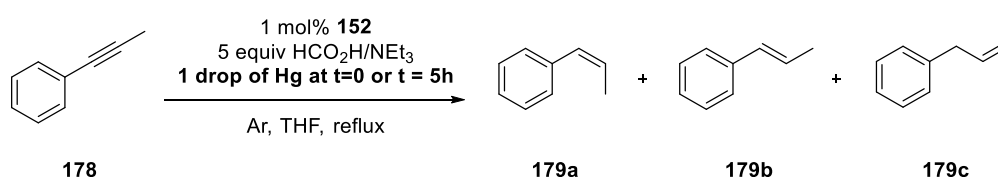


Scheme 45 : Possible allene intermediate.

The next question was to know if the active species might have been $[\text{Pd}_3]^+$ species. To answer the question, we monitored the reaction on model substrate **178** by UPLC-ES-HRMS

(See supporting information). A sample of the reaction was taken each hour from time 0 to full conversion (10 hours) and they were analyzed by HRMS. Each sample was analyzed by GC-MS too to see the conversion of the substrate. The results showed that the isotopic pattern of $[\text{Pd}_3]^+$ **152** centered at $m/z = 1373$ was visible till complete conversion of the alkyne even though its intensity decreased with time. Besides traces of decomposition at lower m/z , the main species observed was around $m/z = 695$. It possessed too the isotopic pattern of $[\text{Pd}_3]^+$ complex and could correspond to $[\text{Pd}_3\text{P}(\text{C}_7\text{H}_7)_3\text{THF}]^+$ fragment. At present time we cannot conclude about the catalytic role of **152**. Isolation of reaction intermediates could help for future determination.

We next wondered if our catalyst was homogeneous or heterogeneous. Several additional experiments were performed in order to get more information. The first one was the test of the mercury drop.¹⁴⁰ Liquid mercury was known to form an amalgam with heterogeneous catalyst and also with nano-particles and should, in theory, let the homogenous metallic complexes untouched. We realized two reactions, one by adding a drop of liquid mercury at the beginning of the reaction and the second by adding the mercury drop after five hours (Scheme 46).



Scheme 46 : Mercury drop test.

The reactions were followed by GC-MS. Addition of mercury at $t = 0$ provided no conversion even if the reaction was warmed for 10 hours. The plot of alkyne conversion and the distribution of products were presented in the following chart (Figure 59)

¹⁴⁰ G. M. Whitesides, M. Hackett, R. L. Brainard, J.-P. P. M. Lavalleye, A. F. Sowinski, A. N. Izumi, S. S. Moore, D. W. Brown, E. M. Staudt, *Organometallics*, **1985**, 4 1819-1830.

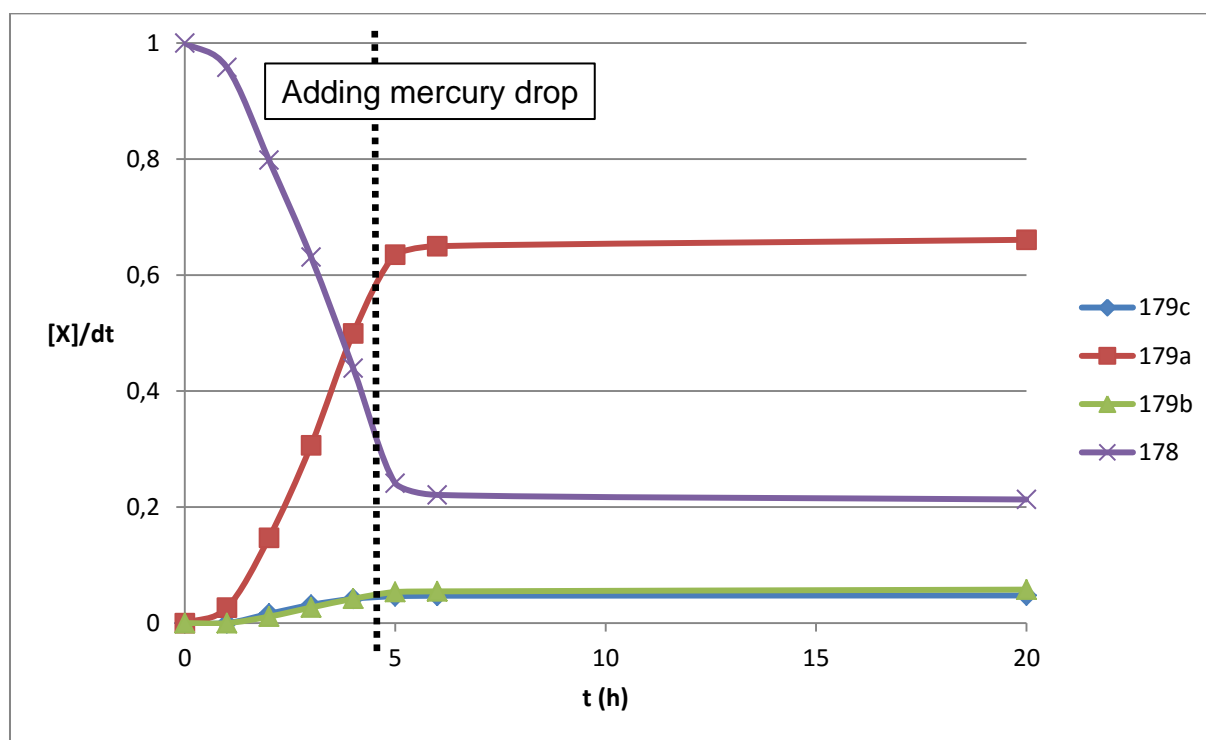


Figure 59 : GC-MS analysis for mercury drop test.

Before adding a mercury drop to the solution, the conversion was comparable with the one observed with classical conditions. After adding mercury, the conversion rate decreased a lot but alkyne was still converted from 75 to 78% after one hour of heating. Then, the previously red solution turned to colorless and no conversion was observed for the next 14 hours of heating. This experiment presented a slight clue towards the fact that the catalyst could be homogeneous. Unfortunately, this proof was not significant enough to be conclusive.

We thus turned to the Sheldon test.¹⁴¹ Sheldon test consisted of a filtration through a celite pad at 50% of conversion to remove the heterogeneous species of the batch. We realized this test on the classical reaction with phenylprop-1-yne. At 50% of conversion, a filtration over celite was realized and the resulting filtrate was put to heat instantly. The GC-MS analysis was plotted on figure 60.

¹⁴¹ H. E. B. Lepmers, R. A. Sheldon, *J. Catal.*, **1998**, *175*, 62-69.

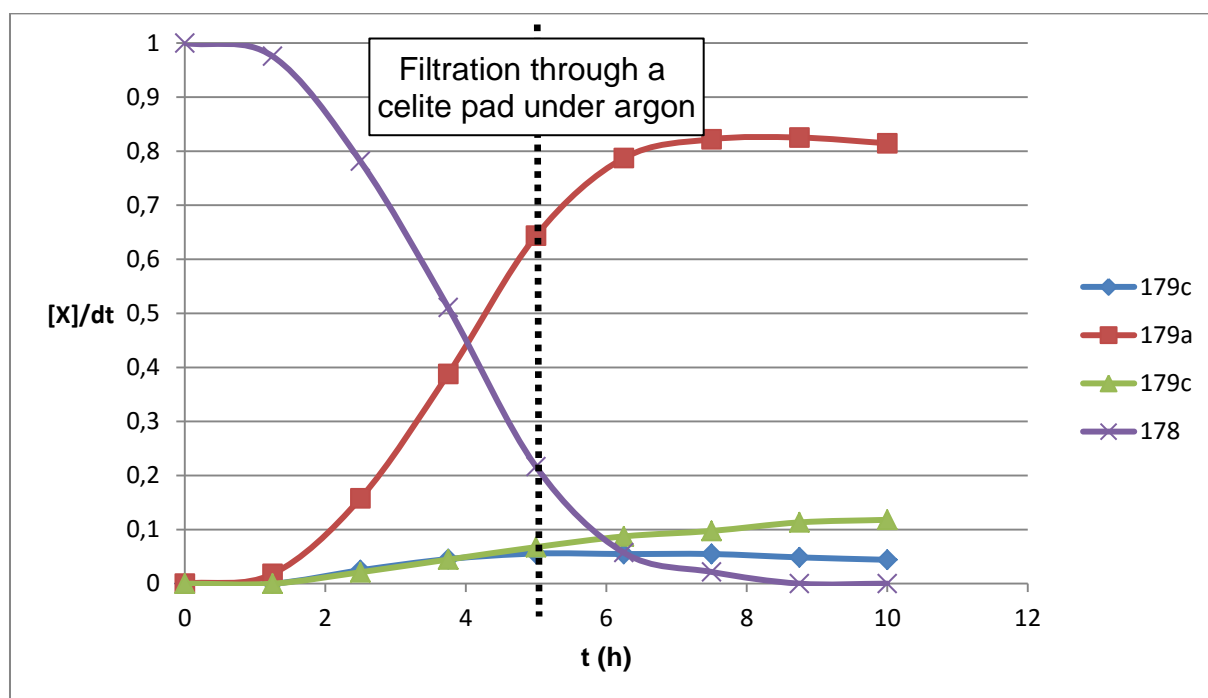


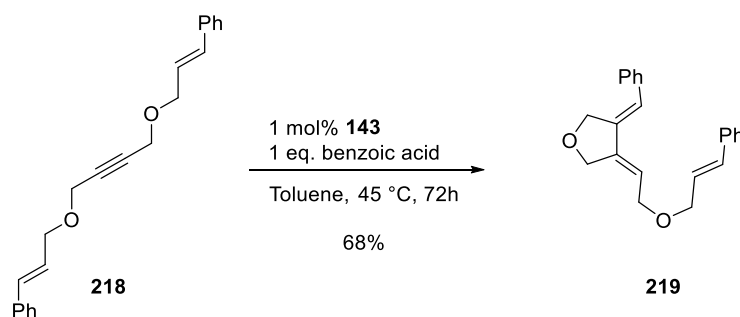
Figure 60 : GC-MS analysis for Sheldon test.

This chart showed that conversion still went on to 100% after removing all the heterogeneous particles. Even if a loss of the selectivity was observed during this experiment, the active species of the reaction should be homogeneous. In addition to that, the celite which contained heterogeneous species was put into another Schlenk vessel and a new batch of solvent, reactants and reagents were added. The suspension was heated to reflux of THF but no conversion was detected.

3.3. Cycloisomerization of enynes

In the latter part, we showed that tripalladium complex **152** could be a very efficient catalyst to realize semi-hydrogenation of alkynes. To go further, we wondered if the Lewis acidic character of these cationic clusters was strong enough to perform cycloisomerization of enynes. Usually, cycloisomerization catalysts are mostly based on mononuclear Pt or Au

complexes.¹⁴² We wanted to exploit the reaction with the dienyne **218** and 1 mol% of catalyst **143** (Scheme 47).



Scheme 47 : Cycloisomerization reaction.

This reaction surprisingly afforded cycloisomerized compound **219** in 68% isolated yield in mild conditions. Whereas this reaction is not yet optimized, these preliminary observations showed that the Lewis acidic behavior of this family of clusters can catalyze cycloisomerization reactions. However, a scope of differently substituted enynes should be investigated to explore the limits of this catalyst.

¹⁴² a) T. Caneque, F. Truscott, R. Rodriguez, G. Maestri, M. Malacria, *Chem. Soc. Rev.*, **2014**, *43*, 2916-2926. b) C. Obradors, A. M. Echavarren, *Acc. Chem. Res.*, **2014**, *47*, 902-912. c) A. Fürstner *Chem. Soc. Rev.*, **2009**, *38*, 3208-3221.

3.4. Conclusions

The presented work showed the first application of tripalladium aromatic clusters into catalytic reactions.¹⁴³ Even if the purpose of this work was to prove that this new family of complexes could have catalytic activities, the relevant chemoselectivity of the catalyst was beyond our greatest expectations. The trinuclear catalyst showed efficiencies at least as good as mononuclear complexes and provided Z-alkenes without any traces of over-reduced products. The high tolerance towards various chemical groups and the small amount of catalyst used made this new semi-hydrogenation reaction competitive. Preliminary studies suggest that the catalyst could operate through molecular mechanisms that differ from those observed for mononuclear catalyst. However, the nature of the active specie is still not known and will be further investigated. Seminal work on cycloisomerisation of enynes showed that $[\text{Pd}_3]^+$ cluster are also able to catalyse this reaction but reaction conditions need to be further improved.

¹⁴³ P-A. Deyris, T. Caneque, Y. Wang, P. Retailleau, F. Bigi, R. Maggi, G. Maestri, M. Malacria, *ChemCatChem*, **2015**, 7, 3266-3269.

SUPPORTING INFORMATION – PART 3

3.5. Supporting Information

3.5.1. General Remarks

All chemicals those syntheses are not reported hereafter were purchased from commercial sources and used as received. Solvents were dried and stored over 4 Å molecular sieves previously activated in a household microwave oven (five minutes at 900 W). Prior to use, they were degassed by bubbling argon for at least 30 minutes. For catalytic reductions, M_3 catalysts did not require the use of dry solvents. THF directly taken from bottles was simply degassed prior to use. Reactions and filtrations were carried out under argon using standard Schlenk technique. ^1H NMR, ^{13}C NMR, ^{19}F NMR and ^{31}P NMR spectra were recorded at 300 K on a Bruker 300 AVANCE spectrometer fitted with a QNP probehead at 300.1 and 75.4 MHz respectively, using the solvent as internal standard (7.26 ppm for ^1H NMR and 77.00 ppm for ^{13}C NMR for CDCl_3) and 85% H_3PO_4 as external standard for ^{31}P (0.00 ppm). Reported assignments are based on decoupling, COSY, NOESY, HSQC and HMBC correlation experiments. The terms m, s, d, t, q and quint represent multiplet, singlet, doublet, triplet, quadruplet and quintuplet respectively, and the term br means a broad signal. Exact masses were recorded on a LCT Premier XE (Waters) equipped with an ESI ionization source and a TOF detector. IR spectra were recorded with a PerkinElmer Spectrum 100 FT-IR Spectrometer. Hydrogenation reactions were followed on a Shimadzu GCMS-QP2010. Calculations were performed with Gaussian 09 at DFT level.¹⁴⁴ The geometries of complexes here reported were optimized without any constraints at the generalized gradient approximation using the M06 hybrid functional of Zhao and Truhlar.¹⁴⁵ Optimizations were carried out using LACVP(d)¹⁴⁶ and Def2-svp basis sets.¹⁴⁷ Harmonic frequencies were calculated at the DFT level to characterize stationary points by the absence of imaginary frequency in the Hessian matrix.

¹⁴⁴ Gaussian 09, Revision A.1, Frisch, M. J.; Trucks, G. W.; Schlegel, H. B.; Scuseria, G. E.; Robb, M. A.; Cheeseman, J. R.; Scalmani, G.; Barone, V.; Mennucci, B.; Petersson, G. A.; Nakatsuji, H.; Caricato, M.; Li, X.; Hratchian, H. P.; Izmaylov, A. F.; Bloino, J.; Zheng, G.; Sonnenberg, J. L.; Hada, M.; Ehara, M.; Toyota, K.; Fukuda, R.; Hasegawa, J.; Ishida, M.; Nakajima, T.; Honda, Y.; Kitao, O.; Nakai, H.; Vreven, T.; Montgomery, Jr., J. A.; Peralta, J. E.; Ogliaro, F.; Bearpark, M.; Heyd, J. J.; Brothers, E.; Kudin, K. N.; Staroverov, V. N.; Kobayashi, R.; Normand, J.; Raghavachari, K.; Rendell, A.; Burant, J. C.; Iyengar, S. S.; Tomasi, J.; Cossi, M.; Rega, N.; Millam, N. J.; Klene, M.; Knox, J. E.; Cross, J. B.; Bakken, V.; Adamo, C.; Jaramillo, J.; Gomperts, R.; Stratmann, R. E.; Yazyev, O.; Austin, A. J.; Cammi, R.; Pomelli, C.; Ochterski, J. W.; Martin, R. L.; Morokuma, K.; Zakrzewski, V. G.; Voth, G. A.; Salvador, P.; Dannenberg, J. J.; Dapprich, S.; Daniels, A. D.; Farkas, Ö.; Foresman, J. B.; Ortiz, J. V.; Cioslowski, J.; Fox, D. J. Gaussian, Inc., Wallingford CT, 2009.

¹⁴⁵ Y. Zhao, D. G. Truhlar, *Theor. Chem. Account* **2008**, *120*, 215.

¹⁴⁶ a) F. Weigen, R. Ahlrichs, *Phys. Chem. Chem. Phys.* **2005**, *7*, 3297. b) D. Andrae, U. Haeussermann, M. Dolg, H. Stoll, H. Preuss, *Theor. Chim. Acta* **1990**, *77*, 123. c) K. A. Peterson, G. Figgen, E. Goll, H. Stoll, M. Dolg, *J. Chem. Phys.* **2003**, *119*, 11113.

¹⁴⁷ a) J. P. Hay, W. R. Wadt, *J. Chem. Phys.* **1985**, *82*, 299. b) R. A. Friesner, R. B. Murphy, M. D. Beachy, M. N. Ringlanda, W. T. Pollard, B. D. Dunietz, Y. X. Cao, *J. Phys. Chem. A*, **1999**, *103*, 1913.

3.5.2. General procedures

General procedure 1 (GP1): Synthesis of aromatic alkynes.

The desired aryl iodide (1.0 mmol), the terminal alkyne (1.1 mmol, 1.1 eq.) and THF (10 mL, 0.1 mol/L) were added to a Schlenk-type flask previously dried at 600°C under vacuum. The mixture put under stirring and Pd(PPh₃)Cl₂ (35.1 mg, 0.05 mmol, 0.05 eq.), CuI (11.4 mg, 0.06 mmol, 0.06 eq.) and triethylamine (200 μL, 2.0 mmol, 2.0 eq.) are sequentially added. The resulting black mixture was stirred for 5h at room temperature and then diluted with 30 mL of ethyl acetate. The solution was extracted with brine (3 x 20 mL). The organic layers was dried over MgSO₄, filtered and evaporated under vacuum. The desired internal alkyne was isolated by flash chromatography on silica gel.

General procedure 2 (GP2): Synthesis of compound **184**.

1-ethynyl-2-(trifluoromethyl)benzene (500 mg, 2.94 mmol) was added into a three-neck balloon and diluted by 20 mL of dry THF. Then the solution was cooled to -15 °C tanks to an ice/salt bath. *n*-Butyllithium (3 mL of a 1.6 mol.L⁻¹ solution in THF, 4.41 mmol, 1.5 eq.) was added dropwise and the solution was stirred for 1h. Methyl iodide (709 mg, 5.00 mmol, 1.7 eq.) was then added dropwise and the mixture was stirred for one more hour. The solution was let to room temperature and stirred overnight. 20 mL of ethyl acetate and then 20 mL of saturated ammonium chloride solution were added and the organic layer was washed by 3 x 20 mL of saturated ammonium chloride solution. The resulting organic layer was dried under MgSO₄ and then evaporated. After chromatography column on silica gel, the desired product was isolated (116 mg, 63% yield).

General procedure 3 (GP3): Synthesis of aliphatic alkynes.

To a previously dried at 600°C under vacuum Schlenk-type flask, were added sodium hydride 60% w/w (314 mg, 7.85 mmol, 1.1 eq.) and 20 mL of dry THF. The suspension was cooled to 0 °C with an ice bath and then but-2-yn-1-ol (500 mg, 7.14 mmol) was added dropwise. The solution was stirred until bubbles disappeared. The desired benzylbromide (7.85 mmol, 1.1 eq.) was then added. The solution was let warm to room-temperature and was stirred overnight. 10 mL of water were put dropwise and the THF was removed under vacuum. The resulting suspension was extracted by 3 x 25 mL of MTBE and the organic layers were

collected and dry over MgSO_4 . The desired compound was isolated after chromatography column.

General procedure 4 (GP4): Synthesis of propargylic esters.

The desired organo-halide (3.00 mmol) and degassed DCM (15mL) were added to a 50mL Schlenk-type flask previously dried at 600°C under vacuum. The mixture was stirred until complete solubilization and triethylamine (3.30 mmol, 1.1 eq.) and 2-butyne-1-ol (4.50 mmol, 1.5 equiv.) were then added via syringe. The resulting suspension was stirred at room temperature and samples were periodically taken for TLC analyses. Upon complete consumption of starting material (2-16 h), the mixture was diluted with ethyl acetate (40 mL) and washed with brine (3 x 40 mL). The organic layer was dried over MgSO_4 and evaporated. Products were purified by flash chromatography on silica gel.

General procedure 5 (GP5): Synthesis of Z-alkenes from corresponding alkynes.

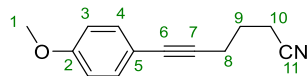
The tripod catalyst (5.0 mg, 0.0031 mmol, 1 mol%, see table 1 entry 7) and freshly degassed THF (3.1 mL, 0.1 mol of alkyne/L) are added under argon to a Schlenk-type flask. *The same results are obtained using either dry THF or wet solvent taken from its bottle.* The desired alkyne (0.31 mmol, 1 eq.), triethylamine (210 μL , 1.55 mmol, 5 eq.), formic acid (58 μL , 1.55 mmol, 5 eq.) and *p*-xylene for reaction followed also *via* GC (38 μL , 0.31 mmol, 1 eq.) were sequentially added via syringes. The mixture was heated to reflux and the conversion was followed analyzing samples *via* GC-MS using *p*-xylene as internal standard (100 μL of crude each, diluted with 900 μL of MeOH). Upon complete conversion of the alkyne, the solution was diluted with 20 mL of ethyl acetate and washed with brine (3 x 20 mL). The organic layer was dried over MgSO_4 and evaporated under vacuum. Desired alkenes were then isolated by flash chromatography on silica gel.

General procedure 6 (GP6): Synthesis of tetrahydrofuran derivatives.

Tripod catalyst **143** (5.3 mg, 0.00317 mmol, 1 mol%) is solubilized in degassed toluene (5.2 mL) under argon. Benzoic acid (39 mg, 0.319 mmol, 1 eq.) and enyne (100 mg, 0.314 mmol) are then sequentially added. The solution is kept under stirring at 45° for 72 hours. The

mixture is then filtered through a celite pad and concentrated under reduced pressure. the product was purified by flash column chromatography.

3.5.3. Synthesis of aromatic alkynes

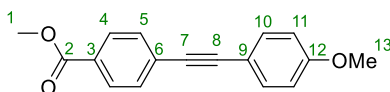
Compound 6-(4-methoxyphenyl)hex-5-ynenitrile: **183**

Following **GP1**, from hex-5-ynenitrile and 4-methoxyphenyl iodide was obtained 159 mg (80% yield) of **183** as a white powder.

¹H NMR (300 MHz, CDCl₃) δ (ppm): 7.32 (d, 2H, *J* = 8.7 Hz, **H4**), 6.82 (d, 2H, *J* = 9.0 Hz, **H3**), 3.80 (s, 3H, **H1**), 2.58 (t, 2H, *J* = 6.9 Hz, **H8**), 2.56 (t, 2H, *J* = 7.2 Hz, **H10**), 1.95 (quint., 2H, *J* = 6.9 Hz, **H9**).

¹³C NMR (75 MHz, CDCl₃) δ (ppm) 159.3 (**C2**), 132.9 (**C4**), 119.2 (**C11**), 115.3 (**C5**), 113.9 (**C3**), 85.3 (**C7**), 82.2 (**C6**), 55.2 (**C1**), 24.7 (**C9**), 18.6 (**C8**), 16.2 (**C10**).

HRMS calcd. for C₁₃H₁₃NO⁺ 199.0992, found 199.0985.

Compound methyl 4-((4-methoxyphenyl)ethynyl)benzoate: **188**

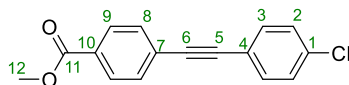
Following **GP1**, from methyl 4-ethynylbenzoate and 4-methoxyphenyl iodide was obtained 218 mg (82% yield) of **188** as a white powder. Spectroscopic data correspond to the literature.¹⁴⁸

¹H NMR (300 MHz, CDCl₃) δ (ppm): 8.00 (d, 2H, *J* = 5.1 Hz, **H4**), 7.55 (d, 2H, *J* = 4.8 Hz, **H5**), 7.48 (d, 2H, *J* = 5.1 Hz, **H10**), 6.89 (d, 2H, *J* = 5.4 Hz, **H11**), 3.92 (s, 3H, **H1**), 3.83 (s, 3H, **H13**).

¹³C NMR (75 MHz, CDCl₃) δ (ppm): 166.6 (**C2**), 160.0 (**C12**), 133.2 (**C10**), 131.3 (**C5**), 129.5 (**C4**), 129.1 (**C3**), 128.4 (**C6**), 114.7 (**C9**), 114.1 (**C11**), 92.6 (**C8**), 87.5 (**C7**), 55.3 (**C13**), 52.2 (**C1**).

HRMS calcd. for C₁₇H₁₄O₃⁺ 266.0937, found 266.0929.

¹⁴⁸ M. J. Mio, L. C. Kopel, J. B. Braun, T. L. Gadzikwa, K. L. Hull, R. G. Brisbois, C. J. Markworth, P. A. Grieco, *Org. Lett.*, **2002**, *4*, 3199.

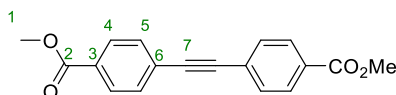
Compound methyl 4-((4-chlorophenyl)ethynyl)benzoate: 189

Following **GP1**, from methyl 4-ethynylbenzoate and 4-chlorophenyl iodide was obtained 254 mg (94% yield) of **189** as a white powder.

¹H NMR (300 MHz, CDCl₃) δ (ppm): 8.02 (d, 2H, *J* = 8.7 Hz, **H9**), 7.57 (d, 2H, *J* = 8.7 Hz, **H8**), 7.47 (d, 2H, *J* = 8.7 Hz, **H3**), 7.34 (d, 2H, *J* = 8.4 Hz, **H2**), 3.93 (s, 3H, **H12**).

¹³C NMR (75 MHz, CDCl₃) δ (ppm) 166.5 (**C11**), 134.8 (**C1**), 132.9 (**C3**), 131.5 (**C8**), 129.7 (**C10**), 129.5 (**C9**), 128.8 (**C2**), 127.6 (**C7**), 121.2 (**C4**), 91.1 (**C5**), 89.5 (**C6**), 52.2 (**C12**).

HRMS calcd. for C₁₆H₁₁ClO₂⁺ 270.0442, found 270.0433.

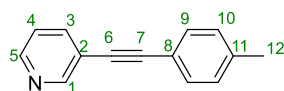
Compound dimethyl 4,4'-(ethyne-1,2-diyl)dibenzoate: 190

Following **GP1**, from methyl 4-ethynylbenzoate and methyl 4-iodobenzoate was obtained 177 mg (60% yield) of **190** as a white powder.

¹H NMR (300 MHz, CDCl₃) δ (ppm): 8.03 (d, 4H, *J* = 8.1 Hz, **H4**), 7.60 (d, 4H, *J* = 8.1 Hz, **H5**), 3.93 (s, 6H, **H1**).

¹³C NMR (75 MHz, CDCl₃) δ (ppm): 166.4 (**C2**), 131.6 (**C5**), 130.0 (**C3**), 129.6 (**C4**), 127.4 (**C6**), 91.4 (**C7**), 52.3 (**C1**).

HRMS calcd. for C₁₈H₁₄O₄⁺ 294.0881, found 294.0874.

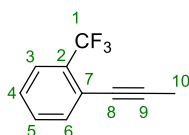
Compound 3-(p-tolylethynyl)pyridine: 191

Following **GP1**, from 3-ethynylpyridine and 4-iodotoluene was obtained 178 mg (92% yield) of **191** as a white powder. Spectroscopic data correspond to the literature.¹⁴⁹

¹H NMR (300 MHz, CDCl₃) δ (ppm): 8.75 (dd, 1H, *J* = 2.1, 0.6 Hz, **H1**), 8.53 (dd, 1H, *J* = 8.7 Hz, **H5**), 7.79 (ddd, 1H, *J* = 7.9, 2.0, 2.0 Hz, **H3**), 7.43 (d, 2H, *J* = 8.1 Hz, **H9**), 7.27 (ddd, 1H, *J* = 8.1, 4.8, 1.0 Hz, **H4**), 7.17 (d, 2H, *J* = 8.1 Hz, **H10**), 2.38 (s, 3H, **H12**).

¹³C NMR (75 MHz, CDCl₃) δ (ppm): 152.2 (**C1**), 148.4 (**C5**), 139.0 (**C11**), 138.3 (**C3**), 131.6 (**C9**), 129.2 (**C10**), 123.0 (**C4**), 120.7 (**C2**), 119.5 (**C8**), 92.9 (**C7**), 85.3 (**C6**), 21.5 (**C12**).

HRMS calcd. for C₁₄H₁₁N⁺ 193.0886, found 193.0879.

Compound 1-(prop-1-yn-1-yl)-2-(trifluoromethyl)benzene: 184

Following **GP2**, from 1-ethynyl-2-(trifluoromethyl)benzene and methyl iodide was obtained 116 mg (63% yield) of **184** as a colorless oil.

¹H NMR (300 MHz, CDCl₃) δ (ppm): 7.61 (d, 1H, *J* = 7.5 Hz, **H3**), 7.52 (d, 1H, *J* = 7.5 Hz, **H6**), 7.44 (dd, 1H, *J* = 7.5, 7.5 Hz, **H4**), 7.34 (dd, 1H, *J* = 7.5, 7.5 Hz, **H5**), 3.80 (s, 3H, **H10**).

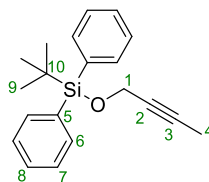
¹³C NMR (75 MHz, CDCl₃) δ (ppm): 134.0 (**C6**), 131.3 (m, **C2**), 131.2 (**C4**), 127.2 (**C5**), 125.7 (q, *J* = 5.0 Hz, **C3**), 123.6 (q, *J* = 271.3 Hz, **C1**), 122.4 (m, **C7**), 92.1 (**C9**), 75.8 (**C8**), 4.5 (**C10**).

¹⁹F NMR (CDCl₃) δ (ppm): - 62.6.

HRMS calcd. for C₁₀H₇F₃⁺ 184.0494, found 184.0489.

¹⁴⁹ S. Voltrova, J. Srogl, *Org. Chem. Front.* **2014**, *1*, 1067.

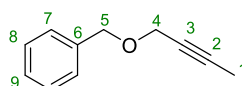
3.4.4. Synthesis of aliphatic alkynes

Compound (but-2-yn-1-yloxy)(tert-butyl)diphenylsilane: **193**

Following **GP3**, from *tert*-butylchlorodiphenylsilane and but-2-yn-1-ol was obtained 758 mg (82% yield) of **193** as a colorless oil.

$^1\text{H NMR}$ (300 MHz, CDCl_3) δ (ppm): 7.75-7.71, (m, 4H, **H6**), 7.46-7.37 (m, 6H, **H7**, **H8**), 4.29 (q, 2H, $J = 2.4$ Hz, **H1**), 1.81 (t, 3H, $J = 2.4$ Hz, **H4**), 1.08 (s, 9H, **H9**).

$^{13}\text{C NMR}$ (75 MHz, CDCl_3) δ (ppm) 135.4 (**C6**), 133.1 (**C5**), 129.4 (**C8**), 127.4 (**C7**), 81.0 (**C3**), 77.3 (**C2**), 52.7 (**C1**), 26.5 (**C9**), 18.9 (**C10**), 3.4 (**C4**).

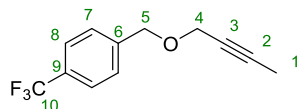
Compound ((but-2-yn-1-yloxy)methyl)benzene: **194**

Following **GP3**, from benzylbromide and but-2-yn-1-ol was obtained 250 mg (52% yield) of **194** as a pale yellow oil. Spectroscopic data correspond to the literature.¹⁵⁰

$^1\text{H NMR}$ (300 MHz, CDCl_3) δ (ppm): 7.38-7.27 (m, 5H, **H7**, **H8**, **H9**), 4.59 (s, 2H, **H5**), 4.13 (q, 2H, $J = 2.1$ Hz, **H4**), 1.88 (t, 3H, $J = 2.1$ Hz, **H1**)

$^{13}\text{C NMR}$ (75 MHz, CDCl_3) δ (ppm): 137.7 (**C6**), 128.4 (**C8**), 128.0 (**C7**), 127.7 (**C9**), 82.6 (**C3**), 75.1 (**C2**), 71.5 (**C5**), 57.7 (**C4**), 3.6 (**C1**).

¹⁵⁰ D. V. Kadnikov, R. C. Larock, *J. Org. Chem.*, **2003**, 68, 9423.

Compound 1-((but-2-yn-1-yloxy)methyl)-4-(trifluoromethyl)benzene: 195

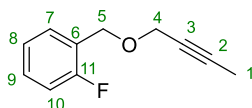
Following **GP3**, from (4-trifluoromethyl)benzylbromide and but-2-yn-1-ol was obtained 616 mg (90% yield) of **195** as a colorless oil.

$^1\text{H NMR}$ (500 MHz, CDCl_3) δ (ppm): 7.60 (d, 2H, $J = 8.1$ Hz, **H8**), 7.47 (d, 2H, $J = 8.1$ Hz, **H7**), 4.64 (s, 2H, **H5**), 4.17 (q, 2H, $J = 2.4$ Hz, **H4**), 1.87 (t, 3H, $J = 2.4$ Hz, **H3**).

$^{13}\text{C NMR}$ (125 MHz, CDCl_3) δ (ppm): 141.9 (**C6**), 129.8 (q, $J = 32.5$ Hz, **C9**), 127.8 (**C7**), 125.3 (d, $J = 3.8$ Hz, **C8**), 124.2 (q, $J = 270.6$ Hz, **C10**), 83.1 (**C3**), 74.7 (**C2**), 70.6 (**C5**), 58.2 (**C4**), 3.6 (**C1**).

$^{19}\text{F NMR}$ (CDCl_3) δ (ppm): - 62.5.

HRMS calcd. for $\text{C}_{12}\text{H}_{11}\text{F}_3\text{O}^+$ 228.0754, found 228.0749.

Compound 1-((but-2-yn-1-yloxy)methyl)-2-fluorobenzene: 196

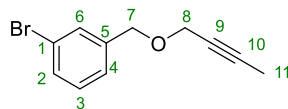
Following **GP3**, from 2-fluorobenzylbromide and but-2-yn-1-ol was obtained 213 mg (40% yield) of **196** as a colorless oil.

$^1\text{H NMR}$ (300 MHz, CDCl_3) δ (ppm): 7.43 (ddd, 1H, $J = 7.2, 7.2, 1.5$ Hz, **H7**), 7.27 (ddd, 1H, $J = 13.2, 7.5, 1.5$ Hz, **H9**), 7.13 (ddd, 1H, $J = 7.6, 5.5, 1.3$ Hz, **H8**), 7.04 (ddd, 1H, $J = 9.4, 8.6, 0.9$ Hz, **H10**), 4.65 (s, 2H, **H5**), 4.17 (q, 2H, $J = 2.4$ Hz, **H4**), 1.88 (t, 3H, $J = 2.4$ Hz, **H1**).

$^{13}\text{C NMR}$ (75 MHz, CDCl_3) δ (ppm) : 160.8 (d, $J = 245.3$ Hz, **C11**), 130.2 (d, $J = 4.4$ Hz, **C7**), 129.4 (d, $J = 7.7$ Hz, **C9**), 124.8 (d, $J = 14.2$ Hz, **C6**), 124.0 (d, $J = 3.2$ Hz, **C8**), 115.2 (d, $J = 21.8$ Hz, **C10**), 82.8 (**C2**), 74.9 (**C3**), 64.9 (d, $J = 3.2$ Hz, **C5**), 58.1 (**C4**), 3.6 (**C1**).

$^{19}\text{F NMR}$ (300 MHz, CDCl_3) δ (ppm): - 118.8.

HRMS calcd. for $\text{C}_{11}\text{H}_{11}\text{FO}^+$ 178.0788, found 178.0779.

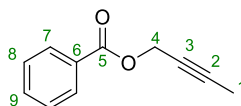
Compound 1-bromo-3-((but-2-yn-1-yloxy)methyl)benzene: 197

Following **GP3**, from 2-fluorobenzylbromide and but-2-yn-1-ol was obtained 294 mg (41% yield) of **197** as a colorless oil.

¹H NMR (300 MHz, CDCl₃) δ (ppm): 7.52 (dd, 1H, *J* = 1.5, 1.5 Hz, **H2**), 7.42 (ddd, 1H, *J* = 7.8, 1.2, 1.2 Hz, **H6**), 7.27 (ddd, 1H, *J* = 7.5, 1.5, 1.5 Hz, **H4**), 7.21 (dd, 1H, *J* = 7.5, 7.5 Hz, **H5**), 4.56 (s, 2H, **H7**), 4.14 (q, 2H, *J* = 2.4 Hz, **H8**) 1.88 (t, 3H, *J* = 2.4 Hz, **H11**).

¹³C NMR (75 MHz, CDCl₃) δ (ppm): 140.1 (**C1**), 130.8 (**C2**), 130.7 (**C6**), 129.9 (**C5**), 126.3 (**C4**), 122.5 (**C3**), 83.0 (**C10**), 74.8 (**C9**), 70.5 (**C7**), 58.0 (**C8**), 3.6 (**C11**).

HRMS calcd. for C₁₁H₁₁BrO⁺ 237.9988, found 237.9979.

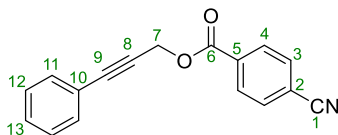
Compound but-2-yn-1-yl benzoate: 198

Following **GP4**, from benzoyl chloride and but-2-yn-1-ol was obtained 449 mg (86% yield) of **198** as a colorless oil.

¹H NMR (300 MHz, CDCl₃) δ (ppm): 8.10 – 8.06 (m, 2H, **H7**), 7.60 – 7.54 (m, 1H, **H9**), 7.47 – 7.41 (m, 2H, **H8**), 4.90 (q, 2H, *J* = 2.1 Hz, **H4**), 1.88 (t, 3H, *J* = 2.4 Hz, **H1**).

¹³C NMR (75 MHz, CDCl₃) δ (ppm): 166.0 (**C5**), 133.1 (**C9**), 129.8 (**C6**, **C7**), 128.4 (**C8**), 83.2 (**C2**), 73.2 (**C3**), 53.3 (**C4**), 3.7 (**C1**)

HRMS calcd. for C₁₁H₁₀O₂⁺ 174.0675, found 174.0671.

Compound 3-phenylprop-2-yn-1-yl 4-cyanobenzoate: 199

Following **GP4**, from benzoyl chloride and but-2-yn-1-ol was obtained 353 mg (45% yield) of **199** as a white powder.

¹H NMR (300 MHz, CDCl₃) δ (ppm): 8.20 (d, 2H, J = 8.1 Hz, **H4**), 7.76 (d, 2H, J = 8.1 Hz, **H3**), 7.50 – 7.45 (m, 2H, **H11**), 7.36 – 7.30 (m, 3H, **H12**, **H13**), 5.19 (s, 2H, **H7**).

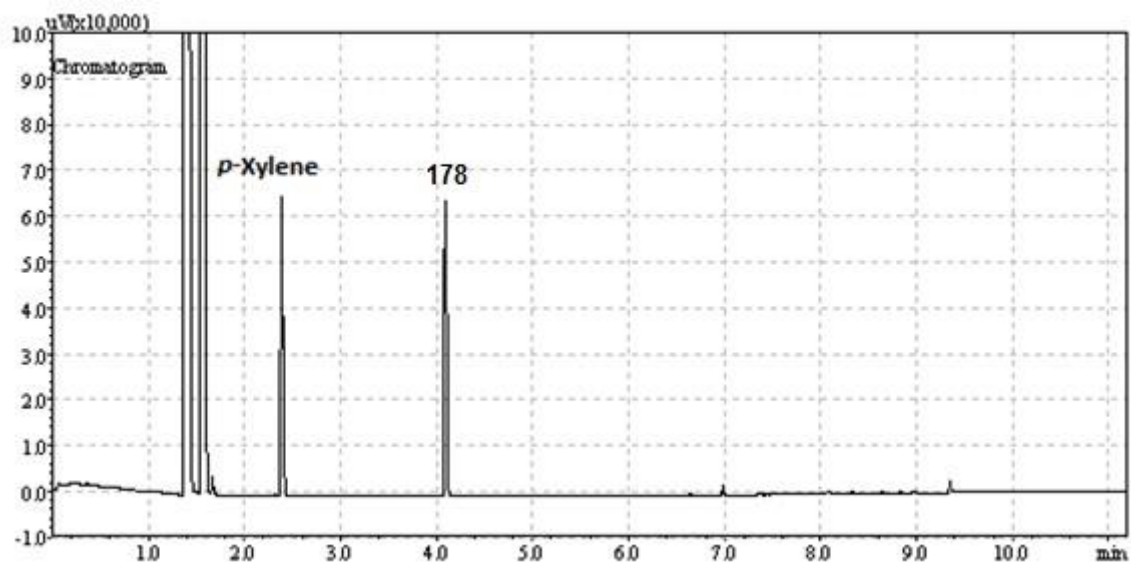
¹³C NMR (75 MHz, CDCl₃) δ (ppm): 164.3 (**C6**), 133.4 (**C5**), 132.3 (**C3**), 131.9 (**C11**), 130.3 (**C4**), 128.9 (**C13**), 128.3 (**C12**), 121.9 (**C10**), 117.9 (**C1**), 116.7 (**C2**), 87.2 (**C9**), 82.3 (**C8**), 54.1 (**C7**).

HRMS calcd. for C₁₇H₁₁NO₂⁺ 261.0784, found 261.0779.

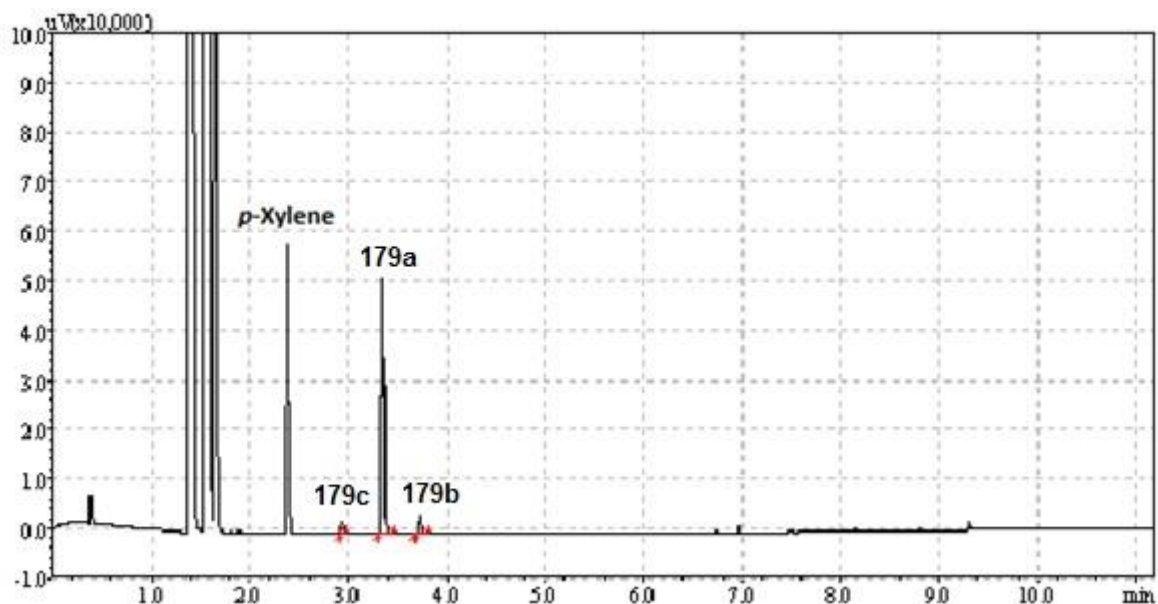
3.4.5. Catalytic semi-reductions of alkynes

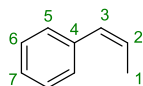
Following **GP5**, from Phenylprop-1-yne **178**, a mixture of **179a**, **179b** and **179c** was obtained as a colorless oil (37 mg, quantitative yield). The ratio between isomers of 93/3/4 was determined by GC-FID and GC-MS and NMR spectra were obtained after chromatography column.

GC at time 0



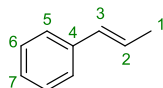
GC at 10h





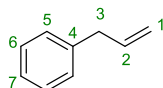
¹H NMR (300 MHz, CDCl₃) δ (ppm): 7.39-7.18 (m, 5H, **H5**, **H6**, **H7**), 6.47 (dq, 1H, $J = 11.7, 1.8$ Hz, **H3**), 5.82 (dq, 1H, $J = 11.7, 7.2$ Hz, **H2**) 1.93 (dd, 3H, $J = 7.2, 1.5$ Hz, **H1**).

¹³C NMR (75 MHz, CDCl₃) δ (ppm): 137.6 (**C4**), 129.8 (**C3**), 128.9 (**C5**), 128.1 (**C6**), 126.8 (**C2**), 125.7 (**C7**), 14.6 (**C1**).



¹H NMR (300 MHz, CDCl₃) δ (ppm): 7.39-7.18 (m, 5H, **H5**, **H6**, **H7**), 6.42 (m, 1H, **H3**), 6.27 (dq, 1H, $J = 15.6, 6.6$ Hz, **H2**) 1.91 (m, 3H, **H1**).

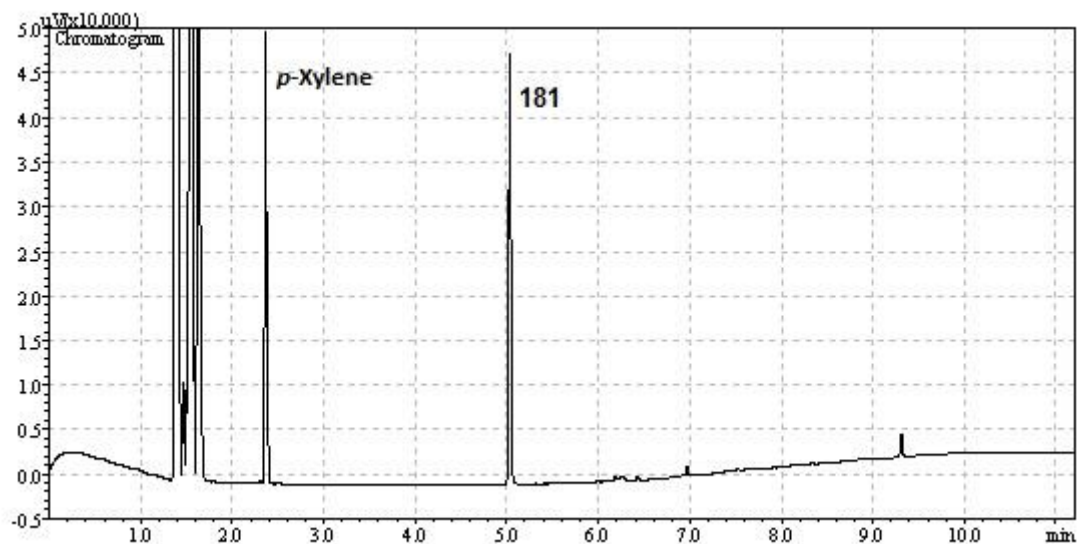
¹³C NMR (75 MHz, CDCl₃) δ (ppm): 137.9 (**C4**), 131.0 (**C3**), 128.9 (**C7**), 128.4 (**C5**), 125.8 (**C6**), 125.6 (**C2**), 18.5 (**C1**).



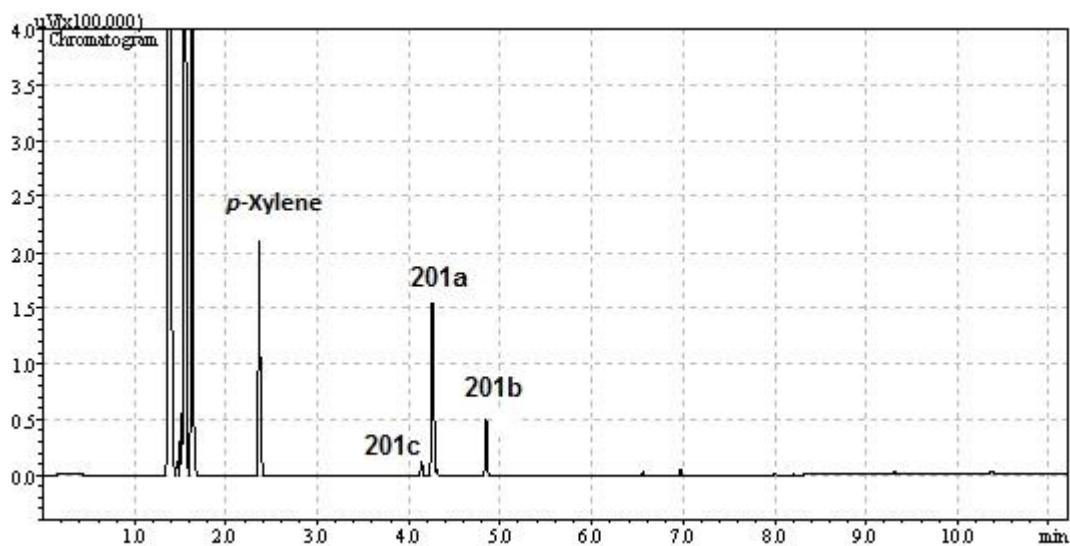
¹H NMR (300 MHz, CDCl₃) δ (ppm): 6.08-5.93 (m, 1H, **H2**), 5.16-5.06 (m, 2H, **H1**), 3.42 (d, 2H, **H3**).

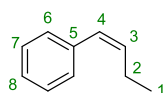
Following **GP5**, from Phenylbut-1-yne **181**, a mixture of **201a**, **201b** and **201c** was obtained as a colorless oil (41 mg, quantitative yield). The ratio between isomers of 78/21/1 was determined by GC-FID and GC-MS and NMR spectra were obtained after chromatography column.

GC at time 0:



GC at t = 22h:

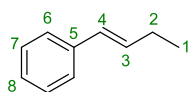




$^1\text{H NMR}$ (300 MHz, CDCl_3) δ (ppm): 7.41 – 7.15 (m, 5H, **H6**, **H7**, **H8**), 6.45 – 6.35 (m, 1H, **H4**), 5.74 – 5.62 (m, 1H, **H3**), 2.37 (pentet of d, 2H, $J = 7.5, 1.8$ Hz, **H2**), 1.10 (t, 3H, $J = 7.5$ Hz, **H1**).

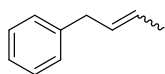
$^{13}\text{C NMR}$ (75 MHz, CDCl_3) δ (ppm): 137.9 (**C5**), 134.7 (**C3**), 128.7 (**2C_{Ar}**), 128.4 (**2C_{Ar}**), 128.1 (**C4**), 126.4 (**C8**), 22.0 (**C2**), 14.5 (**C1**).

HRMS calcd. for $\text{C}_{10}\text{H}_{12}^+$ 132.0939, found 132.0932.



$^1\text{H NMR}$ (300 MHz, CDCl_3) δ (ppm): 7.41 – 7.15 (m, 5H, **H6**, **H7**, **H8**), 6.45 – 6.35 (m, 1H, **H4**), 6.29 (dt, 1H, $J = 15.8, 6.1$ Hz, **H3**), 2.31 – 2.19 (m, 2H, **H2**), 1.10 (t, 3H, $J = 7.5$ Hz, **H1**).

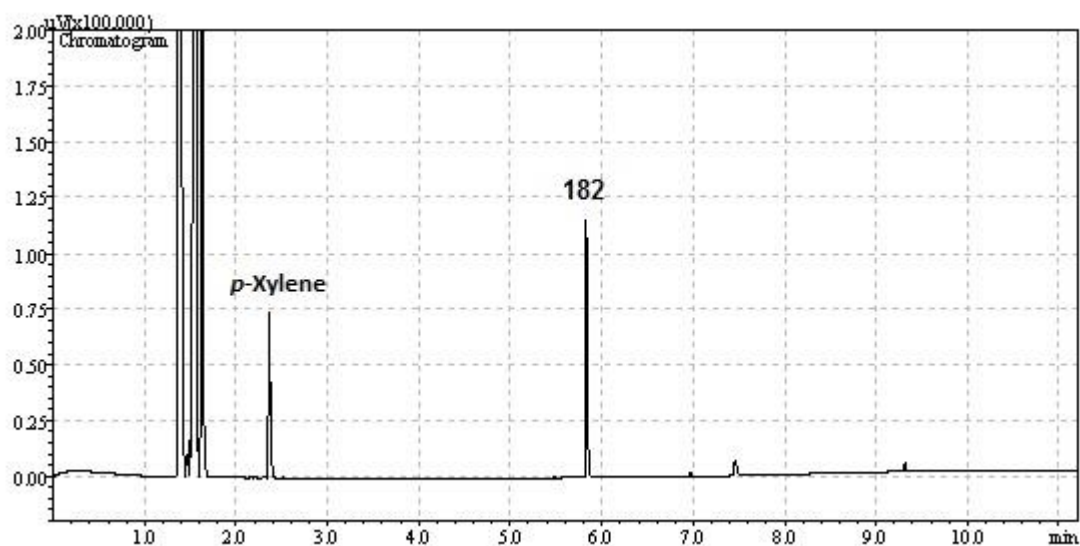
$^{13}\text{C NMR}$ (75 MHz, CDCl_3) δ (ppm): 137.7 (**C5**), 132.6 (**C3**), 128.3 (**C4**), 128.2 (**2C_{Ar}**), 126.7 (**C8**), 125.9 (**2C_{Ar}**), 26.1 (**C2**), 13.6 (**C1**).



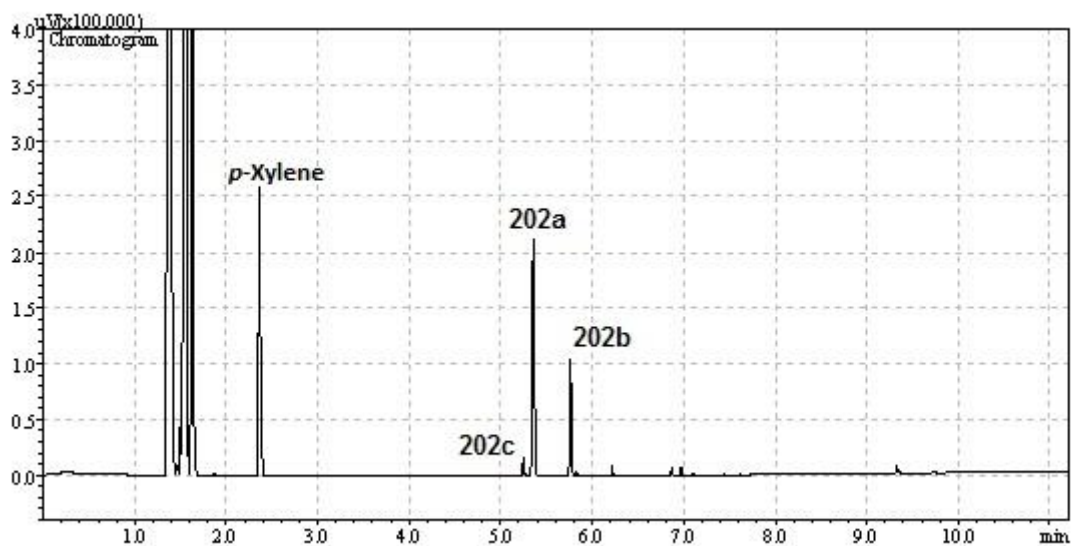
$^1\text{H NMR}$ (300 MHz, CDCl_3) δ (ppm): 7.41 – 7.15 (m, 5H, **H6**, **H7**, **H8**), 5.53 – 5.45 (m, 2H, **Hvinyl**), 3.43, 3.34 (2 d, 2H, $J = 5.0$ and 6.0 Hz, **CH₂ allyl**), 1.75, 1.71 (2 d, further split, 3H each, $J = 5.0$ and 6.0 Hz, **CH₃**).

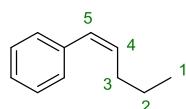
Following **GP5**, from Phenylpent-1-yne **182**, a mixture of **202a**, **202b** and **202c** was obtained as a colorless oil (45 mg, quantitative yield). The ratio between isomers of 70/29/1 was determined by GC-FID and GC-MS and NMR spectra were obtained after chromatography column.

GC at time 0



GC at t = 66h

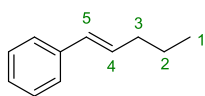




$^1\text{H NMR}$ (300 MHz, CDCl_3) δ (ppm): 7.44 – 7.16 (m, 5H, H_{Ar}), 6.54 – 6.37 (m, 1H, H_5), 5.72 (dt, $J = 11.7, 7.2$ Hz, 1H, H_4), 2.36 (ddd, $J = 14.9, 7.3, 1.8$ Hz, 2H, H_3), 1.62 – 1.44 (m, 2H, H_2), 1.07 – 0.94 (m, 3H, H_1).

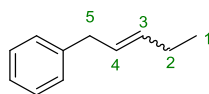
$^{13}\text{C NMR}$ (75 MHz, CDCl_3) δ (ppm): 137.9 (C_{Ar}), 133.2 (C_5), 129.1 (C_{Ar}), 128.9 (C_{Ar}), 128.2 (C_4), 126.5 (C_{Ar}), 30.9 (C_3), 23.4 (C_2), 14.0 (C_1).

HRMS calcd. for $\text{C}_{11}\text{H}_{14}^+$ 146.1090, found 146.1087.



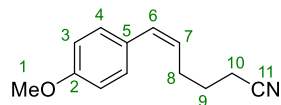
$^1\text{H NMR}$ (300 MHz, CDCl_3) δ (ppm): 7.44 – 7.16 (m, 5H, H_{Ar}), 6.54 – 6.37 (m, 1H, H_5), 6.27 (dt, $J = 15.8, 6.8$ Hz, 1H, H_4), 2.29 – 2.18 (m, 2H, H_3), 1.62 – 1.44 (m, 2H, H_2), 1.07 – 0.94 (m, 3H, H_1).

$^{13}\text{C NMR}$ (75 MHz, CDCl_3) δ (ppm): 138.1 (C_{Ar}), 131.1 (C_5), 130.0 (C_{Ar}), 128.6 (C_{Ar}), 126.9 (C_4), 126.1 (C_{Ar}), 35.3 (C_3), 22.8 (C_2), 13.9 (C_1).



$^1\text{H NMR}$ (300 MHz, CDCl_3) δ (ppm): 7.44 – 7.16 (m, 5H, H_{Ar}), 5.64 – 5.54 (m, 2H, H_3, H_4), 3.45, 3.38 (2d, $J = 5.9$ and 5.0 Hz, 2H, H_5), 2.08 – 2.00 (m, 2H, H_2), 1.09 – 1.02 (m, 3H, H_1).

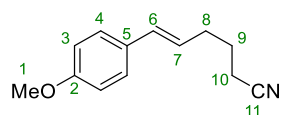
Following **GP5**, from **183**, a mixture of **203a**, **203b** and **203c** was obtained as a white solid (63 mg, 99% yield). The ratio between isomers of 83/13/4 was determined by GC-FID and GC-MS and NMR spectra were obtained after chromatography column.



¹H NMR (300 MHz, CDCl₃) δ (ppm): 7.20 (d, 2H, *J* = 8.7 Hz, **H4**), 6.91-6.81 (m, 2H, **H3**), 6.45 (d, 1H, *J* = 11.4 Hz, **H6**), 5.49 (dt, 1H, *J* = 11.4, 7.2 Hz, **H7**), 3.81 (s, 3H, **H1**), 2.47 (qd, 2H, *J* = 7.5, 1.5 Hz, **H8**), 2.34 (t, 2H, *J* = 7.5 Hz, **H10**), 1.81 (quint, 2H, *J* = 7.5 Hz, **H9**).

¹³C NMR (75 MHz, CDCl₃) δ (ppm): 158.5 (**C2**), 130.3 (**C6**), 129.8 (**C4**), 129.6 (**C5**), 128.1 (**C7**), 119.5 (**C11**), 113.7 (**C3**), 55.2 (**C1**), 27.4 (**C8**), 25.7 (**C9**), 16.6 (**C10**).

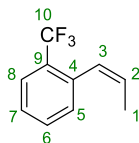
HRMS calcd. for C₁₃H₁₅NO⁺ 201.1148, found 201.1142.



¹H NMR (300 MHz, CDCl₃) δ (ppm): 7.28 (d, 2H, *J* = 8.7 Hz, **H4**), 6.91-6.81 (m, 2H, **H3**), 6.40 (d, 1H, *J* = 15.0 Hz, **H6**), 5.97 (dt, 1H, *J* = 15.0, 7.2 Hz, **H7**), 3.80 (s, 3H, **H1**), 2.57 (dt, 2H, *J* = 9.0, 6.6 Hz, **H8**), 2.40-2.36 (m, 2H, **H10**), 1.95 (quint, 2H, *J* = 6.6 Hz, **H9**).

¹³C NMR (75 MHz, CDCl₃) δ (ppm): 159.0 (**C2**), 131.4 (**C6**), 127.1 (**C4**), 125.3 (**C7**), 119.5 (**C11**), 113.9 (**C3**), 55.2 (**C1**), 31.6 (**C8**), 25.1 (**C9**), 16.4 (**C10**).

Following **GP5**, from **184**, a mixture of **204a**, **204b** and **204c** was obtained as a colorless oil (57 mg, 99% yield). The ratio between isomers of 92/4/4 was determined by GC-FID and GC-MS and NMR spectra were obtained after chromatography column.

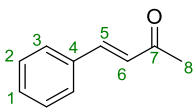


¹H NMR (300 MHz, CDCl₃) δ (ppm): 7.66 (d, 1H, $J = 8.0$ Hz, **H8**), 7.50 (dd, 1H, $J = 7.5, 7.5$ Hz, **H6**), 7.35-7.32 (m, 2H, **H5**, **H7**) 6.65 (d, 1H, $J = 11.5$ Hz, **H3**), 5.92 (dq, 1H, $J = 11.5, 7.0$ Hz, **H2**) 1.73 (dd, 3H, $J = 7.0, 2.0$ Hz, **H1**).

¹³C NMR (75 MHz, CDCl₃) δ (ppm): 136.3 (**C4**), 131.1 (**C6**), 131.1 (**C5**), 128.8 (**C2**), 128.5 (q, $J = 29.5$ Hz, **C9**), 126.7 (**C3**), 126.6 (**C7**), 125.7 (q, $J = 4.5$ Hz, **C8**), 124.3 (q, $J = 272.4$ Hz, **C10**), 14.3 (**C1**).

¹⁹F NMR (CDCl₃) δ (ppm): - 60.9.

Following **GP5**, from **185**, **205b** was obtained via rapid isomerization of **205a** as a colorless oil (45 mg, quantitative yield).

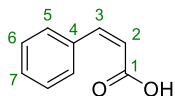


¹H NMR (300 MHz, CDCl₃) δ (ppm): 7.56-7.49 (m, 2H + 1H, **H3**, **H5**), 7.41-7.38 (m, 2H + 1H, **H1**, **H2**) 6.72 (d, 1H, *J* = 16.2 Hz, **H6**), 2.38 (s, 3H, **H8**).

¹³C NMR (75 MHz, CDCl₃) δ (ppm): 198.3 (**C7**), 143.4 (**C5**), 134.4 (**C4**), 130.5 (**C1**), 128.9 (**C3**), 128.2 (**C2**), 127.1 (**C6**), 27.5 (**C8**).

HRMS calcd. for C₁₀H₁₁O⁺ 147,0804, found 147.0798.

Following **GP5**, from **186**, a mixture of **206a**, **206b** was obtained as a colorless oil (46 mg, quantitative yield). The ratio between isomers of 97/3 was determined by NMR after chromatography column. For intensity reasons, vinylic protons only of *trans*-cinnamic acid were detectable in ^1H NMR spectrum.



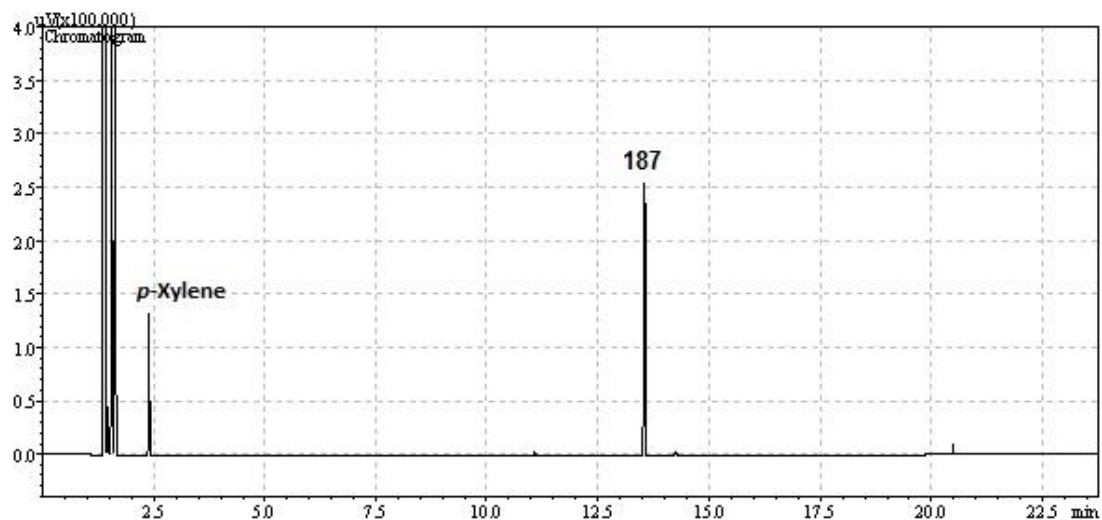
^1H NMR (300 MHz, CDCl_3) δ (ppm): 7.61-7.58 (m, 2H, **H5**), 7.41-7.31 (m, 1H + 2H, **H6**, **H7**), 7.05 (d, 1H, $J = 12.3$ Hz, **H2**), 5.97 (d, 1H, $J = 12.3$ Hz, **H3**).

^{13}C NMR (75 MHz, CDCl_3) δ (ppm): 169.9 (**C1**), 145.4 (**C2**), 134.4 (**C4**), 129.9 (**C5**), 129.3 (**C7**), 128.1 (**C6**), 118.6 (**C3**).

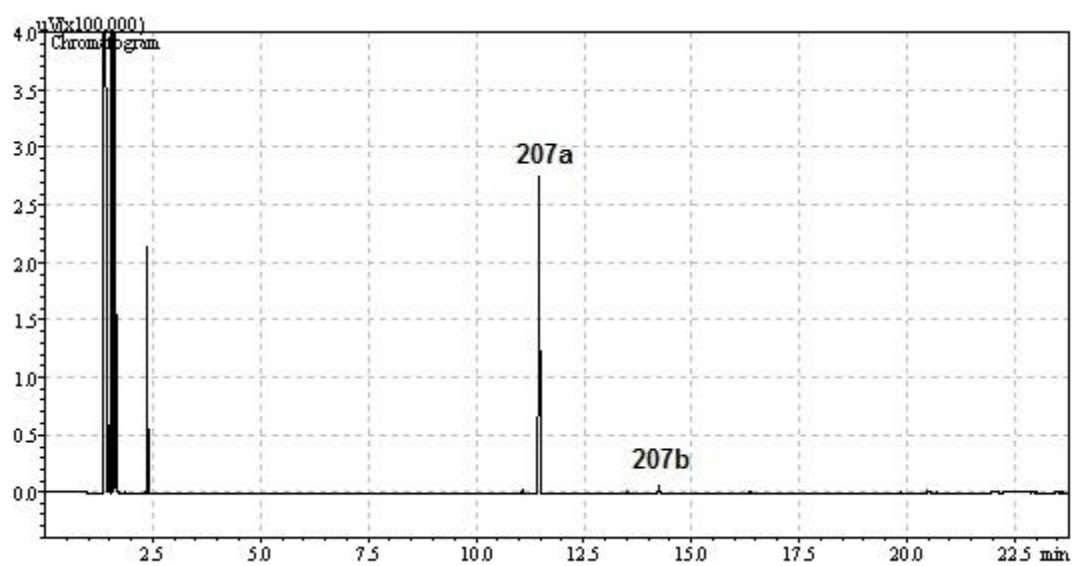
HRMS calcd. for $\text{C}_9\text{H}_8\text{O}_2^+$ 148.0519, found 148.0515.

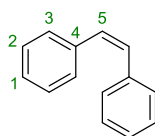
Following **GP5**, from **187**, a mixture of **207a**, **207b** was obtained as a white solid (56 mg, quantitative yield). The ratio between isomers of 98/2 was determined by GC-FID and GC-MS and NMR spectra were obtained after chromatography column.

GC at time 0



GC at t = 7h



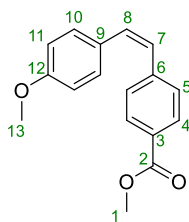


$^1\text{H NMR}$ (300 MHz, CDCl_3) δ (ppm): 7.18-7.03 (m, 10H, Ph), 6.57 (s, 2H, H5).

$^{13}\text{C NMR}$ (75 MHz, CDCl_3) δ (ppm): 137.2 (C4), 130.2 (C5), 128.9 (C3), 128.2 (C2), 127.1 (C1).

HRMS calcd. for $\text{C}_{14}\text{H}_{12}^+$ 180.0934, found 180.0934.

Following **GP5**, from **188**, a mixture of **208a**, **208b** was obtained as a white solid (83 mg, quantitative yield). The ratio between isomers of 99/1 was determined by GC-FID and GC-MS and NMR spectra were obtained after chromatography column. For intensity reasons, resonances of **208b** were not clearly detectable in NMR spectra.

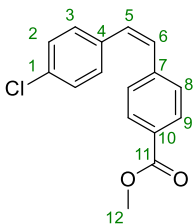


¹H NMR (300 MHz, CDCl₃) δ (ppm): 7.89 (d, 2H, J = 8.4 Hz, **H4**), 7.33 (d, 2H, J = 8.1 Hz, **H5**), 7.15 (d, 2H, J = 8.4 Hz, **H10**), 6.76 (d, 2H, J = 8.7 Hz, **H11**), 6.63 (d, 2H, J = 12.3 Hz, **H7**), 6.51 (d, 2H, J = 12.3 Hz, **H8**) 3.90 (s, 3H, **H1**), 3.79 (s, 3H, **H13**).

¹³C NMR (75 MHz, CDCl₃) δ (ppm): 166.9 (**C2**), 159.0 (**C12**), 142.5 (**C6**), 131.7 (**C7**), 130.2 (**C10**), 129.5 (**C4**), 129.0 (**C9**), 128.8 (**C5**), 128.4 (**C3**), 127.7 (**C8**), 113.7 (**C11**), 55.2 (**C13**), 52.0 (**C1**).

HRMS calcd. for C₁₇H₁₆O₃⁺ 268.1090, found 268.1084.

Following **GP5**, from **189**, a mixture of **209a**, **209b** was obtained as a white solid (84 mg, quantitative yield). The ratio between isomers of 99/1 was determined by GC-FID and GC-MS and NMR spectra were obtained after chromatography column. For intensity reasons, resonances of **209b** were not clearly detectable in NMR spectra.

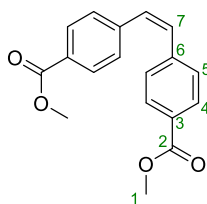


¹H NMR (300 MHz, CDCl₃) δ (ppm): 7.90 (d, 2H, *J* = 8.4 Hz, **H9**), 7.27 (d, 2H, *J* = 8.4 Hz, **H8**), 7.19 (d, 2H, *J* = 8.7 Hz, **H3**), 7.12 (d, 2H, *J* = 8.4 Hz, **H2**) 6.63 (s, 2H, **H5**, **H6**), 3.90 (s, 3H, **H12**).

¹³C NMR (75 MHz, CDCl₃) δ (ppm): 166.8 (**C11**), 141.6 (**C7**), 135.0 (**C4**), 133.2 (**C1**), 130.8 (**C10**), 130.2 (**C2**), 129.9 (**C5**, **C6**), 129.6 (**C9**), 128.8 (**C8**), 128.5 (**C3**), 52.0 (**C12**).

HRMS calcd. for C₁₆H₁₃ClO₂⁺ 272.0599, found 272.0596.

Following **GP5**, from **190**, **210a**, was obtained as a white solid (92 mg, quantitative yield).

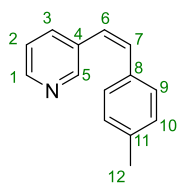


¹H NMR (300 MHz, CDCl₃) δ (ppm): 7.88 (d, 4H, *J* = 8.4 Hz, Z, **H4**), 7.25 (d, 4H, *J* = 8.4 Hz, **H5**), 6.70 (s, 2H, **H7**), 3.88 (s, 6H, **H1**).

¹³C NMR (75 MHz, CDCl₃) δ (ppm): 166.6 (**C2**), 141.3 (**C6**), 131.0 (**C7**), 129.6 (**C4**), 128.9 (**C3**), 128.8 (**C5**), 52.0 (**C1**).

HRMS calcd. for C₁₈H₁₆O₄⁺ 296.1049, found 296.1049.

Following **GP5**, from **191**, **211a**, was obtained as a white solid (92 mg, quantitative yield).

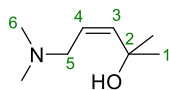


¹H NMR (300 MHz, CDCl₃) δ (ppm): 8.48 (d, 1H, $J = 1.8$ Hz, **H5**), 8.41 (dd, 1H, $J = 4.5, 1.5$ Hz, **H1**), 7.53 (ddd, 1H, $J = 8.1, 1.5, 1.5$ Hz, **H3**), 7.13-7.03 (m, 5H, **H2**, **H9**, **H10**), 6.73 (d, 1H, $J = 12.3$ Hz, **H7**), 6.48 (d, 1H, $J = 12.3$ Hz, **H6**) 2.31 (s, 3H, **H12**).

¹³C NMR (75 MHz, CDCl₃) δ (ppm): 150.1 (**C5**), 147.9 (**C1**), 137.4 (**C11**), 135.8 (**C3**), 133.4 (**C4**), 133.2, (**C8**), 132.6 (**C7**), 129.1 (**C10**), 128.5 (**C9**), 125.6 (**C6**), 122.9 (**C2**), 21.2 (**C12**).

HRMS calcd. for C₁₄H₁₃N⁺ 195.1043, found 195.1038.

Following **GP5**, from **192**, **212a**, was obtained as a colorless oil (44 mg, 99% yield).

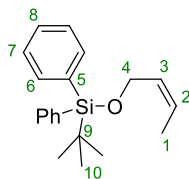


¹H NMR (500 MHz, CDCl₃) δ (ppm): 6.00 (d, 1H, *J* = 11.5 Hz, **H3**), 5.47 (dt, 1H, *J* = 11.5, 8.0 Hz, **H4**), 3.99 (d, 2H, *J* = 7.1 Hz, **H5**), 2.79 (s, 6H, **H6**), 1.40 (s, 6H, **H1**).

¹³C NMR (125 MHz, CDCl₃) δ (ppm): 149.4 (**C3**), 115.1 (**C4**), 72.7 (**C2**), 54.2 (**C5**), 42.8 (**C6**), 30.9 (**C1**).

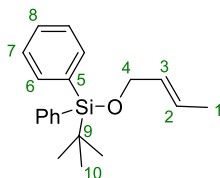
HRMS calcd. for C₈H₁₈NO⁺ (M+H)⁺ 144.1383, found 144.1381.

Following **GP5**, from **193**, a mixture of **213a**, **213b** and **213c** was obtained as a white solid (91 mg, 99% yield). The ratio between isomers of 90/6/4 was determined by GC-FID and GC-MS and NMR spectra were obtained after chromatography column.

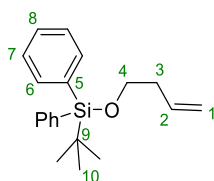


¹H NMR (300 MHz, CDCl₃) δ (ppm): 7.73-7.66 (m, 2H, **H6**), 7.47-7.36 (m, 2H, **H7**, **H8**), 5.68-5.85 (m, 1H, **H3**), 5.55-5.44 (m, 1H, **H2**), 4.27 (d, 2H, *J* = 6 Hz, **H4**), 1.47 (d, 3H, *J* = 6.9 Hz, **H1**), 1.06 (s, 9H, **H10**).

¹³C NMR (75 MHz, CDCl₃) δ (ppm): 135.6 (**C6**), 133.9 (**C5**), 129.9 (**C3**), 129.5 (**C8**), 127.6 (**C7**), 125.2 (**C2**), 60.0 (**C4**), 26.8 (**C10**), 19.1 (**C9**).

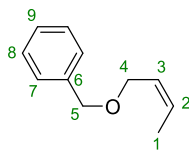


¹H NMR (300 MHz, CDCl₃) δ (ppm): 7.73-7.66 (m, 2H, **H6**), 7.47-7.36 (m, 2H, **H7**, **H8**), 5.68-5.85 (m, 1H, **H3**), 5.55-5.44 (m, 1H, **H2**), 4.14 (dt, 2H, *J* = 4.8, 1.5 Hz, **H4**), 1.72-1.67 (m, 3H, **H1**).



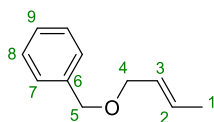
¹H NMR (300 MHz, CDCl₃) δ (ppm): 5.92-5.77 (m, 1H, **H2**), 5.10-4.99 (m, 2H, **H1**), 3.72 (t, 2H, *J* = 6.9 Hz, **H4**), 2.41-2.29 (m, 2H, **H3**).

Following **GP5**, from **194** and after 86% conversion, a mixture of **214a**, **214b** and **214c** was obtained as a colorless oil (50 mg, 86% + 14% starting material). The ratio between isomers of 83/14/3 was determined by GC-FID and GC-MS and NMR spectra were obtained after chromatography column.



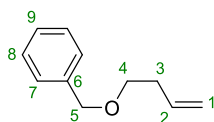
¹H NMR (300 MHz, CDCl₃) δ (ppm): 7.47-7.27 (m, 5H, **H7**, **H8**, **H9**), 5.76-5.57 (m, 2H, **H2**, **H3**), 4.52 (s, 2H, **H5**), 4.11-4.08 (m, 2H, **H4**), 1.65 (d, 3H, *J* = 6.0 Hz, **H1**).

¹³C NMR (75 MHz, CDCl₃) δ (ppm): 138.4 (**C6**), 128.4 (**C7** or **C8**), 128.1 (**C9**), 127.8 (**C8** or **C7**), 127.6 (**C3** or **C2**), 126.8 (**C2** or **C3**), 72.1 (**C5**), 65.4 (**C4**), 13.2 (**C1**).



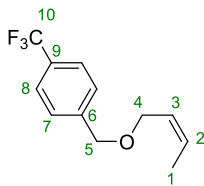
¹H NMR (300 MHz, CDCl₃) δ (ppm): 7.47-7.27 (m, 5H, **H7**, **H8**, **H9**), 5.76-5.57 (m, 2H, **H2**, **H3**), 4.50 (s, 2H, **H5**), 3.99-3.94 (m, 2H, **H4**), 1.73 (dd, 3H, *J* = 6.0, 0.9 Hz, **H1**).

¹³C NMR (75 MHz, CDCl₃) δ (ppm): 136.1 (**C6**), 71.9 (**C5**), 70.9 (**C4**), 17.9 (**C1**).



¹H NMR (300 MHz, CDCl₃) δ (ppm): 5.83-5.75 (m, 1H, **H2**), 5.15-5.01 (m, 2H, **H1**), 3.53 (t, 2H, *J* = 6.9 Hz, **H4**), 2.43-2.36 (m, 2H, **H3**).

Following **GP5**, from **194**, a mixture of **214a**, **214b** and **214c** was obtained as a white solid (72 mg, quantitative yield). The ratio between isomers of 76/19/5 was determined by GC-FID and GC-MS and NMR spectra were obtained after chromatography column.

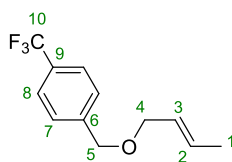


¹H NMR (500 MHz, CDCl₃) δ (ppm): 7.60 (d, 2H, *J* = 8.0 Hz, **H8**), 7.46 (d, 2H, *J* = 8.0 Hz, **H7**), 5.75-5.69 (m, 1H, **H3**), 5.64-5.60 (m, 1H, **H2**), 4.57 (s, 2H, **H5**), 4.12 (d, 2H, *J* = 6.5 Hz, **H4**), 1.66 (d, 3H, *J* = 7.0 Hz, **H1**).

¹³C NMR (125 MHz, CDCl₃) δ (ppm): 142.7 (**C6**), 129.7 (q, *J* = 25.5 Hz, **C9**), 128.4 (**C2**), 127.6 (**C7**), 126.2 (**C3**), 125.3 (q, *J* = 14.5 Hz, **C8**), 124.2 (q, *J* = 270.6 Hz, **C10**), 71.2 (**C5**), 65.8 (**C4**), 13.2 (**C1**).

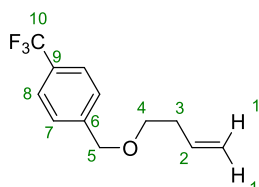
¹⁹F NMR (CDCl₃) δ (ppm): - 62.5.

HRMS calcd. for C₁₂H₁₃F₃O⁺ 230.0913, found 230.0902.



¹H NMR (500 MHz, CDCl₃) δ (ppm): 4.56 (s, 2H, **H5**), 3.99 (m, 2H, **H4**), 1.74 (dd, 3H, *J* = 6.5, 1.0 Hz, **H1**).

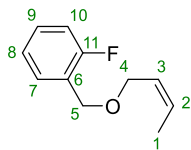
¹³C NMR (125 MHz, CDCl₃) δ (ppm): 142.7 (**C6**), 130.1 (**C2**), 128.5 (**C3**), 71.3 (**C4**), 71.0 (**C5**), 17.7 (**C1**).



¹H NMR (500 MHz, CDCl₃) δ (ppm): 5.85 (ddt, 1H, *J* = 17.0, 10.3, 6.7 Hz, **H2**), 5.12 (dq, 1H, *J* = 17.0, 1.5 Hz, **H1**), 5.07 (m, 1H, **H1'**), 3.56 (t, 2H, *J* = 6.5 Hz, **H4**), 2.40 (m, 3H, **H3**).

¹³C NMR (125 MHz, CDCl₃) δ (ppm): 135.0 (**C2**), 116.6 (**C1**), 72.1 (**C5**), 70.0 (**C4**), 34.2 (**C3**).

Following **GP5**, from **195**, a mixture of **215a**, **215b** and **215c** was obtained as a white solid (56 mg, 99% yield). The ratio between isomers of 74/21/5 was determined by GC-FID and GC-MS and NMR spectra were obtained after chromatography column.

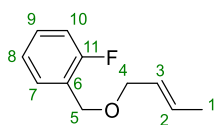


¹H NMR (300 MHz, CDCl₃) δ (ppm): 7.49-7.40 (m, 1H, **H7**), 7.32-7.22 (m, 1H, **H9**), 7.17-7.10 (m, 1H, **H8**), 7.08-7.00 (m, 1H, **H10**), 5.79-5.57 (m, 2H, **H2**, **H3**), 4.59 (s, 2H, **H5**), 4.13 (d, 2H, *J* = 6.3 Hz, **H4**), 1.67 (d, 3H, *J* = 5.1 Hz, **H1**).

¹³C NMR (75 MHz, CDCl₃) δ (ppm): 160.7 (d, *J* = 245.0 Hz, **C11**), 130.0 (d, *J* = 4.2 Hz, **C7**), 129.2 (d, *J* = 8.1 Hz, **C9**), 128.3 (**C2** or **C3**), 126.6 (**C3** or **C2**), 125.5 (d, *J* = 14.8 Hz, **C6**), 124.0 (d, *J* = 3.5 Hz, **C8**), 115.9 (d, *J* = 21.4 Hz, **C10**), 65.7 (**C4**), 65.4 (d, *J* = 3.7 Hz, **C5**), 13.2 (**C1**).

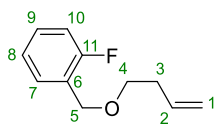
¹⁹F NMR (CDCl₃) δ (ppm): - 119.1.

HRMS calcd. for C₁₁H₁₃FO⁺ 180.0945, found 180.0939.



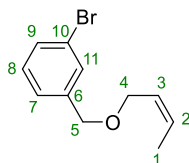
¹H NMR (300 MHz, CDCl₃) δ (ppm): 7.49-7.40 (m, 1H, **H7**), 7.32-7.22 (m, 1H, **H9**), 7.17-7.10 (m, 1H, **H8**), 7.08-7.00 (m, 1H, **H10**), 5.79-5.57 (m, 2H, **H2**, **H3**), 4.57 (s, 2H, **H5**), 4.00 (d, 2H, *J* = 6.9 Hz, **H4**), 1.73 (d, 3H, *J* = 6.3 Hz, **H1**).

¹³C NMR (75 MHz, CDCl₃) δ (ppm): 160.7 (d, *J* = 245.0 Hz, **C11**), 130.1-129.9 (m, **C7**), 129.1 (d, *J* = 7.8 Hz, **C9**), 127.3 (**C2** or **C3**), 126.6 (**C3** or **C2**), 125.5 (d, *J* = 14.6 Hz, **C6**), 124.0 (m, **C8**), 115.9 (d, *J* = 21.4 Hz, **C10**), 71.2 (**C4**), 65.2 (d, *J* = 3.7 Hz, **C5**), 17.8 (**C1**).



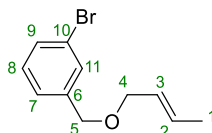
¹H NMR (300 MHz, CDCl₃) δ (ppm): 5.90-5.82 (m, 1H, **H2**), 5.15-5.03 (m, 2H, **H1**), 3.57 (t, 2H, *J* = 6.9 Hz, **H4**), 2.43-2.35 (m, 2H, **H3**).

Following **GP5**, from **196** and after 86% conversion, a mixture of **216a**, **216b** and **216c** was obtained as a colorless oil (75 mg, 86% + 14% starting material). The ratio between isomers of 87/11/2 was determined by GC-FID and GC-MS and NMR spectra were obtained after chromatography column.



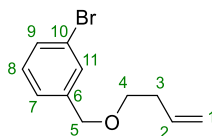
¹H NMR (300 MHz, CDCl₃) δ (ppm): 7.52 (s, 1H, **H11**), 7.41 (dd, 1H, *J* = 7.5, 1.5 Hz, **H9**), 7.37-7.17 (m, 2H, **H7**, **H8**), 5.77-5.55 (m, 2H, **H2**, **H3**), 4.48 (s, 2H, **H5**), 4.09 (d, 2H, *J* = 6.3 Hz, **H4**), 1.66 (d, 3H, *J* = 6.6 Hz, **H1**).

¹³C NMR (75 MHz, CDCl₃) δ (ppm): 140.8 (**C10**), 130.6 (2C, **C9**, **C11**), 129.9 (**C8**), 128.4 (**C2**), 127.8 (**C7**), 126.4 (**C3**), 122.3 (**C6**), 71.1 (**C5**), 65.6 (**C4**), 13.2 (**C1**).



¹H NMR (300 MHz, CDCl₃) δ (ppm): 7.52 (s, 1H, **H11**), 7.45-7.37 (m, 1H, **H9**), 7.37-7.17 (m, 2H, **H7**, **H8**), 5.77-5.55 (m, 2H, **H2**, **H3**), 4.46 (s, 2H, **H5**), 3.96 (d, 2H, *J* = 6.0 Hz, **H4**), 1.75-1.71 (m, 3H, **H1**).

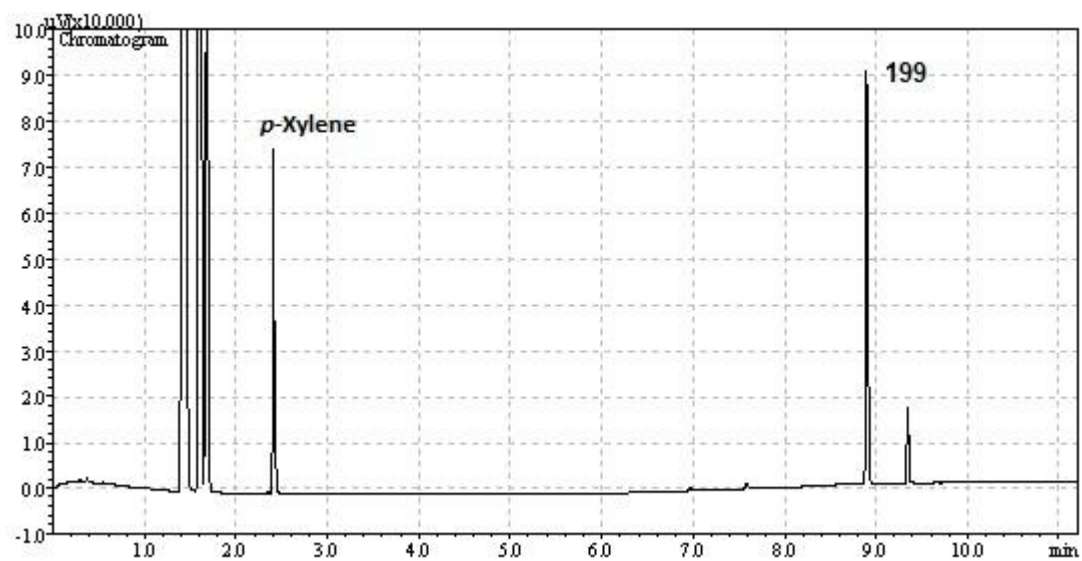
¹³C NMR (75 MHz, CDCl₃) δ (ppm): 138.4 (**C10**), 122.3 (**C6**), 72.1 (**C4**), 71.0 (**C5**), 17.8 (**C1**).



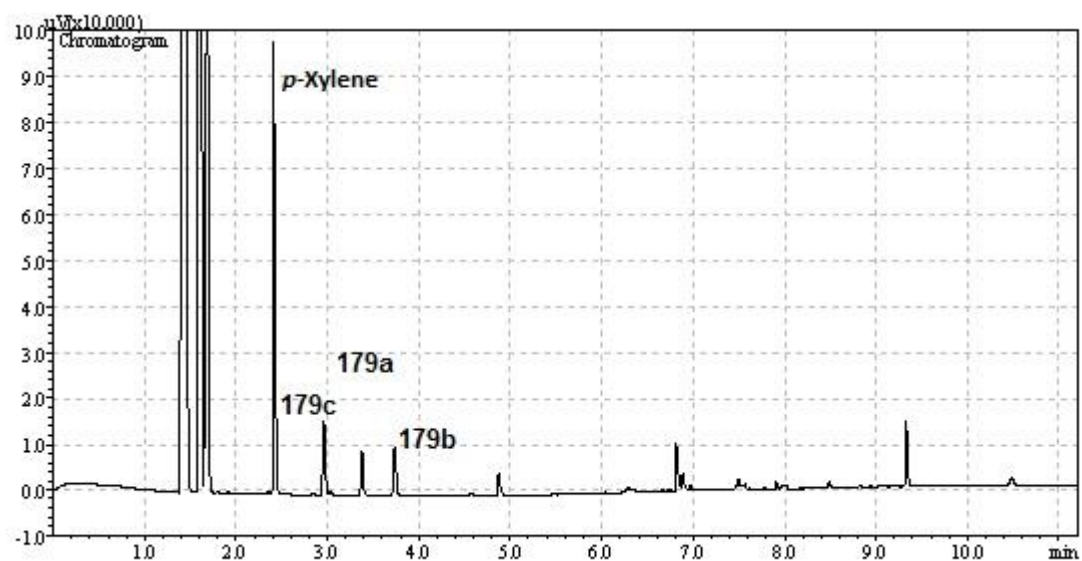
¹H NMR (300 MHz, CDCl₃) δ (ppm): 5.95-5.84 (m, 1H, **H2**), 5.19-5.01 (m, 2H, **H1**), 3.53 (t, 2H, *J* = 6.6 Hz, **H4**), 3.96 (d, 2H, *J* = 6.0 Hz, **H4**), 2.44-2.31 (m, 3H, **H1**).

Following **GP5**, from **199**, a mixture of **179a**, **179b** and **179c** was observed and a ratio between isomers of 29/27/44 was determined by GC-FID and GC-MS.

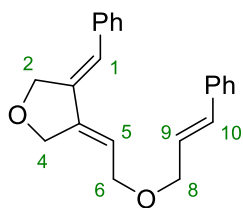
GC at t₀



GC at t = 20h

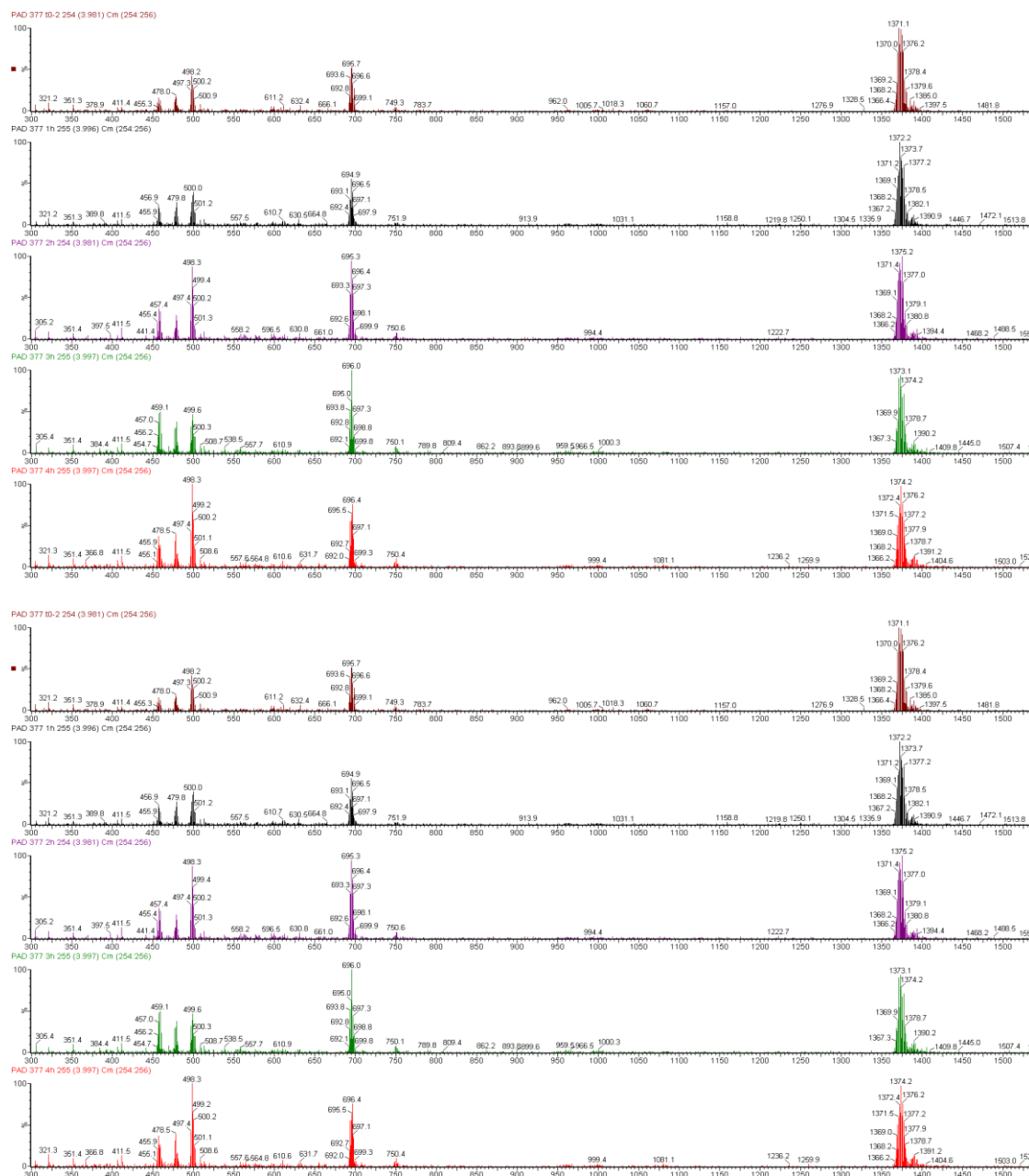


Following **GP6**, from product **218**, was obtained 68 mg (68% yield) of **219** as a white powder.



$^1\text{H NMR}$ (400 MHz, CDCl_3) δ (ppm): 7.18-7.41 (m, 10H, Ar), 6.85 (s, 1H, **H1**), 6.65 (d, $J = 15.96$ Hz, 1H, **H10**), 6.32 (m, 1H, **H9**), 6.12(m, 1H, **H5**), 4.79 (s, 2H, **H6**), 4.58 (m, 2H, **H8**), 4.19 (dd, $J = 6.06, 1.36$ Hz, 2H, **H2**), 4.14 (d, $J = 6.68$, 2H, **H4**)

$^{13}\text{C NMR}$ (75 MHz, CDCl_3) δ (ppm): 140.9 (**CAr**), 137.3 (**CAr**), 136.8 (**C4a**), 136.6 (**C1a**), 133.3 (**C10**), 132.7 (**C1**), 128.65 (2x**CAr**), 128.61 (2x**CAr**), 126.5 (2x**CAr**), 119.7 (**C9**), 114.5 (**C5**), 71.5 (**C4**), 71.0 (**C8**), 69.7 (**C2**), 67.6 (**C6**).

Conversion
199 (%)

For sake of comparison, a plot of alkyne conversion through time is provided below MS spectra. These data came from GC-FID analyses, containing p-xylene as internal standard, over the same samples used for the above-mentioned UPLC ones.

GENERAL CONCLUSION

GENERAL CONCLUSION

During this Ph.D. work we were able to synthesize four natural benzo[*c*]phenanthridines by using palladium/norbornene joint organometallic catalysis. We bypassed the issue of the deprotection of acetal motifs present on these natural alkaloids by introducing an excess of norbornene. It acts both as a cocatalyst and as a sacrificial olefin, ensuring yields between 60 and 74% for the key dual catalytic step and therefore the synthesis of these natural compounds with over-all yields between 35 and 42%.

The second project concerned tripalladium all-metal aromatic complexes, first noble metal analogue of the cyclopropenyl cation $[C_3H_3]^+$ which was previously isolated in our group. These structures were obtained in four steps from commercial compounds. We developed a second-generation synthesis one-pot synthesis using readily available chemicals. This highly tunable method proved practical, efficient and tolerant towards a significantly broader scope of functionalities, delivering a large palette of $[M_3]^+$ clusters in 80%-99% yields. It allowed to access triplatinum $[Pt_3]^+$ and heterometallic $[Pd_2Pt]^+$ and $[PdPt_2]^+$ complexes. They parallel core structural and electronic properties of their $[Pd_3]^+$ peers. Heterometallic complexes are analogues of traditional heteroaromatics. Unlike those built assembling main-group elements, $[Pd_2Pt]^+$ and $[PdPt_2]^+$ complexes present asymmetric crystallographic units identical to their homonuclear peer. Bond-length equalization in heteronuclear system could be observed thanks to lanthanide contraction that makes suitably delocalized M-M and M-M' bonds degenerate. DFT modeling suggested that these $[M_3]^+$ clusters possessed a potentially strong Lewis basic character as regular donor ligands. Despite their electrostatic charge they quadrupolar moment should have allowed them to bind other cationic species. We proved that cationic metal-aromatic platform can act as neutral and anionic ligands by synthesizing $[M''(M_3)(L_n)]^{2+}$ complexes. The coordination can deliver stable species, as 18-electron silver(I) complexes in which four ancillary ligands arrange in an almost perfect tetrahedral geometry around Ag^+ ions. Three can be neutral species and the first coordination sphere of silver nuclei can be filled by a $[M_3]^+$ unit in spite of the charge repulsion between two cations.

In order to better understand the chemistry of metal-aromatic species through these $[M_3]^+$ clusters, we then wanted to study their behavior in catalysis. We developed a method for the selective semi-reduction of alkynes. The best $[M_3]^+$ cluster presented an interesting activity at low loadings and provided good stereoselectivity for Z-alkenes. Furthermore, the use of these

complexes enables to achieve complete chemoselectivity towards C-C triple bonds, completely excluding any over-reduced product. Unlike most mononuclear electron-rich species, they might trigger electrophilic activation of alkynes. This hypothesis is supported by encouraging preliminary results on enyne cycloisomerizations.

RESUME EN FRANÇAIS

RESUME EN FRANCAIS

Depuis plusieurs décennies, la chimie du palladium a connu un véritable essor. Afin de continuer dans cette voie, plusieurs axes de recherche ont été étudiés dans le cadre de cette thèse. Grâce aux récents développements de la catalyse duale palladium/norbornène, plusieurs structures polycycliques azotées complexes ont pu être synthétisées, comme par exemple les dibenzoazépines, les carbazoles ou encore les phénanthridines. Concernant ces dernières, notre groupe a mis au point la réaction de couplage entre des iodures aryliques et des partenaires bromobenzylamines permettant ainsi l'accès rapide au motif benzo[*c*]phénanthridine avec de bons rendements. Cette méthodologie permet de créer une liaison C-C ainsi qu'une liaison C-N pour former la dihydrobenzo[*c*]phénanthridine correspondante. Grâce au palladium encore présent dans le milieu et à l'ajout d'un ballon de dioxygène à la fin de la conversion, l'oxydation de la liaison C-N conduit à la formation de la benzo[*c*]phénanthridine désirée de manière monotopée. Cependant, aucune benzo[*c*]phénanthridine naturelle n'a été produite en utilisant cette méthode et c'est dans ce contexte que le projet a vu le jour. Le but était de synthétiser quatre produits naturels *via* la méthode de couplage séquentiel palladium/norbornène préalablement mise au point dans notre groupe. Le problème de l'hydrolyse des groupements acétals pendant l'étape de couplage a été identifié et résolu après optimisation des conditions réactionnelles. En effet, un excès de norbornène a permis non seulement d'assurer son rôle de co-catalyseur mais également de servir d'oléfine sacrificielle en acceptant formellement une molécule de dihydrogène générée lors de l'oxydation pallado-catalysée de la liaison C-N. Ces conditions optimales ont été appliquées et quatre benzo[*c*]phénanthridines naturelles, à savoir la Noravicine, la Norvitidine, la *O*-Methylnorfagaronine et la Norallonitidine, ont pu être isolées en seulement quatre étapes avec des rendements globaux allant de 35 à 42%.

Quelques mois avant le commencement de cette thèse, une nouvelle famille de complexes triangulaires de palladium a été isolée dans notre groupe à partir d'isothiourées. Cette espèce arborant 44 électrons de valence et une charge positive délocalisée sur son cœur trimétallique, est la première molécule stable qui présente un caractère métallo-aromatique de type δ . De manière contre-intuitive, les calculs DFT effectués sur ces molécules ont prédit un fort caractère basique au sens de Lewis malgré la présence d'une charge positive. Durant cette thèse, nous avons mis au point une nouvelle voie d'accès à cette famille de complexes $[Pd_3]^+$ à partir de disulfures. Cette synthèse, plus efficace en termes de rendements globaux, est

également plus tolérante envers divers groupements fonctionnels. Elle présente l'avantage d'être économe en atome mais aussi de partir de réactifs commercialement disponibles et d'utiliser une purification par précipitation, évitant ainsi la chromatographie sur silice. Avec les conditions optimales en main, cette synthèse a été étendue à des analogues de platine de type $[\text{Pt}_3]^+$ qui possèdent une configuration électronique sensiblement proche des complexes $[\text{Pd}_3]^+$ et qui présentent également une aromaticité de type δ . Utilisant la même synthèse, des complexes hétéro-métalliques de type $[\text{Pd}_2\text{Pt}]^+$ et $[\text{PdPt}_2]^+$ ont aussi pu être obtenus et de manière intéressante, ceux-ci possèdent la même unité asymétrique que leurs pairs homo-nucléaires.

Malgré l'inévitable répulsion entre deux charges positives, le caractère base de Lewis de ces complexes s'est révélé assez fort pour coordiner d'autres espèces cationiques. En effet nous avons réussi à synthétiser et à isoler des espèces tétraédrique de type $[\text{Pd}_3\text{M}]^{2+}$ dans lesquelles M est un cation Au^+ , Ag^+ , ou même Cu^+ . Ces complexes présentent une stabilité appréciable qui nous a permis de les manipuler sans précautions drastiques et ainsi d'obtenir des cristaux adaptés pour des analyses R-X.

D'autre part, au-delà des propriétés spéciales des complexes de type $[\text{Pd}_3]^+$, nous voulions savoir s'ils possédaient une activité catalytique. Notre étude s'est portée sur la réaction de semi-hydrogénation d'alcynes. Suite au processus d'optimisation de la réaction, un de nos catalyseurs $[\text{Pd}_3(\text{SMe})_3\{\text{P}(\text{C}_7\text{H})_3\}_3]^+$ a montré des résultats allant au-delà de nos espérances. En effet, ce complexe produit sélectivement des alcènes de configuration Z, thermodynamiquement moins stables sans présence de produit doublement réduit. Une totale chimio-sélectivité envers les alcynes internes a été prouvée par la tolérance de ce catalyseur pour plusieurs groupements fonctionnels ordinairement sensibles aux conditions d'hydrogénation.

Titre : Voie d'accès aux benzophenanthridines naturelles et la chimie des composés métallo-aromatiques stables

Mots clés : Benzo[*c*]phenanthridines, Metallo-aromaticité, Hydrogénation, Palladium, Catalyse

Résumé : Depuis plusieurs décennies, la chimie du palladium a connu un véritable essor. Afin de continuer dans cette optique, plusieurs axes de recherche ont été investigués dans le cadre de cette thèse. Grâce aux récents développements de la catalyse duale palladium/norbornène des motifs benzophénanthridines naturels. En parallèle, une nouvelle famille de complexes triangulaires de palladium a été isolée dans notre groupe. Cette espèce arborant 44 électrons de valence et une charge positive délocalisée sur son cœur trimétallique, est la première molécule stable qui présente un caractère

métallo-aromatique de type δ . Après l'optimisation d'une nouvelle voie de synthèse, nous avons pu accéder à des analogues de platine mais aussi à des composés hétéro-métalliques possédant des unités asymétriques similaires. Le caractère base de Lewis de ces complexes a permis l'isolation de composés tétraédraux de type $[M''(M_3)(L_n)]^{2+}$ malgré la répulsion des charges positives. Ces espèces triangulaires aromatiques ont aussi prouvé leur habileté en tant que catalyseur pour la réaction de semi-hydrogénation d'alcynes. En effet, ce complexe transforme chimiosélectivement les alcynes en alcènes de configuration *Z* sans présence de produit doublement réduit.

Title : Convergent assembly of natural benzophenanthridines and the chemistry of stable all-metal aromatic complexes

Keywords : Benzo[*c*]phenanthridines, All-Metal aromaticity, Hydrogenation, Palladium, Catalysis

Abstract : Recent developments on dual palladium/norbornene catalytic reactions led to one-pot synthesis of complexes polyheterocyclic molecules. By extension of this reaction, the coupling of aryl triflates and bromobenzylamines permitted us to synthesize natural benzophenanthridine. In parallel, a new family of triangular palladium complexes has been isolated in our research group. These 44 valence electrons complexes possessing a positive charge delocalized on the trimetallic core were the first stable compounds which presented δ -type aromaticity. After optimization of a new synthetic route, we could be able to isolate platinum analogues and also heterometallic clusters which interestingly had the same asymmetric unit than their homonuclear peers. Despite the unavoidable charge repulsion, the Lewis basic character

revealed to be strong enough to bind other cationic species. Indeed, we reached to synthesize tetrahedral $[M''(M_3)(L_n)]^{2+}$ complexes. In another side, we wondered if the stability and special properties of $[Pd_3]^+$ clusters could confer to it some catalytic activities. Our studies were focused on semi-reduction reactions of alkynes. After optimization process, the catalyst $[Pd_3(SMe)_3\{P(C_7H_3)_3\}]^+$ showed results beyond our greatest expectations. Indeed, this cluster selectively produced thermodynamically less stable *Z*-alkene without traces of over-reduced compound. Total chemoselectivity towards alkynes was proved by the reaction on several molecules bearing functional groups which are sensitive to hydrogenation conditions.

